Synthesis and biological evaluation of various heterocyclic compounds

Clemens Zwergel

Thèse

présentée en vue de l'obtention du grade de

DOCTEUR DE L'UNIVERSITE DE LORRAINE

Mention : Chimie Moléculaire

par

Clemens ZWERGEL

Synthesis and biological evaluation of various heterocyclic compounds: Aurones from Coumarins and Chromones, Quinolines and Pyrimidines as DNMTi, Coumarins as potential NFkB-Inhibitors

Rapporteurs:

Ahcène Boumendjel	Professeur à l'Université de Grenoble (France)
Joachim Jose	Professeur à l'Université de Münster (Allemagne)
André Luxen	Professeur à l'Université de Liège (Belgique)

Membres du jury:

Claus Jacob	Professeur à l'Université de la Sarre (Allemagne)
Jean-Bernard Regnouf de Vains	Professeur à l'Université de Lorraine (France)
Gilbert Kirsch	Professeur à l'Université de Lorraine (Directeur de thèse)

The work presented here was part of the Red Cat Training Network. This project was funded by the European Community's Seventh Framework Programme (FP7/2007-2013) under grant agreement n° 215009.

The ‚Red Cat' Training Network comprises ten partners from universities, research institutes and companies from five European countries. It addresses emerging issues in Medicine and Agriculture, such disease-preventive antioxidants for an ageing population, antibiotics against bacteria and 'green' pesticides for an ecologically acceptable agriculture of the future. They provide training for four ER and ten ESR in natural products, antioxidants, intracellular redox processes, green pesticides, and innovative ways of selectively killing cancer cells. The scientific part is reflected in training, which will be highly multidisciplinary, and allow mobility across partners and countries, including industry. Training in modern scientific methods will go hand in hand with acquisition of complementary skills, organized in four training modules, which reflect the training needs of ESR/ER, e.g. in scientific background, communication, languages, IT, IPR, comercialization, science and society and bioethics. Research and training will be implemented by qualified, experienced supervisors supported by external experts (associated partners, external advisors). ESR and ER will receive cross- discipline training in competitive, emerging areas of research with direct relevance to society and high demand for skilled researchers to provide excellent career prospects in academia and industry.

Financial support of European Commission, Seventh Framework Programme (FP7/2007-20139] Marie Curie grant agreement nº 215009

RedCat Project

Acknowledgements

Le présent travail a été réalisé au Laboratoire d'Ingénierie Moléculaire et Biochimie Pharmacologique (LIMBP), désormais Laboratoire « Structure et Réactivité des Systèmes Moléculaires Complexes » (SRSMC) de l'Université de Lorraine (ex-Université Paul Verlaine-Metz), sous la direction du Professeur Gilbert Kirsch, comprenant également un stage chez le Professeur Antonello Mai à l'Université de Rome „La Sapienza".

Je tiens tout d'abord à remercier le professeur Gilbert Kirsch pour m'avoir accueilli dans son laboratoire et pour m'avoir donné la possibilité de réaliser cette thèse. Je lui suis également reconnaissant pour sa disponibilité, ses conseils et ses qualités pédagogiques. J'exprime toute ma gratitude au Professeur Antonello Mai, mon superviseur en Italie, et au Professeur Claus Jacob, mon co-directeur de thèse, pour leur encadrement et leurs discussions précieuses. J'ai beaucoup appris à leurs côtés.

Je tiens à exprimer toute ma gratitude au Dr. Sergio Valente. Je suis reconnaissant pour son introduction au côté pratique de la chimie organique à Metz et plus tard, de retour à Rome, pour m'avoir aidé pendant mon stage dans le groupe du Professeur Mai. Durant notre temps ensemble dans le laboratoire et en dehors, il est devenu un très bon ami ainsi que sa famille.

Je remercie tous les membres du jury pour l'intérêt qu'ils ont bien voulu porter à ce travail et pour avoir honoré de leur présence le jury de thèse.

Je souhaite également remercier les équipes biologiques notamment de l'Université de Lorraine, surtout celle dirigée par le Professeur Denyse Bagrel, les équipes de l'Université de Naples II en Italie, dirigées par les professeurs Lucia Altucci et Ettore Novellino, celle de l'Université Emroy, Atlanta aux États-Uni, dirigée par Professeur Xiaodong Cheng, celle du Laboratoire de Biologie Moléculaire et Cellulaire du Cancer, Luxembourg, dirigée par le Professeur Marc Diederich, celle de l'USR3388 CNRS-Pierre Fabre Toulouse, dirigée par le Dr. Paola Arimondo et celles de l'Université de Rome „La Sapienza", dirigées par les professeurs Elisabetta Ferretti et Alberto Gulino.

Je remercie tous les collaborateurs de Red Cat et plus particulièrement Oualid Talhi et François Gaascht, qui ont effectué un stage à Metz, et les Professeurs Artur Silva et Marc Diederich pour leurs conseils et leurs coopérations scientifiques.

Ces travaux n'auraient pu se réaliser sans les techniciennes d'analyse. Je remercie donc Véronique Vaillant, Stéphanie Phillipot et Sandrine Rup pour tous leurs efforts et conseils.
Je remercie l'ITN training network „Red Cat" de l'Union Européenne pour le financement de ces trois années, l'école doctorale SESAMES avec son directeur, Professeur Assfeld pour son aide pendant ce temps, ainsi que l'Université de Lorraine (ex-Université Paul Verlaine-Metz) et l'Université de Rome „La Sapienza" pour leurs formations.

Je tiens à remercier tous mes collègues, qui ont participé à la vie du laboratoire à Metz pour leur soutien de tous les défis de la vie scientifique et de la culture française: Stéphanie Hesse, Germain Revelant, Zhanjie Xu, Charlène Gadais, Ismail Abdillahi, Wafaa Chaouni ainsi que les nombreux stagiaires.

Je souhaite également remercier mes collègues du laboratoire du Professeur Mai, mieux connu sous le nom de « neverlab » , et plus particulièrement: Dante Rotili, Donatella Labella, Stefano Tomassi, Alessia Lenoci, Biagina Marrocco, Maria Tardugno et tous les stagiaires en master.

Enfin je souhaite remercier toute ma famille, mon père, ma mère et mon frère Constantin sans oublier les autres membres de la famille pour leur soutien durant toutes ces années et sans lesquels je ne serais pas là aujourd'hui. J'associe également à ces remerciements tous mes amis pour les moments passés ensemble: Felix pour sa patience, ses idées et visites mémorables à Metz et à Rome, Matze et sa copine Jana pour leur support sans fin et les promenades amusantes. Tiziano et Angelo, mes colocataires italiens, qui m'ont appris la cuisine italienne, Jeannine, Emilie et Alex qui m'ont fait découvrir le mode de vie français; et tous ceux que j'ai oublié de mentionner.

Table of contents

English summary

Today, cancer is becoming a major public health problem with 12.7 million new cancer cases and 7.6 million cancer deaths registered in 2008. Although the number of people cured of cancer is increasing, people still die because of cancer. The reasons, besides an early and correct diagnosis, are the lack of effective treatments and the emergence of drug-resistant cancers.

Therefore, researchers are interested in new approaches to develop potent and selective therapies to fight cancer.

To start with, we developed a series of natural compound derivatives related to aurones. Aurones play an important role in the bright yellow pigmentation of some flowers and fruits exhibiting a strong and broad variety of biological activities. We combined the benzofuranone motif of the aurone with other coumarin and chromone motifs inspired by nature. These new compounds displayed promising anticancer activity because they are able to block the cell cycle in K562 cancer cells and are able to induce apoptosis being an interesting scaffold for further development.

Secondly, we focused on an epigenetic target. DNA methyltransferases (DNMTs) are considered as an interesting target in oncology. The use of specific inhibitors of DNMT (DNMTi) might reactivate tumor suppressor genes and induce the reprogramming of cancer cells, leading to their proliferation arrest and ultimately to their death. We improved the known compound SGI1027 through structure modification leading to novel non-nucleoside DNMT inhibitors, more potent and more selective than the lead compound. The anticancer activity of our quinoline and pyrimidine based compounds - tested in different cancer cell lines - suggests their use as possible potent and selective future cancer therapy.

A third series of coumarin-based curcuminoid analogues were prepared and tested for their potential ability to modulate the TNF-alpha induced NF-κB pathway in K562 cancer cells. However, we were not able to demonstrate the involvement of the targeted pathway so far. Complementary and deeper investigations need to be conducted in order

to elicit deeper biological properties of these compounds with the possible involvement of different pathways.

Résumé de la thèse en français

Aujourd'hui, le cancer est devenu un problème majeur de santé publique avec 12,7 millions de nouveaux cas de cancer et 7,6 millions de décès enregistrés en 2008. Même si le nombre de personnes, qui guérissent, augmente, les décès sont toujours importants. Les raisons, malgré un diagnostic précoce et correct, sont l'absence de traitements efficaces et l'émergence de résistances à la thérapie anticancéreuse.

C'est pourquoi les chercheurs s'intéressent aux nouvelles approches pour développer des traitements puissants et sélectifs pour vaincre le cancer.

Dans notre première approche, nous avons développé une série de dérivés de composés naturels appelés aurones. Les aurones jouent un rôle important dans la pigmentation jaune lumineuse de certaines fleurs et certains fruits et présentent de nombreuses activités biologiques. Nous avons combiné le motif benzofuranone des aurones avec d'autres motifs de la coumarine et chromone issus de la nature. Ces nouveaux composés montrent une activité anticancéreuse prometteuse, car ils sont capables de bloquer le cycle cellulaire dans les cellules cancéreuses K562 et peuvent y induire l'apoptose. Ils sont donc un motif intéressant pour un développement ultérieur de recherches.

Ensuite nous avons concentré notre attention sur un objectif épigénétique. Les méthyltransférases de l'ADN (DNMT) sont considérées comme une cible intéressante en oncologie. L'usage d'inhibiteurs spécifiques de la méthyltransferase de l'ADN (DNMTi) pourrait réactiver les gènes suppresseurs de tumeurs et induire la reprogrammation des cellules cancéreuses, conduisant à l'arrêt de leur prolifération et finalement à leur mort. Nous avons amélioré le composé connu SGI1027 par une modification de la structure. Nous avons obtenu de nouveaux inhibiteurs non- nucléosidiques de la méthyltransferase de l'ADN, plus puissants et plus sélectifs que le composé principal. L'activité anti-cancéreuse de nos composés quinoléiniques et pyrimidiniques est testée sur différentes lignées cellulaires de cancer indiquant leur future utilisation possible dans un traitement anti-cancéreux puissant et sélectif.

Une troisième série d'analogues de curcuminoïdes à base de coumarine a été préparée et testée pour sa capacité potentielle à moduler la voie TNF-alpha induite par NF-κB dans les cellules cancéreuses K562. Cependant, nous n'avons pas été capable de montrer

l'implication de la voie ciblée jusqu'à maintenant. Des études complémentaires et plus approfondies doivent être menées afin d'estimer les propriétés biologiques de ces composés dans la participation éventuelle à différentes voies.

CHAPTER 1

- GENERAL INTRODUCTION -

1. General introduction

Known since the ancient Greeks, studied by Hippocrates who gave its name (from the Greek word *"Karkinos"),* cancer has been an incurable disease for a long time. „Cancer" is a general term for a disease that can affect any part of the body caused by the proliferation of cells, with implications for the entire organism. Other terms used are malignant tumours and neoplasms. Many of them can be cured nowadays through the advances in medicine.

Although the number of people cured of cancer is increasing, people still die because of cancer. It is currently one of the three lead causes of death worldwide, among cardiovascular and infectious diseases, representing about 13% of global mortality rates (7.6 million victims in 2008) [1, 2].

The reasons besides a therapeutic point of view and an early as well as a correct diagnosis are the lack of effective treatments and the emergence of drug-resistant cancers [3-8].

Cancer is a complex disease, managed by many biological mechanisms. It arises from one single cell transforming from a healthy one into a tumourous one via multistage processes from a pre-cancerous lesion to malignant tissue. These changes are the result of personal genetic risk factors in combination with external influences, e.g.:

- physical tumourigenic agents, such as ultraviolet and ionizing radiation
- chemical tumourigenic agents, such as asbestos, components of tobacco smoke, aflatoxin as nutrition contamination and arsenic as potable water contaminant
- biological tumourigenic agents, such as infections from certain viruses, bacteria or parasites [1].

Despite of the already existing therapies, the estimates of the WHO show that the number of cancer victims will double by 2030. This highlights the importance of developing new treatments that are targeted, more effective and with fewer side

effects.

Today, modern research tries to synthesize, isolate, identify and elucidate how both natural and synthetic molecules work and researchers improve drug efficiency in a way to increase the number of therapeutic compounds to fight against different type of cancers [9-13].

During my PhD research I wanted to study chemical, biochemical and biological aspects of new agents to fight cancer.

Within my project I anticipated developing new competences in drug design. I wanted to focus on improving my synthetic chemistry skills particularly in the area of natural derivatives working closely together with biologists and biochemists in order to create new bioactive compounds.

To start with, we developed a series of natural compound derivatives related to aurones. Aurones play an important role in the bright yellow pigmentation of some flowers and fruits exhibiting a strong and broad variety of biological activities. We combined the benzofuranone motif of the aurones with other coumarin and chromone motifs inspired by nature. We will present new compounds displaying promising anticancer activity in K562 cancer cells.

Secondly, we focused on an epigenetic target. DNA methyltransferases are considered as an interesting target in Oncology. The use of specific inhibitors of DNMT (DNMTi) might reactivate tumour suppressor genes and induce the reprogramming of cancer cells, leading to their proliferation arrest and ultimately to their death. We prepared new quinoline and pyrimidine based compounds based on the known compound SGI1027 leading to promising selective novel non-nucleoside DNMT inhibitors.

As a third series, coumarin-based chalcone analogues were projected and prepared for their potential ability to modulate the TNF-alpha induced NFκB pathway in K562 cancer cells.

References

1. WHO. *Cancer Fact Sheet*. 2013 [cited 2013 16. September]; Available from: http://www.who.int/medicantre/factsheets/fs297.
2. J. Ferlay, D.M. Parkin, and E. Steliarova-Foucher, *Estimates of cancer incidence and mortality in Europe in 2008.* Eur J Cancer, 2010. **46**(4): p. 765-81.
3. M. Dean, *ABC transporters, drug resistance, and cancer stem cells.* J Mammary Gland Biol Neoplasia, 2009. **14**(1): p. 3-9.
4. S. Dermime, *Cancer Diagnosis, Treatment and Therapy.* J Carcinogene Mutagene S, 2013. **14**.
5. J. Ferlay, H.R. Shin, F. Bray, D. Forman, C. Mathers, and D.M. Parkin, *Estimates of worldwide burden of cancer in 2008: GLOBOCAN 2008.* Int J Cancer, 2010. **127**(12): p. 2893-917.
6. F.S. Liu, *Mechanisms of chemotherapeutic drug resistance in cancer therapy--a quick review.* Taiwan J Obstet Gynecol, 2009. **48**(3): p. 239-44.
7. R. Siegel, C. DeSantis, K. Virgo, K. Stein, A. Mariotto, T. Smith, D. Cooper, T. Gansler, C. Lerro, S. Fedewa, C. Lin, C. Leach, R.S. Cannady, H. Cho, S. Scoppa, M. Hachey, R. Kirch, A. Jemal, and E. Ward, *Cancer treatment and survivorship statistics, 2012.* CA Cancer J Clin, 2012. **62**(4): p. 220-41.
8. R. Siegel, D. Naishadham, and A. Jemal, *Cancer statistics, 2012.* CA Cancer J Clin, 2012. **62**(1): p. 10-29.
9. G.M. Cragg and D.J. Newman, *Natural products: A continuing source of novel drug leads.* Biochim Biophys Acta, 2013.
10. T. Efferth, P.C. Li, V.S. Konkimalla, and B. Kaina, *From traditional Chinese medicine to rational cancer therapy.* Trends Mol Med, 2007. **13**(8): p. 353-61.
11. D.J. Newman and G.M. Cragg, *Natural products as sources of new drugs over the 30 years from 1981 to 2010.* J Nat Prod, 2012. **75**(3): p. 311-35.
12. S. Nobili, D. Lippi, E. Witort, M. Donnini, L. Bausi, E. Mini, and S. Capaccioli, *Natural compounds for cancer treatment and prevention.* Pharmacol Res, 2009. **59**(6): p. 365-78.
13. M. Schumacher, M. Kelkel, M. Dicato, and M. Diederich, *Gold from the sea: marine compounds as inhibitors of the hallmarks of cancer.* Biotechnol Adv, 2011. **29**(5): p. 531-47.

CHAPTER 2

- AURONES -

2. Aurones

2.1 General introduction

Flavonoids represent a large class of natural products in the plant kingdom, exhibiting multiple biological activities [14]. Aurones play an important role in the pigmentation of some flowers and fruits and contribute especially to the bright yellow colour of flowers [15]. They also exhibit a strong and broad variety of biological activities. For example they have been described as antifungal agents [16], as insect antifeedant agents [17], as inhibitors of tyrosinase [18], and as antioxidants [19]. Not widely distributed in nature, aurones, (*Z*)-2-benzylidene-benzofuran-3(2H)-ones, are one of the less common and lesser-known representatives of a flavonoid subclass [20]. This is probably the reason why they have received little attention in comparison to the structurally similar and widely investigated flavones and isoflavones [21].

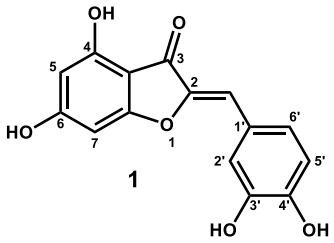

1

Figure 1: Aureusidin, an example of a common aurone

There are, however, a few notable exceptions. Aureusidin, a common aurone (**1**), is an inhibitor of iodothyronine- deiodinase, an enzyme involved in hormone synthesis and regulation [22]. Synthetic aurones bind to the nucleotide-binding domain of P-glycoprotein [23], to inhibit cyclin-dependent kinases in connection with antiproliferative properties [24], and to act as anticancer agents [25].

2.2 Synthesis of aurone derivatives

A very popular way to prepare aurones was developed by Varma *et al.* His method is based on the aldol–like condensation of benzofuran-3(2H)-ones with benzaldehydes [26]. This and some other classical methods for the synthesis were reviewed by Boumendjel *et al.* in 2003 [20]. Since then, several new or refined methods have been published:

Lawrence *et al.* studied the naturally occurring aurone **1**, isolated from *Uvaria hamiltonii*, and prepared a series of analogues structurally based on known tubulin binding agents, which were subsequently evaluated for anticancer activity [21]. The authors employed well-known methods to afford their aurone derivatives. The synthetic avenue described by Lawrence *et al.*, for example, consisted of the preparation of benzofuranone (**4**) (Scheme 1) via a polyphosphoric acid (PPA) cyclisation of the phenoxyacetic acid **3**, which was in turn prepared by the condensation of phenol **2** with chloroacetic acid.

The synthesis of aurone **1** required the use of the TBDMS-protected benzaldehyde **5**, prepared in high yield from 3,4-dihydroxybenzaldehyde using *tert*-butyldimethylsilyl chloride in the presence of imidazole [27].

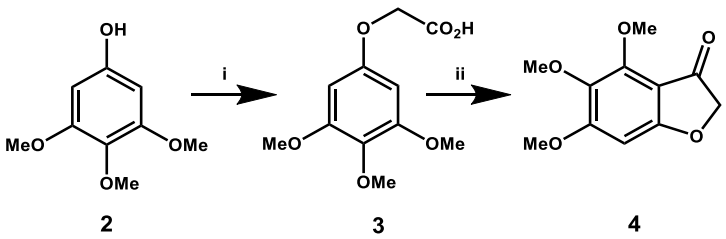

Scheme 1: Reagents and conditions (i) $ClCH_2CO_2H$, NaH, DMF, rt, overnight; (ii) PPA, 80ºC, 8h [21].

To obtain the aurone, the protected benzaldehyde is condensed with the appropriate benzofuranone **4** in the presence of neutral alumina. This method was

originally described by Varma *et al.* [26]. Subsequent treatment with tetra-butylammonium fluoride afforded the deprotected aurone **1** (Scheme 2).

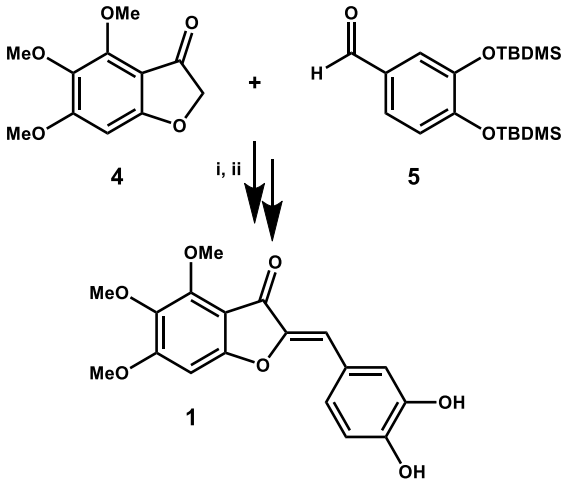

Scheme 2: (i) Al_2O_3, DCM, rt, overnight, (ii) to remove TBDMS: TBAF, DCM, rt, 30 min.

As for all the natural derivatives isolated by Atta ur Rahman and Choudhary *et al.* [31], an example of which is aurone **1**, the synthetic approach yielded the geometric (*Z*)-isomer, this being generally more stable thermodynamically than the (*E*)-isomer.

As part of an alternative synthetic approach, Kraus *et al.*, employed a Steglich esterification followed by a Suzuki coupling [28]. They started with the esterification of commercially available phenol **2** with 3,3-dibromoacrylic acid **6**. A Fries rearrangement led from the ester **7** to ketone **8.** After cyclisation of **8,** the authors initially expected a bromoketone, originally assigned as **9.** However, Suzuki coupling with phenylboronic acid **11** provided a different compound. After considering alternative structures through NMR studies, they revised **9** to **10.** This implies that the Suzuki coupling led to aurone **12** (Scheme 3).

The Suzuki reaction is more commonly conducted with aryl bromides or iodides than with chlorides [29]. Interestingly, when the authors exchanged 3,3-dibromoacrylic acid to 3,3-dichloroacrylic acid the reaction led to flavones **9** and not

to aurones. The rationale for the remarkable divergence still remains unclear.

As a further alternative synthetic pathway, Harkat *et al.* described a three-step procedure to form aurone derivatives using a gold(I)-catalyzed cyclisation of 2-(1-hydroxyprop-2-ynyl)phenols. The classical aldol-like coupling reaction sometimes results in low yields and requires the synthesis of benzofuran-3(2H)-ones from substituted 2-phenoxyacetic acids by an intramolecular Friedel – Craft reaction. Such a reaction is usually carried out under harsh conditions and yields are modest [30].

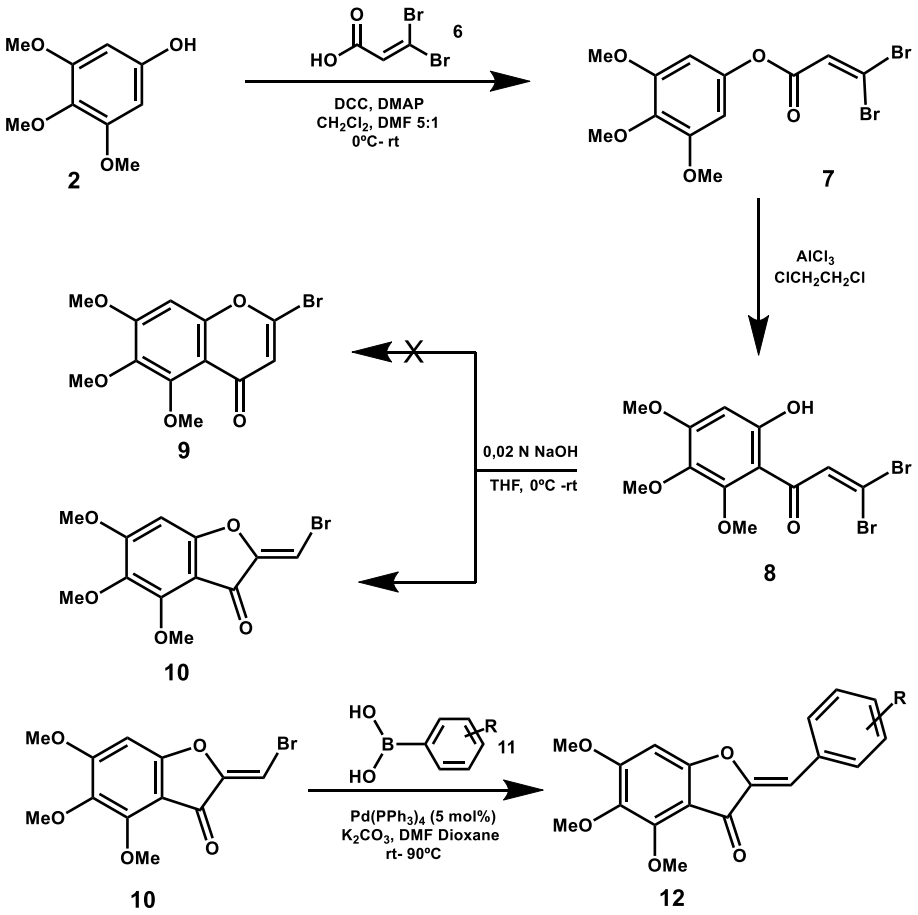

Scheme 3: Synthetic route towards aurones via Steglich esterification followed by Suzuki coupling [28].

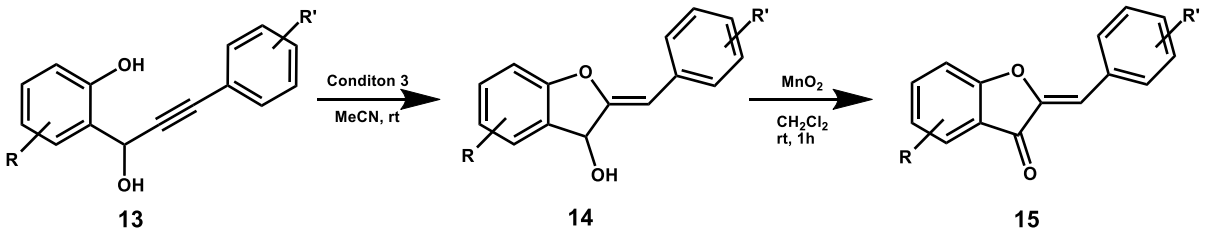

13 14 15

Scheme 4: Three-step procedure to form aurone derivatives using a gold (I)-catalyst R= H- , Br- , MeO-, NO_2- and R' Cl-, MeO- [30].

Conditions	Catalyst (mol%)	Additive (mol%)	Time (h)	yield (%)
1	none	K_2CO_3 (10)	24	0
2	AuCl (10)	none	0.5	*a*
3	AuCl (10)	K_2CO_3 (10)	2	78
Conditions	Catalyst (mol%)	Additive (mol%)	Time (h)	yield (%)
1	none	K_2CO_3 (10)	24	0
2	AuCl (10)	none	0.5	*a*
3	AuCl (10)	K_2CO_3 (10)	2	78

Table 1: Reaction conditions for catalytic condensation of aurones.
a: decomposition

In contrast, the group prepared various 2-(1-hydroxy-3-arylprop-2-ynyl) phenols **(13**) by addition of 2 equivalents of lithium arylacetylides, with or without substituents, at low temperature in THF to yield several substituted salicylaldehydes (Scheme 4). The propynol obtained was then subjected to cyclisation (Table 1).

Only the combination of gold(I) chloride and potassium carbonate enabled the cyclisation to the arylidene alcohol **14**. Oxidation with MnO_2 afforded the corresponding aurones (**15**). Using this method, the synthesis of different natural aurones was achieved, including the 4'chloroaurone from *Spatoglossum variabile,*

which has been isolated previously by Atta ur Rahman and Choudhary [31].

Agrawal *et al.* described a similar cyclisation using pyridine-Hg $(OAc)_2$, as well as $CuBr_2$, in dimethylsulfoxide (Scheme 5). As part of this procedure, to a molar amount of Hg($OAc)_2$ in cold pyridine the 2'-hydroxychalcone **16** was added and the solution refluxed for 10-15 min. Then the reaction was cooled, treated with diluted HCl, and then diluted with ice-cold water. Recrystallization led to the pure *Z*-isomer of **17**. As part of a second method, the authors used a few milligram of $CuBr_2$ in DMSO and 2-hydroxychalcones. After refluxing this mixture for about 60 to 90 min, the reaction was cooled and quenched with water. Filtration and recrystallization in EtOH yielded the desired aurones (**17**) [32].

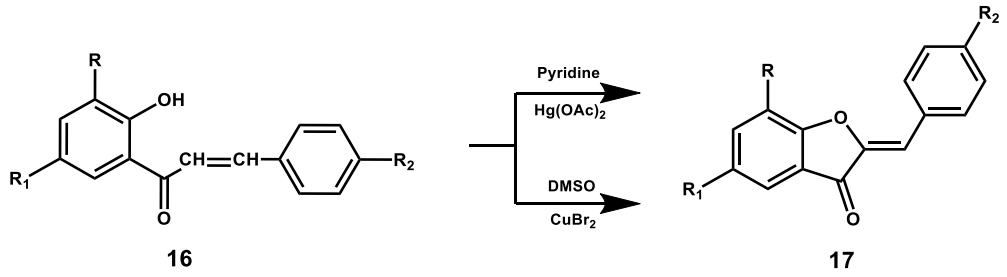

16 17

Scheme 5: Cyclisation by mercury(II) acetate in pyridine and cupric bromide in dimethylsulfoxide R= H-, Br-; R_1= H-, CH_3-; R_2= H-, OCH_3-, Cl- [32].

Thanigaimalai and Yang described a synthetic route to aurones via oxidation of 2-hydroxy-6-cyclohexylmethoxychalcones with thallium (III) nitrate (Scheme 6) [33]. In continuation of their previous work [34, 35] they treated different chalcones (**18**) with thallium (III) nitrate in methanol, first at room temperature for 24 h, and then heated to 65°C, followed by addition of hydrochloric acid in a one pot oxidative cyclisation to achieve the corresponding isoflavones (not shown) and/or aurones (**19**) depending on the electronic nature of substituents on ring B of the chalcones. The strong electron donating groups in the para-position of ring B led to isoflavones, the weak electron donating group to a mixture of both aurones and isoflavones, and the electron withdrawing groups ended with aurones (**19**). Again NMR studies of the aurone derivatives revealed that their oxidative cyclisation method gave only

Z- isomers, as reported in the literature [36, 37].

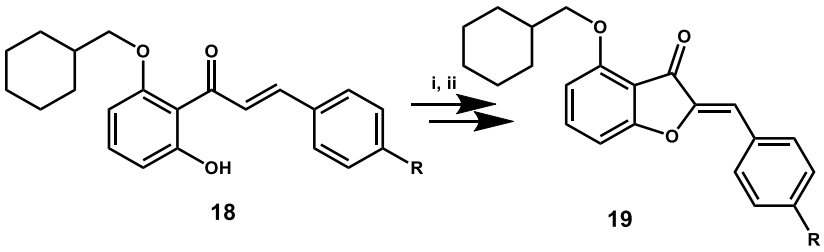

18 19

Scheme 6: (i) Thallium (III) nitrate (TTN), methanol, overnight at rt; (ii) hydrochloric acid, 50°C, 5 h. R= -H, -Cl, -CHO, -$COOCH_3$, -NO_2, -COOH [33].

2.3 Aurones and their role in colouring flowers

There are many beautiful flowers in nature in a variety of shapes and colours. Such diversity is acquired through evolutionary processes to ensure successful reproduction by attracting pollinators or by promotion of wind pollination [38]. The colour is especially important to attract pollinators, such as insects and birds. For plant breeders, the colour of flowers is one of their most important targets. Such breeders have come up with many different-coloured hybrids and cultivars using natural mutants or genetically related species. Recent advances in genetic modification techniques enable the production of desirable and novel flower colours [39]. Many researchers exploit the knowledge of flavonoid biosynthesis effectively to obtain unique flower colours. Transgenic blue-violet flowers, for instance, are already on the market today and transgenic blue roses have been reported [40].

For creating transgenic plants with yellow colours, aurones are often used as pigments of choice. Ono and Fukuchi-Mizutani revealed that regulation of aurone biosynthesis led to production of yellow flowers in a *Torenia* hybrid [15].

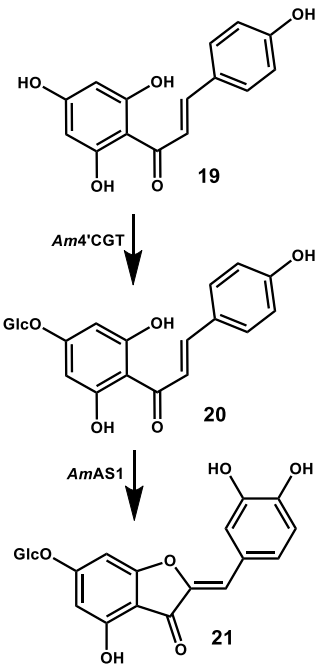

Scheme 7: Biosynthetic route towards aurones.

Interestingly, the biosynthetic avenue leading to aurones differs somewhat from

the chemical synthetic pathways discussed earlier. In transgenic flowers, the coexpression of *Antirrhinum majus* chalcone 4'-*O*-glucosyltransferase (*Am4'CGT)* in the cytoplasm and *A. majus* aureusidin synthase *(AmAS1)* in the vacuole combined with down-regulation of anthocyanin biosynthesis by RNA interference (RNAi) resulted in yellow flowers. These two enzymes will produce aureusidin 6-*O*-glucoside (**21**) via a 2',4',6',4-tetrahydroxychalcone 4'-*O*-glucoside **20**. The authors suggested that the chalcones (**19**) are 4'-*O*-glucosylated in the cytoplasm, their 4'-*O*-glucosides transported to the vacuole, and therein enzymatically converted to aurone 6-*O*-glucosides (Scheme 7).
Shrestha *et al.* found aureusidin also *in Rhus parviflora* (Anacardiaceae) [41]

Since chalcones are common throughout the plant kingdom, the strategy to generate yellow flowers by production of aureusidin 6-*O*-glucoside is widely applicable to most plant species producing chalcones. Furthermore, this genetic "trick" opens the door to molecular breeding strategies, which generate monotonous yellow flowers that dominantly produce aurone 6-*O*-glucoside [15].

2.4 Aurones as fluorescent probes with potential applications

Organic molecules that fluoresce in the visible region of the electromagnetic spectrum might be useful as probes in biological systems [42]. Such probes should cause minimal perturbation of the biological macro-molecule, they possess background fluorescence and are easy to use. There are three general types of fluorophores of interest here: xanthenes (fluorescein, rhodamine), boron dipyrromethenes and cyanines. Some of them already absorb and fluoresce in the visible region, but most of these molecules are relatively bulky with small Stokes' shifts [1, 2]. Shanker and Dilek recently published aurone derivatives as potential fluorescent probes for biomolecules that can be observed with visible light [42]. Even the largest molecule they prepared for this study is smaller than the xanthene dyes. The UV–Vis absorption characteristics of naturally occurring aurones have been well documented [14, 15]. An amine substituent at the 4-position of aurone **22** leads to the largest red shift in the absorption maximum compared with that of the parent molecule. Acetylation of the amine (aurone **23**) shifts the absorption and emission maxima to shorter wavelengths, while restricting the rotation of the amine nitrogen in **24** shifts the absorption and emission maxima to longer wavelengths.

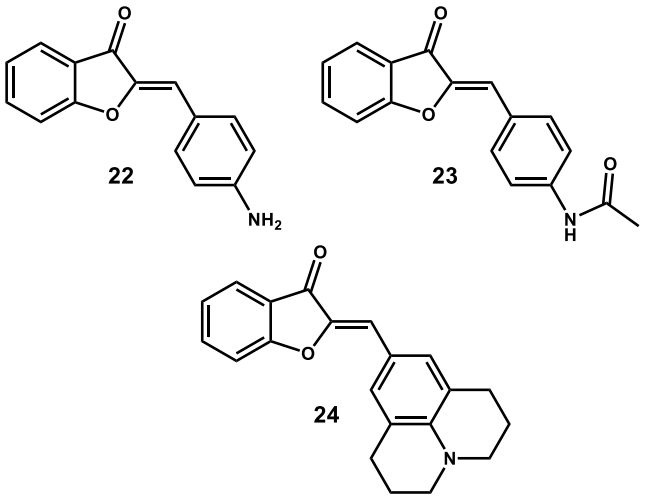

Figure 2: Aurones which may serve as potential fluorescent probes [42].

On one hand, xanthenes have high quantum yields in polar environments, while on the other hand the aminoaurones investigated need to have a hydrophobic environment to be useful fluorescent probes. The molecules investigated can also be observed using common microscopy excitation sources. The authors further speculated that *Z*- and *E*-isomers can be interconverted photochemically and, therefore, may have applications as photoactivated switches. As a proof of the concept, they showed that the absorption and emission maxima of aurones may be varied to suit a particular application through functional group selection [42].

2.5 Aurones as chemosensors

Chen *et al.* developed novel aurones as chemosensors for cyanide anions like **25**. These compounds exhibit remarkable response to cyanide anions with obvious changes , colour and fluorescence change owing to a hydrogen bonding reaction between cyanide anions and the O–H moiety of the sensors, which allows to use the naked eye to detect cyanide anions [43].

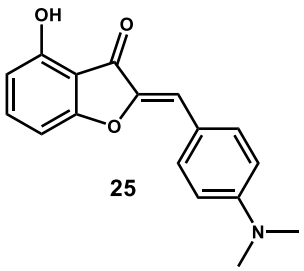

25

Figure3: Aurone as chemosensor for cyanide anions [43].

2.6 Biological roles, targets and activities

Aurones and others sub-classes of flavonoids, such as flavones and chalcones, have been studied for their numerous biological activities. Aurones, however, are only studied sparingly compared with the others sub-classes [44, 45]. Nevertheless, recent studies have revealed promising biological properties of this group of natural molecules. We described the most relevant biological properties of aurones discovered so far in our recently published review too [46].

i. Aurones as antiparasitic agents

Recently, Souard *et al.* synthesized and analysed 35 aurones for their potential as antimalarial drugs. All of these compounds were found to be non- cytotoxic in human cell lines and among them, seven had an IC_{50} below 5 µM in the antiplasmodial assay. The most active compound was tested *in vivo* on mice and was not toxic to the mouse itself, but the antiplasmodial effect appeared to be less efficient compared with the *in vitro* studies due to its low solubility. The structure–activity relationship analysis revealed that dimethoxylation at positions C4 and C6, a halogen atom at position 4', and the substitution of the intracyclic oxygen atom with an N-H group increased the activity of the compounds. However, a long chain had an adverse effect. Concerning the azaaurones, an ethyl moiety at C4' rather than C2', substitution of the ethyl group by an ethynyl group, methoxylation at the 4'-position, and a dimethylamino moiety improve the efficiency of the molecules (**26**) [47].

ii. Aurones as antimicrobial agents

Aurones also exert antibacterial and antifungal properties. A recent article published in 2010 reported that a series of synthetic aurone analogues are efficient antibacterial and antifungal molecules. All of these compounds exhibited moderate to good antibacterial activity against *E.coli*, *B. subtilis*, *S. aureus*, *K. pneumoniae* and

P. vulgaris. Concerning their antifungal activity, all of these compounds were able to inhibit different fungal strains, including *A. fumigatus*, *A. niger*, *T. virdie*, *C. albicans* and *P. chrysogenum* at a concentration of 25 μg/mL and with different efficiency (**27**) [48].

Tiwari *et al.* synthesised ferrocene-substituted aurones and tested them against antibiotic- sensitive and antibiotic-resistant strains of S. aureus and a resist- ant strain of S. epidermidis as well as human breast cancer cells. The most active compound **28** showed not only a bactericidal effect from time-kill assays but it is also active in human breast carcinoma, with IC_{50} value in the low micromolar range [49].

iii. Aurones as anti-viral agents

A series of different flavonoids has been analysed for neuraminidase inhibition potency, a glycoprotein involved in the infection process of the influenza virus. Among this list of 25 flavonoids, most of the aurones tested were described as good neuraminidase inhibitors. The structure–activity relationship revealed that a glycosyl group at any position, and a hetero-function at C3 or C4 decrease this effect, and an OH group at C6 or C4', a double bond between C-2 and the phenylidene, and a hetero-function at C3 are essential for the activity (**29**) [50].

Several aurone derivatives synthesized by Haudecoeur and Belkacem were analysed to target the hepatitis C virus RNA-dependent RNA polymerase. The authors identified the aurone target site by site–directed mutagenesis as the thumb pocket I of the polymerase. They identified seven aurone derivatives as potent inhibitor molecules with an IC_{50} below 5 μM. Interestingly, all of these compounds are non-cytotoxic towards cultured human Huh7 and HEK293 cells. This data permitted the authors to identify important substituents for biological activity: on the A ring, a hydroxy group at position C4 or a dihydroxy substitution at positions C4 and C6; on the B ring, hydroxy groups at positions C2', C4' – or C3', C4' or a hydrophobic and a bulky substituent or an alternative core (**30**) [51].

iv. Aurones as anti-inflammatory agents

The aurone derivatives synthesized by Bandgar and Patil, described as antibacterial and antifungal molecules, also show anti-inflammatory properties. They are able to inhibit the production of TNF-α (tumour necrosis factor-alpha) and IL-6 (interleukin-6), two cytokines that are often involved in diseases, such as autoimmune diseases, diabetes, arthrosclerosis and cancer [48].

The anti-inflammatory potential of aurone derivatives was confirmed by a second study. Several aurones were synthesized as derivatives of sulfuretin, a molecule already described as an anti-inflammatory agent able to reduce the production of nitric oxide and prostaglandin E_2, two pro-inflammatory molecules. Results show that these synthetic compounds are less cytotoxic and some of them are more efficient than sulfuretin. Analysis of the structure–activity relationships revealed that a hydroxyl-function at C6 is important to decrease the synthesis of prostaglandin E_2 and that methoxy groups on the B ring are useful to reduce the production of nitric oxide (**27, 31**) [52].

v. Aurones as anti-cancer agents

A series of aurones have been synthesized and analysed for their ability to target ABCG2 (ATP – binding cassette sub – family G member 2), an ABC protein transporter responsible for the breast cancer multidrug resistance mechanism. Results have shown that aurones are able to inhibit the ABCG2 efflux transporter in a dose-dependent manner and have a low cytotoxic effect against several cancer and healthy cell lines (**32**) [53]. Lewin *et al.* synthesised a series of novel aurones and evaluated them on KB human buccal carcinoma cells. The best aurone **33** has an IC_{50} =0,4 µM [54]

In another study, Cheng and Zhang synthesized a series of 4'–substituted 5–hydroxyaurone derivatives. These compounds have been tested for their cytotoxic effects on both cancer and non-cancer cell lines. Results show that some aurones are cytotoxic toward cancer cell lines, but exert weaker activities against non-cancer cell lines. These compounds have also been tested *in vitro* regarding their ability to

inhibit cell motility and angiogenesis, two processes implicated in cancer cell invasion and metastasis development. The authors identified two synthetic compounds that are able to beneficially modulate these two mechanisms involved in cancer development (**34**) [25].

vi. Aurones to treat skin diseases

Some aurones are able to inhibit human tyrosinase, an enzyme which plays a role in the melanin synthesis pathway. Melanin is the natural pigment of human skin and has been implicated in several dermatological diseases. Analysis of the structure–activity relationship indicates that hydroxyl groups on the B ring are necessary for the activity and hydroxyl groups at the 4,6 and 4' positions strongly increase efficiency (**35**) [18].

vii. Aurones in Alzheimer's disease

A novel series of aurone derivatives has been synthesized as radiolabelled probes to detect β-amyloid plaques in Alzheimer's disease. *In vitro* results show that these compounds have only one high affinity binding site for β-amyloid peptides. Biodistribution performed on mice revealed that these molecules have a good brain uptake and a fast clearance from the brain, which are two important properties for *in vivo* amyloid probes [55]. Shrestha *et al.* found aureusidin, above mentioned for colouring *Antirrhinum majus,* also *in Rhus parviflora* (Anacardiaceae). They tested this compound **36** against CDK5/p25, which could be useful in the treatment of Alzheimer's disease showing a significant in vitro inhibition capacity (IC_{50} value of 4.81 μM [41]

viii. Aurones as SIRT1 inhibitors

Manjulatha *et al.* introduced a new procedure to synthesize aurones. They performed their reaction of benzofuran- 3(2H)-one with a benzaldehydes in the presence of the mild base Ethylenediamine diacetate (EDDA) under ultrasonic

conditions. Some of the obtained compounds showed SIRT1 inhibiting as well as anti-proliferative properties against two cancer cell lines in vitro. Compound **37** was identified as the potent inhibitor of SIRT1 (IC_{50} = 1 μM) which showed a dose dependent increase in the acetylation of p53 resulting in induction of apoptosis. [56]

ix. Aurones as potential biological herbicides

Zhang *et al.* prepared aurones with herbicidal activity. (*Z*)- 2-Phenylmethylene-4,6-dimethoxy-3(2*H*)-benzofuranone(**38**) was their most active compound against the dicotyledonous plant *Brassica campestris*. [57] Their promising results might lead *to* herbicides against dicotyledonous weeds with further structure modification.

x. Aurones as radical scavenger

Shakya *et al.* introduced into crops the capability to synthesize the yellow antioxidant, aureusidin. For this purpose, the snapdragon (Antirrhinum majus) chalcone 4'-O-glucosyltransferase (Am4'CGT) and aureusidin synthase (AmAs1) genes were expressed in tobacco (Nicotiana tabacum) and lettuce (Lactuca sativa) which possess a functionally active chalcone ⁄ flavanone biosynthetic pathway. Afterwards these plants displayed higher superoxide dismutase (SOD) inhibiting and oxygen radical absorbance capacity (ORAC) activities than the control plants. Through the introduction of aurone biosynthetic pathways according to the authors, the nutritional qualities of leafy vegetables could be enhanced [58].

Another research group isolated and elucidated a new natural prenylated aurone from *Artocarpus altilis* The structure was elucidated as 6-hydroxy-2-[8-hydroxy-2-methyl-2-(4-methyl-3-pentenyl)-2*H*-1-benzopyran-5-ylmethylene]-3(2*H*)-benzofuranone **39** exhibiting moderate nitric oxide radical scavenging activity. [59]

Tronina et al. transferred xanthohumol with the help of the *Aspergillus ochraceus* bacterium to the novel aurone **40.** The antioxidant properties of starting xanthohumol and its metabolite were investigated using the 2,2'- diphenyl-1-

picrylhydrazyl (DPPH) radical scavenging method. The new biotransformation product, was 8.6-fold potent antioxidant than xanthohumol [60].

Table 2: Overview of some most bioactive aurones reported so far

Effect/Target	**Structure**
Antimalarial [47]	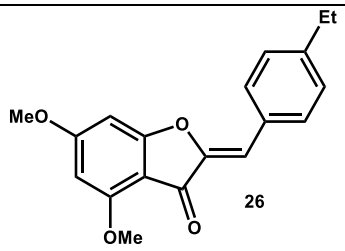 26
Antimicrobial (antifungal and bacterial) [48] [49]	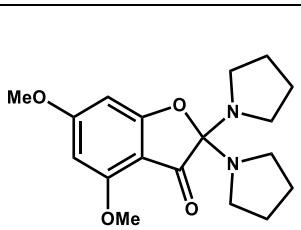 27 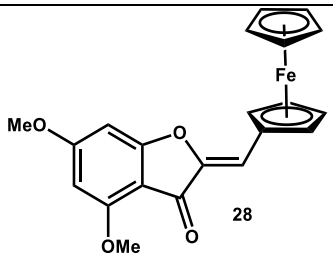 28
Anti-viral (Influenza virus) [50]	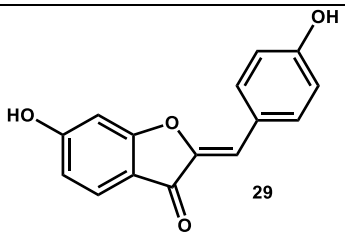 29
Anti-viral (Hepatitis C virus) [51]	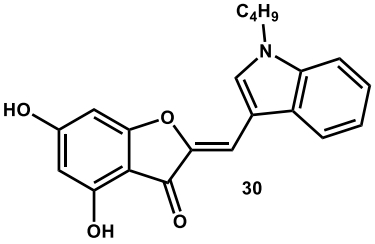 30
Anti-inflammatory [52] [48]	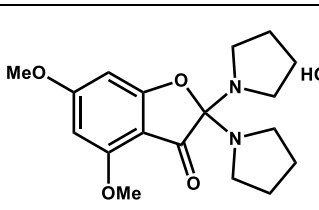 27 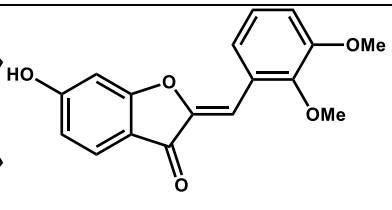 31

Anti-cancer (breast cancer) [53] (buccal cancer) [54]	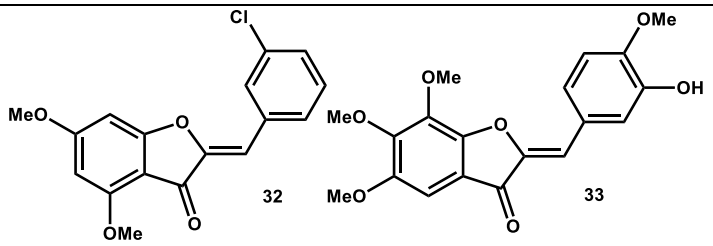 32 33
Anti-cancer (anti-motility and angiogenesis) [25]	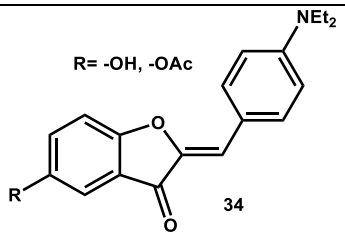 34
Skin disease [18]	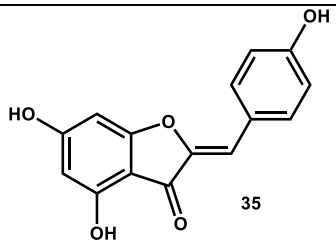 35
Alzheimer's disease [41]	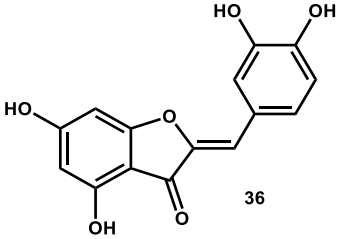 36
SIRT1 inhibitor [56]	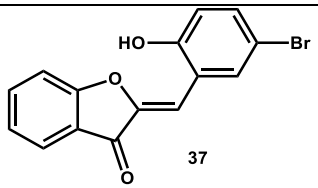 37
Herbicides [57]	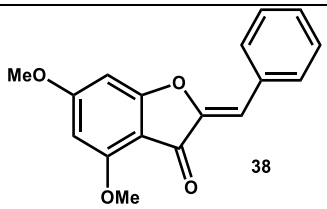 38
Radical scavengers [59, 60]	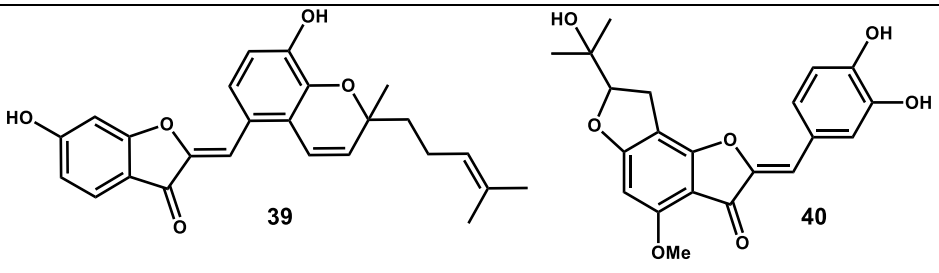 39 40

2.7 Summary of the literature survey

In conclusion, aurones seem to provide a promising scaffold for medicinal chemistry. Our research group has prepared already in the early 1970' several aurone derivatives: for example one of the first selenoaurones [61]. Using this experience combined with the possibility to access other heterocyclic analogues of benzofuranes, as well as an almost unlimited number of arylaldehydes available, there are ample opportunities to produce libraries of aurones or related aza-, thio-, and seleno-aurones for studies of their possible biological activities.

2.8 Novel benzopyran-2- and 4-one-containing aurones

synthesis and biological activity in K562 human leukemia cells

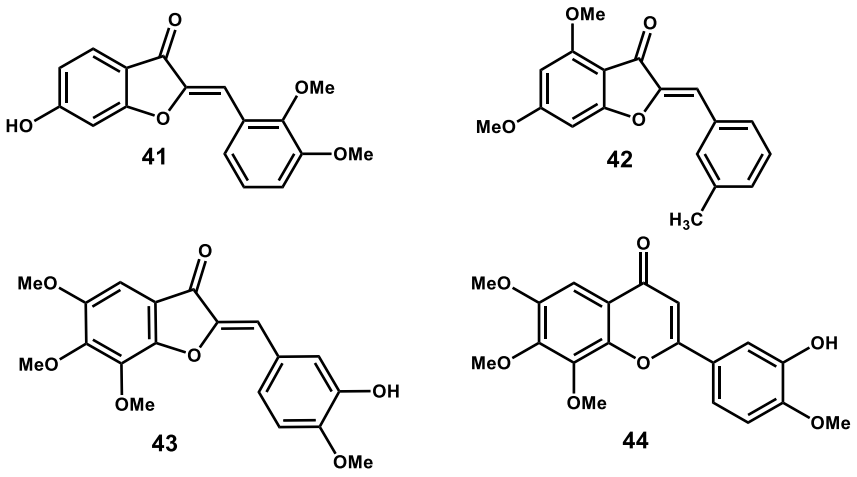

Figure 4: Aurones (**41**-**43**) and the isomeric flavone (**44**) with postulated anticancer properties [21, 25, 53]

In recent literature[53] [25] several aurones such as **41** and **42** have been described with anti-cancer properties. Lawrence *et al.*[21] studied the aurones isolated from *Uvaria hamiltonii* for the total synthesis as well as for their anticancer properties in K562 cells. Among them compound **43** was the most active with a growth inhibition IC_{50} value of 50 µM.

By reaction with potassium cyanide the aurone **43** converted into the flavone **44** providing a more active compound with an IC_{50} value of 40 µM.

Flavones as well as the aurones belong to the class of flavonoids and are known to possess anticancer activity, besides other biological activities such as being anti-oxidative or anti-inflammatory [62, 63]. They might also prevent cardiovascular diseases when they form part of a daily diet[64]. Besides other activities, various chromones exhibit anticancer properties[65]. Their constitutional isomers, the coumarins, show similar biological activities, which have been recently reviewed [66].

Therefore our idea was to combine the benzofurane structure from aurones with the different chromone motif or the isomeric coumarine motif, to obtain potential novel anticancer agents.

In this study we describe the preparation of 26 chromone- and coumarin-based benzofurane derivatives and their biological effects in K562 human leukemia cells when tested at 50 µM for 48 h. In particular, the effects of our new derivatives on the K562 cell cycle as well as induction of apoptosis (pre-G1 peak) have been determined.

2.8.1 Chemistry

We have chosen only the 7-Methoxy-coumarine-4-aldehyde 49 as the only coumarine as it was the most biological active structure in previous studies of our lab [67]. The standard method to prepare coumarin-4-aldehyde **49** is reported using 4-methylcoumarin **45** and SeO_2[68]. The disadvantage of this method is that you loose some product during the hot filtration as the desired compound **49** is not very soluble in xylene. Therefore we tried different solvents to improve the solublity leading to higher yields: in dioxane the solubility was slightly better but it employed more time than with xylene (18 hours compared to 12hours), we switched to chlorobenzene which proved to be the best solvent regarding our above mentioned goals (Table 3). To avoid the toxic seleniumdioxide as well as the hazardous solvents, we applied two more eco friendly methods: 4-chloromethylcoumarin **46** was boiled in water for 12 hrs to obtain 4-(hydroxymethyl)coumarin **47**, which was then oxidised with manganese dioxide in ethanol to the desired aldehyde **49.** The second method is based on a Kröhnke's oxidation[69] starting from 4-(chloromethyl)coumarine **46** achieving the corresponding aldehyde **49** much faster (1hour compared to 12-18 hours) with a very good yield (90%). The reaction is carried out with *p*-nitrosodimethylaniline as oxidising agent at room temperature in basic conditions followed by an acidic hydrolysis of the intermediate **48** to yield the desired aldehyde **49** (Scheme 8).

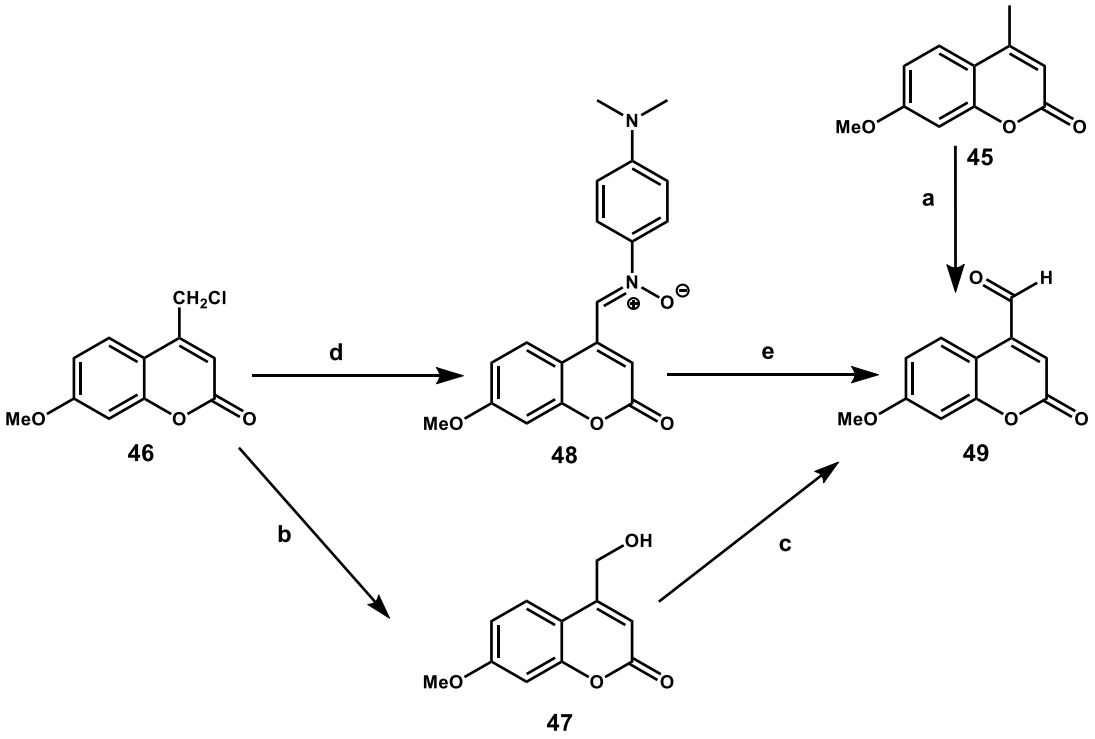

Scheme 8: Synthesis of coumarin-4-aldehyde **49 a)** SeO_2, different solvents, reflux for 12-18 hours (see table below) **b)** water, reflux, 12 hours **c)** MnO_2, THF, 70 ^{0}C, 18hours **d)** *p*-nitrosodimethylaniline, sodium ethanolate, ethanol, room temperature, 20 mins, 95% **e)** hydrolysis 5N H_2SO_4 room temperature, 30 mins, 95%

Solvent	**Temp.**	**Solubility**	**Result/Yield**
Xylene	reflux	low (cold) good (hot)	no byproducts 40-50% yield
Chlorobenzene	reflux	high	no byproducts 40-60% yield
Dioxane	reflux	high	Little by-products 40-45% yield

Table 3 Influence of solvent for Riley Oxidation

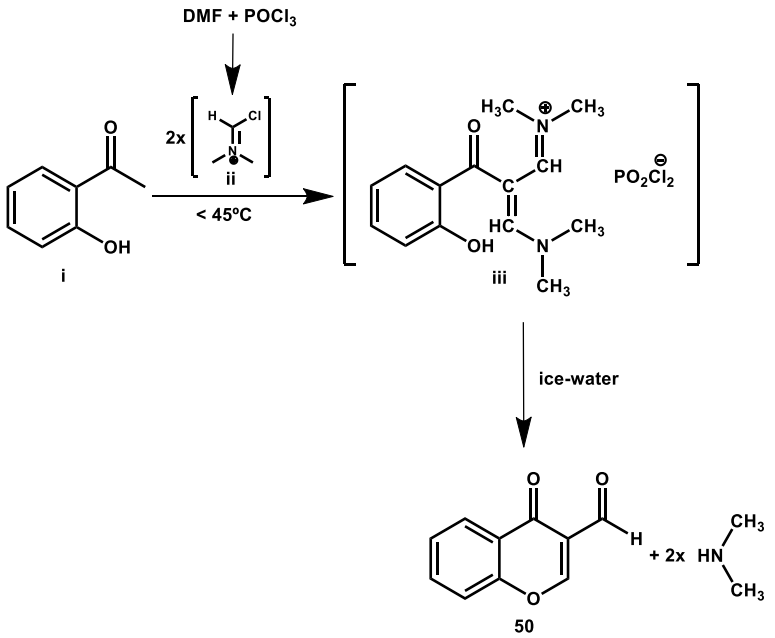

Scheme 9: Synthesis of chromone aldehydes via Vilsmeier-Haack reaction: example **50**

i benzophenone derivative, **ii** Vilsmeier reagent, **iii** iminium intermediate

To test the different subsitutional effects of various functional groups, the compounds **50-58** were prepared through the Vilsmeier–Haack reaction [21, 25, 53, 70-80]. This method can be used to formylate activated aromatic systems in the sense of a Friedl-Crafts-acylation, as free formylchloride is not stable[81].

The reaction of dimethylformamide with phosphorus oxychloride produces an electrophilic chloroiminium cation **ii**, also called the Vilsmeier reagent. The subsequent (in our case double) electrophilic substitution on the keton **i** produces a substituted iminium ion **iii**, which is hydrolyzed to give the desired aryl aldehyde, here as example **50**. The above shown iminium ion **iii** has been proposed by Harnisch [70] (Scheme 9). However we could not isolate this intermediate to proof this suggested mechanism.

Despite the commercial availablity of compound **59a**, it can been prepared like **59b** and **60** following a procedure of Cagniant and Kirsch [61, 82].

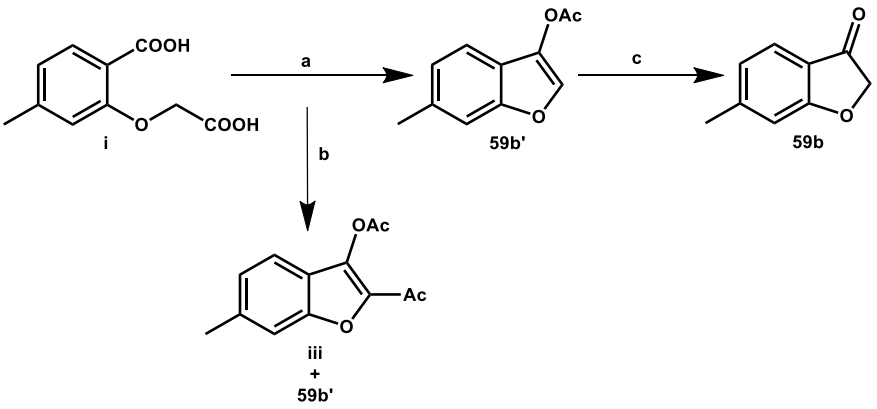

Scheme 10: Synthesis of benzofuranone derivatives: example **59b a)** AcONa, AcOH, AcO_2 (1:3:5 ratio), reflux for 3-4 hours **b)** prolonged heating 12-15 hours **c)** HCl, EtOH, reflux, 1,5 hours [82]

2-(Carboxymethoxy)-4-methylbenzoic acid **i** is refuluxed in a mixture of sodium acetate, acetic acid and acetic anhydride for 3-4 hours leading to the cyclised compound **59b'** in good yields (about 75%). However prolonged heating (12-15 hours) is giving a mixture of the monoacetylated compound **59b'** and bis-acetylated compound **iii**. Compound ii is easily hydrolyzed to in this case compound **59b** (Scheme 10).

A common way to prepare aurones is based on the method of an aldol–like condensation of benzofuran-3(*2H*)-ones with benzaldehydes. These aldol reactions are usually carried out with catalytic amounts of acid (hydrochloric acid) or base (pyrrolidine) in ethanol or THF under reflux[20]. The aurone **71** has been prepared by this known literature method [83].

Firstly we used these conditions to synthesize the desired compounds (**61**-**70**)in very low yields (about 5-10%) containing numerous impurities. Then we decided to perform the aldolic condensation through the use of acidic Al_2O_3 (Brockmann I) [26]. The desired compounds were obtained at room temperature within 2 to 6 days in acceptable yields (Table 4). No purification was necessary or in some cases recrystallization from ethanol was suffcient to obtain the pure compounds **61-70** (Scheme 11).

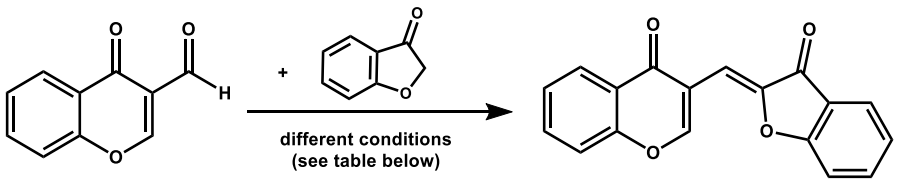

Catalyst	Solvent	Temperature	Result/Yield
Pyridine Piperidine	THF	reflux	numerous by-products low yield (approx. 10%)
HCl	Ethanol Methanol THF	reflux	numerous by-products low yield (approx. 10%)
Al_2O_3	CH_2Cl_2	RT	very little by-products 40-50% yield

Table 4: Different approaches to achieve aurone hybrids

Although an unambiguous assignment of the isomeric structures of our series of compounds was not carried out, the values are consistent with those present in the literature for known (*Z*)-aurones[31]' [84].

The synthetic yields, melting points, elemental analyses, ^{1}H and ^{13}C NMR spectra of all compounds are described in the experimental section.

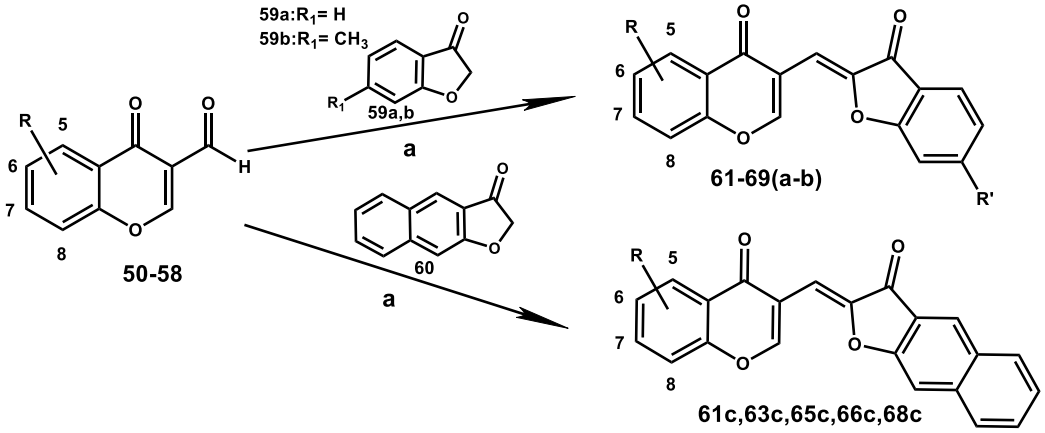

61a: R=H; R'=H
61b: R=H; R'=Me
61c: R=H
62a: R=6-Me; R'=H
62b: R=6-Me; R'=Me

63a: R=6-Me, 7-Me; R'=H
63b: R=6-Me, 7-Me; R'=Me
63c: R=6-Me, 7-Me
64a: R=7-Cl; R'=H
64b: R=7-Cl; R'=Me

65a: R=6-Cl; R'=H
65b: R=6-Cl; R'=Me
65c: R=6-Cl
66a: R=6-F; R'=H
66b: R=6-F; R'=Me

66c: R=7-F
67a: R=7-OMe; R'=H
67b: R=7-OMe; R'=Me
68a: R=5-OMe; R'=H
68b: R=5-OMe; R'=Me

68c: R=5-OMe
69a: R=7-OMe, 8-OMe; R'=H
69b: R=7-OMe, 8-OMe; R'=Me

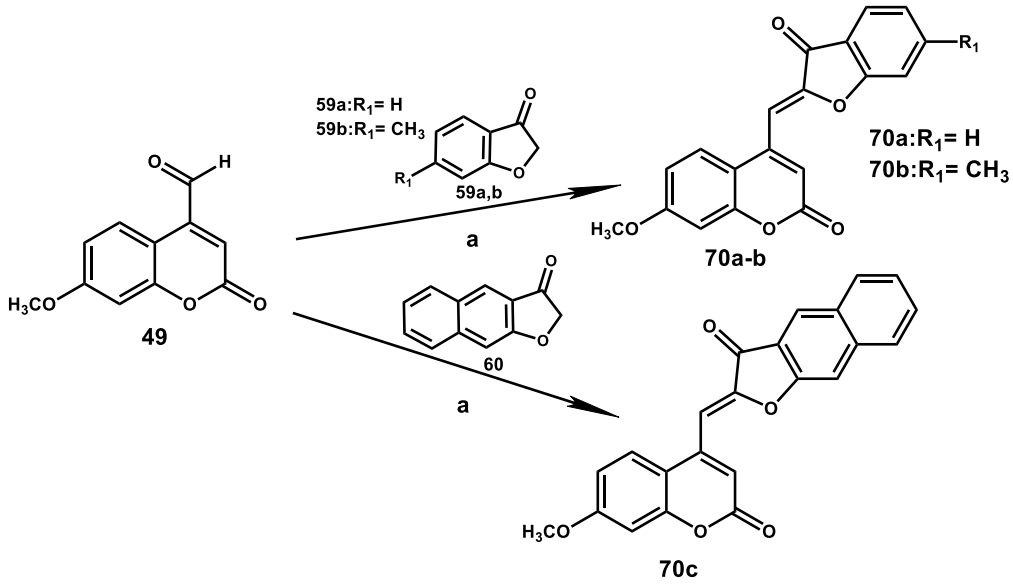

Scheme 11: Synthetic route **a** acid Al_2O_3, anhydrous DCM, room temperature, 2-6 d

2.8.2 Biology

Effect of compounds 61-70 on cell cycle distribution and apoptosis induction in human K562 cells.

The described compounds **61**-**70** were tested at 50 µM for 48 h in K562 human leukemia cells to determine their effects on the cell cycle and apoptosis induction (**Fig. 5 A** and **B**). The HDAC inhibitor SAHA (Vorinostat®) was included as a positive control.

Analysing the results, we could observe that compound **62b** and, to a lesser extent, **63c**, **68c** and **70b** displayed slight cell cycle arrest in the G1 phase, whereas with some other derivatives (**61b**, **62a**, **64b**, **65b**, **66a and 66b**) a block in the S phase occurred. Only one among the new described compounds, **70c,** was able to arrest the cell cycle in G2 phase.

Taking into account the pre-G1 peak in **Fig. 5B** as an index of pro-apoptotic properties of the compounds, it results that **61a**, **61c**, **63c**, **65c**, **67a** and **68c** exhibit 17 to 22% of apoptosis induction in this assay, while **62b**, **70b** and **70c** showed the strongest effect with around 24%.

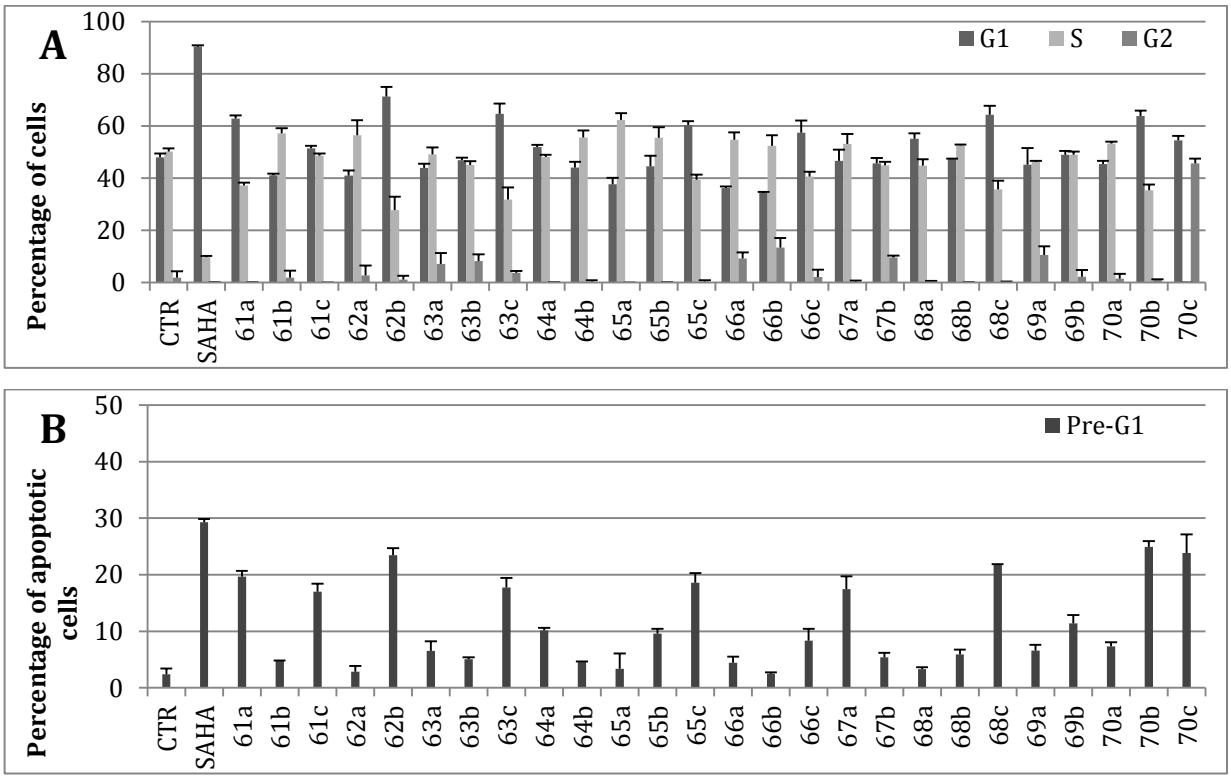

C

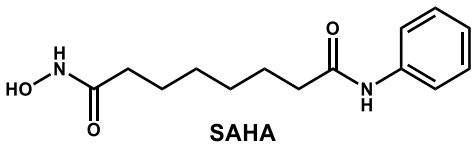

Figure 5: (A) Cell-cycle analysis and **(B)** apoptosis induction in K562 cells treated with **61**-**70** at 50 µM for 48 h; **(C)** structure of SAHA (Vorinostat ®)

Structure-activity relationship analysis highlighted that the different substitutions (halogen, methyl and methoxy) on the chromanone (**61**-**69**) do not influence the potency of the compounds. Instead, exchanging the furanone or methylfuranone moiety with a napthofuranone seems to exert a more powerful effects toward apoptosis with the exception of **61a**, **62b** and **70b**.

The replacement of the chromone moiety (**61-69**) with the isomeric coumarin (**70**) led to the only one compound able to block the cell cylce in G2 (**70c**).

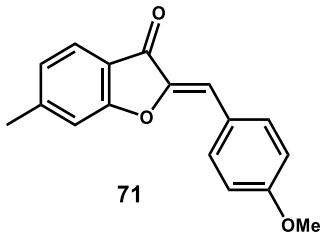

Figure 6: Aurone used as reference compound

To better ascertain the pro-apoptotic property of these oxobenzofuran-chromone and –coumarin derivatives, we selected **70b** as a lead compound, and we tested it in K562 cells at doses ranging from 5 to 100 µM, in comparison with **49**, the comarin-4-aldheyde used for the synthesis of **70b**, and with the (*Z*)-2-(4-methoxybenzylidene)-6-methylbenzofuran-3(2*H*)-one (**71**), a compound showing a simple, classic aurone structure (**Fig. 6**). After 48 h as well as 72 h of treatment, **70b** showed at higher doses (50 and 100 µM) the strongest apoptosis induction, being more efficient than **49** and **71** (Figure 7). This data suggest that the combination of an aurone-like template with a chromone or coumarin scaffold can lead to new compounds endowed with interesting apoptotic effect in K562 leukemia cells.

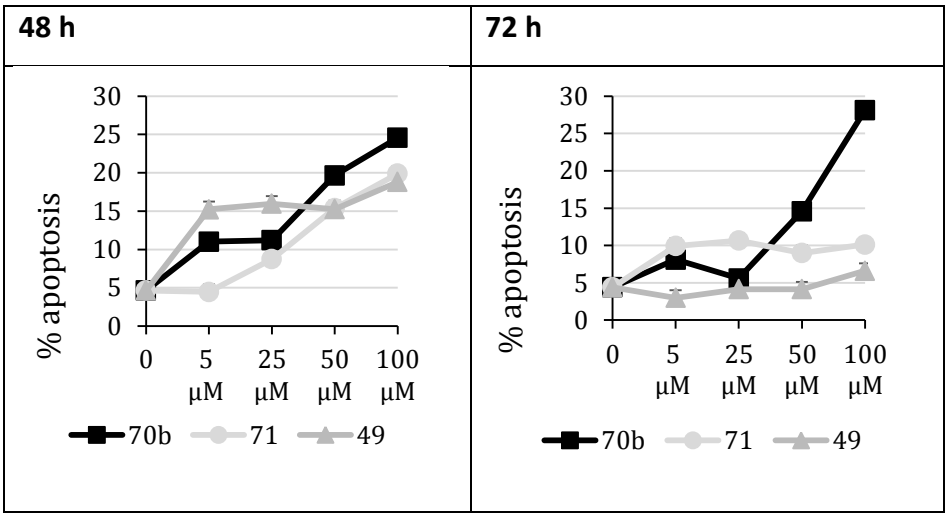

Figure 7: Dose-dependent apoptosis induction in K562 cells treated with **70b**, **49** and **71** for 48 (**A**) and 72 (**B**) h.

2.9 Conclusion and Outlook

In summary, new benzofuran-chromone and –coumarine derivatives have been synthesized and evaluated against K562 human leukeima cells. Both these chemical structures displayed anticancer acitivity because they are able to block the K562 cell cycle in G1 (**62b** 72%), S (**65a** 63%) or G2 (**70c** 46%) phase, and to induce high (around 24%) apoptosis (**62b**, **70b** and **70c)**. These new compounds seem to provide a promising scaffold for medicinal chemistry bearing in mind the possibility to access heterocyclic analogues of benzofuranes. Complementary investigations must be launched into the discovery of other biological properties as well as their molecular mechanism of action. This work has been accepted by ChemMedComm (late September 2013).

2.10 Experimental part

2.10.1 Chemistry

2.10.1.1 General introduction

Melting points

Melting points (mp), expressed in degrees Celsius (° C), were determined with a Stuart SMP3 or Buchi 530 apparatus and are uncorrected.

Nuclear magnetic resonance spectra (NMR)

The proton (^{1}H NMR) and carbon (^{13}C NMR) NMR spectra were recorded on a Bruker AC 250 or Bruker AC400 spectrometer.

The solvents used ($CDCl_3$ or DMSO-d_6) are shown in parentheses.

The chemical shifts are expressed in parts per million (ppm) relative to an internal standard (Me_4Si). The following abbreviations are used: s: singlet, d: doublet, t: triplet, m: multiplet.

Mass spectra

Mass spectra were recorded with a MicroTof-Q 98 or a Fisons Trio 1000 spectrometer.

Elemental analysis

The determination of the mass fractions of carbon, hydrogen, nitrogen and oxygen has been conducted on a CHN microanalysis device Thermo Scientific Flash 2000. Elemental analysis has been used to determine the purity of the described compounds, that is >95%.

Chromatography

All reactions were routinely monitored by TLC (Merck DC, Alufolien Kieselgel 60 F254) with spots visualized by UV light. Column chromatography was performed on

silica gel LC 60A (70-200 micron, Sigma Aldrich). All solvents were reagent grade and, when necessary, were purified and dried by standard methods. Concentration of solutions after reactions and extractions involved the use of a rotary evaporator operating at a reduced pressure of approx. 20 Torr. Organic solutions were dried over anhydrous magnesium sulphate.

Sources for the consumables

The solvents used were purchased from Carlo Erba (France) or Sigma Aldrich (Italy) and the reactives from Sigma Aldrich (France and Italy), Acros Organics (France) ou Alfa Aesar (Germany).

2.10.1.2 Synthesis of the aurone derivatives

Preparation of the starting materials and compound 30

Synthesis of 7-Methoxy-4methylcoumarin (45) and 7-Methoxy-4(chloromethyl)coumarin (46)

A mixture of 3-methoxyphenol (0,030 M) and ethyl 4-chloroacetoacetate or ethylacetoacetate (0,033 M) was added drop wise to concentrated sulphuric acid while the temperature was kept below 10 ^{o}C. The reaction was then allowed to reach RT and stirred for 24 hrs. Quenching the mixture with ice-cold water (200 mL) gave the crude product, which was first filtered and then recrystallized from ethanol.

45) 7-Methoxy-4methylcoumarin [68]

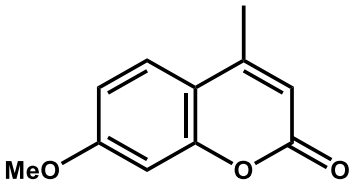

Melting point: 160-162 °C

Appearance: colourless solid

Yield: 63%

^{1}H NMR (250 MHz, $CDCl_3$) d 2.37 (s, 3H, $–CH_3$), 3.83 (s, 3H, $–OCH_3$), 6.18 (s, 1H, -CHCOO-), 6.92–6.95 (m, 2H, aromatic protons) 7.64-7.68 (d, 1H, J=10.0 Hz, aromatic proton) ppm

^{13}C NMR (62.5 MHz, $CDCl_3$) δ 18.67, 55.73, 100.83, 111.95, 112.26, 113.57, 125.51, 152.55, 155.29, 161.28, 162.64 ppm

46) 7-Methoxy-4(chloromethyl)coumarin [79]

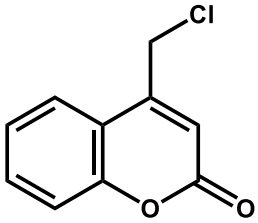

Melting point: 195-197 °C

Appearance: colourless solid

Yield: 51%

^{1}H NMR (250 MHz, $CDCl_3$) δ 3.86 (s, 3H, –OCH_3), 4.98 (s, 2H, –CH_2Cl), 6.49 (s, 1H, -C*H*COO-), 6.98–7.04 (m, 2H, aromatic protons) 7.74-7.77 (d, 1H, *J*=7.5 Hz, aromatic proton) ppm

^{13}C NMR (62.5 MHz, $CDCl_3$) δ 41.33, 55.82, 101.24, 110.79, 112.64, 125.14, 131.03, 149.59, 155.78, 160.74, 163.00 ppm

Synthesis of 7-Methoxy-4 (hydroxymethyl)coumarin (47)

7-Methoxy-4(chloromethyl)coumarin **46** (0,02 M) was suspended in deionized water and refluxed for 12 hrs obtaining a clear solution. Back to room temperature, 2 N HCl was slowly added until pH 5.0. The colourless solid was filtered and washed with water to obtain pure **47**.

47) 7-Methoxy-4(hydroxymethyl)coumarin [83]

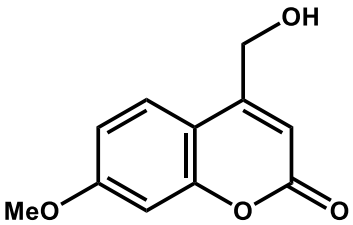

Melting point: 187-188 °C

Appearance: colourless solid

Yield: 85%

^{1}H NMR (250 MHz, $CDCl_3$) d 3.82 (s, 3H, –OCH_3), 4.69 (s, 2H, –CH_2-), 6.19 (s, 1H, -C*H*COO-), 6.94–6.99 (m, 2H, aromatic protons) 7.63-7.67 (d, 1H, J=10.0 Hz, aromatic proton) ppm

^{13}C NMR (62.5 MHz, $CDCl_3$) δ 55.81, 65.94, 100.08, 111.02, 111.73, 113.35, 125.87, 147.30, 154.39, 160.24, 160.86 ppm

Synthesis of 7-Methoxy-coumarin-4-aldehyde (49)

*a) Riley oxidation of 7-Methoxy-4-methylcoumarine **45*** [85]

Seleniumoxide (0,015M) was heated to 100 °C in xylene, dioxane and chlorobenzol for 30 mins and then 7-Methoxy-4-methylcoumarine **6a** (0,01M) was added and the heating was continued for -12-18 hrs. The reaction was filtered hot through paper in the case of xyelene and dioxane and cold thorugh celite in the case of chlorobenzene in order to remove the seleniumoxide. Evaporation oft he solvent gave the desired 7-Methoxy-coumarine-4-aldhyde **49** pure enough for further use.

*b) oxidation of 7-Methoxy-4-(hydroxymethyl)coumarine **47** with manganese dioxide*

Magnese dioxide (0,05M) and Methoxy-4-(hydroxymethyl)coumarine **47** (0,01M) were heated to 70 °C in THF for 18hrs. The reaction was filtered through celite in order to remove the manganese dioxide. Evaporation oft he solvent gave the desired 7-Methoxy-coumarine-4-aldhyde **49** pure enough for further use.

*c) Synthesis of **48** (*E)-*N-[4-(dimethylamino)phenyl)-1-(7-methoxy-2-oxo-2*H-*chromen-4-yl]methanimine oxide*

A mixture of 7-methoxy-4(chloromethyl)coumarin **46** (1 mmol) and *p*-nitrosodimethylaniline (3 mmol) in ethanol was added dropwise to sodium ethanolate (1 mmol) in ethanol at room temperature. An orange nitrone salt was almost immediately

35 precipitating. After 20 minutes the solid was filtered and washed with an excess of ethanol. The product was used without further purification for the next step.

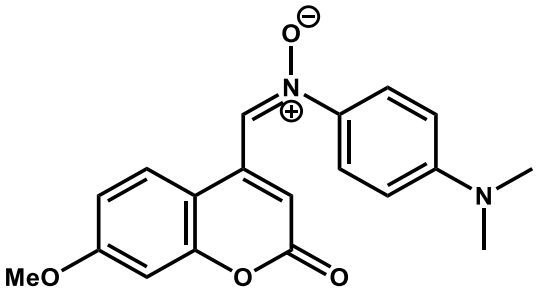

Melting point: 207-209 °C

Appearance: solide orange-rouge

Yield: 95%

^{1}H NMR (250 MHz, $CDCl_3$) δ 3.06 (s, 6H, 2x –C*H*$_3$), 3.88 (s, 3H, –OC*H*$_3$), 6.67-6.70 (d, 2H, *J*=7.5 Hz, aromatic protons), 6.85–6.89 (m, 2H, =C*H*COO– and C=C-C*H*=N), 7.53–7.56 (d, 1H, *J*=7.5 Hz, aromatic proton), 7.66–7.69 (d, 2H, *J*=15.0 Hz, aromatic protons), 8.26 (s, 1H, aromatic proton), 8.46 (s, 1H, aromatic proton) ppm

^{13}C NMR (62.5 MHz, $CDCl_3$) δ 40.28, 55.76, 101.62, 109.73, 110.40, 111.16, 111.35, 122.64, 123.34, 123.46, 138.62, 139.09, 151.96, 155.51, 162.22, 162.29 ppm

HRMS (ESI) [M+Na]+ $C_{19}H_{19}N_2O_4$ found: 339.1339, : 339.1338.

Elemental analysis: calculated: C: 67.44%; H: 5.36%; N: 8.28%; O: 18.91% : C: 67.22%; H: 5.49%

Compound **48** is added slowly into vigorously stirring diluted sulphuric acid (5M). After 30 minutes of stirring the reaction is quenched with water and extracted with DCM. The organic phased is washed with diluted Hall (2M), dried with magnesium sulphate and the evaporated giving pure 7-methoxycoumarine-4-aldehyde **49**.

59) 7-Methoxy-coumarine-4-aldehyde [68]

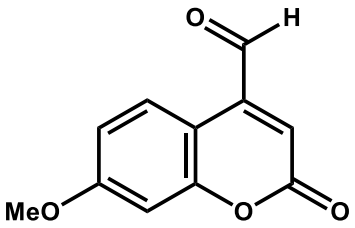

Melting point: 194-196 °C

Appearance: yellow solid

Yield: 95%

^{1}H NMR (250 MHz, $CDCl_3$) δ 3.89 (s, 3H, $–OCH_3$), 6.72 (s, 1H, -CHCOO-), 6.88–6.95 (m, 2H, aromatic protons) 7.48-7.52 (d, 1H, *J*=10.0 Hz, aromatic proton), 10.08 (s, 1H -CHO) ppm

^{13}C NMR (62.5 MHz, $CDCl_3$) δ 55.81, 110.10, 108.17, 113.27, 122.17, 127.37, 143.75, 156.51, 160.75, 163.35, 191.75 ppm

General procedure for the synthesis of 3-formylchromones:

To a stirred solution of corresponding *o*-hydroxy- acetophenone (30mmol) in dimethylformamide (40mL), phosphorous oxychloride (60mmol) was added drop-wise at 0°C over 20-30 mins. The mixture was stirred on ice for further 30 mins and then continued at RT for 3-5 hrs. The mixture was treated with ice-cold water (100 mL). The resulting solid was filtered, washed with plenty of water and purified if necessary by recrystallization from ethanol.

50) 3-Formylchromone [71]

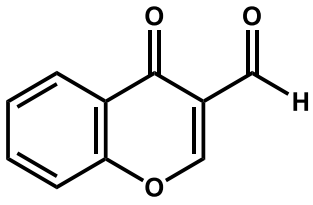

Melting point: 152-154 °C

Appearance: yellow solid

Yield: 63%

^{1}H NMR (250 MHz, $CDCl_3$) δ 7.48–7.56 (m, 2H, aromatic protons), 7.73–7.79 (m, 1H, aromatic proton), 8.28-8.32 (d, 1H, *J*=10.0 Hz, aromatic proton), 8.55 (s, 1H, -O-C*H*=C-), 10.40 (s, 1H –C*H*O) ppm

^{13}C NMR (62.5MHz, $CDCl_3$) δ 118.64, 120.32, 125.31, 126.13, 126.65, 134.86, 156.22, 160.74, 175.85, 188.53 ppm

51) 6-Methyl-3-formylchromone [72]

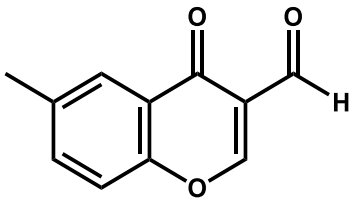

Melting point: 169-170 °C

Appearance: yellow solid

Yield: 20%

^{1}H NMR (250 MHz, $CDCl_3$) δ 2.44 (s, 1H; -CH_3), 744–7.48 (m, 2H, aromatic protons), 7.55(s, 1H, aromatic proton), 8.06 (s, 1H, aromatic proton), 8.52 (s, 1H, -O-C*H*=C-), 10.37 (s, 1H –C*H*O) ppm

^{13}C NMR (62.5 MHz, $CDCl_3$) δ 21.02, 118.69, 120.17, 124.81, 125.75, 136.14, 137.12, 154.74, 160.29, 173.97, 188.95 ppm

52) **6,7-Dimethyl-3-formylchromone** [73]

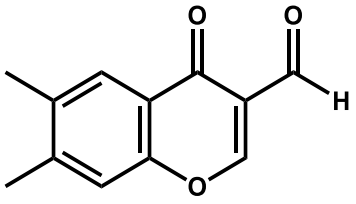

Melting point: 157-159 °C

Appearance: yellow solid

Yield: 14%

^{1}H NMR (250 MHz, $CDCl_3$) δ 2.39 (s, 1H; -CH_3), 2.42 (s, 1H; -CH_3), 7.44–7.60 (m, 2H, aromatic protons), 7.31 (s, 1H, aromatic proton), 8.03 (s, 1H, aromatic proton), 8.51 (s, 1H, -O-C*H*=C-), 10.39 (s, 1H –C*H*O) ppm

^{13}C NMR (62.5 MHz, $CDCl_3$) δ 19.41, 20.51, 118.69, 120.17, 123.03, 125.75, 136.14, 145.51, 154.74, 160.29, 175.97, 188.95 ppm

53) **7-Chloro-3-formylchromone** [74]

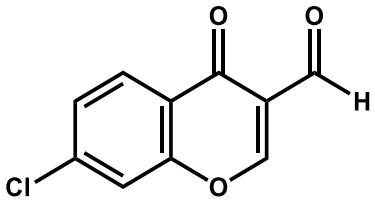

Melting point: 184-186 °C

Appearance: yellow solid

Yield: 41%

^{1}H NMR (250 MHz, $CDCl_3$) δ 7.46–7.50 (d, 2H, *J*=10.0Hz, aromatic protons), 7.57 (s, 1H, aromatic proton), 8.23-8.26 (d, 1H, *J*=7.5 Hz, aromatic proton), 8.52 (s, 1H, -O-C*H*=C-), 10.38 (s, 1H, –C*H*O) ppm

^{13}C NMR (62.5 MHz, $CDCl_3$) δ 118.75, 120.50, 123.02, 123.81, 127.49, 141.06, 156.24, 160.55, 175.14, 188.16 ppm

54) **6-Chloro-3-formylchromone** [75]

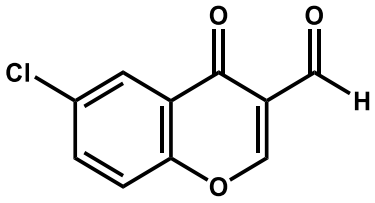

Melting point: 170-172 °C

Appearance: yellow solid

Yield: 66%

^{1}H NMR (250 MHz, $CDCl_3$) δ 7.50–7.53 (d, 1H, *J*=7.5Hz, aromatic proton), 7.68–7.72 (dd, 1H, *J*=10.0Hz, aromatic proton), 8.25-8.26 (d, 1H, *J*=2.5 Hz, aromatic proton), 8.55 (s, 1H, -O-C*H*=C-), 10.36 (s, 1H, –C*H*O) ppm

RMN ^{13}C (62.5 MHz, $CDCl_3$) δ 120.24, 120.31, 125.63, 126.30, 132.84, 135.02, 154.50, 160.68, 174.87, 188.15 ppm

55) **6-Fluoro-3-formylchromone** [76]

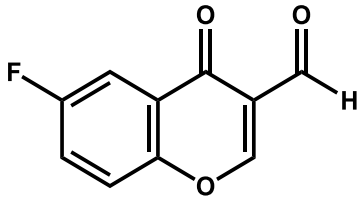

Melting point: 157-159

Appearance: yellow solid

Yield: 40%

^{1}H NMR (250 MHz, $CDCl_3$) δ 7.44–7.60 (m, 2H, aromatic protons), 7.68–7.72 (dd, 1H, *J*=10.0Hz, aromatic proton), 8.92-8.96 (dd, 1H, *J*=10.0 Hz, aromatic proton), 8.56 (s, 1H, -O-C*H*=C-), 10.38 (s, 1H, –C*H*O) ppm

^{13}C NMR (62.5 MHz, $CDCl_3$) δ 110.05, 120.34, 121.30, 122.05, 125.33, 126.60, 153.88, 160.32, 175.01, 188.20 ppm

56) **7-Methoxy-3-formylchromone** [72, 74]

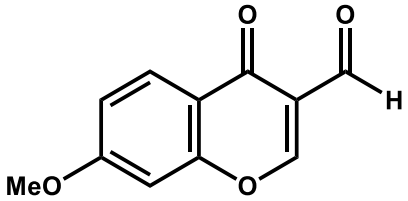

Melting point: 188-190 °C

Appearance: yellow solid

Yield: 12%

^{1}H NMR (250 MHz, $CDCl_3$) δ 3.92 (s, 3H, –OCH_3), 6.92–6.93 (d, 1H, *J*=2.5Hz, aromatic proton), 7.03–7.08 (dd, 1H, *J*=12.5Hz, aromatic proton), 8.19-8.22 (d, 1H, *J*=7.5Hz, aromatic proton), 8.50 (s, 1H, -O-C*H*=C-), 10.40 (s, 1H –C*H*O) ppm

^{13}C NMR (62.5 MHz, $CDCl_3$) δ 55.93, 101.35, 115.54, 118.82, 120.16, 127.34, 158.04, 160.24, 164.82, 175.27, 189.02 ppm

57) **5-Methoxy-3-formylchromone** [78]

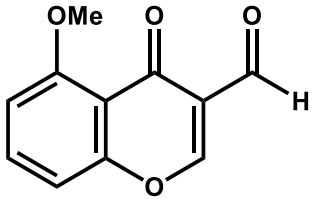

Melting point: 127-129 °C

Appearance: yellow solid

Yield: 36%

^{1}H NMR (250 MHz, $CDCl_3$) δ 4.02 (s, 3H, –OC*H*$_3$), 6.89–6.92 (d, 1H, *J*=7.5Hz, aromatic proton), 7.06–7.09 (d, 1H, *J*=7.5Hz, aromatic proton), 7.61-7.64 (m, 1H, aromatic proton), 8.39 (s, 1H, -O-C*H*=C-), 10.34 (s, 1H, –C*H*O) ppm

^{13}C NMR (62.5 MHz, $CDCl_3$) δ 56.57, 107.93, 110.40, 115.53, 121.21, 134.93, 158.07, 158.74, 160.35, 175.83, 189.16 ppm

58) 7,8-Dimethoxy-3-formylchormone [72]

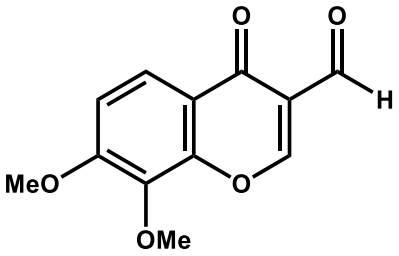

Melting point: 230-232 °C

Appearance: yellow solid

Yield: 32%

^{1}H NMR (250 MHz, $CDCl_3$) δ 3.99 (s, 3H, –OC*H*$_3$), 4.02 (s, 3H, –OCH_3), 7.09–7.12 (d, 1H, *J*=7.5Hz, aromatic proton), 8.00-8.04 (d, 1H, *J*=10.0Hz, aromatic proton), 8.52 (s, 1H, -O-C*H*=C-), 10.37 (s, 1H, –C*H*O) ppm

^{13}C NMR (62.5 MHz, $CDCl_3$) δ 56.45, 61.64, 110.94, 119.37, 119.67, 121.38, 137.19, 150.43, 157.55, 160.38, 175.45, 188.68 ppm

General procedure for the synthesis of the benzofuranones 59a, 59b and 60:

A stirred solution of corresponding 2-(carboxymethoxy)-4-methylbenzoic acid (30mmol) is refluxed in a mixture of sodium acetate, acetic acid and acetic anhydride (1:3:5 ratio) for 3-4 hours. The cooled mixture was diluted with water and extracted with petroleum. The extract was washed in turn with water, saturated sodium hydrogen carbonate solution and finally saturated brine. The residue left upon removal of the solvent was distilled under reduce pressure giving the cyclized compound **59a', 59b'** and **60'**in good yields.

59a') Benzofuran-3-yl acetate [82, 86]

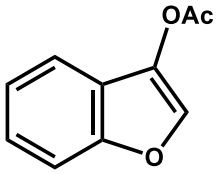

Appearance: yellow oil

Yield: 70%

^{1}H NMR (250 MHz, $CDCl_3$) δ 2.29 (s, 3H, OCOC*H*$_3$), 7.05-7.60 (4 H, m, aromatic protons), and 8.10 (1 H, s, C*H*)

^{13}C NMR (62.5 MHz, $CDCl_3$) δ 20.30, 111.56, 118.87, 121.11, 123.35, 124.73, 131.64, 143.62, 156.58, 169.02

59b') 6-Methylbenzofuran-3-yl acetate [82, 87]

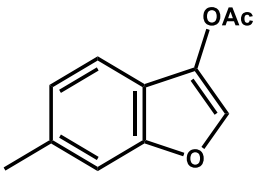

Melting point: 37-39 °C

Appearance: yellow solid

Yield: 85%

^{1}H NMR (250 MHz, $CDCl_3$) δ 2.43 (s, 3H, C*H*$_3$), 2.14 (s, 3H, $OCOCH_3$), 7.26 (m, 2H, aromatic protons), 7.79 (d, J = 8.0 Hz, 1H, aromatic proton), 8.14 (1 H, s, C*H*)

^{13}C NMR (62.5 MHz, $CDCl_3$) δ 20.32, 21.67, 111.64, 120.88, 121.13, 123.60, 128.67,

132.92, 143.69, 152.52, 169.05

60') Naphtho[2,3-b]furan-3-yl acetate [61]

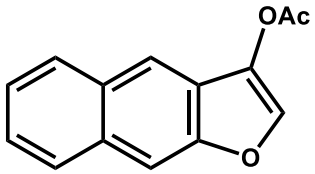

Melting point: 78-80 °C

Appearance: orange solid

Yield: 74%

^{1}H NMR (250 MHz, $CDCl_3$) δ 2.46 (s, 3H, $OCOCH_3$), 7.43-7.46 (m, 2H, aromatic protons), 7.79 (d, J = 8.0 Hz, 2H, aromatic proton), 7.91-7.44 (m, 2H, aromatic protons), 8.14 (1 H, s, C*H*)

^{13}C NMR (62.5 MHz, $CDCl_3$) δ 20.32, 120.48, 121.13, 127.27 (2C), 127.36 (2C), 128.39, 128.78, 129.71, 131.64, 143.67, 156.50, 169.04

The previously described esters **59a', 59b'** and **60'** are hydrolysed with concentrated hydrochloric acid (2 ml) in ethanol (80 ml) under 1,5 hours reflux. The cooled solution was diluted with diethyl ether and crystallization from an appropriate solvent gave the desired benzofuranones **59a, 59b** and **60** in good yields. (28) (4.6 g, 69%).

59a) Benzofuran-3(2H)-one[82, 86]

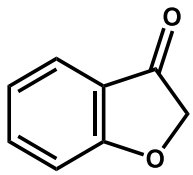

Melting point: 99-100 °C

Appearance: yellow solid

Yield: 87%

^{1}H NMR (250 MHz, $CDCl_3$) δ 4.63 (s, 2H, CH_2), 7.10 (t, J = 7.4 Hz, 1H, aromatic

proton), 7.15 (d, J = 8.4 Hz, 1H, aromatic proton), 7.62 (t, J= 7.8 Hz, 1 H, aromatic proton), 7.68 (d, J = 7.7 Hz, 1H, aromatic proton)

^{13}C NMR (62.5 MHz, $CDCl_3$) δ 74.83, 113.82, 121.37, 122.21, 124.24, 138.09, 174.25, 200.18

59b) 6-Methylbenzofuran-3(2H)-one [82, 87]

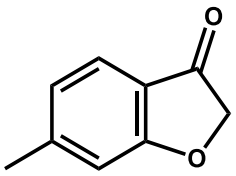

Melting point: 84-86 °C

Appearance: yellow solid

Yield: 80%

^{1}H NMR (250 MHz, $CDCl_3$) δ 2.45 (s, CH_3), 4.63 (s, 2H, CH_2), 6.94 (t, J = 8.4 Hz, 2H, aromatic protons), 7.57 (d, J = 8.0 Hz, 1H, aromatic proton)

^{13}C NMR (62.5 MHz, $CDCl_3$) δ 22,49, 74.97, 113.63, 118.85, 123.62, 123.65, 149.97, 174.60, 199.27

60) Naphtho[2,3-b]furan-3(2H)-one [61]

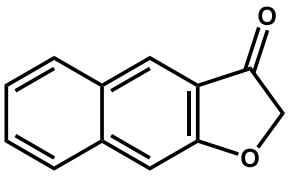

Melting point: 146-148°C

Appearance: orange solid

Yield: 79%

^{1}H NMR (250 MHz, $CDCl_3$) δ 4.98 (s, 2H, CH_2), 7.46-7.57 (m, 2H, aromatic protons), 7.86-7.92 (m, 4H, aromatic protons)

^{13}C NMR (62.5 MHz, $CDCl_3$) δ 74.56, 106.14, 124.73, 126.53, 126.88, 127.17, 129.18 (2C), 132.20, 137.59, 155.51, 197.23

Synthesis of (*Z*)-2-(4-methoxybenzylidene)-6-methylbenzofuran-3(2*H*)-one (71)

A mixture of the 4- methoxybenzaldehyde (5 mmol) and **59b** (5 mmol) were refluxed in ethanol (5 mL) with 3 drops of glacial acetic acidic and 5 drops of pyrrolidine for 1h. The mixture was allowed to cool down to room temperature and precipitated product **30** was filtered, washed with a small amount of ice-cold ethanol and recrystallized from ethanol [20].

71) (*Z*)-2-(4-Methoxybenzylidene)-6-methylbenzofuran-3(2*H*)-one [88]

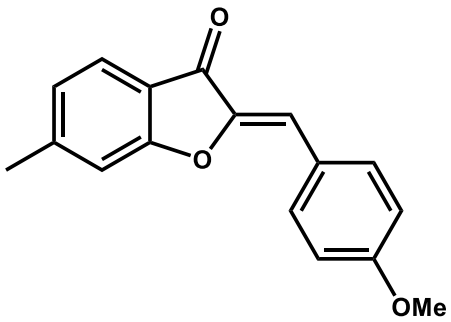

Melting point: 114-116 °C

Appearance: yellow solid

Yield: 64%

RMN ^{1}H (250 MHz, $CDCl_3$) δ 2.53 (s, 3H, –C*H*$_3$), 3.90 (s, 3H, –OC*H*$_3$), 6.88 (s, 1H, =C*H*COO–), 6.99-7.06 (m, 3H, aromatic protons), 7.16 (s, 1H, =C-C*H*=C), 7.70–7.72 (d, 1H, *J*=5.0 Hz, aromatic proton) ppm, 7.89–7.92 (d, 2H, *J*=7.5 Hz, aromatic protons) ppm

RMN ^{13}C (62.5 MHz, $CDCl_3$) δ 21.62, 55.87, 112.84, 113.65, 114.21, 114.30, 119.47, 123.74, 124.69, 130.53, 132.81, 132.90, 146.92, 150.06, 159.82, 166.17, 182.62 ppm

HRMS (ESI) [M+H]+ $C_{17}H_{14}O_3$ calculated: 266.296 found: 266.289.

Elemental analysis: calculated: C: 76.86%; H: 5.30%; O: 18.02% found: C: 76.78%; H: 5.35%

Synthesis of the benzofuran-chromone and –coumarinderivatives:

A mixture of the chromone-3 aldehydes or coumarine-4- aldehydes (5 mmol) and different benzofurane derivatives (5 mmol) were stirred at room temperature in dichloromethane (5 mL) with acidic Al_2O_3 (Beckmann I, 1g) for 2 to 6 days. The suspension was filtered through celite and washed with dichloromethane/THF to remove all traces of aluminium oxide. After distillation of the solvent in vacuo the obtained solid was recrystallized from ethanol.

61a) (*Z*)-3-[(6-Methyl-3-oxobenzofuran-2(3*H*)-ylidene)methyl)]-chromone

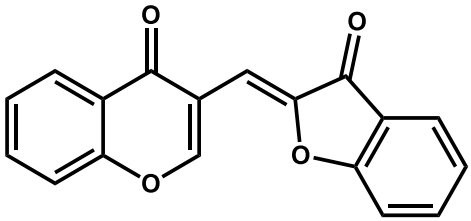

Melting point: 233-234 °C

Appearance: yellow solid

Yield: 36%

^{1}H NMR (250 MHz, $CDCl_3$) δ 7.23-7.33 (d, 2H, *J*= 10.0 Hz, aromatic protons), 7.38 (s, 1H =C-C*H*=C), 7.44–7.54 (m, 2H, aromatic protons), 7.64–7.77 (m, 2H, aromatic protons), 7.81–7.84 (d, 1H, *J*= 7.5 Hz, aromatic proton), 8.29-8.33 (d, 1H, *J*=10.0 Hz, aromatic proton), 9.09 (s, 1H –O-C*H*=C-) ppm

^{13}C NMR (62.5 MHz, $CDCl_3$) δ 102.25, 112.75, 118.13, 118.27, 121.75, 123.62, 123.83, 124.87, 125.84, 126.53, 134.15, 136.92, 147.15, 155.90, 158.77, 165.58, 175.13, 183.57 ppm

HRMS (ESI) [M+H]+ $C_{18}H_{11}O_4$ calculated: 291.0652 found: 291.0663.

Elemental analysis: calculated: C: 74.48%; H: 3.47%; O: 22.05% found: C: 74.48%; H: 3.47%

61b) (*Z*)-3-[(6-Methyl-3-oxobenzofuran-2(3*H*)-ylidene)methyl]-chromone

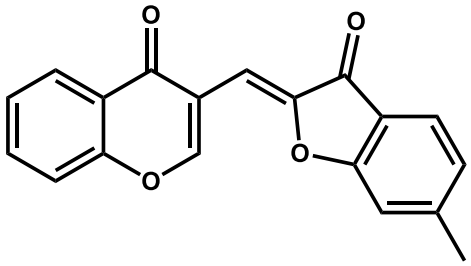

Melting point: 210-212 °C

Appearance: yellow solid

Yield: 66%

^{1}H NMR (250 MHz, $CDCl_3$) δ 2.51 (s, 3H, –C*H*$_3$), 7.04-7.08 (d, 1H, *J*= 10.0 Hz, aromatic proton), 7.11 (s, 1H, aromatic proton), 7.33 (s, 1H =C-C*H*=C), 7.43–7.54 (m, 2H, aromatic protons), 7.68–7.76 (m, 2H, aromatic protons), 8.29-8.33 (d, 1H, *J*= 10.0 Hz, aromatic proton), 9.06 (s, 1H –O-C*H*=C-) ppm

^{13}C NMR (62.5 MHz, $CDCl_3$) δ 22.66, 101.70, 112.91, 118.18, 118.27, 119.39, 123.60, 124.50, 125.17, 125.80, 126.51, 134.12, 147.62, 149.13, 155.89, 158.61, 166.14, 175.17, 183.17 ppm

HRMS (ESI) [M+H]+ $C_{19}H_{13}O_4$ calculated: 305.0808 found: 305.0811.

Elemental analysis: calculated: C: 74.99%; H: 3.97%; O: 21.03% found: C: 74.42 H: 4.22

61c) (*Z*)-2-[(Chromon-3-yl)methylene]naphtho[2,3-*b*]furan-3(2*H*)-one

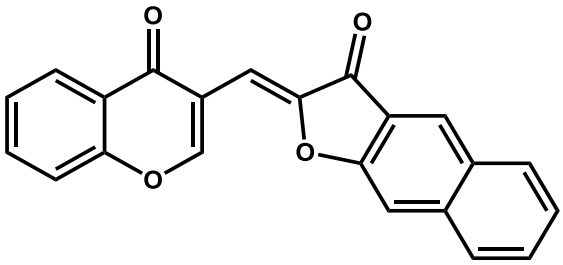

Melting point: 243-245 °C

Appearance: yellow solid

Yield: 21%

^{1}H NMR (250 MHz, $CDCl_3$) δ 7.37 (s, 1H =C-C*H*=C), 7.43-7.55 (m, 3H, aromatic proton), 7.59–7.65 (m, 2H, aromatic protons), 7.70–7.76 (t, 1H, *J*=7.5 Hz, aromatic proton), 7.87–7.90 (d, 1H, *J*=7.5 Hz, aromatic proton), 7.98–8.01 (d, 1H, *J*=7.5 Hz,

aromatic proton), 8.30–8.33 (d, 1H, *J*=7.5 Hz, aromatic proton), 8.40 (s, 1H, aromatic proton), 9.16 (s, 1H –O-C*H*=C-) ppm

^{13}C NMR (62.5 MHz, $CDCl_3$) δ 101.07, 107.74, 118.29, 121.75, 123.61, 125.53, 126.54, 126.64, 127.84, 129.69, 130.05, 130.73, 130.90, 134.12, 138.26, 147.84, 155.92, 158.58, 159.44, 175.19, 183.95 ppm

HRMS (ESI) [M+H]+ $C_{22}H_{13}O_4$ calculated: 341.0808 found: 341.0803.

Elemental analysis: calculated: C: 77.64%; H: 3.55%; O: 18.80% found: C: 77,78%; H: 3.11%

62a) (*Z*)-6-Methyl-3-[3-oxobenzofuran-2((3*H*)-ylidene)methyl]-chromone

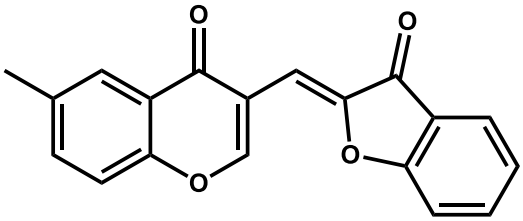

Melting point: 218-220 °C

Appearance: pale yellow solid

Yield: 37%

^{1}H NMR (250 MHz, $CDCl_3$) δ 2.48 (s, 3H, –CH_3), 7.21-7.28 (m, 1H, aromatic proton), 7.32 (s, 1H =C-C*H*=C), 7.37 (s, 1H, aromatic proton), 7.33–7.34 (d, 1H, *J*= 10.0 Hz, aromatic proton), 7.50–7.54 (d, 1H, *J*=10.0 Hz, aromatic proton), 7.63–7.70 (t, 1H, *J*=7.5 Hz, aromatic proton), 7.80–7.83 (d, 1H, *J*=7.5 Hz, aromatic proton), 8.07 (s, 1H, aromatic proton), 9.06 (s, 1H –O-C*H*=C-) ppm

^{13}C NMR (62.5 MHz, $CDCl_3$) δ 20.98, 102.54, 112.75, 117.87, 118.03, 121.77, 123.25, 123.78, 124.84, 125.81, 135.97, 136.88, 147.02, 154.18, 158.74, 165.55, 175.21, 183.59 ppm

HRMS (ESI) [M+H]+ $C_{19}H_{13}O_4$ calculated: 305.0808 found: 305.0820.

Elemental analysis: calculated: C: 74.99%; H: 3.97%; O: 21.03% found: C: 75.24%; H: 4.03%

62b) (*Z*)-6-Methyl-3-[(6-methyl-3-oxobenzofuran-2(3*H*)-ylidene)methyl]-chromone

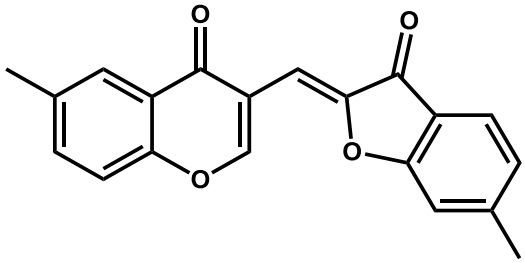

Melting point: 255-257 °C

Appearance: pale orange solid

Yield: 37%

^{1}H NMR (250 MHz, $CDCl_3$) δ 2.48 (s, 3H, –CH_3), 2.50 (s, 3H, –CH_3), 7.03-7.06 (d, 1H, *J*= 7.5 Hz, aromatic proton), 7.10 (s, 1H, aromatic proton), 7.33 (s, 1H =C-C*H*=C), 7.39–7.43 (d, 1H, *J*=10.0 Hz, aromatic proton), 7.50–7.53 (d, 1H, J=7.5 Hz, aromatic proton), 7.67–7.70 (d, 1H, *J*=7.5 Hz, aromatic proton), 8.08 (s, 1H, aromatic proton), 9.03 (s, 1H –O-C*H*=C-) ppm;

^{3}C NMR (62.5 MHz, $CDCl_3$) δ 20.98, 22.64, 101.99, 112.89, 117.95, 118.01, 119.44, 123.31, 124.48, 125.13, 125.82, 135.33, 135.90, 147.51, 149.05, 154.18, 158.57, 166.22, 175.31, 183.32 ppm

HRMS (ESI) [M+H]+ $C_{20}H_{15}O_4$ calculated: 319.0965 found: 319.0961.

Elemental analysis: calculated: C: 75.46%; H: 4.43%; O: 20.10% found: C: 75.64% H: 4.50%

63a) (*Z*)-6,7-Dimethyl-3-[(3-oxobenzofuran-2(3*H*)-ylidene)methyl]chromone

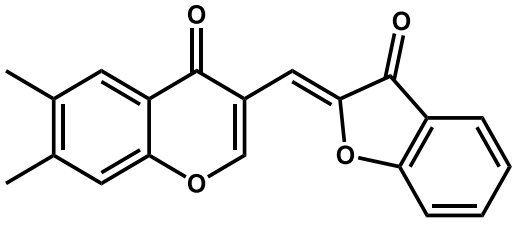

Melting point: 238-240 °C

Appearance: pale yellow solid

Yield: 42%

^{1}H NMR (250 MHz, $CDCl_3$) δ 2.38-2.41 (d, 6H, *J*=7.5 Hz, 2 –CH_3), 7.21-7.29 (m, 2H, aromatic protons), 7.31 (s, 1H =C-C*H*=C), 7.38 (s, 1H, aromatic proton), 7.63–7.69 (t,

1H, *J*=7.5 Hz, aromatic proton), 7.79–7.82 (d, 1H, *J*=7.5 Hz, aromatic proton), 8.01 (s, 1H, aromatic proton), 9.02 (s, 1H –O-C*H*=C-) ppm

^{13}C NMR (62.5 MHz, $CDCl_3$) δ 19.34, 20.46, 102.77, 112.73, 117.80, 118.35, 121.42, 121.81, 123.73, 124.81, 126.06, 135.26, 136.81, 144.78, 146.94, 154.45, 158.61, 165.53, 175.04, 183.57 ppm

HRMS (ESI) [M+H]+ $C_{20}H_{15}O_4$ calculated: 319.0965 found: 319.0977.

Elemental analysis: calculated: C: 75.46%; H: 4.43%; O: 20.10% found: C: 75.40%; H: 4.40%

63b) (*Z*)-6,7-Dimethyl-3-[(6-methyl-3-oxobenzofuran-2(3*H*)-ylidene)methyl]chromone

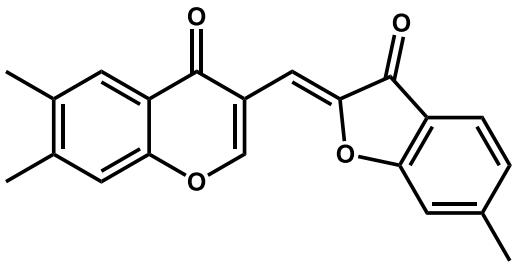

Melting point: 286-288 °C

Appearance: pale yellow solid

Yield: 44%

^{1}H NMR (250 MHz, $CDCl_3$) δ 2.37-2.40 (d, 6H, *J*=7.5 Hz, 2 –CH_3), 2.50 (s, 3H, –CH_3), 7.03-7.06 (d, 1H, *J*= 7.5 Hz, aromatic proton), 7.10 (s, 1H, aromatic proton), 7.28 (s, 1H =C-C*H*=C), 7.33 (s, 1H, aromatic proton), 7.67–7.70 (d, 1H, *J*=7.5 Hz, aromatic proton), 8.02 (s, 1H, aromatic proton), 8.99 (s, 1H –O-C*H*=C-) ppm

^{13}C NMR (62.5 MHz, $CDCl_3$) δ 19.34, 20.45, 22.63, 102.20, 112.88, 117.87, 118.34, 119.47, 121.43, 124.44, 125.07, 126.05, 135.20, 144.71, 147.42, 148.97, 154.45, 158.43, 166.09, 175.07, 183.16 ppm

HRMS (ESI) [M+H]+ $C_{21}H_{17}O_4$ calculated: 333.1121 found: 333.1120.

Elemental analysis: calculated: C: 75.89%; H: 4.85%; O: 19.26% found: C: 75.80%; H: 4.74%

63c) (*Z*)-2-[(6,7-Dimethylchromon-3-yl)methylene]naphtho[2,3-*b*]furan-3(2*H*)-one

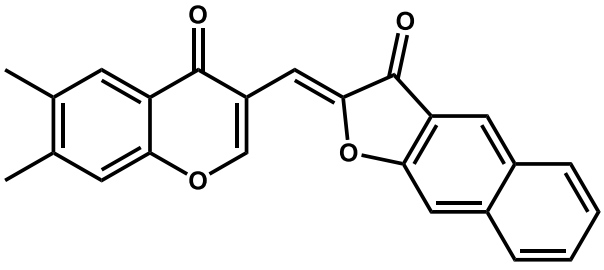

Melting point: 207-209 °C

Appearance: yellow solid

Yield: 41%

^{1}H NMR (250 MHz, $CDCl_3$) δ 2.38-2.42 (d, 6H, J=10.0 Hz, 2 –CH_3), 7.30 (s, 1H =C-

C*H*=C), 7.39 (s, 1H, aromatic proton), 7.45–7.51 (m, 1H, aromatic proton), 7.59–7.63 (m, 2H, aromatic protons), 7.87–7.90 (d, 1H, *J*=7.5 Hz, aromatic proton) 7.98–8.04 (m, 2H, aromatic protons), 8.41 (s, 1H, aromatic proton), 9.12 (s, 1H –O-C*H*=C-) ppm

^{13}C NMR (62.5 MHz, $CDCl_3$) δ 18.82, 19.15, 113.96, 114.03, 115.58, 119.52, 120.88, 124.53, 124.95, 126.07, 129.03, 129.29, 129.34, 130.71, 130.90, 131.55, 133.46, 149.02, 149.37, 151.05, 153.39, 154.13, 177.51, 182.66 ppm

HRMS (ESI) [M+Na]+ $C_{24}H_{17}O_4$ calculated: 369.1121 found: 369.1117.

Elemental analysis: calculated: C: 78.25%; H: 4.38%; O: 17.37% found: C: 78.34%; H: 4.36%;

64a) (*Z*)-7-Chloro-3-[(3-oxobenzofuran-2(3*H*)-ylidene)methyl] chromone

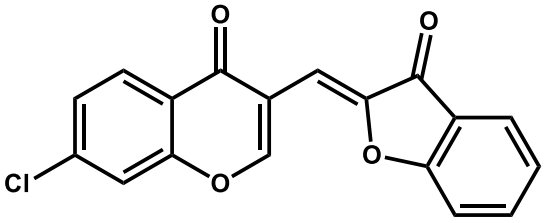

Melting point: 253-255 °C

Appearance: pale yellow solid

Yield: 45%

^{1}H NMR (250 MHz, $CDCl_3$) δ 7.23 (s, 1H =C-C*H*=C), 7.29–7.33 (m, 2H, aromatic proton), 7.40-7.45 (d, 1H, *J*=12.5Hz, aromatic protons), 7.65–7.72(m, 2H, aromatic protons), 7.80–7.84 (d, 1H, *J*=10.5 Hz, aromatic proton) 8.22-8.26 (d, 1H, *J*=10.0 Hz, aromatic proton), 9.06 (s, 1H –O-C*H*=C-) ppm

^{13}C NMR (62.5 MHz, $CDCl_3$) δ 101.57, 112.76, 118.36, 118.50, 121.65, 122.08, 123.95, 124.93, 126.72, 127.91, 137.05, 140.35, 147.33, 155.94, 158.59, 165.59, 174.36, 183.54 ppm

HRMS (ESI) [M+H]+ $C_{18}H_{10}ClO_4$ calculated: 325.0262 found: 325.0286.

Elemental analysis: calculated: C: 66.58%; H: 2.79%; Cl: 10.92%; O: 19.71% found: C: 66.65%, H: 2.83%

64b) (*Z*)-7-Chloro-3-[(6-methyl-3-oxobenzofuran-2(3*H*)-ylidene)methyl]chromone

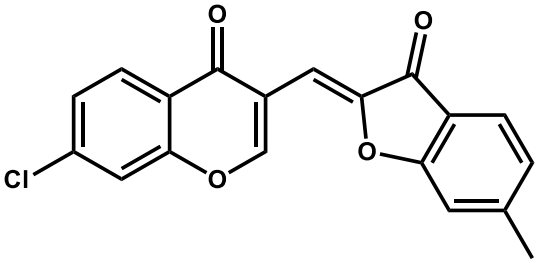

Melting point: 267-269 °C

Appearance: pale yellow solid

Yield: 55%

^{1}H NMR (250 MHz, $CDCl_3$) δ 2.51 (s, 3H, –C*H*$_3$), 7.04 (s, 1H =C-C*H*=C), 7.07-7.11 (d, 1H, *J*=10.0 Hz, aromatic protons), 7.40–7.44 (d, 1H, *J*=10.0 Hz, aromatic proton), 7.54 (s, 1H, aromatic proton), 7.68–7.70 (d, 1H, *J*=5.0Hz, aromatic proton) 8.21-8.25 (d, 1H, *J*=10.0 Hz, aromatic proton), 9.01 (s, 1H –O-C*H*=C-) ppm

^{13}C NMR (62.5 MHz, $CDCl_3$) δ 22.68, 101.01, 112.92, 118.34, 118.57, 119.31, 122.09, 124.55, 125.28, 126.66, 127.90, 140.28, 147.82, 149.28, 155.94, 158.41, 166.15, 174.38, 183.10 ppm

HRMS (ESI) [M+H]+ $C_{19}H_{12}ClO_4$ calculated: 339.0419 found: 339.0428.

Elemental analysis: calculated: C: 67.37%; H: 3.27%; Cl: 10.47%; O: 18.89% found: C: 67.55%, H: 3.26%

65a) (*Z*)-6-Chloro-3-[(3-oxobenzofuran-2(3*H*)-ylidene)methyl] chromone

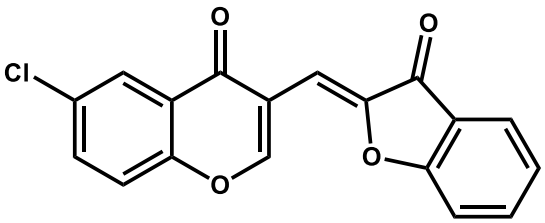

Melting point: 250-252 °C

Appearance: yellow solid

Yield: 42%

^{1}H NMR (250 MHz, $CDCl_3$) δ 7.23 (s, 1H =C-C*H*=C), 7.29–7.32 (d, 2H, *J*=7.5 Hz, aromatic proton), 7.47-7.51 (d, 1H, *J*=10.0Hz, aromatic protons), 7.64–7.71 (m, 2H, aromatic protons), 7.80–7.83 (d, 1H, J=7.5 Hz, aromatic proton) 8.26-8.27 (d, 1H,

J=2.5 Hz, aromatic proton), 9.07 (s, 1H –O-C*H*=C-) ppm

^{13}C NMR (62.5 MHz, $CDCl_3$) δ 101.60, 112.75, 118.21, 120.03, 121.64, 123.95, 124.46, 124.93, 125.90, 131.88, 134.39, 137.04, 147.29, 154.20, 158.66, 165.59, 174.06, 183.52 ppm

HRMS (ESI) [M+Na]+ $C_{18}H_9ClNaO_4$ calculated: 347.0082 found: 347.0092.

Elemental analysis: calculated: C: 66.58%; H: 2.79%; Cl: 10.92%; O: 19.71% found: C: 66.78%; H: 2.80%

65b) (*Z*)-6-Chloro-3-[(6-methyl-3-oxobenzofuran-2(3*H*)-ylidene)methyl]chromone

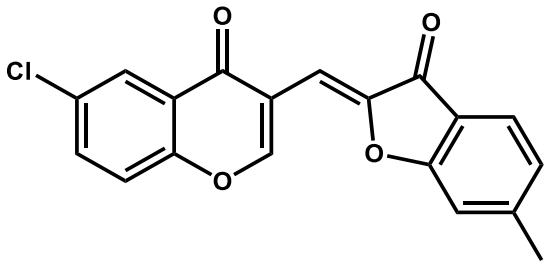

Melting point: 253-255 °C

Appearance: pale yellow solid

Yield: 37%

^{1}H NMR (250 MHz, $CDCl_3$) δ 2.51 (s, 3H, –C*H*$_3$), 7.04–7.07 (d, 2H, *J*=7.5 Hz, aromatic proton), 7.13 (s, 1H =C-C*H*=C), 7.26 (s, 1H, aromatic proton), 7.47-7.50 (d, 1H, *J*=7.5Hz, aromatic protons), 7.63–7.64 (d, 1H, *J*=2.5 Hz, aromatic proton), 7.67–7.70 (m, 1H, aromatic proton) 8.25-8.26 (d, 1H, *J*=2.5 Hz, aromatic proton), 9.03 (s, 1H –O-C*H*=C-) ppm

^{13}C NMR (62.5 MHz, $CDCl_3$) δ 22.76, 101.04, 112.91, 118.28, 119.31, 120.01, 124.47, 124.55, 125.28, 125.89, 131.34, 134.34, 147.78, 149.27, 154.20, 158.49, 166.51, 174.08, 183.08 ppm

HRMS (ESI) [M+H]+ $C_{19}H_{12}ClO_4$ calculated: 339.0419 found: 339.0422.

Elemental analysis: calculated: C: 67.37%; H: 3.27%; Cl: 10.47%; O: 18.89% found: C: 67.37%; H: 3.29%

65c) (*Z*)-2-[(6-Chloro-chromon-3-yl)methylene]naphtho[2,3-*b*]furan-3(2*H*)-one

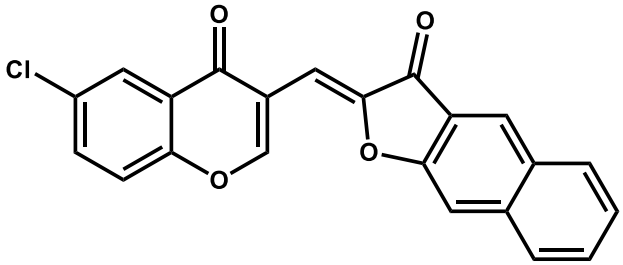

Melting point: 310-312 °C

Appearance: yellow solid

Yield: 25%

^{1}H NMR (250 MHz, $CDCl_3$) δ 7.32 (s, 1H =C-C*H*=C), 7.46–7.52 (m, 2H, aromatic protons), 7.60–7.71 (m, 3H, aromatic protons), 7.87–7.90 (d, 1H, *J*=7.5 Hz, aromatic proton) 7.99–8.03 (d, 1H, *J*=10.0 Hz, aromatic proton), 8.29 (s, 1H, aromatic proton), 8.42 (s, 1H, aromatic proton), 9.15 (s, 1H –O-C*H*=C-) ppm

^{13}C NMR (62.5 MHz, $CDCl_3$) δ 100.41, 107.76, 118.39, 120.03, 124.48, 125.61, 125.92, 126.75, 127.85, 129.78, 130.09, 130.93, 131.83, 134.34, 138.28, 148.02, 154.26, 157.99, 158.45, 159.40, 174.21, 183.81 ppm

HRMS (ESI) [M+H]+ $C_{22}H_{12}ClO_4$ calculated: 375.0419 found: 375.0426.

Elemental analysis: calculated: C: 74.48%; H: 3.47%; O: 22.05% found: C: 74.53%; H: 3.56%

66a) (*Z*)-6-Fluoro-3-[(3-oxobenzofuran-2(3*H*)-ylidene)methyl] chromone

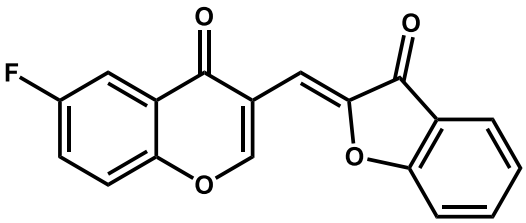

Melting point: 249-251 °C

Appearance: pale yellow solid

Yield: 44%

^{1}H NMR (250 MHz, $CDCl_3$) δ 7.23 (s, 1H =C-C*H*=C), 7.29 (s, 1H, aromatic proton), 7.32 (s, 1H, aromatic proton), 7.41-7.48 (m, 1H, aromatic proton), 7.52–7.58 (m, 1H, aromatic proton), 7.65–7.71 (t, 1H, *J*=7.5 Hz, aromatic proton), 7.81–7.84 (d, 1H,

J=7.5 Hz, aromatic proton), 7.92-7.95 (d, 1H, *J*=7.5 Hz, aromatic proton), 9.09 (s, 1H –O-C*H*=C-) ppm

^{13}C NMR (62.5 MHz, $CDCl_3$) δ 22.66, 101.76, 111.23, 111.61, 112.75, 117.53, 120.41, 120.54, 121.68, 122.62, 123.92, 124.92, 136.65, 147.30, 158.72, 165.59, 174.47, 183.52 ppm

HRMS (ESI) [M+H]+ $C_{18}H_{12}FO_4$ calculated: 309.0558 found: 309.0557.

Elemental analysis: calculated: C: 70.13%; H: 2.94%; F: 6.16%; O: 20.76% found: C: 70.39%; H: 2.76%

66b) (*Z*)-6-Fluoro-3-[(6-methyl-3-oxobenzofuran-2(3*H*)-ylidene)methyl]chromone

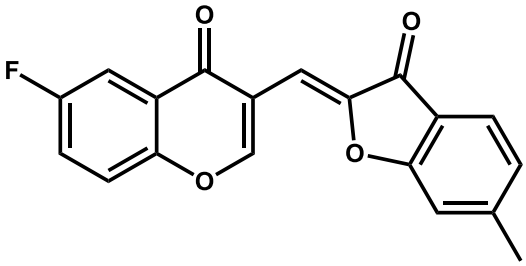

Melting point: 230-232 °C

Appearance: pale yellow solid

Yield: 38%

^{1}H NMR (250 MHz, $CDCl_3$) δ 2.51 (s, 3H, –CH_3), 7.05–7.11 (t, 2H, *J*=7.5 Hz, aromatic proton), 7.28 (s, 1H =C-C*H*=C), 7.44-7.48 (m, 1H, aromatic proton), 7.52–7.57 (m, 1H, aromatic proton), 7.68–7.71 (d, 1H, *J*=7.5 Hz, aromatic proton) 7.92-7.95 (d, 1H, *J*=7.5 Hz, aromatic proton), 9.05 (s, 1H –O-C*H*=C-) ppm

^{13}C NMR (62.5 MHz, $CDCl_3$) δ 22.66, 101.20, 111.60, 112.90, 117.62, 119.35, 120.38, 124.47, 124.55, 124.55, 124.83, 125.25, 147.79, 149.22, 152.13, 157.86, 166.15, 174.50, 183.09 ppm

HRMS (ESI) [M+H]+ $C_{19}H_{12}FO_4$ calculated: 323.0714 found: 323.0715.

Elemental analysis: calculated: C: 70.81%; H: 3.44%; F: 5.89%; O: 19.86% found: C: 69.81%; H: 3.44%

66c) (*Z*)-2-[(6-Fluoro-chromon-3-yl)methylene]naphtho[2,3-*b*]furan-3(2*H*)-one

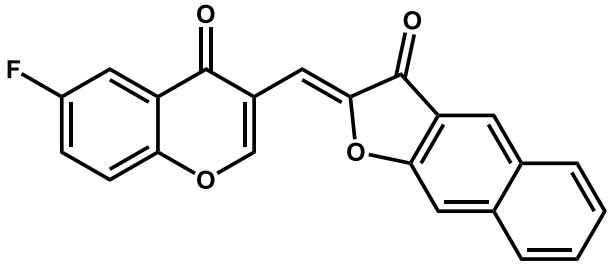

Melting point: 303-305 °C

Appearance: yellow solid

Yield: 38%

^{1}H NMR (250 MHz, $CDCl_3$) δ 7.32 (s, 1H =C-C*H*=C), 7.41–7.67 (m, 5H, aromatic protons), 7.87–8.01 (m, 3H, aromatic protons), 8.41 (s, 1H, aromatic proton), 9.16 (s, 1H –O-C*H*=C-) ppm

^{13}C NMR (62.5 MHz, $CDCl_3$) δ 100.60, 107.77, 120.43, 120.56, 121.66, 122.61, 125.61, 126.75, 127.85, 129.78, 130.08, 130.94, 131.83, 134.34, 138.28, 142.61, 148.01, 157.99, 158.56, 159.43, 174.26, 184.89 ppm

HRMS (ESI) [M+H]+ $C_{22}H_{12}FO_4$ calculated: 359.0714 found: 359.0710.

Elemental analysis: calculated: C: 73.74%; H: 3.09%; F: 5.30%; O: 17.86% found: C: 73.75%, H: 3.14%

67a) (*Z*)-7-Methoxy-3-[(3-oxobenzofuran-2(3*H*)-ylidene)methyl]chromone

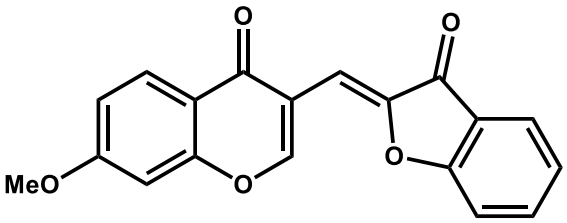

Melting point: 233-235 °C

Appearance: pale yellow solid

Yield: 45%

^{1}H NMR (250 MHz, $CDCl_3$) δ 3.93 (s, 3H, –OCH_3), 6.88 (s, 1H, aromatic proton), 6.98–7.03 (d, 1H, *J*=12.5 Hz, aromatic proton), 7.21-7.32 (m, 2H, aromatic protons), 7.37 (s, 1H =C-C*H*=C), 7.54 (s, 1H, aromatic proton), 7.63-7.67 (m, 1H, aromatic protons), 7.80–7.83 (d, 1H, J=7.5Hz, aromatic proton), 8.18-8.22 (d, 1H, *J*=10.0 Hz, aromatic

proton), 9.00 (s, 1H –O-C*H*=C-) ppm

^{13}C NMR (62.5 MHz, $CDCl_3$) δ 55.92, 100.57, 102.49, 112.74, 114.98, 117.43, 117.97, 121.78, 123.78, 124.84, 127.94, 136.86, 147.08, 157.64, 158.43, 164.44, 165.54, 174.42, 183.56 ppm

HRMS (ESI) [M+H]+ $C_{19}H_{13}O_5$ calculated: 321.0757 found: 321.0764.

Elemental analysis: calculated: C: 71.25%; H: 3.78%; O: 24.98% found: C: 71.13% H: 3.83%

67b) (*Z*)-7-Methoxy-3-[(6-methyl-3-oxobenzofuran-2(3*H*)-ylidene)methyl]chromone

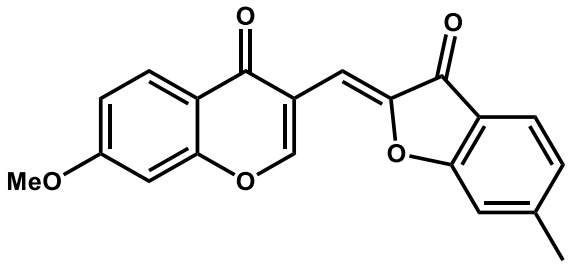

Melting point: 222-224 °C

Appearance: pale yellow solid

Yield: 41%

^{1}H NMR (250 MHz, $CDCl_3$) δ 2.50 (s, 3H, –C*H*$_3$), 3.93 (s, 3H, –OC*H*$_3$), 6.88 (s, 1H, aromatic proton), 6.97-7.09 (m, 3H, aromatic protons), 7.32 (s, 1H =C-C*H*=C), 7.40–7.44 (d, 1H, *J*= 10.0 Hz, aromatic proton), 7.54 (s, 1H, aromatic proton), 7.66–7.69 (d, 1H, *J*= 7.5Hz, aromatic proton), 8.17-8.21 (d, 1H, *J*=10.0 Hz, aromatic proton), 8.97 (s, 1H –O-C*H*=C-) ppm

^{13}C NMR (62.5 MHz, $CDCl_3$) δ 22.64, 55.90, 100.54, 101.90, 112.89, 114.93, 117.43, 118.03, 119.43, 124.45, 125.11, 127.91, 147.54, 149.04, 157.62, 158.24, 164.40, 166.09, 174.44, 183.13 ppm

HRMS (ESI) [M+H]+ $C_{20}H_{15}O_5$ calculated: 335.0914 found: 335.0924.

Elemental analysis: calculated: C: 71.85%; H: 4.22%; O: 23.93% found: C: 71.60%; H: 4.31%

68a) (*Z*)-5-Methoxy-3-[(3-oxobenzofuran-2(3*H*)-ylidene)methyl]chromone

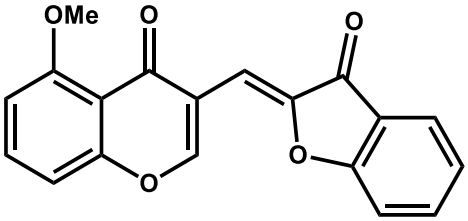

Melting point: 236-238 °C

Appearance: pale yellow solid

Yield: 33%

^{1}H NMR (250 MHz, $CDCl_3$) δ 4.01 (s, 3H, –OC*H*$_3$), 6.84–6.88 (d, 1H, *J*=10.0 Hz, aromatic proton), 7.04–7.08 (d, 1H, *J*=10.0 Hz, aromatic proton), 7.21-7.31 (m, 3H, aromatic protons), 7.37 (s, 1H =C-C*H*=C), 7.54 (s, 1H, aromatic proton), 7.56–7.69 (m, 2H, aromatic protons), 7.80-7.83 (d, 1H, *J*=7.5 Hz, aromatic proton), 8.90 (s, 1H –O-C*H*=C-) ppm

^{13}C NMR (62.5 MHz, $CDCl_3$) δ 56.53, 102.66, 107.05, 110.16, 112.71, 114.24, 119.13, 121.84, 123.72, 124.82, 134.28, 136.80, 147.10, 157.10, 157.80, 160.28, 165.48, 174.41, 183.55 ppm

HRMS (ESI) [M+H]+ $C_{19}H_{13}O_5$ calculated: 321.0757 found: 321.0762.

Elemental analysis: calculated: C: 71.25%; H: 3.78%; O: 24.98% found: C: 71.03%; H: 3.78%

68b) (*Z*)-5-Methoxy-3-[(6-methyl-3-oxobenzofuran-2(3*H*)-ylidene)methyl]chromone

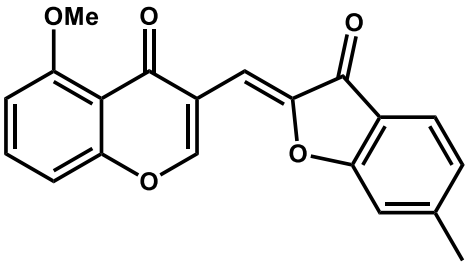

Melting point: 260-262 °C

Appearance: yellow solid pâle

Yield: 43%

^{1}H NMR (250 MHz, $CDCl_3$) δ 2.51 (s, 3H, –C*H*$_3$), 4.00 (s, 3H, –OC*H*$_3$), 6.83–6.87 (d, 1H, *J*=10.0 Hz, aromatic proton), 7.02-7.08 (m, 3H, aromatic protons), 7.32 (s, 1H =C-

C*H*=C), 7.40–7.44 (d, 1H, *J*=10.0 Hz, aromatic proton), 7.54 (s, 1H, aromatic proton), 7.55–7.62 (m, 1H, aromatic proton), 7.66-7.69 (d, 1H, *J*=7.5 Hz, aromatic proton), 8.90 (s, 1H –O-C*H*=C-) ppm

^{13}C NMR (62.5 MHz, $CDCl_3$) δ 22.64, 56.52, 102.08, 106.99, 110.15, 112.86, 114.24, 119.20, 119.49, 124.43, 125.06, 134.22, 147.57, 148.94, 156.90, 157.80, 160.27, 166.03, 174.44, 183.12 ppm

HRMS (ESI) [M+H]+ $C_{20}H_{15}O_5$ calculated: 335.0914 found: 335.0914.

Elemental analysis: calculated: C: 71.85%; H: 4.22%; O: 23.93% found: C: 71.60%; H: 4,26%

68c) (*Z*)-2-[(5-Methoxy-chromon-3-yl)methylene]naphtho[2,3-*b*]furan-3(2*H*)-one

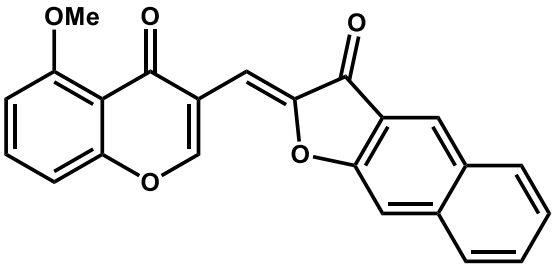

Melting point: 286-288 °C

Appearance: yellow solid

Yield: 37%

^{1}H NMR (250 MHz, $CDCl_3$) δ 4.02 (s, 3H, –OCH_3), 6.85-6.88 (m, 1H, aromatic proton), 7.07-7.10 (m, 1H, aromatic proton), 7.37 (s, 1H =C-CH=C), 7.45–7.49 (m, 1H, aromatic proton), 7.54–7.67 (m, 3H, aromatic protons), 7.83–7.92 (m, 1H, aromatic proton), 7.95–8.03 (m, 1H, aromatic proton), 8.40 (s, 1H, aromatic proton), 9.02 (s, 1H –O-C*H*=C-) ppm

^{13}C NMR (62.5 MHz, $CDCl_3$) δ 56.52, 101.47, 107.00, 107.66, 110.18, 114.25, 119.30, 121.88, 125.44, 126.51, 127.81, 129.59, 130.02, 130.86, 134.23, 138.22, 147.79, 156.90, 157.83, 159.40, 160.29, 174.46, 183.89 ppm

HRMS (ESI) [M+H]+ $C_{23}H_{15}O_5$ calculated: 371.0914 found: 371.0920.

Elemental analysis: calculated: C: 74.59%; H: 3.81%; O: 21.60% found: C: 74.19%; H: 3.44%

69a) (*Z*)-7,8-Dimethoxy-3-[(3-oxobenzofuran-2(3*H*)-ylidene)methyl]chromone

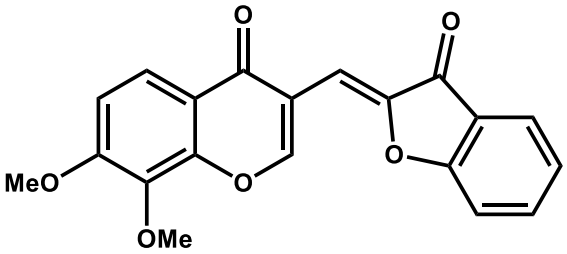

Melting point: 250-252 °C

Appearance: yellow solid pâle

Yield: 40%

RMN ^{1}H (250 MHz, $CDCl_3$) δ 2.51 (s, 3H, –CH_3), 4.03 (s, 6H, 2 –OCH_3), 7.07–7.10 (d, 1H, *J*= 7.5Hz, aromatic proton), 7.22-7.31 (m, 2H, aromatic protons), 7.36 (s, 1H =C-C*H*=C), 7.61-7.64 (m, 1H, aromatic proton), 7.81–7.84 (d, 1H, *J*= 7.5Hz, aromatic proton), 8.02-8.06 (d, 1H, *J*=10.0 Hz, aromatic proton), 9.11 (s, 1H –O-C*H*=C-) ppm

RMN ^{13}C (62.5 MHz, $CDCl_3$) δ 56.49, 61.73, 102.31, 110.51, 112.74, 117.58, 118.20, 121.76, 121.98, 123.81, 124.86, 147.17, 150.23, 156.92, 158.55, 165.55, 174.61, 183.57 ppm

HRMS (ESI) [M+H]+ $C_{20}H_{15}O_6$ found: 351.0863 : 351.0853.

Elemental analysis: calculated: C: 68.57%; H: 4.03%; O: 27.40% : C: 68.90%; H: 4.14%

69b) (*Z*)-7,8-Dimethoxy-3-[(6-methyl-3-oxobenzofuran-2(3*H*)-ylidene)methyl] chromone

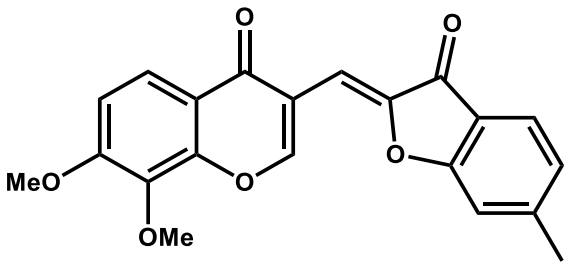

Melting point: 214-216 °C

Appearance: pale yellow solid

Yield: 34%

^{1}H NMR (250 MHz, $CDCl_3$) δ 2.51 (s, 3H, –C*H*$_3$), 4.03 (s, 6H, 2 –OC*H*$_3$), 7.04-7.10 (m, 3H, aromatic protons), 7.31 (s, 1H =C-C*H*=C), 7.68–7.71 (d, 1H, *J*= 7.5Hz, aromatic proton), 8.02-8.05 (d, 1H, *J*=7.5 Hz, aromatic proton), 9.07 (s, 1H –O-C*H*=C-) ppm

^{13}C NMR (62.5 MHz, $CDCl_3$) δ 22.66, 56.48, 61.72, 101.75, 110.46, 112.87, 117.65, 118.23, 119.43, 121.98, 124.49, 125.16, 136.77, 147.65, 149.11, 150.23, 156.87, 158.36, 166.12, 174.64, 183.16 ppm

HRMS (ESI) [M+H]+ $C_{21}H_{17}O_6$ calculated: 365.1020 found: 365.1006.

Elemental analysis: calculated: C: 69.23%; H: 4.43%; O: 26.35% found: C: 69.47%, H: 4.49%

70a) (*Z*)-7-Methoxy-4-[(3-oxobenzofuran-2(3*H*)-ylidene)methyl]-2*H*-coumarine

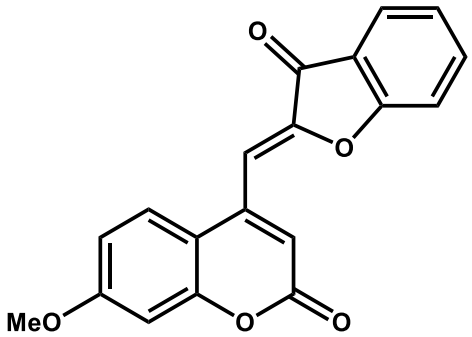

Melting point: 225-227 °C

Appearance: yellow solid

Yield: 36%

^{1}H NMR (250 MHz, $CDCl_3$) δ 3.91 (s, 3H, –OC*H*$_3$), 6.88-6.95 (m, 2H, aromatic

protons), 7.03 (s, 1H, =C*H*COO–), 7.17 (s, 1H, =C-C*H*=C), 7.33–7.38 (m, 2H, aromatic protons), 7.71–7.76 (m, 2H, aromatic protons), 7.82–7.85 (d, 1H, *J*=7.5 Hz, aromatic proton) ppm

^{13}C NMR (62.5 MHz, $CDCl_3$) δ 55.84, 101.46, 102.00, 111.72, 112.64, 113.28, 114.73, 120.67, 124.54, 125.15, 125.18, 138.18, 143.68, 151.00, 155.64, 161.29, 162.95, 166.66, 184.19 ppm

HRMS (ESI) [M+Na]+ $C_{19}H_{12}NaO_5$ calculated: 343.057 found: 343.059.

Elemental analysis: calculated: C: 71.25%; H: 3.78%; O: 24.98% :found C: 70.96%; H: 3.90%

70b) (*Z*)-7-Methoxy-4-[(6-methyl-3-oxobenzofuran-2(3*H*)-ylidene)methyl]-2*H*-coumarine

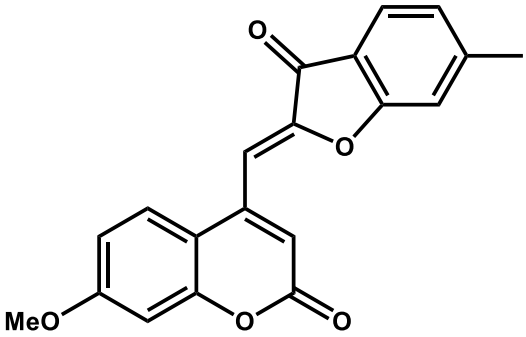

Melting point: 238-240 °C

Appearance: yellow solid

Yield: 40%

^{1}H NMR (250 MHz, $CDCl_3$) δ 2.53 (s, 3H, –CH_3), 3.88 (s, 3H, –OCH_3), 6.87-6.95 (m, 2H, aromatic protons), 6.97 (s, 1H, =C*H*COO–), 7.09–7.15 (m, 3H, aromatic protons,=C-C*H*=C), 7.69–7.76 (t, 2H, *J*=9.5 Hz, aromatic protons) ppm

^{13}C NMR (62.5 MHz, $CDCl_3$) δ 22.84 55.83, 101.43, 101.52, 111.77, 112.60, 113.41, 114.53, 118.34, 124.82, 125.18, 125.86, 143.83, 150.75,151.57, 155.62, 161.34, 162.90, 167.11, 183.65 ppm

HRMS (ESI) [M+Na]+ $C_{20}H_{14}NaO_5$ calculated: 357.0733, found: 357.0742.

Elemental analysis: calculated: C: 71.85%; H: 4.22%; O: 23.93% found: C: 71.67%; H: 4.32%

70c) (*Z*)-2-[(7-Methoxycoumarin-yl)methylene]naphtho[2,3-*b*]furan-3(2*H*)-one

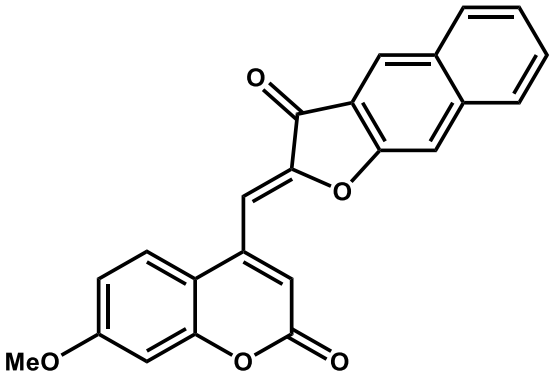

Melting point: 291-293 °C

Appearance: orange solid

Yield: 38%

^{1}H NMR (250 MHz, $CDCl_3$) δ 3.91 (s, 3H, –OCH_3), 6.89-6.96 (m, 2H, aromatic protons), 7.01 (s, 1H, =C*H*COO–), 7.26 (s, 1H, =C-C*H*=C), 7.49–7.54 (m, 1H, aromatic proton), 7.64–7.70 (m, 2H, aromatic protons), 7.76–7.80 (d, 1H, *J*=10.0 Hz, aromatic proton) ppm, 7.90–7.94 (d, 1H, *J*=10.0 Hz, aromatic proton) ppm, 8.00–8.03 (d, 1H, *J*=7.5 Hz, aromatic proton) 8.45 (s, 1H, aromatic proton) ppm

^{13}C NMR (62.5 MHz, $CDCl_3$) δ 55.83, 100.65, 101.45, 108.47, 111.78, 112.60, 114.43, 120.48, 125.13, 126.03, 127.47, 128.23, 130.27, 130.40, 131.07, 138.70, 143.83, 151.93, 155.65, 159.79, 161.42, 162.90, 184.53 ppm

HRMS (ESI) [M+Na]+ $C_{23}H_{14}NaO_5$ calculated: 393.074 found: 393.074.

Elemental analysis: calculated: C: 74.59%; H: 3.81%; O: 21.60% found: C: 74.63%; H: 3.82%

2.10.2 Biology

2.10.2.1 General

The experiments described in this chapter have been conducted by the following research groups: Prof Denyse Bagrel of the Université de Lorraine, Prof Lucia Altucci of University of Naples in Italy.

2.10.2.2 Cell culture

K562 (chronic myeloid leukemia) cells were cultured in RPMI (Invitrogen) with 10% fetal calf serum (Hyclone), 100 U/mL penicillin.

2.10.2.3 Cell Cycle Analysis on K562 Cells

2.5×10^5 treated (containing the tested compound and 0. 1% DMSO) and untreated (containing 0.1% DMSO) cells were collected, fixed and resuspended in 500 µL of a hypotonic buffer (0.1% Triton X-100, 0.1% sodium citrate, 50 µg/mL propidium iodide (PI), RNAse A). Cells were incubated in the dark for 30 min. Samples were acquired on a FACS-Calibur flow cytometer using the Cell Quest software (Becton Dickinson) and analysed with standard procedures using the Cell Quest software (Becton Dickinson) and the ModFit LT version 3 Software (Verity) as previously reported [89]. All the experiments were performed in triplicates.

2.11 References

14. V. Cody, E. Middleton, and Meeting Plant Flavonoids in Biology and Medicine, *Plant flavonoids in biology and medicine : biochemical, pharmacological, and structure-activity relationships ; proceedings of a symposium held in Buffalo, New York, July 22 - 26, 1985*. Progress in Clinical and Biological Research. 1986, New York, USA: Liss. XXI, 592 S.
15. E. Ono, M. Fukuchi-Mizutani, N. Nakamura, Y. Fukui, K. Yonekura-Sakakibara, M. Yamaguchi, T. Nakayama, T. Tanaka, T. Kusumi, and Y. Tanaka, *Yellow flowers generated by expression of the aurone biosynthetic pathway.* Proceedings of the National Academy of Sciences of the United States of America, 2006. **103**(29): p. 11075-80.
16. C.J.W. Brooks and D.G. Watson, *Phytoalexins.* Natural Product Reports, 1985. **2**(5): p. 427-459.
17. M. Morimoto, H. Fukumoto, T. Nozoe, A. Hagiwara, and K. Komai, *Synthesis and insect antifeedant activity of aurones against Spodoptera litura larvae.* Journal of agricultural and food chemistry, 2007. **55**(3): p. 700-5.
18. S. Okombi, D. Rival, S. Bonnet, A.M. Mariotte, E. Perrier, and A. Boumendjel, *Discovery of benzylidenebenzofuran-3(2H)-one (aurones) as inhibitors of tyrosinase derived from human melanocytes.* Journal of medicinal chemistry, 2006. **49**(1): p. 329-33.
19. S. Venkateswarlu, G.K. Panchagnula, and G.V. Subbaraju, *Synthesis and antioxidative activity of 3',4',6,7-tetrahydroxyaurone, a metabolite of Bidens frondosa.* Bioscience, biotechnology, and biochemistry, 2004. **68**(10): p. 2183-5.
20. A. Boumendjel, *Aurones: a subclass of flavones with promising biological potential.* Current medicinal chemistry, 2003. **10**(23): p. 2621-30.
21. N.J. Lawrence, D. Rennison, A.T. McGown, and J.A. Hadfield, *The total synthesis of an aurone isolated from Uvaria hamiltonii: aurones and flavones as anticancer agents.* Bioorganic & medicinal chemistry letters, 2003. **13**(21): p. 3759-63.
22. M. Auf'mkolk, J. Koehrle, R.D. Hesch, and V. Cody, *Inhibition of rat liver iodothyronine deiodinase. Interaction of aurones with the iodothyronine ligand-binding site.* The Journal of biological chemistry, 1986. **261**(25): p. 11623-30.
23. M. Hadjeri, M. Barbier, X. Ronot, A.M. Mariotte, A. Boumendjel, and J. Boutonnat, *Modulation of P-glycoprotein-mediated multidrug resistance by flavonoid derivatives and analogues.* Journal of medicinal chemistry, 2003. **46**(11): p. 2125-31.
24. J. Schoepfer, H. Fretz, B. Chaudhuri, L. Muller, E. Seeber, L. Meijer, O. Lozach, E. Vangrevelinghe, and P. Furet, *Structure-based design and synthesis of 2-benzylidene-benzofuran-3-ones as flavopiridol mimics.* Journal of medicinal chemistry, 2002. **45**(9): p. 1741-7.
25. H. Cheng, L. Zhang, Y. Liu, S. Chen, H. Cheng, X. Lu, Z. Zheng, and G.-C. Zhou, *Design, synthesis and discovery of 5-hydroxyaurone derivatives as growth inhibitors against HUVEC and some cancer cell lines.* European journal of medicinal chemistry, 2010. **45**(12): p. 5950-5957.
26. R.S. Varma and M. Varma, *Alluminia-mediated condensation. A simple synthesis of Aurones.* Tetrahedron Letters, 1992. **33**(40): p. 5937-5940.
27. D. Kim, Y. Li, B.A. Horenstein, and K. Nskanishi, *Synthesis of tunichromes mm-l and mm-2, blood pigments of the iron.Assimilating tunicate, molgula manhattensis.* Tetrahedron Letters, 1990. **31**(49): p. 7119-7122.
28. G.A. Kraus and V. Gupta, *Divergent approach to flavones and aurones via dihaloacrylic acids. Unexpected dependence on the halogen atom.* Organic

letters, 2010. **12**(22): p. 5278-80.
29. J.P. Corbet and G. Mignani, *Selected patented cross-coupling reaction technologies.* Chemical reviews, 2006. **106**(7): p. 2651-710.
30. H. Harkat, A. Blanc, J.M. Weibel, and P. Pale, *Versatile and expeditious synthesis of aurones via Au I-catalyzed cyclization.* The Journal of organic chemistry, 2008. **73**(4): p. 1620-3.
31. R. Atta ur, M. Choudhary, S. Hayat, A.M. Khan, and A. Ahmed, *Two new aurones from marine brown alga Spatoglossum variabile.* Chemical & pharmaceutical bulletin, 2001. **49**(1): p. 105-7.
32. N.N. Agrawal and P.A. Soni, *A new process for the synthesis of aurones by using mercury (II) acetate in pyridine and cupric bromide in dimethyl sulfoxide.* Indian journal of Chemistry, 2006. **45B**: p. 1301-1303.
33. P. Thanigaimalai, H.M. Yang, V.K. Sharma, Y. Kim, and S.H. Jung, *The scope of thallium nitrate oxidative cyclization of chalcones; synthesis and evaluation of isoflavone and aurone analogs for their inhibitory activity against interleukin-5.* Bioorganic & medicinal chemistry, 2010. **18**(12): p. 4441-5.
34. S.H. Jung, S.H. Cho, T.H. Dang, J.H. Lee, J.H. Ju, M.K. Kim, S.H. Lee, J.C. Ryu, and Y. Kim, *Structural requirement of isoflavonones for the inhibitory activity of interleukin-5.* European journal of medicinal chemistry, 2003. **38**(5): p. 537-45.
35. H.M. Yang, H.R. Shin, S.C. Bang, K.C. Lee, T.A. Hoang le, I.J. Lee, Y. Kim, and S.H. Jung, *The role of alkoxy group on the A ring of isoflavones in the inhibition of interleukin-5.* Archives of pharmacal research, 2007. **30**(8): p. 950-4.
36. K. Thakkar and M. Cushman, *A Novel Oxidative Cyclization of 2'-Hydroxychalcones to 4,5-Dialkoxyaurones by Thallium(III) Nitrate.* The Journal of organic chemistry, 1995. **60**(20): p. 6499-6510.
37. A. Detsi, M. Majdalani, C.A. Kontogiorgis, D. Hadjipavlou-Litina, and P. Kefalas, *Natural and synthetic 2'-hydroxy-chalcones and aurones: synthesis, characterization and evaluation of the antioxidant and soybean lipoxygenase inhibitory activity.* Bioorganic & medicinal chemistry, 2009. **17**(23): p. 8073-85.
38. A.M. Henry, D. Manicacci, M. Falque, and C. Damerval, *Molecular evolution of the Opaque-2 gene in Zea mays L.* Journal of molecular evolution, 2005. **61**(4): p. 551-8.
39. M. Nishihara and T. Nakatsuka, *Genetic engineering of flavonoid pigments to modify flower color in floricultural plants.* Biotechnology letters, 2011. **33**(3): p. 433-41.
40. Y. Tanaka, Y. Katsumoto, F. Brugliera, and J.P.C.T.O.C. Mason, 1–24., *Genetic engineering in floriculture.* Journal of Plant Biotechnology, 2005. **80**: p. 1-24.
41. S. Shrestha, S. Natarajan, J.H. Park, D.Y. Lee, J.G. Cho, G.S. Kim, Y.J. Jeon, S.W. Yeon, D.C. Yang, and N.I. Baek, *Potential neuroprotective flavonoid-based inhibitors of CDK5/p25 from Rhus parviflora.* Bioorg Med Chem Lett, 2013. **23**(18): p. 5150-4.
42. N. Shanker, O. Dilek, K. Mukherjee, D.W. McGee, and S.L. Bane, *Aurones: Small Molecule Visible Range Fluorescent Probes Suitable for Biomacromolecules.* Journal of fluorescence, 2011.
43. H. Chen, Y. Sun, C. Zhou, D. Cao, Z. Liu, and L. Ma, *Three hydroxy aurone compounds as chemosensors for cyanide anions.* Spectrochim Acta A Mol Biomol Spectrosc, 2013. **116C**: p. 389-393.
44. B. Orlikova, D. Tasdemir, F. Golais, M. Dicato, and M. Diederich, *The aromatic ketone 4'-hydroxychalcone inhibits TNFalpha-induced NF-kappaB activation via proteasome inhibition.* Biochemical pharmacology, 2011. **82**(6): p. 620-31.
45. B. Orlikova, D. Tasdemir, F. Golais, M. Dicato, and M. Diederich, *Dietary chalcones with chemopreventive and chemotherapeutic potential.* Genes &

nutrition, 2011. **6**(2): p. 125-47.
46. C. Zwergel, F. Gaascht, S. Valente, M. Diederich, D. Bagrel, and G. Kirsch, *Aurones: interesting natural and synthetic compounds with emerging biological potential.* Nat Prod Commun, 2012. **7**(3): p. 389-94.
47. F. Souard, S. Okombi, C. Beney, S. Chevalley, A. Valentin, and A. Boumendjel, *1-Azaaurones derived from the naturally occurring aurones as potential antimalarial drugs.* Bioorganic & medicinal chemistry, 2010. **18**(15): p. 5724-31.
48. B.P. Bandgar, S.A. Patil, B.L. Korbad, S.C. Biradar, S.N. Nile, and C.N. Khobragade, *Synthesis and biological evaluation of a novel series of 2,2-bisaminomethylated aurone analogues as anti-inflammatory and antimicrobial agents.* European journal of medicinal chemistry, 2010. **45**(7): p. 3223-7.
49. K.N. Tiwari, J.P. Monserrat, A. Hequet, C. Ganem-Elbaz, T. Cresteil, G. Jaouen, A. Vessieres, E.A. Hillard, and C. Jolivalt, *In vitro inhibitory properties of ferrocene-substituted chalcones and aurones on bacterial and human cell cultures.* Dalton Trans, 2012. **41**(21): p. 6451-7.
50. A.L. Liu, H.D. Wang, S.M. Lee, Y.T. Wang, and G.H. Du, *Structure-activity relationship of flavonoids as influenza virus neuraminidase inhibitors and their in vitro anti-viral activities.* Bioorganic & medicinal chemistry, 2008. **16**(15): p. 7141-7.
51. R. Haudecoeur, A. Ahmed-Belkacem, W. Yi, A. Fortune, R. Brillet, C. Belle, E. Nicolle, C. Pallier, J.M. Pawlotsky, and A. Boumendjel, *Discovery of Naturally Occurring Aurones That Are Potent Allosteric Inhibitors of Hepatitis C Virus RNA-Dependent RNA Polymerase.* Journal of medicinal chemistry, 2011.
52. S.Y. Shin, M.C. Shin, J.S. Shin, K.T. Lee, and Y.S. Lee, *Synthesis of aurones and their inhibitory effects on nitric oxide and PGE(2) productions in LPS-induced RAW 264.7 cells.* Bioorganic & medicinal chemistry letters, 2011. **21**(15): p. 4520-3.
53. H.M. Sim, C.Y. Lee, P.L. Ee, and M.L. Go, *Dimethoxyaurones: Potent inhibitors of ABCG2 (breast cancer resistance protein).* European journal of pharmaceutical sciences : official journal of the European Federation for Pharmaceutical Sciences, 2008. **35**(4): p. 293-306.
54. G. Lewin, G. Aubert, S. Thoret, J. Dubois, and T. Cresteil, *Influence of the skeleton on the cytotoxicity of flavonoids.* Bioorg Med Chem, 2012. **20**(3): p. 1231-9.
55. M. Ono, Y. Maya, M. Haratake, K. Ito, H. Mori, and M. Nakayama, *Aurones serve as probes of beta-amyloid plaques in Alzheimer's disease.* Biochemical and biophysical research communications, 2007. **361**(1): p. 116-21.
56. K. Manjulatha, S. Srinivas, N. Mulakayala, D. Rambabu, M. Prabhakar, K.M. Arunasree, M. Alvala, M.V. Basaveswara Rao, and M. Pal, *Ethylenediamine diacetate (EDDA) mediated synthesis of aurones under ultrasound: their evaluation as inhibitors of SIRT1.* Bioorg Med Chem Lett, 2012. **22**(19): p. 6160-5.
57. M. Zhang, X.H. Xu, Y. Cui, L.G. Xie, and C.H. Kong, *Synthesis and herbicidal potential of substituted aurones.* Pest Manag Sci, 2012. **68**(11): p. 1512-22.
58. R. Shakya, J. Ye, and C.M. Rommens, *Altered leaf colour is associated with increased superoxide-scavenging activity in aureusidin-producing transgenic plants.* Plant Biotechnol J, 2012. **10**(9): p. 1046-55.
59. T.T. Huong, N.X. Cuong, H. Tram le, T.T. Quang, V. Duong le, N.H. Nam, N.T. Dat, P.T. Huong, C.N. Diep, P.V. Kiem, and C.V. Minh, *A new prenylated aurone from Artocarpus altilis.* J Asian Nat Prod Res, 2012. **14**(9): p. 923-8.
60. T. Tronina, A. Bartmanska, J. Poplonski, and E. Huszcza, *Transformation of xanthohumol by Aspergillus ochraceus.* J Basic Microbiol, 2013.
61. P. Cagniant, G. Kirsch, and P. Legendre, *Contribution à l'étude du naphto-[2.3-b]furanne et de son analogue sélénié le naphto-[2.3-b] sélénophène.* C.

R. Acad. Sci., Ser. C, 1973. **276**(Copyright (C) 2013 American Chemical Society (ACS). All Rights Reserved.): p. 1629-31.
62. J.A. Beutler, E. Hamel, A.J. Vlietinck, A. Haemers, P. Rajan, J.N. Roitman, J.H. Cardellina, and M.R. Boyd, *Structure−Activity Requirements for Flavone Cytotoxicity and Binding to Tubulin.* Journal of medicinal chemistry, 1998. **41**(13): p. 2333-2338.
63. M. Lopez-Lazaro, *Distribution and biological activities of the flavonoid luteolin.* Mini Rev Med Chem, 2009. **9**(1): p. 31-59.
64. J.J. Peterson, J.T. Dwyer, P.F. Jacques, and M.L. McCullough, *Associations between flavonoids and cardiovascular disease incidence or mortality in European and US populations.* Nutrition Reviews, 2012. **70**(9): p. 491-508.
65. R. Ali, Z. Mirza, G.M.D. Ashraf, M.A. Kamal, S.A. Ansari, G.A. Damanhouri, A.M. Abuzenadah, A.G. Chaudhary, and I.A. Sheikh, *New Anticancer Agents: Recent Developments in Tumor Therapy.* Anticancer Res, 2012. **32**(7): p. 2999-3005.
66. C. Kontogiorgis, A. Detsi, and D. Hadjipavlou-Litina, *Coumarin-based drugs: a patent review (2008 – present).* Expert Opin Ther Pat, 2012. **22**(4): p. 437-454.
67. S. Valente, E. Bana, E. Viry, D. Bagrel, and G. Kirsch, *Synthesis and biological evaluation of novel coumarin-based inhibitors of Cdc25 phosphatases.* Bioorg Med Chem Lett, 2010. **20**(19): p. 5827-30.
68. K. Ito and J. Sawanobori, *4-Diazomethyl-7-Methoxycoumarin as a New Type of Stable Aryldiazomethane Reagent.* Synthetic Communications, 1982. **12**(9): p. 665-671.
69. F. Kröhnke and E. Börner, *Über α-Keto-aldonitrone und eine neue Darstellungsweise von α-Keto-aldehyden.* Berichte der deutschen chemischen Gesellschaft (A and B Series), 1936. **69**(8): p. 2006-2016.
70. H. Harnisch, *Chromon-3-carbaldehyde.* Justus Liebigs Annalen der Chemie, 1973. **765**(1): p. 8-14.
71. R. Araya-Maturana, J. Heredia-Moya, H. Pessoa-Mahana, and B. Weiss-López, *Improved Selective Reduction of 3-Formylchromones Using Basic Alumina and 2-Propanol.* Synthetic Communications, 2003. **33**(18): p. 3225-3231.
72. T. Shankar, R. Gandhidasan, and S. Venkataraman, *Synthesis and characterization and anti-inflammatory and antibacterial evaluation of 3-arylidene-7-methoxychroman-4-ones.* Indian J. Chem., Sect. B: Org. Chem. Incl. Med. Chem., 2011. **50B**(Copyright (C) 2012 American Chemical Society (ACS). All Rights Reserved.): p. 1202-1207.
73. A. Caşcaval, *2-Hydroxyketone, V. Darstellung substituierter Chromone.* Liebigs Annalen der Chemie, 1980. **1980**(5): p. 669-672.
74. T. Patonay, A. Kiss-Szikszai, V.M.L. Silva, A.M.S. Silva, D.C.G.A. Pinto, J.A.S. Cavaleiro, and J. Jekő, *Microwave-Induced Synthesis and Regio- and Stereoselective Epoxidation of 3-Styrylchromones.* European Journal of Organic Chemistry, 2008. **2008**(11): p. 1937-1946.
75. P.-L. Zhao, J. Li, and G.-F. Yang, *Synthesis and insecticidal activity of chromanone and chromone analogues of diacylhydrazines.* Bioorganic & Medicinal Chemistry, 2007. **15**(5): p. 1888-1895.
76. K.F. Shelke, B.R. Madje, S.B. Sapkal, B.B. Shingate, and M.S. Shingare, *An efficient ionic liquid promoted Knoevenagel condensation of 4-oxo-4H-benzopyran-3-carbaldehyde with Meldrum's acid.* Green Chemistry Letters and Reviews, 2009. **2**(1): p. 3-7.
77. J. Alderete, J. Belmar, M. Parra, C. Zúñiga, and V. Jimenez, *Esters derived from 7-decanoyloxychromone-3-carboxylic acid: synthesis and mesomorphic properties.* Liquid Crystals, 2003. **30**(11): p. 1319-1325.
78. H. Dueckert, V. Khedkar, H. Waldmann, and K. Kumar, *Lewis Base Catalyzed [4+2] Annulation of Electron-Deficient Chromone-Derived Heterodienes and*

Acetylenes. Chem.--Eur. J., 2011. **17**(Copyright (C) 2012 American Chemical Society (ACS). All Rights Reserved.): p. 5130-5137, S5130/1-S5130/20.
79. A.M. Piloto, A.S.C. Fonseca, S.P.G. Costa, and M.S.T. Gonçalves, *Carboxylic fused furans for amino acid fluorescent labelling.* Tetrahedron, 2006. **62**(39): p. 9258-9267.
80. N. Hadj-Esfandiari, L. Navidpour, H. Shadnia, M. Amini, N. Samadi, M.A. Faramarzi, and A. Shafiee, *Synthesis, antibacterial activity, and quantitative structure-activity relationships of new (Z)-2-(nitroimidazolylmethylene)-3(2H)-benzofuranone derivatives.* Bioorg. Med. Chem. Lett., 2007. **17:** p. 6354-6363.
81. G. Jones and S.P. Stanforth, *The Vilsmeier Reaction of Non-Aromatic Compounds*, in *Organic Reactions*. 2004, John Wiley & Sons, Inc.
82. P. Cagniant and G. Kirsch, *Méthode de synthése des [2H] benzofurannones-3 mono et polysubstituées et des benzo [b] furannes correspondants.* C. R. Acad. Sci., Ser. C, 1976. **282**: p. 993-96.
83. K. Takaoka, Y. Tatsu, N. Yumoto, T. Nakajima, and K. Shimamoto, *Synthesis and photoreactivity of caged blockers for glutamate transporters.* Bioorganic & Medicinal Chemistry Letters, 2003. **13**(5): p. 965-970.
84. R.M. Seabra, P.B. Andrade, F. Ferreres, and M.M. Moreira, *Methoxylated aurones from cyperus capitatus.* Phytochemistry, 1997. **45**(4): p. 839-840.
85. T. Chen, S. Hevi, F. Gay, N. Tsujimoto, T. He, B. Zhang, Y. Ueda, and E. Li, *Complete inactivation of DNMT1 leads to mitotic catastrophe in human cancer cells.* Nat Genet, 2007. **39**(3): p. 391-6.
86. C.F. Carvalho and M.V. Sargent, *Naturally Occurring Dibenzofurans. Part 4. Synthesis of Dibenzofurandiols by Annelation of Benzofurans.* Journal of the Chemical Society, Perkin Transactions 1: Organic and Bio-Organic Chemistry (1972-1999), 1984(7): p. 1605 - 1612.
87. J. Bergman and B. Egestad, *A Study of a Condensation Product Obtained from 6-Methyl-3(2H)-benzofuranone and Acetic Anhydride.* Acta Chemica Scandinavica, Series B: Organic Chemistry and Biochemistry, 1980. **34**(3): p. 177 - 180.
88. S.K. Doifode, M.P. Wadekar, and S. Rewatkar, *Debromination of Aurone Dibromide with Sodium Hydrogen Sulphide.* Oriental Journal of Chemistry, 2011. **27**(2): p. 771-774.
89. A. Nebbioso, N. Clarke, E. Voltz, E. Germain, C. Ambrosino, P. Bontempo, R. Alvarez, E.M. Schiavone, F. Ferrara, F. Bresciani, A. Weisz, A.R. de Lera, H. Gronemeyer, and L. Altucci, *Tumor-selective action of HDAC inhibitors involves TRAIL induction in acute myeloid leukemia cells.* Nat Med, 2005. **11**(1): p. 77-84.

CHAPTER 3

- DNA-METHYLTRANSFERASE INHIBITORS -

3. DNMT Inhibitors

3.1 Introduction to Epigenetics

Epigenetics were initially defined in 1942 by Waddington as “the interactions between genes and their products leading to the realization of the phenotype” [90]. Nowadays it is more precisely described as “the changes happening on a chromosome without altering its DNA sequence, leading to a heritable and stable phenotype” [91, 92].

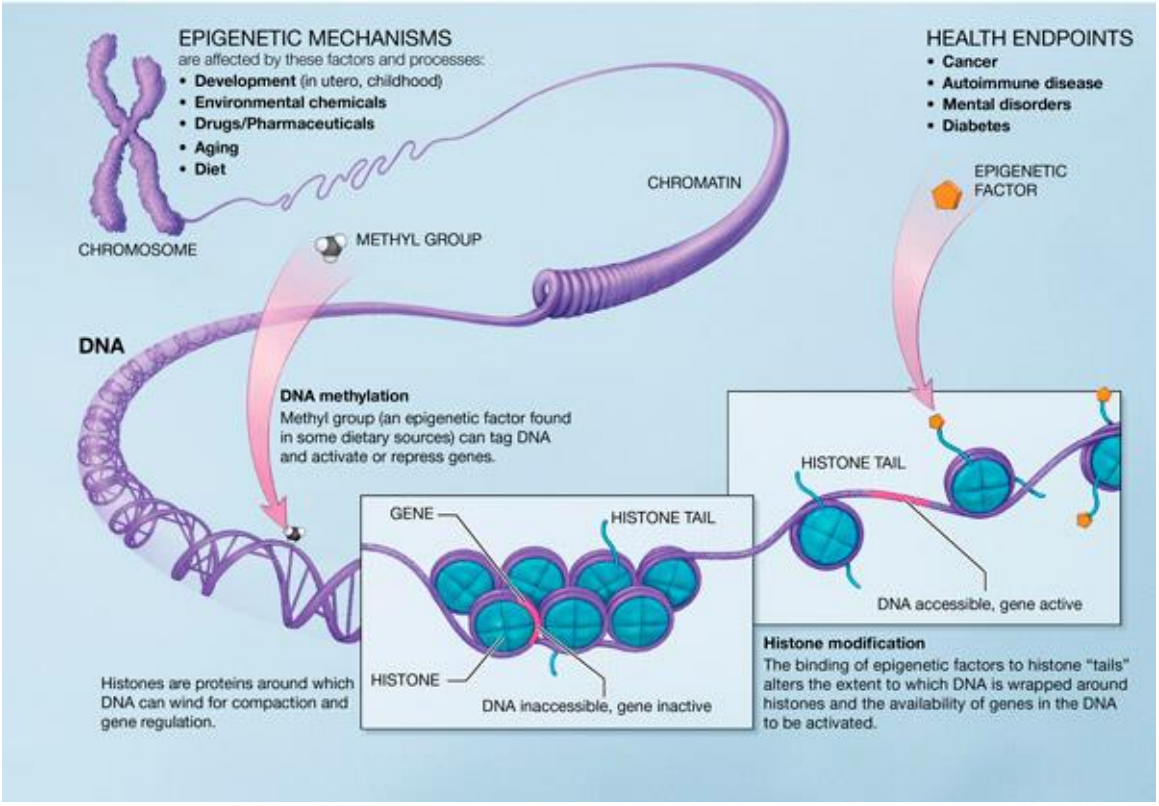

Figure 8: Overview on epigenetic targets

Epigenetic regulation of gene expression is mediated through at least five series of events involving changes of chromatin at molecular levels: DNA modifications, histone modifications, histone variants, noncoding RNAs (miRNA) and nucleosome remodelling. Epigenetic control of transcription is essential to drive cells towards their normal phenotype, and epigenetic dysregulation could lead to initiation and progression of human diseases including cancer [93-95].

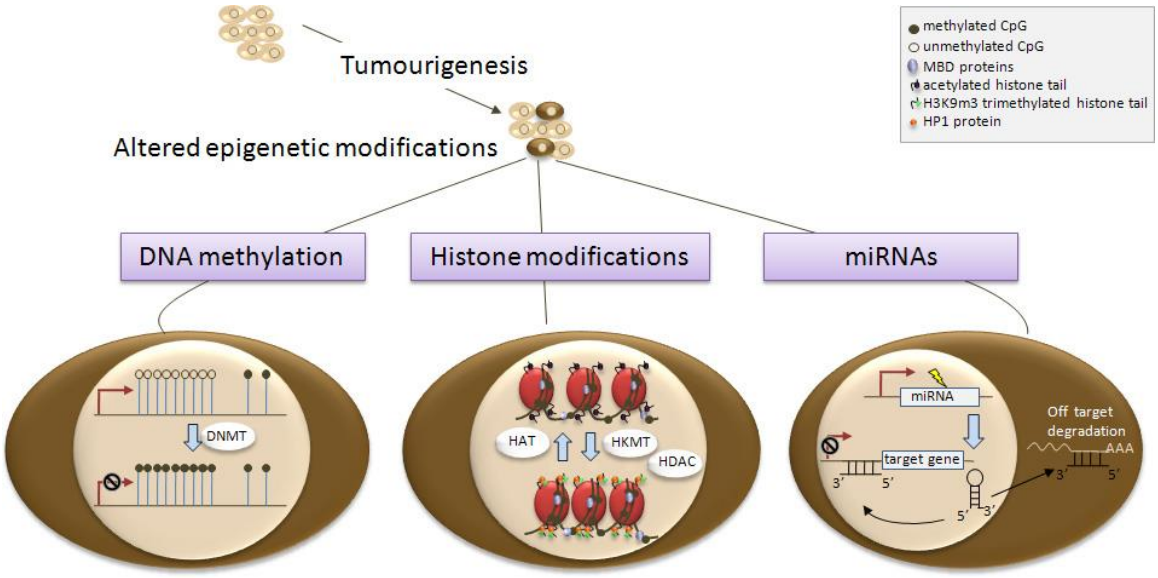

Figure 9: Epigenetic modifications, such as histone acetylation and methylation, and DNA methylation, open or close the chromatin structure, thus controlling gene expression or repression. DNMT for DNA methyltransferases, HATs stands for histone acetyltransferases, HKMT for histone lysinemethyltransferase, HDACs for histone deacetylases, miRNA for micro (noncoding) RNA and MBD for methyl-binding proteins.

3.2 DNA methyltransferases

3.2.1 General introduction

Among the five epigenetic events, DNA methylation has been widely studied. These modifications play an important role in the modulation of gene expression [96]. DNA methylation like other epigenetics events are on one hand crucial for embryonic development or differentiation [85, 97-99] and on the other hand the establishment of aberrant DNA methylation patterns are associated with under or over- expression of certain proteins leading to various pathologies like Alzheimer's disease [100, 101], depression, bipolar disorder, schizophrenia [101, 102] auto-immune diseases [103] and even in some genetic disorders (Crohn disease, atherosclerosis) [104, 105].Furthermore aberrant DNA methylation patterns have been extensively described in literature in numerous cancers as MyeloDysplastic Syndromes (MDS), Acute Myeloid Leukemia (AML) and Chronic Myelomonocytic Leukemia (CMML) [106-109]. Peterson et al. could demonstrate very recently that DNA methylation is depent on individual lifestyle choices such as nutrition or smoking through an epigenome-wide association study. These changes in the epigenome could lead to different pathologies according to the authors. [110]

DNA methylation is regulating gene expression through almost exclusive methylation of CpG islands in promoters, where about 60% of the promoter are lying [111]. Therefore these promoters are no longer recognized by transcription factors, resulting in a repression of the corresponding genes for example Tumour Suppressor Genes (TSG) [112-115]. The methylated CpGs are able to recruit methyl-binding domain proteins e.g. MeCP2, which could interact with other epigenetically important proteins (HDACs, HMTs) creating a repressive chromatin environment (Figure 8 and 9) [113, 115, 116]. In this way CpG methylation is crucial for a well-balanced equilibrium between activation and silencing of various genes in somatic cells. The maintenance of DNA methylation patterns possesses an error frequency of about 5% per cellular division [117] leaving certain flexibility for slight but probable important changes in the methylation patterns. Any disruption in these epigenetic processes might result in various above mentioned disorders [115, 118,

119].

Three DNA methyltransferases (DNMTs), DNMT1, DNMT3A and DNMT3B catalyse the transfer of a methyl group from *S*-adenosyl-L-methionine (AdoMet) to the C5-position of cytosine predominantly in the CpG dinucleotides (Figure 10) [120]. The maintenance methyltransferase DNMT1 was the first one described and characterized containing 1616 amino acids [121, 122]. It is most abundant in somatic cells and has a greater activity for hemi- than unmethylated substrates, intervening mainly after DNA replication to methylate the newly synthesized strand. [123-125]. Bestor *et al*. demonstrated that the disruption of the DNMT1 gene in healthy mice could lead to significant demethylation of the entire genome as well as to strongly reduced embryonic survival rate [126]. In normal healthy cells, partial or total knockout of DNMT1 has been connected with transcriptional silencing of important genes, leading to apoptosis [97], severe mitotic defects [85] and tumorigenesis through chromosomal instability [98, 99, 123].

Differently, de novo methyltransferase DNMT3A is only present in low amounts in somatic cells and shows no preference for hemi- or unmethylated DNA[124, 125, 127]. DNMT3A has been identified to mainly methylate pericentromeric regions of the DNA, whereas DNMT3B mainly centromeric regions [125, 128, 129]. In cancer cells, aberrant DNA methylation leads to hypermethylation at CpG islands, joined to a global hypomethylation, giving rise to genomic instability and inactivation of tumour suppressor genes[130]. Hypermethylation of CpG islands is so biologically relevant and specific that for each cancer a typical hypermethylome can be drawn [131].

Even if genetic origins of cancer are well accepted nowadays, there is clear evidence that epigenetic modifications are early events in tumorigenesis [118, 132, 133]. Interestingly, unlike genetic mutations, the epigenetic alterations are reversible [134]. Bearing in mind these ideas, DNMT inhibitors (DNMTi) are useful tools to reactivate tumour suppressor genes and to reprogram cancer cells towards growth arrest and death [135, 136].

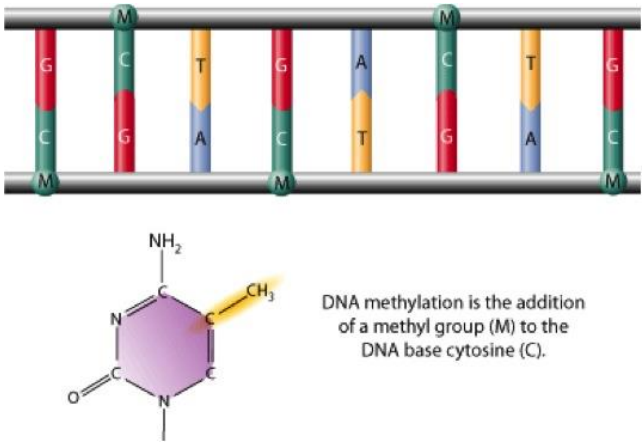

Figure 10: Cytosine DNA methylation- methyl group is transferred from *S*-adenosylmethionine to the C-5 position of cytosine by a family of cytosine (DNA-5)-methyltransferases (DNMT's).

3.2.1 Catalytic mechanism of DNMTs

The different DNMTs share among different species highly conserved[137], common features such as a N-terminal domain binding to DNA and having protein recognition domains to guide the DNMTs for example to the nucleus or to chromatin [138], as well as a catalytic C-terminal domain, which includes the binding site for the cofactor S-Adenosyl-L-Methionine (SAM), the proline-cysteine dipeptide bearing the catalytic thiolate group, the glutamine residue allowing the protonation of the 3-position of the cytosine and the recognition site for the targeted C5 position of the cytosine base [137, 139].

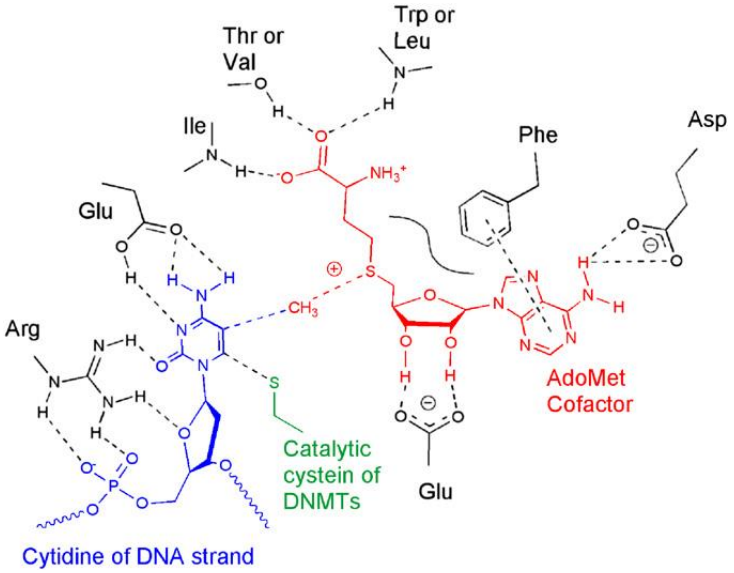

Figure 11: Scheme of catalytic site of the DNMTs [135]

These enzymes are able to transfer a methyl group from the cofactor SAM to the targeted cytosine.

A direct methylation in the 5-position of the cytosine is unlikely to happen in neutral aqueous media due to its poor reactivity [111]. Klimasauskas et al. demonstrated that the targeted cytosine is flipped out of the DNA double helix into the active site of the enzymes (Figure 11) [140].

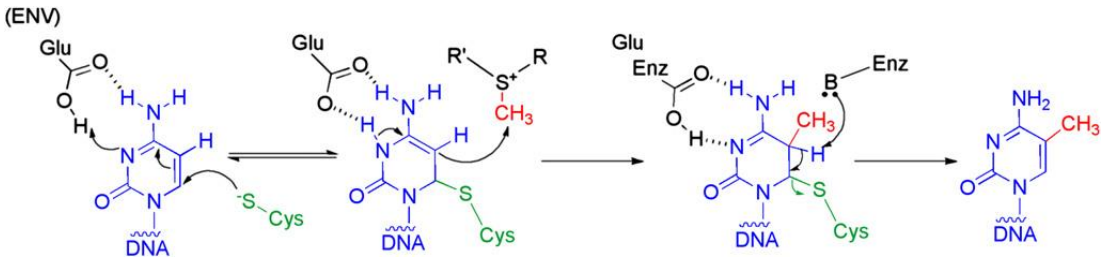

Scheme 12: Catalytic mechanism of C5-DNA methylation. The targeted cytidine is in blue, the methyl group in red and the catalytic thiolate in green. [135]

The enzymatic cascade starts with the nucleophilic attack of thiolate in the 6-position of the catalytic cysteine leading to the corresponding enamine (Scheme 12). After the glutamic acid containing ENV tripeptide is able to protonate the

cytosine in N3-position. A nucleophilic attack of the enamine on the SAM cofactor is leading to the methlygroup in the C5 position. The following deprotonation of the C5 by a base (depending on the DNMT) in the active site, releases at the same time S-Adenosyl-L-Homocysteine (SAH). The transferred methyl group creates a steric hindrance that favours the beta-elimination in order to recycle the enzyme and to release of the methylated cytosine [111, 141].

3.3 Known DNMT inhibitors

As highlighted before, the hypermethylation of tumour suppressor genes is often involved in canceriogenesis and cancer development. Because of the reversibility of the methylation, the demethylation is an interesting approach to fight cancer [93, 142].

Two different classes of DNMT inhibitors have been described in literature: the nucleoside analogues (Figure 13) that are known and studied for many years, and the non-nucleoside inhibitors (Figure 14) with broad structure diversity [143].

3.3.1 Nucleoside-like inhibitors

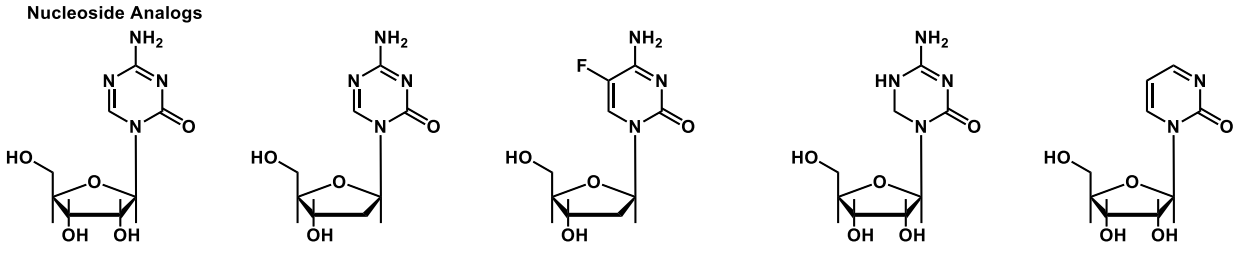

Figure 12: Nucleoside-like inhibitors of DNMTs.

Azacitidine **72** (Vidaza®), decitabine **73** (Dacogen®)and zebularine **76**

The first two molecules described as DNMT inhibitors, 5-azacytidine (azacitidine) **72**and 5-aza-2'- deoxycytidine (decitabine) **73**, are cytidine analogues in which the

carbon atom in position 5 is replaced by a nitrogen atom and linked to a ribose or a deoxyribose, respectively (Figure 13) They were initially used in leukemia chemotherapy as antimetabolites and cytotoxic agents [144]. In 1977 and 1978, Constantinides et al. published their hypomethylating properties [145, 146]. In the following years, several other analogues have been prepared and tested, among them 5,6-dihydro-5-azacytidine **74** and 5-fluoro-2'–deoxycytidine **75** [147].

These compounds are integrated into the genome during the S phase (replication) of the cell cycle, showing a limited specificity towards more rapidly proliferating cancer cells [148]. Once incorporated into the DNA, the cytosine analogues undergo the same DNMT-catalysed reaction as normal cytosines with the formation of a covalent intermediate between the catalytic cysteine of the enzyme and 6-position of cytosine analogs (Scheme 13). The beta- elimination reaction can no longer take place due to the presence of the nitrogen atom in 5-position instead of the carbon atom in cytosine, leading to an irreversible covalent complex [149]. This kind of inhibitor is called a suicide inhibitor, in this case triggering the proteasomal degradation of the DNMT [143, 150].

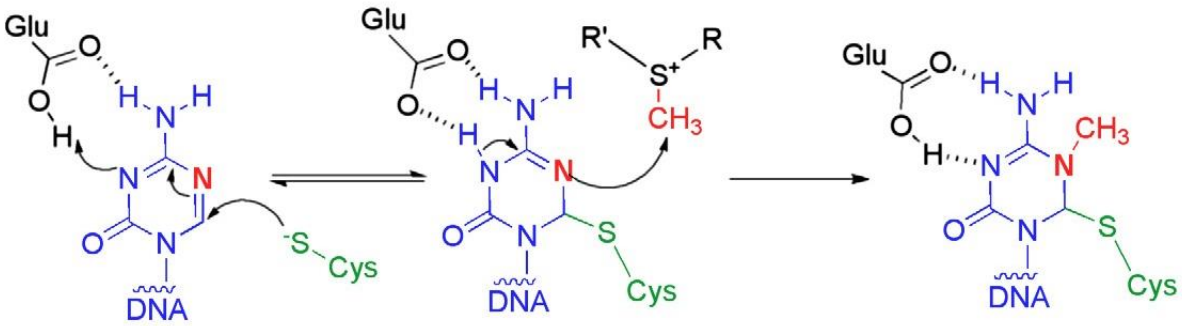

Scheme 13: Mechanism of the 5-azacytidine and 5-aza-2'-deoxycytidine.[135]

Zebularine **76** has a different mode of action [143]. The covalent intermediate is reversible and heat labile [151]. To date no evidence can be found in the literature regarding a possible clinical development of this compound.

Among all the nucleoside inhibitors described, azacitidine **72** and decitabine **73** have been approved by the FDA in 2004 and 2006, respectively, for haematological

malignancies [152]. Further clinical trials also in combination with other anticancer drugs are still on-going: Both approved drugs are in Phase II against melanoma, ovarian and prostate cancer, and in combination with inhibitors of HDACs against metastatic melanomas [143, 153]. However, despite their high efficacy such drugs suffer from poor bioavailability, chemical instability, and toxic side-effects [154]. Therefore they are used at low doses reducing the cytotoxicity in order to achieve mainly the demethylation effect [143].

Single-stranded DNA

Single- stranded DNA molecules including a sequence of 30 bases and a phosphorothioate backbone have been described as allosteric inhibitors of DNMT1 [155]. However such an approach appears to be discontinued as no further studies have been published in regard to severe side effects.

These nucleoside-like inhibitors proved their efficiency in various clinical trials, but their lack of specificity and their strong unwanted side effects is leading to the development of novel more selective DNMT inhibitors.

3.3.2 Non-nucleoside inhibitors

In the last years, a particular interest has emerged from non-nucleoside molecules sharing only a DNA incorporation independent mechanism. Most of the molecules described in literature are compounds that have already demonstrated a biological action against other targets than DNMTi e.g. procainamide, hydralazine, psammaplin A or epigallocatechin-3-O-gallate (EGCG) (see Figure 13) [143].

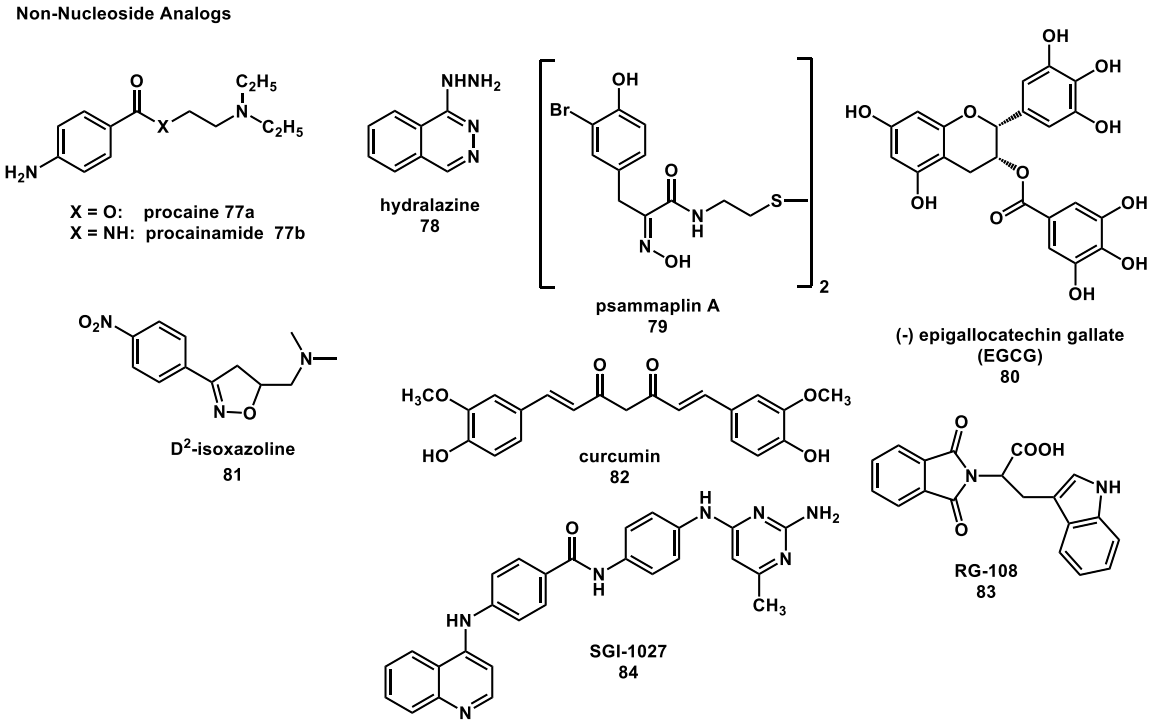

Figure 13: Non-Nucleoside analogs inhibitors of DNMTs.

Procainamide and procaine **77a-b**

Procainamide and its ester analogue, procaine is in use for more than 30 years as antiarrhythmic and anaesthetic agents, respectively. Its DNMT inhibitory effects were discovered through their secondary effects [156]. However different studies [157-161] in vitro and in vivo show no homogeneity in the used protocols and obtained results despite its affinity for the CpG-rich regions of DNA [162], making it difficult to evaluate the DNMT inhibitory activities of procaine and its analogues. Chuang et al as well as Stresemann *et al.* suppose another mechanism than DNA

methylation inhibition as responsible for apoptosis [160, 161].

Hydralazine **78**

Hydralazine is a well-known antihypertensive drug [163]. Similar to procaine, its secondary effects led to the discovery of its DNMT inhibitory properties. Despite its frequent use for many years, its mechanism has not been elucidated so far [93].

Hydralazine activity to inhibit DNMTs is still controversial. Some in vitro studies do not exhibit any specific DNMT inhibition. Like mentioned above Chuang et al., for example, compared hydralazine and procainamide on bladder, prostate and colon cancer cell lines [160]reporting no hypomethylation. In contrast several clinical trials in T-cells, brain and ovary tumours [164-167] revealed the demethylation potential of hydralazine. So it may be possible that the DNMT inhibitory effect of hydralazine is specific to very few cell lines.

This could be an advantage in the future development by decreasing the risk to induce a global demethylation of the entire DNA, which could have unwanted side effects in healthy cells [135]

Psammaplin A **79**

Psammaplin A, a dimer of two derivatives of 3-bromotyrosine, is a natural compound extracted from a sponge, the Psammaplinaplysilla. It was described as inhibitor of different enzymes, such as topoisomerase II [168], DNA gyrase [169], leucine aminopeptidase [52], HDACs or DNMTs [170]. Kim et al suggested that this compound has rather a strong HDAC inhibitory activity than a DNMT one [171].

Epigallocatechin-3-O-gallate (EGCG) **80**

One of the most studied flavonoid is epigallocatechin-3-O-gallate (EGCG). EGCG is the main flavonoid in the green tea. Its preventive anti-cancerous properties as well as numerous targets (protein kinases, highly reactive hydrogen peroxides.) have been extensively studied [172-174].

In vitro studies revealed that EGCG does not act as indirect inhibitors of DNMTs via

an increase of SAH like other catechins, but more like as a direct competitive inhibitor, preventing the cytosine to enter into the active site [175]. However the DNMT inhibition activity of EGCG is still questioned [138] due to the fact that recently published results demonstrated that EGCG is more likely inducing oxidative stress leading to apoptosis but without genomic demethylation [160, 161].
So this compound class could be seen more as chemopreventive drugs rather than actual treatment drugs [174, 176].

Isoxazolines **81**

Based on the procainamide structure Castellano *et al.* used the frozen analogue approach replacing the amide function by an isoxazoline nucleus [177, 178]. Their idea was to reduce the flexibility of the procainamide molecule.
These compounds were revealed to be modest inhibitors of DNMT1 (IC_{50} around 150 mM). As concluded by the authors, further studies are needed to improve the potency of such derivatives [178].

Curcumin **82**

Virtual screening using a DNMT1 homology model revealed two probable binding modes for curcumin in the catalytic domain. Despite the docking results and numerous in vitro and in vivo studies, curcumin is known to interact with different biological targets. Therefore no clear evidence of pharmacological activities has been demonstrated in in vivo models neither in human therapy [179, 180].

RG108 (phthalimido-L-tryptophan) **83**

RG108 is a DNMT inhibitor found by virtual screening on DNMT1 [181, 182] RG108 inhibits in vitro M. SssI and human DNA methylation in HCT116 and NALM6 (leukemia) cells at 100 mM. Stresemann *et al.* demonstrated that, in contrast to most other DNMTs inhibitors, RG108 is neither genotoxic, nor cytotoxic [161]. However the cellular DNMT inhibition potency of RG108 is not clear due to variant observation in different studies [135, 183].

SGI 1027 **84**

SGI-1027 is a lipophilic quinoline inhibiting DNMT1, 3A and 3B that was initially prepared as an antitumour agent. In the late 1970's Denny *et al.* published that quinolinium salts bind strongly but nevertheless reversibly to the DNA minor groove, leading to cell death by a still unknown mechanism [184]. This compound is a weak base and has a relatively good stability in physiological media. Its activity was tested in vitro on bacterial as well as mammalian DNMTs [185]. All DNMTs are inhibited by SGI-1027 because of the very conserved motifs involved in the recognition of the SAM cofactor [111].

3.4 Summary of the literature survey

So why is the design of new DNMT inhibitors interesting? On the one hand, they can be used further elucidate the role of DNA methylation in normal as wells as cancer cells [186] and the other hand DNA methylation is a promising therapeutical target in different cancer types, but also in other diseases such as neurological disorders [187].Although the first non-selective inhibitors were discovered in the 1960, there is still a lot to investigate on the road ahead to effective and selective future therapies. To date none of the previously described non-nucleoside inhibitors have entered clinical development yet, so there is still a long way to go before such compounds might reach the bedside of a patient. Concerning their potential use as drugs, a direct cytotoxic effect is no more wanted, instead the epigenetic therapy treats cancer by reprogramming cells which decide of their own fate [135].

3.5 Optimisation study SGI 1027

Here we report the results of an optimization study on the non-nucleoside lead compound SGI-1027 (**84**) [135]. The rational design, the synthetic routs and the biological evaluation in cancer cells will be presented.

This compound **84** identified among a series of quinoline-based compounds developed as anticancer drugs, has attracted our attention because of its high potency in both enzyme and cell assays[185]. Because the structure of **84** shows four fragments (4-aminoquinoline + 4- 3aminobenzoic acid + 1,4-phenylenediamine + 2,4-diamino-6-methylpyrimidine) linked in sequence with *para*/*para* orientation, we prepared a series of regioisomers of compound **84** by shifting each fragment's linkage from *para* to *meta* or *ortho* position (Fig. 15a), so obtaining compounds **85**-**92** (Figure 14). In addition, we prepared two related compounds (**93**, **94**) showing either a bis-quinoline or bis-pyrimidine structure and two truncated compounds (**95**, **96**) lacking the "right" pyrimidine or the "left" quinolone portion, respectively (Figure 14).

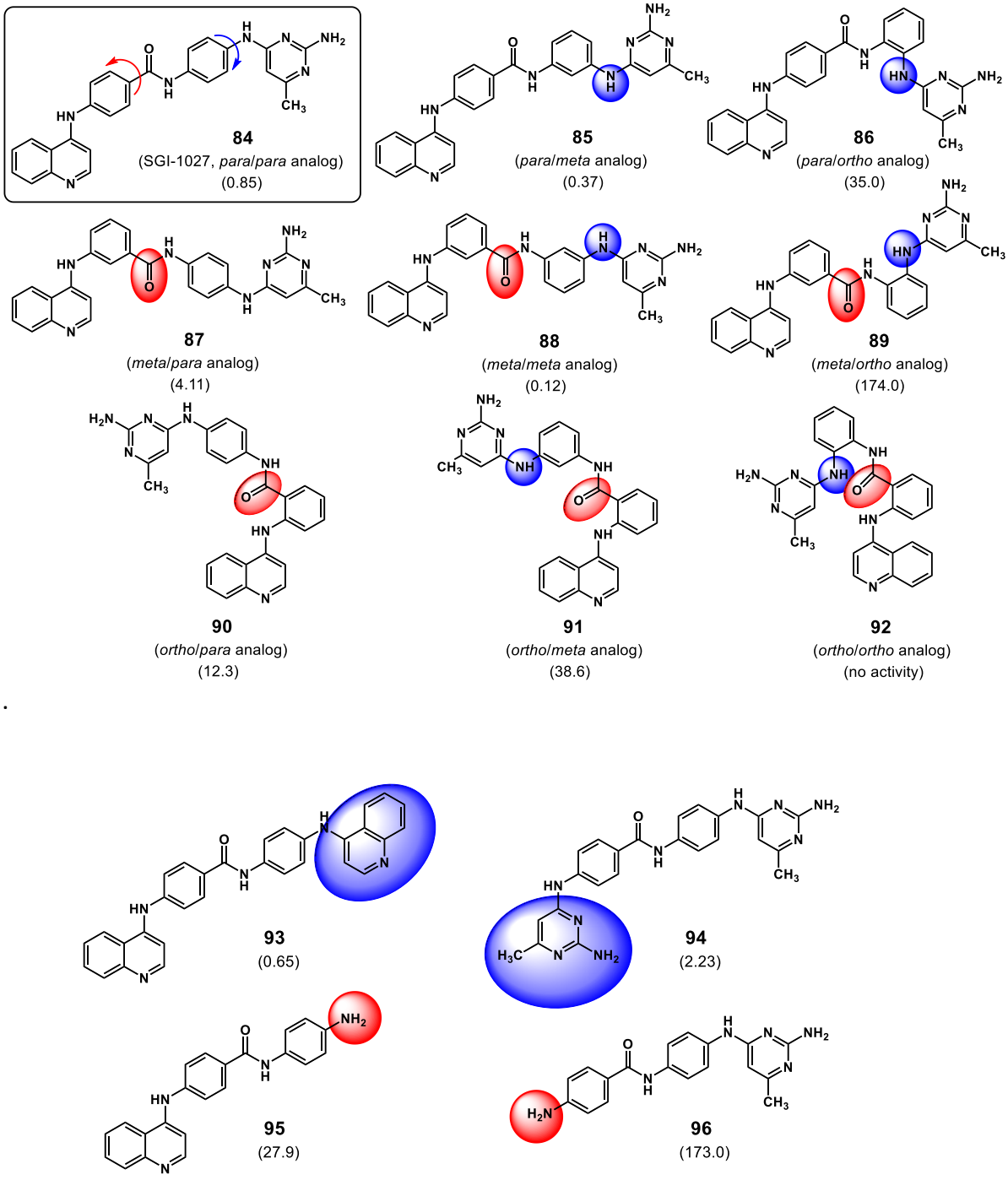

Figure 14: Chemical structures of SGI-1027 **84** and the related analogs **85**-**96** described in this study. Their IC_{50} values (μM) from nanoscale HTS against human DNMT1 are reported in brackets.

3.5.1 Chemical synthesis of compounds 84-96

Compounds **84**-**92** were prepared by coupling the 2-, 3-, or 4-(quinolin-4-ylamino)benzoic acid **97a-c** with the N^4-(2-, 3-, or 4-aminophenyl)-6-methylpyrimidine-2,4-diamine **98a-c**, in the presence of benzotriazol-1-yl-oxytripyrrolidinophosphonium hexafluorophosphate (PyBOP) and triethylamine, in dry *N,N*-dimethylformamide as solvent (Scheme 14).

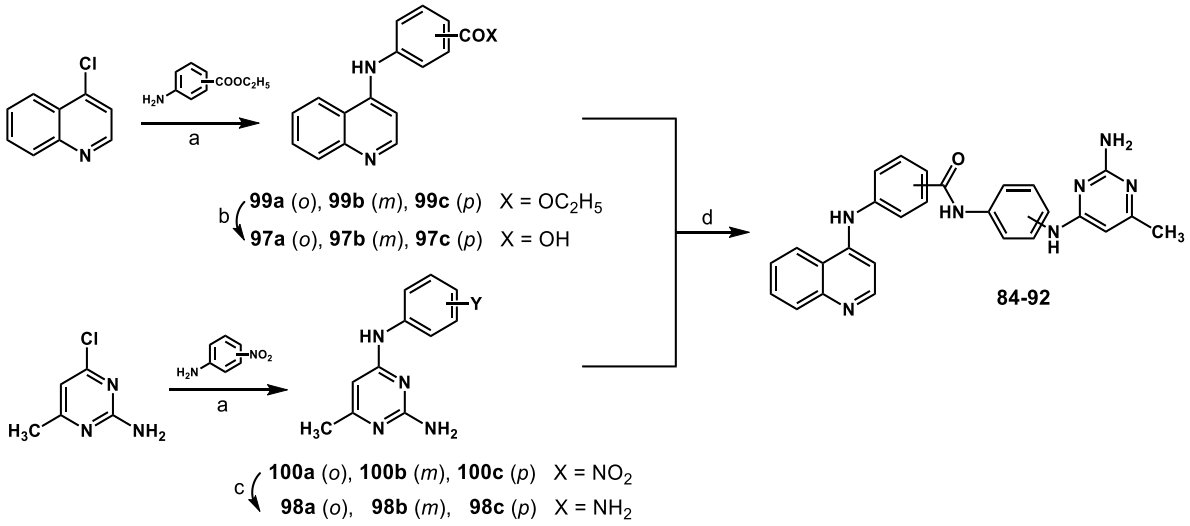

Scheme 14: Reagents and conditions: (a): 37% HCl, CH_3CH_2OH, 80 °C, 2 h; (b): 2 N KOH, CH_3CH_2OH; (c): stannous chloride dihydrate, 37% HCl, CH_3CH_2OH, 1 h, 80 °C; (d): $(C_2H_5)_3N$, PyBOP, anhydrous DMF, N_2 atmosphere, room temperature, 1 h.

PyBOP (benzotriazol-1-yl-oxytripyrrolidinophosphonium hexafluorophosphate) is usually used as a peptide coupling reagent. However it can be used for coupling an acid **i** with an amine **v** to form an amide **vi** (Scheme 15)[188]. We used this reagent as a convenient method to build up our SGI1027 analogues. The not very reactive acid **i** is activated through the phosphonium salt **iv** or the ester **ix** via a base catalyzed nucleophilic attack of the carboxylate on the positively charged phosphor of PyBOP. The so activated acid **iv** can either directly react with a primary amine **v** to the desired amide **vi** or compound iv can undergo a transesterification with 1H-benzo[d][1,2,3]triazol-1-olate **v** to the ester **ix**. The latter one is known to react

slower with the amine **v** to the desired amide **vi**. The driving force of the reaction is the formation of the stable phosphoric triamide **vii**.

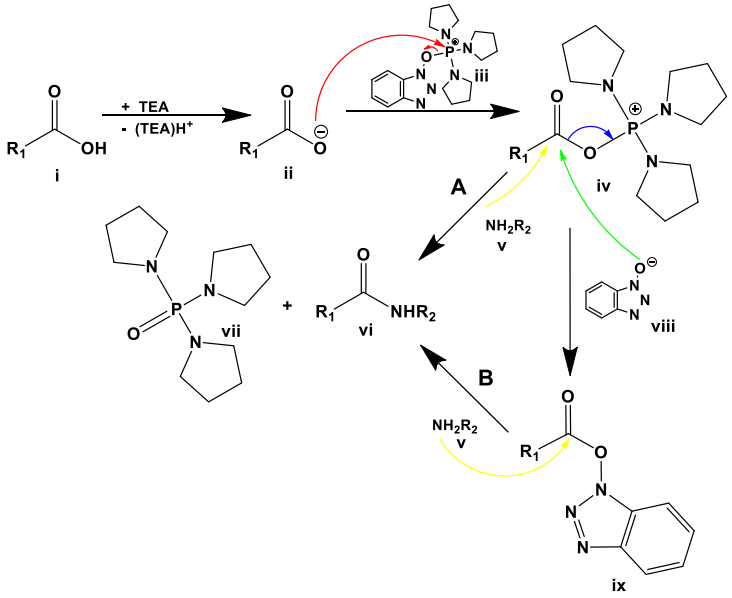

Scheme 15: General reaction mechanism for an amidation via PyBOP, the arrow in red represents a nucleophilic attack of PyBOP to activate the acid, the green one represents the transesterification and the yellow ones the nucleophilic attack to finally form the desired amid

The intermediate compounds **97a-c** (Scheme 14) were prepared by reaction between 4-chloroquinoline with the appropriate ethyl 2-, 3-, or 4-aminobenzoate and 37% hydrochloric acid in ethanol at 80 °C. The obtained ethyl benzoates **99a-c** underwent basic hydrolysis using 2 N potassium hydroxide to afford the corresponding acids **97a-c**. The same reaction conducted with 4-chloro-6-methylpyrimidin-2-amine and the opportune 2-, 3-, or 4-nitroanilines in the presence of 37% hydrochloric acid and ethanol at 80 °C furnished the nitro-intermediates **100a-c** which were in turn reduced with stannous chloride dihydrate and 37% hydrochloric acid in ethanol to the corresponding anilines **98a-c**.

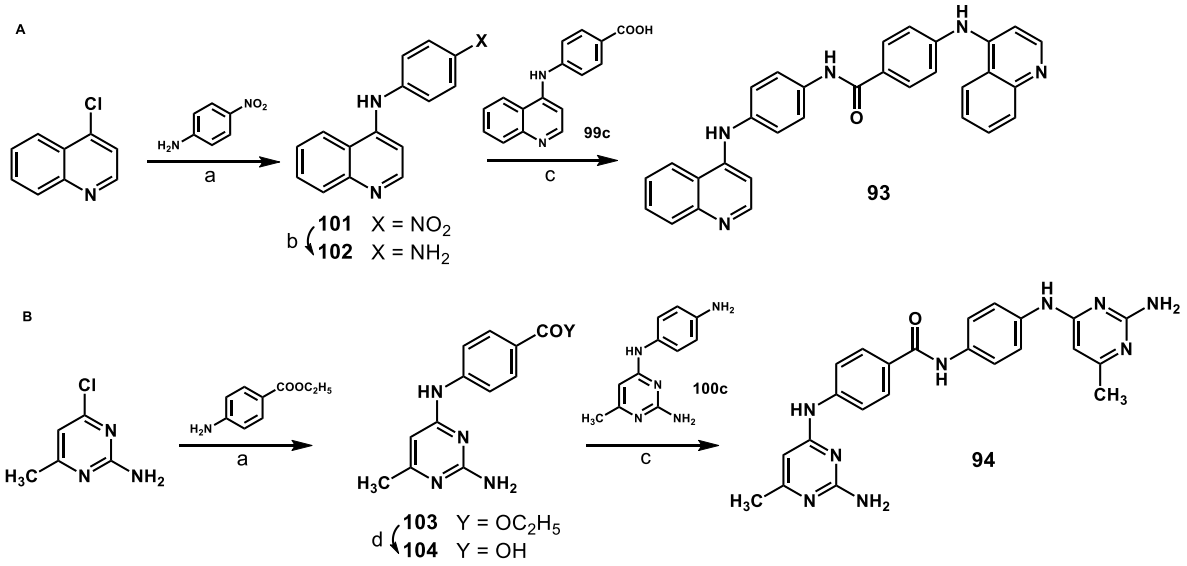

Scheme 16: Reagents and conditions: (a): 37% HCl, CH_3CH_2OH, 80 °C, 2 h; (b): stannous chloride dihydrate, 37% HCl, CH_3CH_2OH, 80 °C, 1 h; (c): $(C_2H_5)_3N$, PyBOP, anhydrous DMF, N_2 atmosphere, room temperature, 1 h; (d): 2 N KOH, CH_3CH_2OH.

The bisquinoline **93** was obtained by treating 4-chloroquinoline with 4-nitroaniline and, after reduction of the nitro group of the resulting intermediate **18** to the corresponding aniline **19**, by coupling **102** with **99c** (Scheme 16A). Treatment of 4-chloro-6-methylpyrimidin-2-amine with ethyl 4-aminobenzoate afforded the intermediate ester **103**, which was hydrolyzed to the acid **104** and then coupled with **100c** to furnish the bispyrimidine **94** (Scheme 16B).

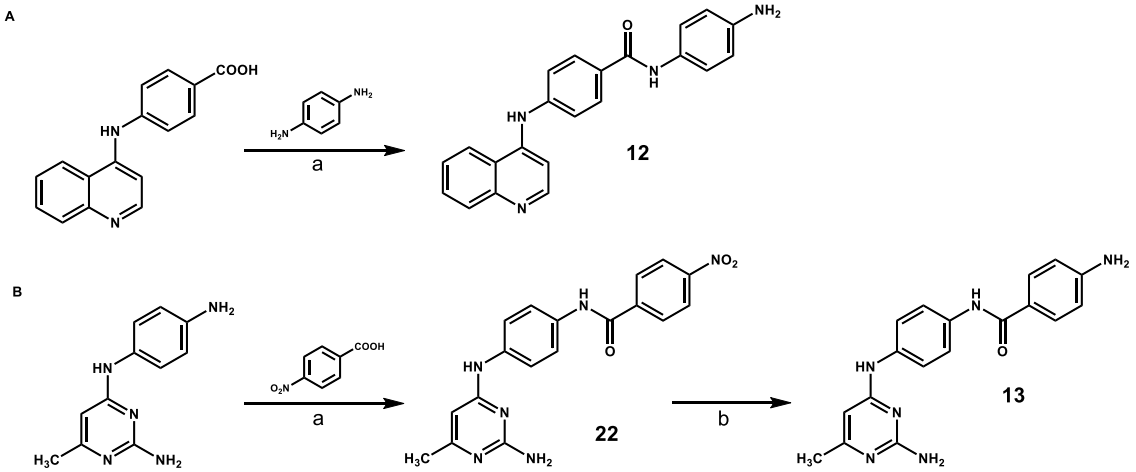

Scheme 17: Reagents and conditions: (a): $(C_2H_5)_3N$, PyBOP, anhydrous DMF, N_2 atmosphere, room temperature, 1 h; (b): stannous chloride dihydrate, 37% HCl, CH_3CH_2OH, 80 °C, 1 h.

The truncated compounds **95** and **96** were prepared by reaction of **99c** with 4-phenylendiamine **95**, or by reaction of **100c** with 4-nitrobenzoic acid and subsequent reduction of the nitro group of the intermediate **105** to the corresponding amine **96** (Scheme 17).

3.5.2 Biochemical and biological results

3.5.2.1 DNMT1, DNMT3A2/3L, PRMT1 and GLP assays

From a nanoscale pre-screening performed on **84**-**96** against human DNMT1 using poly(dI-dC) as substrate, compounds **85**, **87** and **88**, obtained by replacing either or both the *para* with the *meta* linkages in the **84** structure, emerged as highly efficient DNMT1 inhibitors, whereas the *ortho* regioisomers were less potent (**86**, **89**-**91**) or totally inactive (**92**). The bisquinoline **93** displayed similar potency as **84** against DNMT1, while the bispyrimidine **11** was less efficient, and the truncated compounds **95** and **96** showed a severe drop of inhibition (Figure 14 and 15a).

To perform wider and more accurate assays against DNMTs, we tested the most potent compounds **85**, **87**, **88**, **93** and **94** in comparison with **84** against human DNMT1 using a hemimethylated substrate and human DNMT3A2/DNMT3L complex using an unmethylated substrate (Figure 15b). Under these assay conditions, the *meta*/*meta* analog **88** (IC_{50} = 9 μM) displayed a 4-fold higher activity than **84** against DNMT1, while the *para*/*meta* (**85**) and the *meta*/*para* (**87**) analogs were 2.5- and 7.6-fold less potent, respectively. The bisquinoline **93** showed the same DNMT1 inhibiting activity as **84**, while the bispyrimidine **94** was 2-fold less active. Against DNMT3A2/DNMT3L, all the inhibitors were more efficient than against DNMT1, and **88** was again the most potent with IC_{50} = 2.8 μM [IC_{50} (**84)** = 10 μM]. Among the remaining compounds, **94** and **85** were 2-fold less potent than **1**, and lower activities were registered with **93** and **87** (Figure 15b).

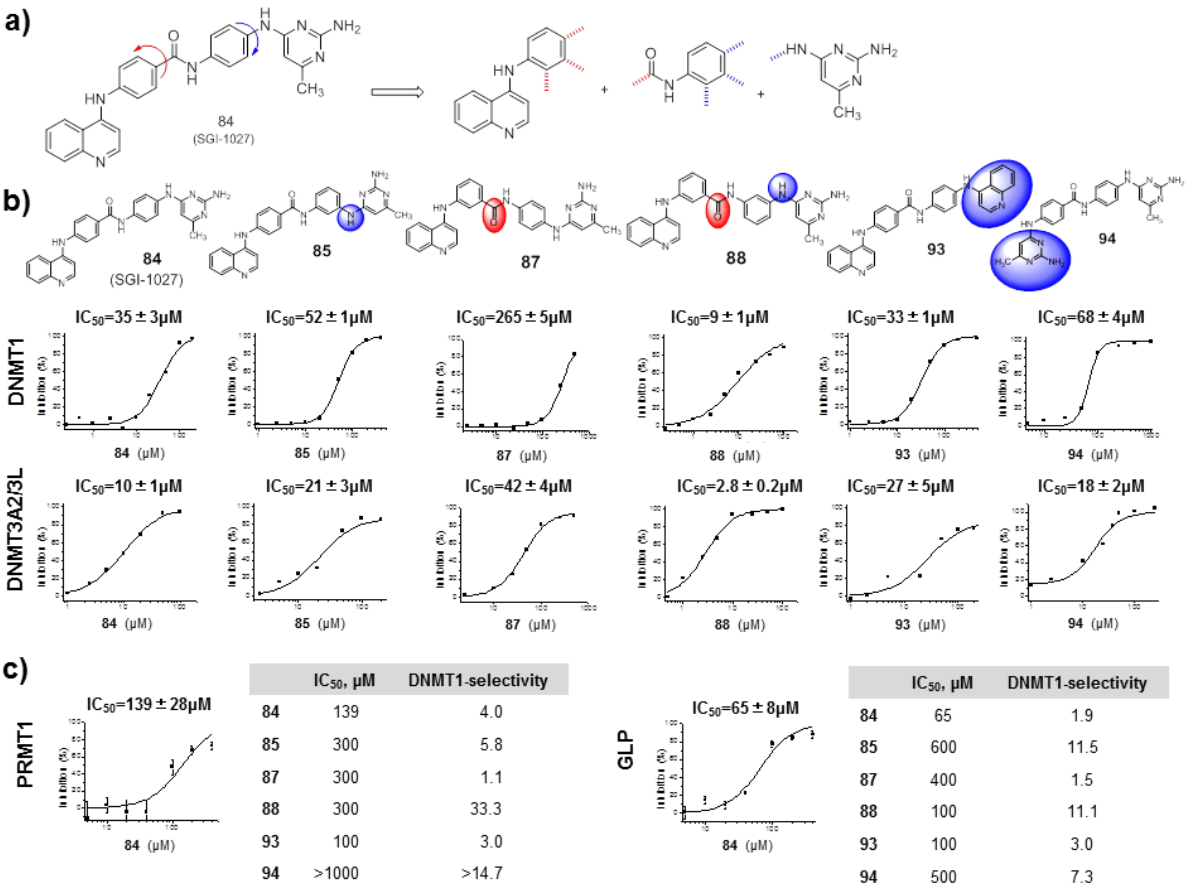

	IC_{50}, μM	DNMT1-selectivity
84	139	4.0
85	300	5.8
87	300	1.1
88	300	33.3
93	100	3.0
94	>1000	>14.7

	IC_{50}, μM	DNMT1-selectivity
84	65	1.9
85	600	11.5
87	400	1.5
88	100	11.1
93	100	3.0
94	500	7.3

Figure 15: Novel quinoline-based non-nucleoside DNMTi. **(a)** Design of **84** regioisomers. **(b)** Inhibitory activities of **84**, **85**, **87**, **88**, **93** and **94** against human DNMT1 (hemimethylated substrate) and the DNMT3A2/DNMT3L complex (unmethylated substrate). **(c)** Inhibitory activities of **84**, **85**, **87**, **88**, **93** and **94** against PRMT1 and GLP. The DNMT1-selectivity (as PRMT or GLP/DNMT1 IC50 ratio) for each compound is reported.

To determine the specificity of **84**, **85**, **87**, **88**, **93** and **94** for DNMTs among other AdoMet-dependent enzymes, we tested them against PRMT1, a protein arginine methyltransferase [189], and G9a-like protein (GLP), a histone H3 lysine 9 methyltransferase [190, 191]. Under the tested conditions, the new derivatives displayed very low (if any) PRMT1 and GLP inhibiting activities, resulting in all cases more DNMTs-selective than **84**, that displayed only 4- and 1.9-fold lower activities against PRMT1 and GLP, respectively, when compared with DNMTs inhibition. In

contrast, **88** was 33- and 11-fold less potent against PRMT1 and GLP than against DNMT1 (Figure 15c).

3.5.2.2 Docking studies of compound 84 and 88 as well as mechanism of action of 88

To better understand the mechanism of inhibition of our compounds against DNMT1, we docked **84** and **88** in two different DNMT1 structures available in Protein Data Bank (PDB), first using DNMT1 (residues 600-1600) crystallized in complex with the cofactor analog sinefungin (PDB 3SWR, Hashimoto and Cheng, unpublished data), and then using DNMT1 (residues 646-1600) in complex with both AdoMet and a 19-base pair DNA duplex (PDB 3PTA)[192]. These two structures share a similar overall three-dimensional arrangement with some conformational differences mainly in the DNA binding CXXC domain region (residues 646–692, Figure 16).

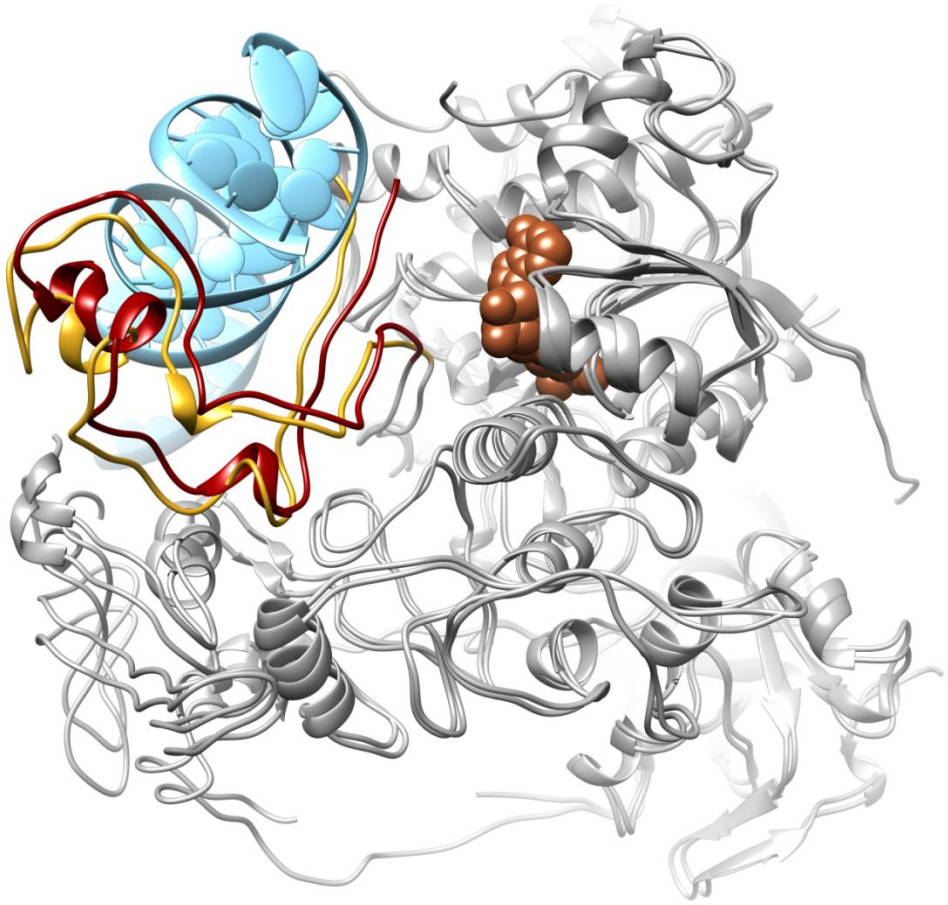

Figure 16: Superimposition of the DNMT1 structures crystallized in complex (PDB 3PTA) and unliganded to DNA (PDB 3SWR). Both the catalytic regions are depicted as grey ribbons, in the 3PTA structure SAH, the CXXC domain and the DNA are depicted as brown spheres, red ribbons and cyan ribbons and ellipsoids, respectively. In the 3SWR structure the CXXC domain is represented as yellow ribbons.

Docking results achieved on the DNMT1 structure alone (unbound to DNA) revealed that both **84** and **88** were able to spam between the AdoMet binding site and the CXXC region (Figure 17a), inserting their 4-aminoquinoline fragments in a lipophilic region normally occupied by AdoMet, and establishing with their 2,4-diamino-6-methylpyrimidine terminal heads a number of hydrogen-bonds at the CXXC domain region. In particular, in **88** the four fragments are optimally assembled so as to maximize its interactions in this region, thus clarifying why **88** is more potent than its structural congener **84**. Almost the same binding orientation was

obtained when **84** was docked in the enzyme/DNA structure (Figure 17b, top panel), in agreement with experimental data demonstrating that this ligand inhibits DNMT1 by competing with AdoMet but not with DNA[185]. On the contrary, the same calculations did not succeed in suggesting a well-defined binding pose for **88**, because the subtle rearrangement of the CXXC domain induced by the presence of DNA sterically hampers **88** to make hydrogen-bonds in this region (Figure 19b, bottom panel). These data suggest that **88**, differently from **84**, binds the enzyme when DNA is absent thereby inhibiting the enzyme by competing with this target substrate. Competition experiments performed with **88** and DNMT1 by varying concentration of either DNA or AdoMet confirmed the mechanism of inhibition of **88** that was competitive with the DNA substrate and not with the AdoMet cofactor (Figure 17c).

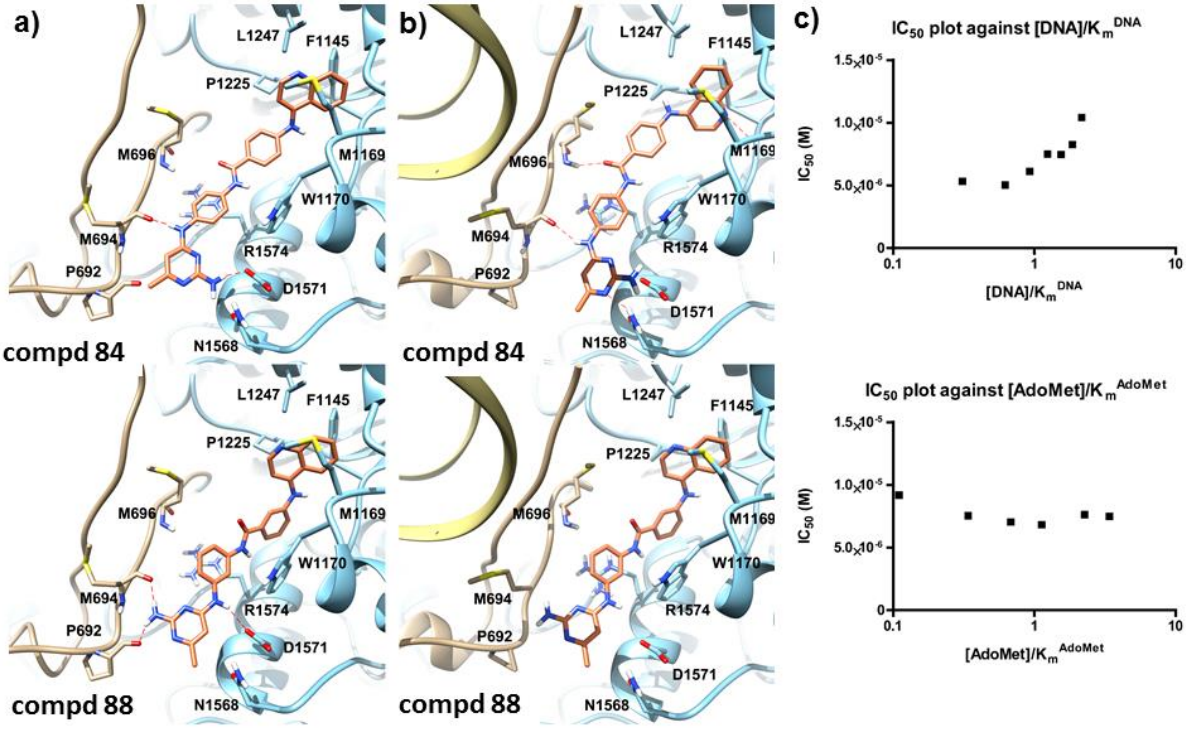

Figure 17: Binding mode and mechanism of action of compound 88. **(a)** Binding modes of **84** (top) and **88** (bottom) to DNA-unliganded DNMT1 (PDB 3SWR). **(b)** Binding modes of **84** (top) and **88** (bottom) to DNA/DNMT1 complex (PDB 3PTA). **(c)** Competition experiments performed with **88** and DNMT1 by varying DNA (top) or AdoMet (bottom) concentrations.

3.5.2.3 Effects of quinoline-based DNMTi in a panel of cancer cell lines.

To study the effects of these DNMTi in a cellular context, we tested **84**, **85**, **87**, **88**, **93** and **94** in a panel of cancer cells (histiocytic lymphoma U-937, breast cancer MDA-MB-231, Burkitt's lymphoma RAJI and prostate cancer PC- 3). Trypan blue exclusion assays were carried out to determine their effects on cell proliferation and viability. The effect of the tested compounds in peripheral blood mononuclear cells (PBMCs) was also determined to assess for differential toxicity. In full agreement with their DNMT inhibition potency, compounds **84**, **85** and **88** displayed the highest antiproliferative effects and the strongest cell death induction in all the cancer cells tested (Figure 18a-d). Compounds **87**, **93** and **94** showed both lower activity and cytotoxicity in these assays (Figure 18f). Compounds **84** showed comparable potency against tumor cells, but **88** was the less toxic in PBMCs (Figure 20e,f). Nuclear morphological changes were further observed by fluorescence microscopy after Hoechst and propidium iodide (PI) staining in both U-937 and RAJI cells treated with increasing doses of **88**, to assess levels of necrosis and apoptosis induced by the compound (Fig. 18g). In U-937 cells, **88** displayed massive apoptosis at 10 μM followed by necrosis at 25μM, while in RAJI cells **88** mainly led to necrosis at 25 μM without triggering any apoptotic response at lower concentrations.

a) Histiocytic lymphoma U-937 cells

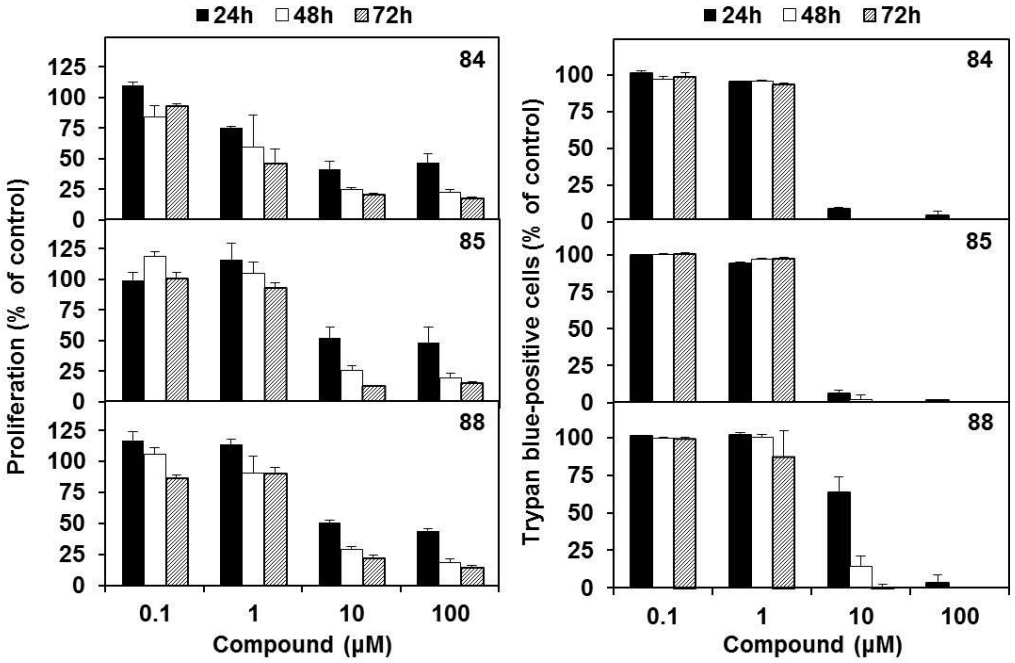

b) Burkitt's lymphoma RAJI cells

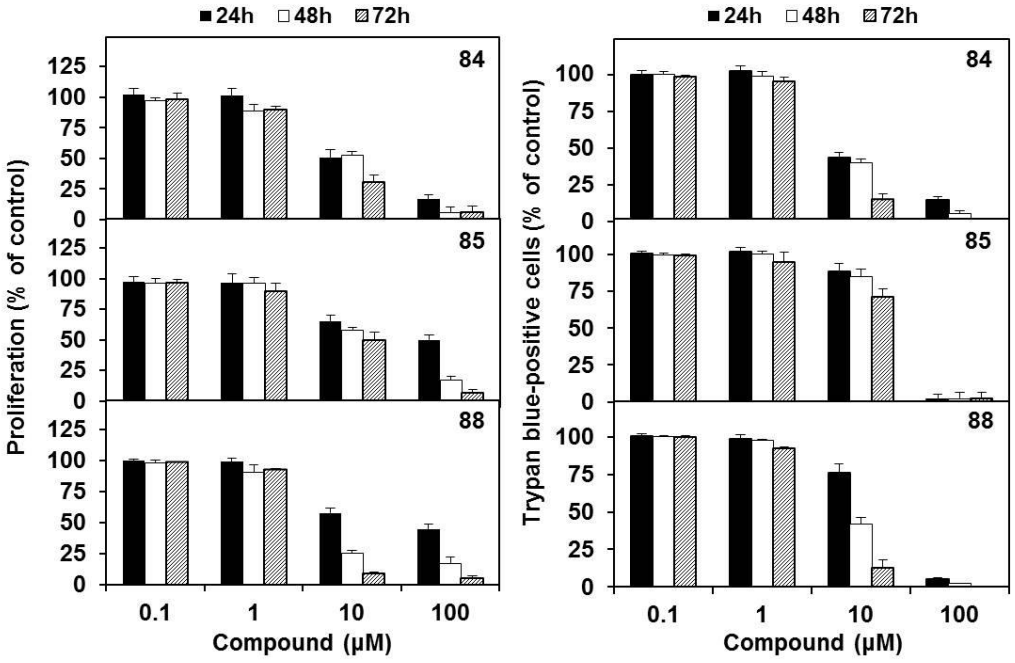

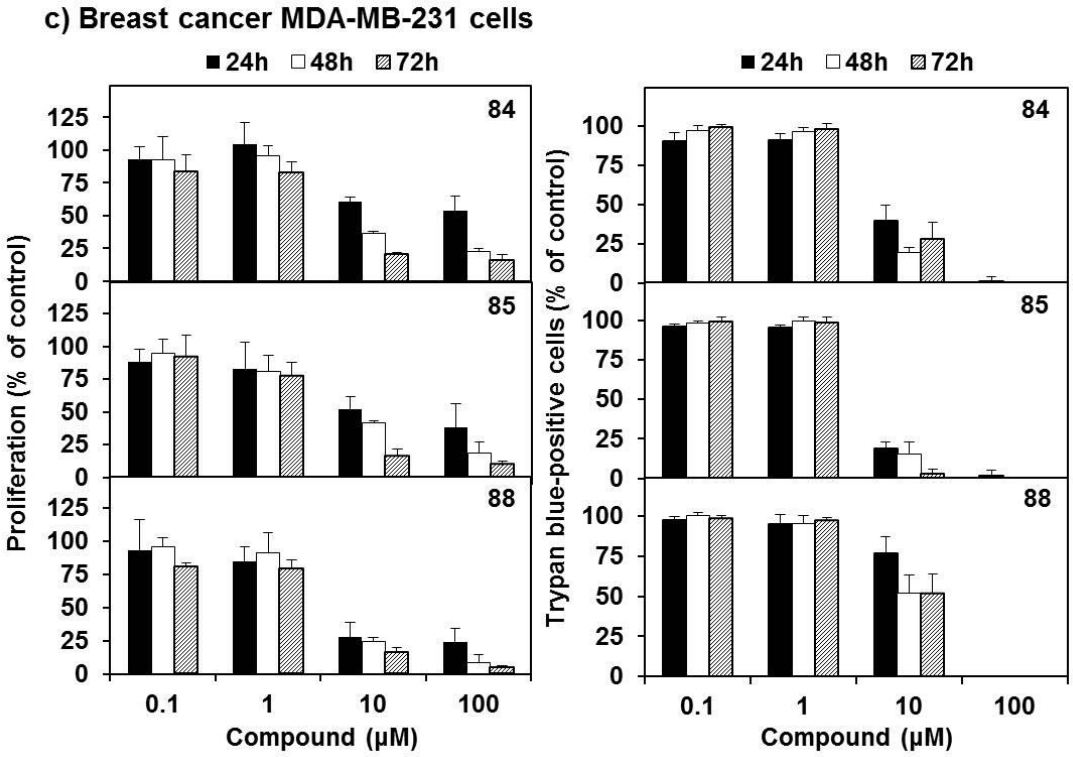
c) Breast cancer MDA-MB-231 cells
24h 48h 72h
Proliferation (% of control)
Trypan blue-positive cells (% of control)
84
85
88
0 25 50 75 100 125
0.1 1 10 100
Compound (µM)

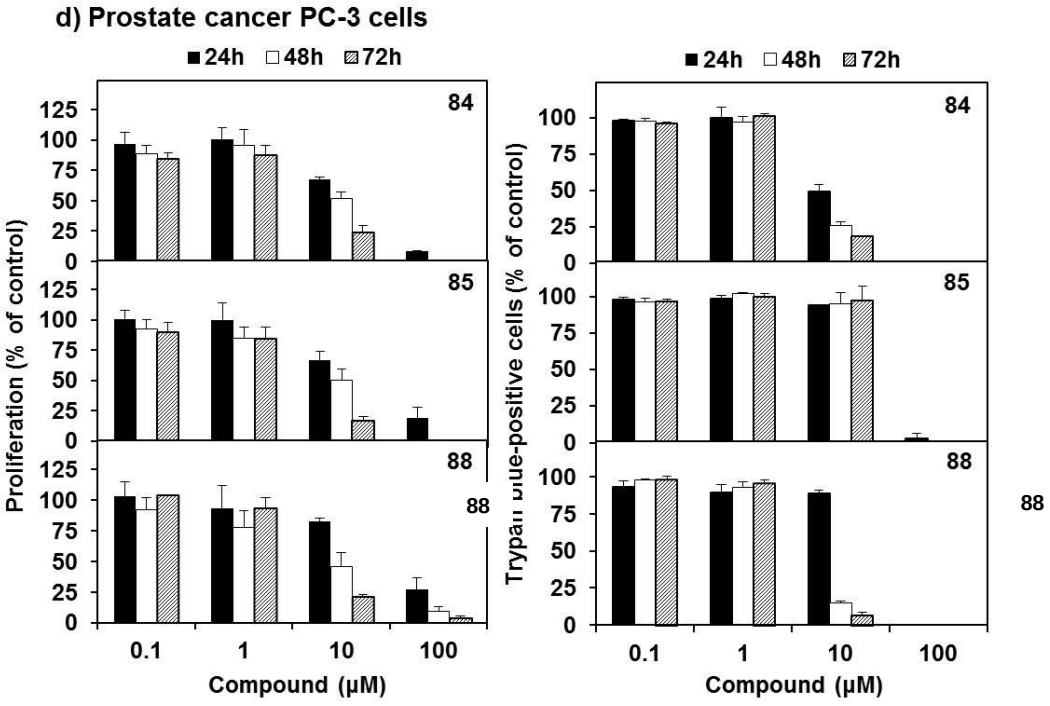
d) Prostate cancer PC-3 cells
24h 48h 72h
Proliferation (% of control)
Trypan blue-positive cells (% of control)
84
85
88
0 25 50 75 100 125
0.1 1 10 100
Compound (µM)

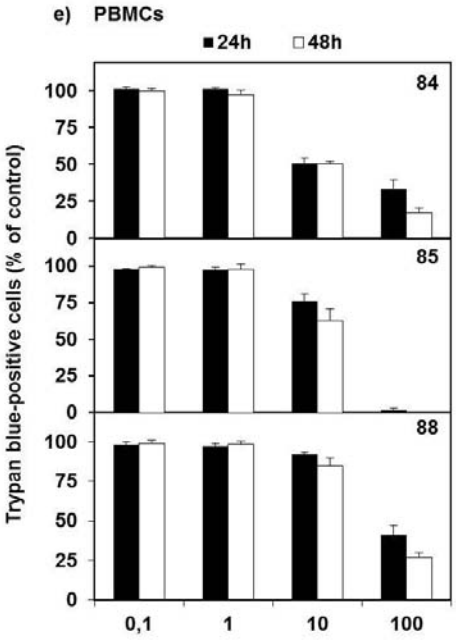

f) IC_{50} values of cellular viability after 48 h

compd	IC_{50}, µM				
	PBMCs	U-937	RAJI	PC-3	MDA-MB-231
84	23.8 ± 8.4	1.7 ± 1.1	9.1 ±0.8	6.5 ± 0.6	4.8 ± 1.6
85	15.2 ± 2.0	2.7 ± 0.9	26.5 ± 3.4	29.8 ± 1.8	7.4 ± 3.0
88	57.4 ± 9.3	4.3 ± 1.7	8.8 ± 0.4	6.6 ± 2.9	9.7 ± 1.5

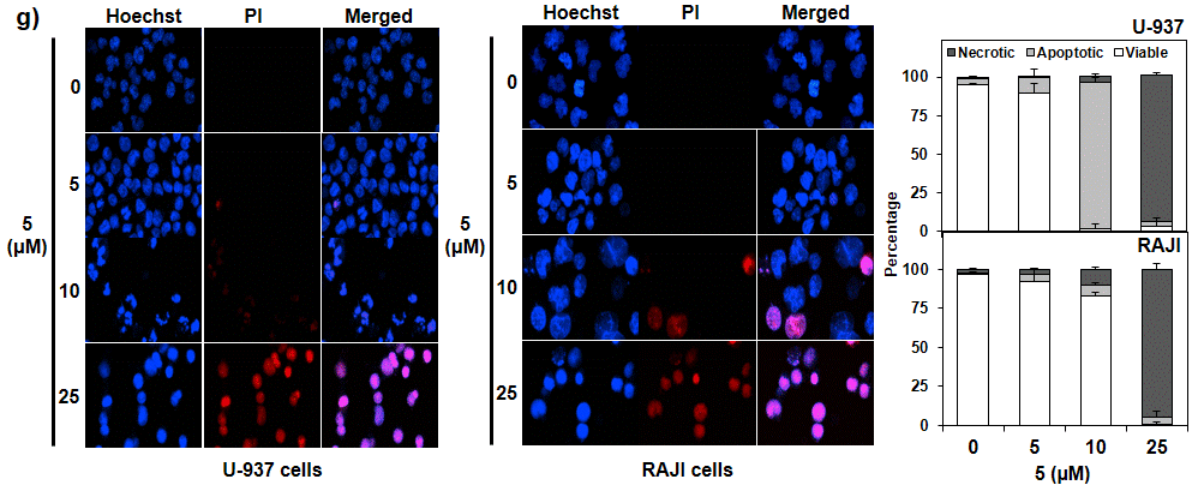

Figure 18: Cellular studies on quinoline-based DNMTi. **(a-e)** Antiproliferative effects (left) and cell death induction (right) of **84**, **85** and **88** on U-937 **(a)**, RAJI **(b)**, MDA-MB-231 **(c)**, PC-3 **(d)** and PBM **(e)** cells. **(f)** IC_{50} values of cell viability relative to the above cells treated with **84**, **85** and **88** for 48 h. **(g)** Nuclear morphology

analysis after Hoechst and PI staining in U-937 and RAJI cells treated with increasing doses of **5** for 72 h. Data represent the mean (±SD) of at least three independent experiments. Pictures are representative of three independent experiments.

3.5.2.4 Effects of 85 and 88 in medulloblastoma stem cells (MbSCs)

When tested in mice MbSCs, expressing high levels of DNMTs (Figure 19), compound **88** arrested the cell clonogenic activity and induced cell adhesion and differentiation, significantly impairing MbSC growth rate, evaluated by quantification of PCNA levels and MTT assay (Figure 20a,b). MbSCs dfferentiation was evaluated by βIII-tubulin and phase contrast images (Figure 20c,d). In these assays, **88** displayed the highest growth arrest, while **85** showed higher differentiation already after treatment with lower doses. To the best of our knowledge, these are the first examples of non-nucleoside DNMTi tested in cancer stem cells (CSCs).

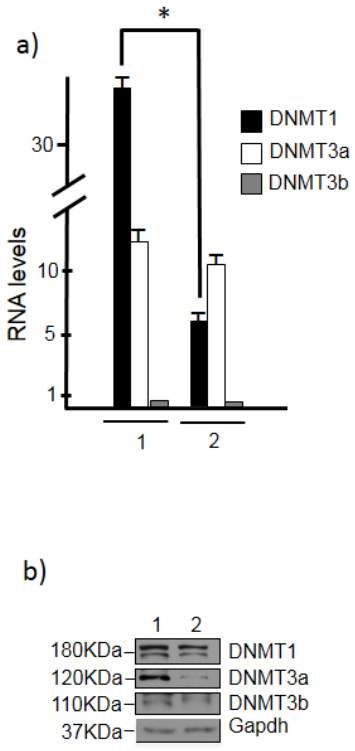

Figure 19: DNMT expression levels in MbSCs. a) mRNA levels of DNMT1, DNMT3a and DNMT3b in MbSCs derived from Ptch1+/- mouse tumors (1) and MbSCs treated for 48 h with PDGF (10 ng/mL) (2). *P<0.05 versus untreated cells. b) Western blot analysis of DNMT1, DNMT3a and DNMT3b in MbSCs derived from Ptch1+/- mouse tumors (1) and MbSCs treated for 48 h with PDGF (10 ng/mL) (2). *P<0.05 versus untreated cells.

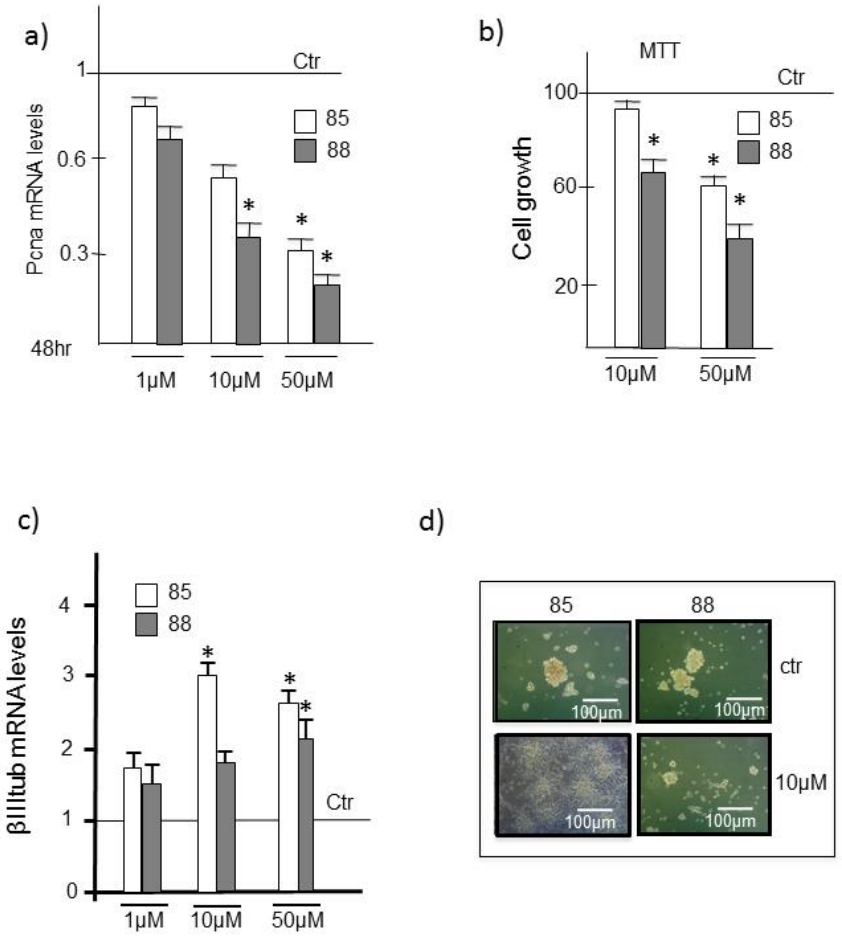

Figure 20: Effects of 85 and 88 in MbSCs. **(a)** PCNA mRNA levels and **(b)** MTT assay of MbSCs after 48 h of **85** and **88** treatment or DMSO as control (Ctr). *P<0.05 versus untreated cells (ctr). **(c)** mRNA levels of βIII-tubulin (βIIItub) in **85**- and **88**-treated MbSCs for 48 h. DMSO was used as control.*P<0.05 versus untreated cells (ctr). **(d)** Representative bright field images of MbSCs after **85** or **88** (48 h, 10 μM) or DMSO as control.

3.6 Conclusion and outlook

In conclusion, through chemical manipulation applied on **84** we identified compound **88**, a novel non-nucleoside DNMTi more potent than **84** and more selective towards other AdoMet- dependent methyltransferases (PRMT1, GLP). Differently from **84**, competitive with AdoMet, **88** was found to be competitive with DNA for its DNMT1 inhibition. Tested on a panel of cancer cells (leukemia U937, breast cancer MDA-MB-231, Burkitt's lymphoma RAJI, and prostate cancer PC- 3) as well as on PBMCs, **88** displayed comparable activity as **84** and less toxicity. In MbSCs, at 10 μM **88** significantly blocked proliferation but required higher doses (50 μM) to induce differentiation, while the related compound **85**, less potent as antiproliferative agent, showed high differentiating activity. The anticancer activity displayed by **85** and **88** in the tested cancer cells including CSCs suggests their use as potent and selective non-nucleoside DNMTi for cancer therapy. This work has been accepted by JMedChem.

3.7 Experimental part

3.7.1 Chemistry

3.7.1.1 General introduction

Please see chapter 2.10.1.1

3.7.1.2 Synthesis of selective non-nucleosidic human DNMTi

General Procedure for the Synthesis of the Ester Intermediates 99a-c, 103, and the Nitro Intermediates 100a-c, 101.

Example: Synthesis of Ethyl 3-(Quinolin-4-ylamino)benzoate (99b).

4-Chloroquinoline (6.11 mmol, 1 g), ethyl 3-aminobenzoate (6.11 mmol, 1 g) and a catalytic amount (4 drops) of 37% hydrochloric acid were refluxed for 2 h. The reaction was allowed to cool down to room temperature and the precipitated solid was filtered off, washed with water (3 × 5 mL) and recrystallized from methanol to afford pure **16b** as hydrochloride salt.

99b Ethyl 3-(Quinolin-4-ylamino)benzoate

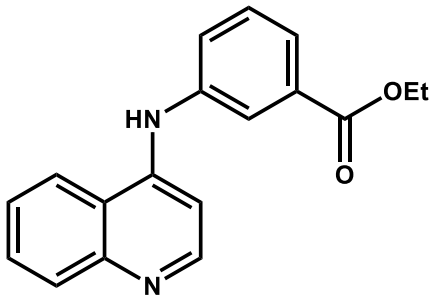

Melting point: 260-263 °C

Appearance: pale yellow solid

Yield: 80%

Recrystallization solvent: methanol

^{1}H NMR (DMSO-d_6, 400 MHz) δ 1.34 (t, 3H, *J* = 7.2 Hz, -COOCH$_2$C*H*$_3$), 4.36 (q, 2H, *J* = 7.2 Hz, -COOC*H*$_2$CH$_3$) 6.88 (d, 1H, *J* = 5.2 Hz, quinoline proton), 7.74 (m, 2H, benzene protons), 7.84 (t, 1H, *J* = 7.4 Hz, benzene proton), 8.00 (d, 1H, *J* = 8.2 Hz, quinoline

proton), 8.06-8.12 (m, 3H, benzene and quinolone protons), 8.56 (d, 1H, *J* = 8.2 Hz, quinoline proton), 8.81 (d, 1H, *J* = 5.2 Hz, quinoline proton), 11.08 (bs, 1H, -N*H*), 14.68 (bs, 1H, H^+) ppm

^{13}C NMR (DMSO-d_6, 100 MHz) δ 14.1, 60.9, 112.8, 114.2, 119.9, 121.6, 122.1, 124.2, 125.7, 129.2, 129.6, 130.9, 133.7, 138.7, 142.3, 149.7, 151.6, 165.9 ppm

HRMS (ESI) m/z $[M]^+$ $C_{18}H_{16}N_2O_2$ calculated: 292.1212 found: 292.1218.

99a Ethyl 2-(Quinolin-4-ylamino)benzoate

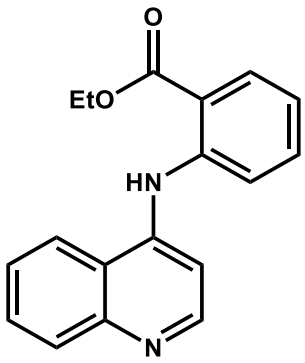

Melting point: 235-237 °C

Appearance: pale yellow solid

Yield: 71%;

Recrystallization solvent: acetonitrile/methanol

^{1}H NMR (DMSO-d_6, 400 MHz) δ 1.30 (t, 3H, *J* = 7.2 Hz, -COOCH$_2$C*H$_3$*), 4.29 (q, 2H, *J* = 7.2 Hz, -COOC*H$_2$*CH$_3$), 6.99 (d, 1H, *J* = 5.2 Hz, quinoline proton), 7.36 (m, 1H benzene proton), 7.62 (m, 1H, benzene proton), 7.80 (t, 1H, *J* = 7.4 Hz, quinoline proton), 7.96-8.02 (m, 2H, benzene and quinoline protons), 8.16 (d, 1H, *J* = 8.2 Hz, quinoline proton), 8.55 (d, 1H, *J* = 5.2 Hz, quinoline proton), 10.26 (bs, 1H, -N*H*), 13.12 (bs, 1H, H^+) ppm

^{13}C NMR (DMSO-d_6, 100 MHz, δ) δ 14.1, 60.9, 110.6, 112.8, 118.6, 117.7, 121.6, 124.2, 125.7, 129.2, 129.6, 130.7, 133.8, 138.7, 149.7, 151.2, 151.6, 167.9 ppm

HRMS (ESI) m/z $[M]^+$ $C_{18}H_{16}N_2O_2$ calculated: 292.1212 found: 292.1208.

99c Ethyl 4-(Quinolin-4-ylamino)benzoate [193]

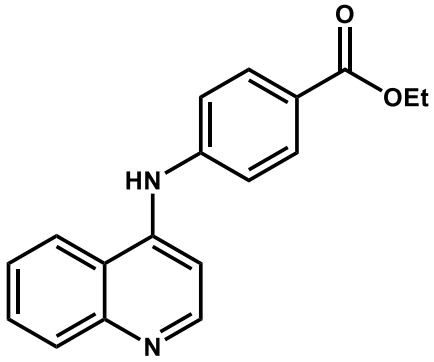

Melting point: 262-265 °C

Appearance: yellow solid

Yield: 83%

Recrystallization solvent: methanol

^{1}H NMR (DMSO-d_6, 400 MHz) δ 1.31 (t, 3H, *J* = 7.2 Hz, -COOCH$_2$C*H*$_3$), 4.29 (q, 2H, *J* = 7.2 Hz, -COOC*H*$_2$CH$_3$) 7.26 (d, 1H, *J* = 5.2 Hz, quinoline proton), 7.44 (m, 2H, benzene protons), 7.56 (t, 1H, *J* = 7.4 Hz, benzene proton), 7.72 (d, 1H, *J* = 8.2 Hz, quinoline proton), 7.87-8.01 (m, 3H, benzene and quinoline protons), 8.35 (d, 1H, *J* = 8.2 Hz, quinoline proton), 8.60 (d, 1H, *J* = 5.2 Hz, quinoline proton), 9.32 (bs, 1H, -N*H*), 13.50 (bs, 1H, H^+) ppm

^{13}C NMR (DMSO-d_6, 100 MHz, δ) δ 14.1, 60.9, 112.8, 119.5, 120.1, 121.6, 125.7, 129.2, 129.6, 130.7, 130.9, 138.7, 149.7, 150.2, 151.6, 165.9 ppm

HRMS (ESI) m/z $[M]^+$ $C_{18}H_{16}N_2O_2$ calculated: 292.1212 found: 292.1215.

100a 6-Methyl-N^4-(2-nitrophenyl)pyrimidine-2,4-diamine

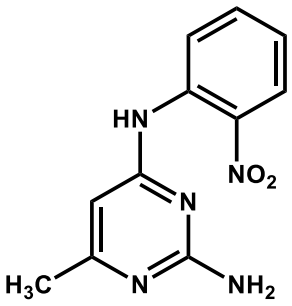

Melting point: 251-253 °C

Appearance: pale yellow solid

Yield: 63%

Recrystallization solvent: methanol

^{1}H NMR (DMSO-d_6, 400 MHz) δ 2.31 (s, 3H, -CH_3), 5.91 (s, 2H, NH_2 of pyrimidine), 6.26 (s, 1H, pyrimidine proton) 7.52 (t, 1H, *J*=8.0 Hz, benzene proton), 7.64 (t, 1H, *J* = 7.4 Hz, benzene proton), 7.78 (t, 1H, *J* = 7.6 Hz, benzene proton), 8.05 (d, 1H, *J* = 8.2 Hz, benzene proton), 11.02 (s, 1H, NH), 13.03 (s, 1H, H+) ppm

RMN ^{13}C (DMSO-d_6, 100 MHz) δ 23.9, 93.8, 110.5, 119.6, 125.9, 129.0, 137.1, 144.6, 163.1, 164.5, 170.2 ppm

HRMS (ESI) m/z $[M]^+$ $C_{11}H_{11}N_5O_2$ calculated: 245.0913 found: 245.0914.

100b 6-Methyl-N^4-(3-nitrophenyl)pyrimidine-2,4-diamine [194]

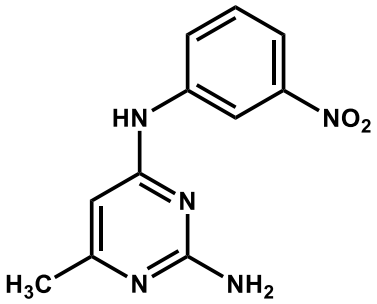

Melting point: 290-292 °C

Appearance: pale yellow solid

Yield: 72%

Recrystallization solvent: methanol

^{1}H NMR (DMSO-d_6, 400 MHz) δ 2.32 (s, 3H, -CH_3), 5.97 (s, 2H, NH_2 of pyrimidine), 6.26 (s, 1H, pyrimidine proton) 7.67 (t, 1H, *J*=8.0Hz, benzene proton), 7.98 (d, 1H, *J* = 7.4 Hz, benzene proton), 8.32 (d, 1H, *J* = 7.6 Hz, benzene proton), 8.53 (s, 1H, benzene proton), 11.10 (s, 1H, NH), 12.97 (s, 1H, H+) ppm

^{13}C NMR (DMSO-d_6, 100 MHz) δ 23.9, 93.8, 109.2, 113.9, 123.9, 130.4, 143.3, 148.7, 163.1, 164.5, 170.2 ppm

HRMS (ESI) $[M]^+$ $C_{11}H_{11}N_5O_2$ calculated: 245.0913 found: 245.0910.

100c 6-Methyl-N^4-(4-nitrophenyl)pyrimidine-2,4-diamine [193]

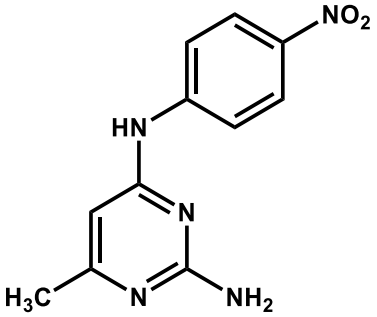

Melting point: >300 °C

Appearance: pale yellow solid

Yield: 67%

Recrystallization solvent: methanol

^{1}H NMR (DMSO-d_6, 400 MHz, δ; ppm) 2.32 (s, 3H, -CH_3), 6.20 (bs, 2H, -NH_2 of pyrimidine), 6.25 (s, 1H, pyrimidine proton), 7.44 (d, 2H, *J* = 8.0 Hz, benzene protons), 8.03 (d, 2H, *J* = 8.0 Hz, benzene protons), 11.10 (s, 1H, NH), 12.99 (s, 1H, H+) ppm

^{13}C NMR (DMSO-d_6, 100 MHz) δ 23.9, 93.8, 119.2 (2C), 124,7 (2C), 137.9, 147.0, 163.1, 164.5, 170.2 ppm

HRMS (ESI) $[M]^+$ $C_{11}H_{11}N_5O_2$ calculated: 245.0913 found: 245.0912.

101 N-(4-nitrophenyl)quinolin-4-amine

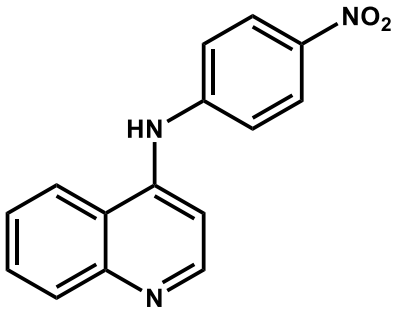

Melting point: >300 °C

Appearance: yellow solid

Yield: 74%

Recrystallization solvent: methanol

^{1}H NMR (DMSO-d_6, 400 MHz) δ 7.24 (d, 1H, *J* = 6.8 Hz, quinoline proton), 7.83-7.86 (m, 3H, benzene and quinoline protons), 8.05-8.09 (m, 1H, quinoline proton), 8.20 (d, 1H, *J* = 8.4 Hz, benzene protons), 8.38 (d, 2H, *J* = 9.2 Hz, benzene protons), 8.69 (d, 1H, *J* = 6.8 Hz, quinoline proton), 8.98 (d, 1H, *J* = 8.4 Hz, quinoline proton), 11.49 (bs, 1H, -N*H*), 15.38 (bs, 1H, H^+) ppm

^{13}C NMR (DMSO-d_6, 100 MHz) δ 112.8, 119.2 (2C), 121.6, 124.2, 124.7 (2C), 125.7, 129.2, 129.6, 137.9, 138.7, 149.7, 151.6, 152.0 ppm

HRMS (ESI) $[M]^+$ $C_{15}H_{11}N_3O_2$ calculated: 265.0851 found: 265.0847.

103 Ethyl 4-((2-amino-6-methylpyrimidin-4-yl)amino)benzoate

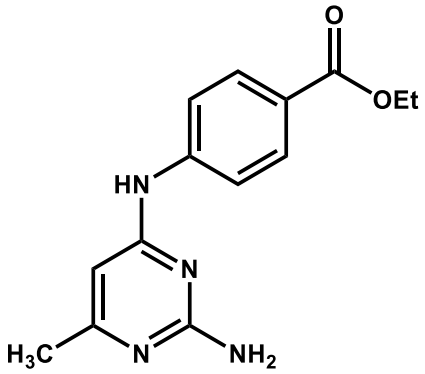

Melting point: 238-240 °C

Appearance: solide beige

Yield: 65%;

Recrystallization solvent: acetonitrile/methanol

^{1}H NMR (DMSO-d_6, 400 MHz) δ 1.34 (t, 3H, *J* = 7.2 Hz, -COOCH$_2$C*H$_3$*), 2.28 (s, 3H, -C*H$_3$*), 4.30 (q, 2H, *J* = 7.2 Hz, -COOC*H$_2$*CH$_3$), 6.30 (s, 2H, N*H$_2$* of pyrimidine), 6.42 (s, 1H, pyrimidine proton) 7.92 (d, 1H, *J* = 8.0 Hz, benzene proton), 8.04 (d, 1H, *J* = 8.0 Hz, benzene proton), 11.30 (BS, 1H, -N*H*), 14.62 (bs, 1H, H^+) ppm

^{13}C NMR (DMSO-d_6, 100 MHz) δ 14.1, 23.9, 60.9, 93.8, 111.2 (2C), 120.1, 130.7 (2C), 145.2, 163.1, 164.5, 165.9, 170.2 ppm

HRMS (ESI) $[M]^+$ $C_{14}H_{16}N_4O_2$ calculated: 272.1273 found: 272.1269.

General Procedure for the Synthesis of the Acid Intermediates 97a-c, 104.

Example: Synthesis of 3-(Quinolin-4-ylamino)benzoic acid (97b). A solution of ethyl 3-(quinolin-4-ylamino)benzoate **99b** (1.71 mmol, 0.5 g) and 2 N KOH (6.84 mmol, 0.38 g) in ethanol (15 mL) was stirred overnight at room temperature. Then the solvent was evaporated, and 2 N HCl was slowly added until the pH 5.0. The colourless solid was filtered, washed first with water and then recrystallized from methanol to obtain pure **97b**.

97b 3-(Quinolin-4-ylamino)benzoic acid

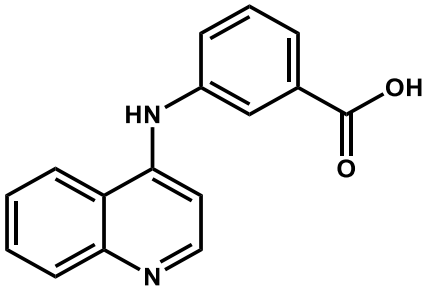

Melting point: >300 °C

Appearance: pale yellow solid

Yield: 90%

Recrystallization solvent: methanol

^{1}H NMR (DMSO-d_6, 400 MHz) δ 7.00 (d, 1H, *J* = 5.2 Hz, quinoline proton), 7.51-7.58 (m, 2H, benzene and quinoline protons), 7.63 (d, 1H, benzene proton), 7.68-7.75 (m, 2H, benzene and quinoline protons), 7.90-7.93 (m, 2H, benzene and quinoline protons), 8.39 (d, 1H, *J* = 8.0 Hz, quinoline proton), 8.51 (d, 1H, *J* = 5.2 Hz, quinoline proton), 9.17 (bs, 1H, N*H*), 12.75 (bs, 1H, COO*H*) ppm

^{13}C NMR (DMSO-d_6, 100 MHz) δ 112.8, 114.6, 120.3, 121.6, 123.0, 124.2, 125.7, 128.9, 129.2, 129.6, 133.7,138.7, 142.3, 149.7, 151.6, 166.3 ppm

HRMS (ESI) $[M]^+$ $C_{16}H_{12}N_2O_2$ calculated: 264.0899 found: 264.0902.

97a 2-(Quinolin-4-ylamino)benzoic acid

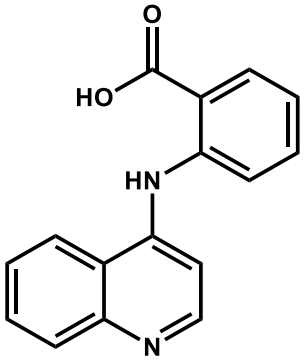

Melting point: >300 °C

Appearance: yellow solid

Yield: 88%

Recrystallization solvent: methanol

^{1}H NMR (DMSO-d_6, 400 MHz) δ 7.21-7.25 (m, 2H, benzene and quinoline protons), 7.61-7.64 (m, 1H, quinoline proton), 7.69 (d, 1H, J=8.0Hz, benzene proton), 7.72 (d, 1H, J=8,0Hz, benzene proton), 7.86-7.90 (m, 2H, benzene and quinoline protons), 7.97 (d, 1H, J=8.0Hz, quinoline proton), 8.07 (d, 1H, J=8.0Hz, quinoline proton), 8.34 (d, 1H, J=8.0Hz, quinoline proton), 8.59 (bs, 1H, N*H*) 12.02 (bs, 1H, COO*H*) ppm

^{13}C NMR (DMSO-d_6, 100 MHz, δ; ppm) δ 108.9, 110.6, 112.8, 118.6, 121.6, 124.2, 125.7, 129.2, 129.6, 131.1, 134.7, 138.7, 149.7, 151.6(2C), 169.3 ppm

HRMS (ESI) $[M]^+$ $C_{16}H_{12}N_2O_2$ calculated: 264.0899 found: 264.0903.

97c 4-(Quinolin-4-ylamino)benzoic acid [193]

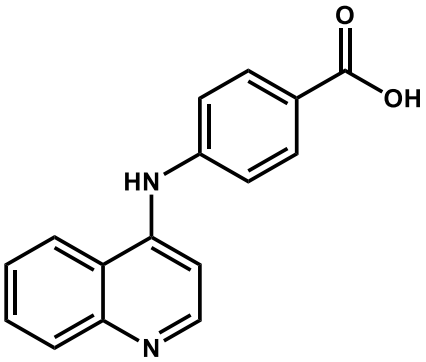

Melting point: >300 °C

Appearance: pale yellow solid

Yield: 85%

Recrystallization solvent: methanol

^{1}H NMR (DMSO-d_6, 400 MHz) δ 7.15 (d, 1H, *J* = 5.2 Hz, quinoline proton), 7.54-7.56 (m, 2H, benzene and quinoline protons), 7.73-7.75 (m, 1H, benzene proton), 7.95-8.04 (m, 4H, benzene and quinoline protons), 8.43 (bs, 1H, N*H*), 8.59-8.64 (m, 2H, quinoline protons), 12.40 (s, 1H, COO*H*) ppm

^{13}C NMR (DMSO-d_6, 100 MHz) δ 112.8, 119.5 (2C), 120.2, 121.6, 124.2, 125.7, 129.2, 129.6, 131.1 (2C), 138.7, 149.7, 151.1, 151.6, 169.3 ppm

HRMS (ESI) $[M]^+$ $C_{16}H_{12}N_2O_2$ calculated: 264.0899 found: 264.0894.

104 4-((2-Amino-6-methylpyrimidin-4-yl)amino)benzoic acid

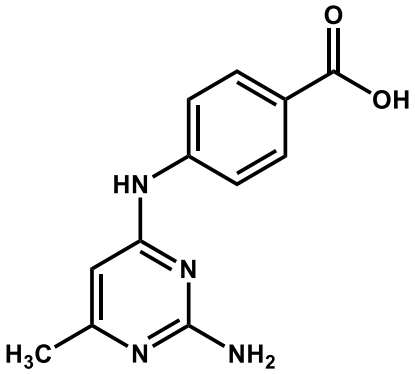

Melting point: >300 °C

Appearance: colorless solid

Yield: 87%

Recrystallization solvent: methanol

^{1}H NMR (DMSO-d_6, 400 MHz) δ 2.12 (s, 3H, -CH_3), 4.30 (q, 2H, *J* = 7.2 Hz, -COOCH_2CH$_3$), 6.28 (s, 1H, pyrimidine proton), 6.30 (s, 2H, NH_2 of pyrimidine), 7.81-7.87 (m, 4H, benzene protons), 8.04 (d, 1H, *J* = 8.0 Hz, benzene proton), 9.30 (bs, 1H, -N*H*), 12.70 (bs, 1H, COO*H*) ppm

^{13}C NMR (DMSO-d_6, 100 MHz) δ 23.9, 93.8, 111.2 (2C), 120.2, 131.1 (2C), 146.1, 163.1, 164.5, 169.3, 170.2 ppm

HRMS (ESI) $[M]^+$ $C_{12}H_{12}N_4O_2$ calculated: 244.0960 found: 244.0964.

General Procedure for the Synthesis of the Anilines 98a-c, 102 and 96.

Example: Synthesis of N^4-(3-Aminophenyl)-6-methylpyrimidine-2,4-diamine (15b).

To a cooled solution of 6-methyl-N^4-(3-nitrophenyl)pyrimidine-2,4-diamine **100b** (1.63 mmol, 0.5 g) and stannous chloride dihydrate (8.15 mmol, 1.84 g) in ethanol (10 mL), 37 % hydrochloric acid solution (0.3 mL) was slowly added at 0 °C. The reaction was then kept at 80 °C for 1 h. Afterwards, the reaction was quenched at room temperature by 2 N sodium carbonate solution (20 mL) and the mixture was extracted with ethyl acetate (3 × 30 mL), washed with brine (3 × 30 mL), then dried with anhydrous sodium sulphate, filtered and concentrated under reduced pressure. The crude solid was recrystallized from cyclohexane to give the pure product **98b**.

98b N^4-(3-Aminophenyl)-6-methylpyrimidine-2,4-diamine [194]

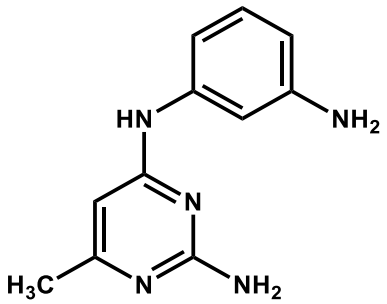

Melting point: 140-142 °C

Appearance: pale brown solid

Yield: 73%

Recrystallization solvent: acetonitrile

^{1}H NMR (DMSO-d_6, 400 MHz) δ 2.06 (s, 3H, -CH_3), 4.92 (bs, 2H, -NH_2 of aniline), 5.87 (s, 1H, pyrimidine proton), 5.97 (bs, 2H, -NH_2 of pyrimidine), 6.19 (d, 1H, *J* = 8.0 Hz, aniline proton), 6.80 (d, 1H, *J* = 8.0 Hz, aniline proton), 6.87-6.91 (m, 2H, aniline protons), 8.64 (bs, 1H, -N*H*) ppm

^{13}C NMR (DMSO-d_6, 100 MHz) δ 23.9, 93.8, 102.7, 105.0, 107.8, 130.3, 143.2, 147.8, 163.1, 164.5, 170.2 ppm

HRMS (ESI) $[M]^+$ $C_{11}H_{13}N_5$ calculated: 215.1171 found: 215.1167.

98a N^4-(2-Aminophenyl)-6-methylpyrimidine-2,4-diamine

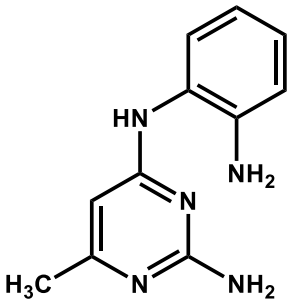

Melting point: 213-215 °C

Appearance: off-white solid

Yield: 64%

Recrystallization solvent: acetonitrile/methanol

^{1}H NMR (DMSO-d_6, 400 MHz) δ 2.02 (s, 3H, -CH_3), 4.81 (bs, 2H, -NH_2 of aniline), 5.59 (s, 1H, pyrimidine proton), 5.91 (bs, 2H, -NH_2 of pyrimidine), 6.56 (d, 1H, *J* = 8.0 Hz, aniline proton), 6.74 (d, 1H, *J* = 8.0 Hz, aniline proton), 6.87-6.90 (m, 2H, aniline protons), 7.93 (bs, 1H, -N*H*) ppm

^{13}C NMR (DMSO-d_6, 100 MHz) δ 23.9, 93.8, 102.7, 105.0, 115.1, 119.5, 126.7 132.3, 136.5, 142.3, 163.1, 164.5, 170.2 ppm

HRMS (ESI) $[M]^+$ $C_{11}H_{13}N_5$ calculated: 215.1171 found: 215.1174.

98c N^4-(4-Aminophenyl)-6-methylpyrimidine-2,4-diamine[193]

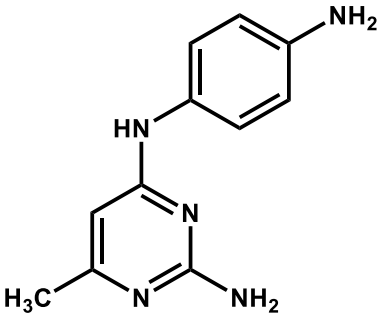

Melting point: 88-90 °C

Appearance: solide brune pâle

Yield: 79%

Recrystallization solvent: cyclohexane

RMN ^{1}H (DMSO-d_6, 400 MHz) δ 2.05 (s, 3H, -CH_3), 4.40 (bs, 2H, -NH_2 of aniline), 5.82 (s, 1H, pyrimidine proton), 6.20 (bs, 2H, -NH_2 de pyrimidine), 6.53 (d, 2H, *J* = 8.0 Hz, aniline proton), 7.16 (d, 2H, *J* = 8.0 Hz, aniline proton), 8.06 (bs, 1H, -N*H*) ppm

RMN ^{13}C (DMSO-d_6, 100 MHz) δ 23.9, 93.8, 117.1 (2C), 118.3 (2C), 130.9, 138.4, 163.1, 164.5, 170.2 ppm

HRMS (ESI) $[M]^+$ $C_{11}H_{13}N_5$ calculated: 215.1171 found: 215.1176.

102 N^1-(Quinolin-4-yl)benzene-1,4-diamine

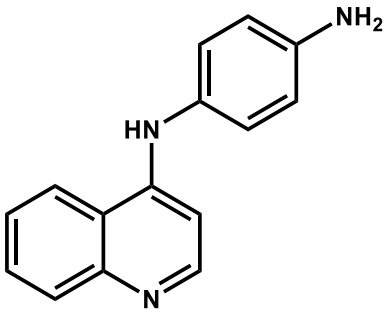

Melting point: 168-170 °C

Appearance: orange solide

Yield: 77%

Recrystallization solvent: acetonitrile/methanol

^{1}H NMR (DMSO-d_6, 400 MHz) δ 5.11 (bs, 2H, -NH_2 of aniline), 6.46 (d, 1H, *J* = 5.2 Hz, quinoline proton), 6.66 (d, 1H, *J* = 8.4 Hz, aniline proton), 7.00 (d, 2H, *J* = 8.4 Hz, aniline protons), 7.44-7.47 (m, 1H, quinoline proton), 7.62-7.66 (m, 1H, quinoline proton), 8.38 (d, 1H, *J* = 8.4 Hz, aniline proton), 8.31 (d, 1H, *J* = 5.6 Hz, quinoline proton), 8.39 (d, 1H, *J* = 8.0 Hz, quinoline proton), 8.68 (bs, 1H, -N*H*) ppm

^{13}C NMR (DMSO-d_6, 100 MHz) δ 112.8, 117.1 (2C), 118.3 (2C), 121.6, 124.2, 125.7, 129.2, 129.6, 135.9, 138.4, 138.7, 149.7, 151.6, ppm

HRMS (ESI) $[M]^+$ $C_{15}H_{13}N_3$ calculated: 235.1109 found: 235.1102.

General Procedure for the Synthesis of the Compounds 84-95 and 105.

105 N-(4-((2-Amino-6-methylpyrimidin-4-yl)amino)phenyl)-4-nitrobenzamide [193, 194]

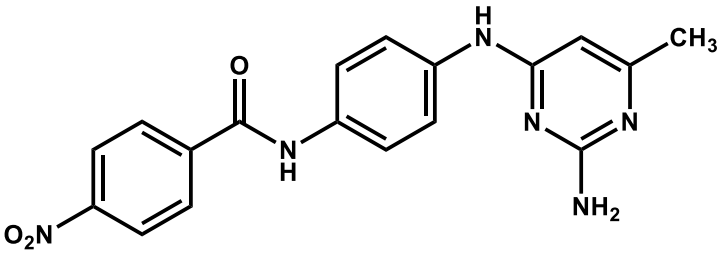

Melting point: >300 °C

Appearance: orange solide

Yield: 76%

Recrystallisation solvent: methanol

^{1}H NMR (DMSO-d_6, 400 MHz) δ 2.10 (s, 3H, -CH_3), 5.90 (s, 1H, pyrimidine proton), 6.26 (bs, 2H, -NH_2 de pyrimidine), 7.74 – 7.66 (m, 4H, benzene protons), 8.20 (d, *J* = 8.7 Hz, 2H, benzene protons), 8.37 (d, *J* = 8.7 Hz, 2H, benzene protons), 9.11 (bs, 1H, -N*H*-), 10.50 (s, 1H, -CON*H*-) ppm

^{13}C NMR (DMSO-d_6, 100 MHz) δ 23.9, 93.8, 117.7 (2C), 122.4 (2C), 124.0, 124.1, 127.9, 129.6, 129.7, 136.5, 136.8, 151.3, 163.1, 164.5, 164.7, 170.2 ppm

HRMS (ESI) $[M]^+$ $C_{18}H_{16}N_6O_3$ calculated: 364.1284 found: 364.1279.

Example: Synthesis of *N*-(3-(2-Amino-6-methylpyrimidin-4-ylamino)phenyl)-3-(quinolin-4-ylamino)benzamide (88).

Triethylamine (3.04 mmol, 0.42 mL) and benzotriazol-1-yl-oxytripyrrolidinophosphonium hexafluorophosphate (PyBOP) (0.91 mmol, 0.47 g) were added to a solution of 3-(quinolin-4-ylamino)benzoic acid **14b** (0.76 mmol, 0.2 g) in anhydrous *N,N*-dimethylformamide (5 mL) under nitrogen atmosphere. The resulting mixture was stirred for 30 minutes at room temperature, afterwards N^4-(3-aminophenyl)-6-methylpyrimidine-2,4-diamine **15b** (0.76 mmol, 0.16 g) was added under nitrogen atmosphere and the reaction was stirred overnight. The reaction was quenched with water (50 mL) and extracted with ethyl acetate (3 × 30 mL). The combined organic extracts were dried and the residue obtained upon evaporation

of solvent was purified by column chromatography (SiO_2 eluting with ethyl acetate/methanol 10/1) to provide pure **88**.

88 *N*-(3-(2-Amino-6-methylpyrimidin-4-ylamino)phenyl)-3-(quinolin-4-ylamino)benzamide

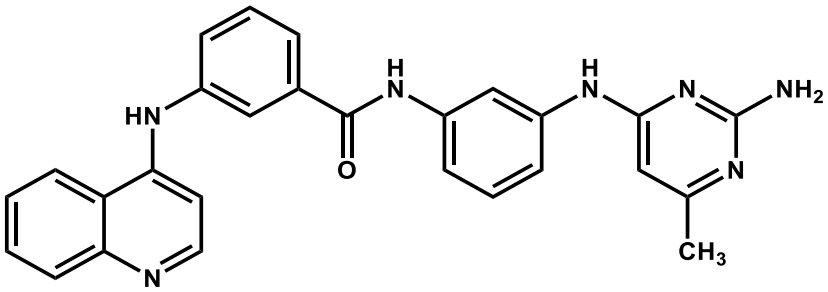

Melting point: 270-272 °C

Appearance: off-white solid

Yield: 80%

Recrystallisation solvent: methanol

^{1}H NMR (DMSO-d_6, 400 MHz) δ 2.10 (s, 3H, -CH_3), 5.94 (s, 1H, pyrimidine proton), 6.07 (bs, 2H, -NH_2-pyrimidine), 7.06 (d, 1H, *J* = 4.8 Hz, quinoline proton), 7.26 (t, 1H, *J* = 8.0 Hz, benzene proton), 7.35 (d, 1H, *J* = 7.6 Hz, quinoline proton), 7.55-7.61 (m, 4H, benzene and quinoline protons), 7.72-7.75 (m, 2H, benzene protons), 7.91 (d, 1H, *J* = 8.0 Hz, quinoline proton), 7.95 (s, 1H, benzene proton), 8.03 (s, 1H, benzene proton), 8.42 (d, 1H, *J* =8.4 Hz, quinoline proton), 8.52 (d, 1H, *J* = 5.6 Hz, quinoline proton), 9.04 (bs, 1H, -N*H*-pyrimidine), 9.16 (bs, 1H, -N*H*-quinoline), 10.18 (bs, 1H, -CON*H*-) ppm

^{13}C NMR (DMSO-d_6, 100 MHz) δ 23.9, 93.8, 108.0, 111.6, 111.8, 112.8, 113.4, 117.5, 121.2, 121.6, 124.2, 125.7, 129.2, 129.6, 129.7, 133.9, 135.0, 136.7, 138.7, 142.5, 142.6, 149.7, 151.6, 163.1, 164.5, 164.7, 170.2 ppm

HRMS (ESI) $[M]^+$ $C_{27}H_{23}N_7O$ calculated: 461.1964 found: 461.1969.

Elemental analysis: calculated: C: 70.27%; H: 5.02%; N: 21.24% found: C: 70.33%; H: 5.08%; N: 21.19%

84 ***N*-(4-(2-Amino-6-methylpyrimidin-4-ylamino)phenyl)-4-(quinolin-4-ylamino) benzamide (SGI-1027)** [185, 193, 194]

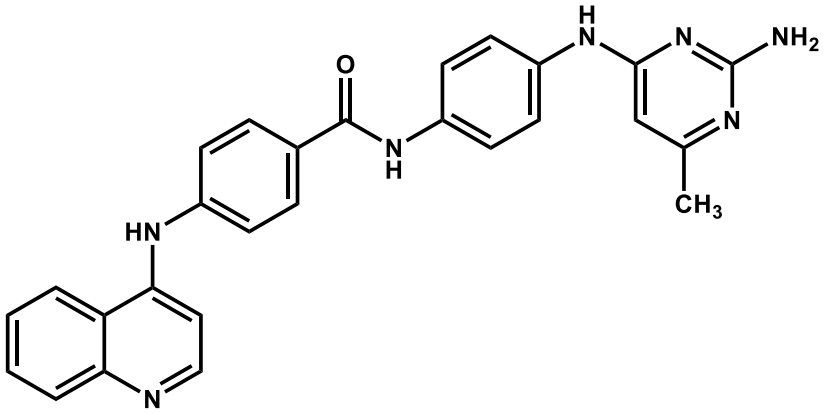

Melting point: >300 °C

Appearance: off-white solid

Yield: 79%

Recrystallization solvent: methanol

^{1}H NMR (DMSO-d_6, 400 MHz) δ 2.10 (s, 3H, -CH_3), 5.88 (s, 1H, pyrimidine proton), 6.14 (bs, 2H, -NH_2-pyrimidine), 7.21 (d, 1H, *J* = 5.4 Hz, quinoline proton), 7.48-7.81 (m, 8H, benzene and quinoline protons), 7.93-8.03 (m, 3H, benzene and quinoline protons), 8.42 (d, 1H, *J* =8.4 Hz, quinoline proton), 8.52 (d, 1H, *J* = 5.6 Hz, quinoline proton), 8.97 (bs, 1H, -N*H*-pyrimidine), 9.25 (bs, 1H, -N*H*-quinoline), 10.06 (bs, 1H, -CON*H*-) ppm

^{13}C NMR (DMSO-d_6, 100 MHz) δ 23.9, 93.8, 111.4 (2C), 112.8, 117.7 (2C), 121.6, 122.4 (2C), 124.2 (2C), 125.7, 127.9, 129.2, 129.6, 130.2 (2C), 136.5, 138.7, 149.3, 149.7, 151.6, 163.1, 164.5, 164.7, 170.2 ppm

HRMS (ESI) $[M]^+$ $C_{27}H_{23}N_7O$ calculated: 461.1964 found: 461.1969.

Elemental analysis: calculated: C: 70.27%; H: 5.02%; N: 21.24% found: C: 70.54%; H: 5.11%; N: 21.09%

85 ***N*-(3-(2-Amino-6-methylpyrimidin-4-ylamino)phenyl)-4-(quinolin-4-ylamino) benzamide** [194]

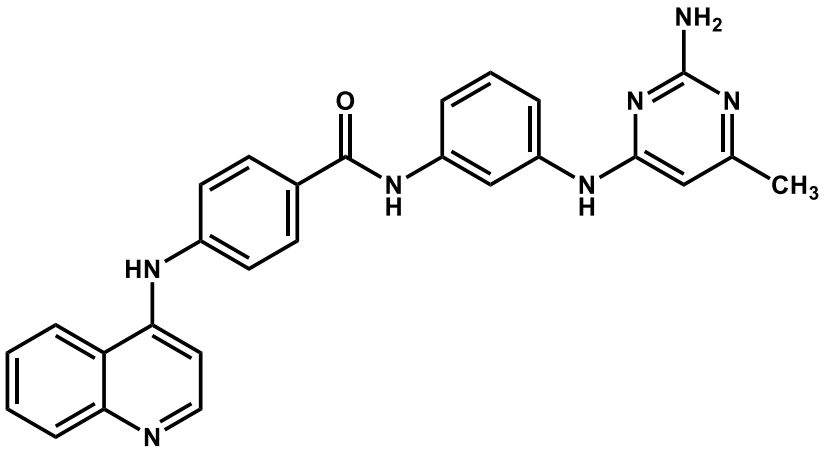

Melting point: 270-272 °C

Appearance: off-white solide

Yield: 81%

Recrystallization solvent: methanol

^{1}H NMR (DMSO-d_6, 400 MHz) δ 2.10 (s, 3H, -CH_3), 5.95 (s, 1H, pyrimidine proton), 6.07 (bs, 2H, -NH_2-pyrimidine), 7.21-7.25 (m, 2H, benzene and quinoline protons), 7.37 (d, 1H, *J* = 8.2 Hz, benzene proton), 7.50-7.61 (m, 4H, benzene and quinoline protons), 7.75 (t, 1H, *J* = 7.4 Hz, quinoline proton), 7.93-8.03 (m, 4H, benzene and quinoline protons), 8.42 (d, 1H, *J* =8.4 Hz, quinoline proton), 8.52 (d, 1H, *J* = 5.6 Hz, quinoline proton), 9.03 (bs, 1H, -N*H*-pyrimidine), 9.25 (bs, 1H, -N*H*-quinoline), 10.05 (bs, 1H, -CON*H*-) ppm

^{13}C NMR (DMSO-d_6, 100 MHz) δ 23.9, 93.8, 108.0, 111.4 (2C), 111.6, 112.8, 113.4, 121.6, 124.2 (2C), 125.7, 129.2, 129.6, 129.7, 130.2 (2C), 136.7, 138.7, 142.6, 149.3, 149.7, 151.6, 163.1, 164.5, 164.7, 170.2 ppm

HRMS (ESI) $[M]^+$ $C_{27}H_{23}N_7O$ calculated: 461.1964 found: 461.1969.

Elemental analysis: calculated: C: 70.27%; H: 5.02%; N: 21.24% found: C: 70.48%; H: 5.10%; N: 21.15%

86 **N-(2-(2-Amino-6-methylpyrimidin-4-ylamino)phenyl)-4-(quinolin-4-ylamino) benzamide**

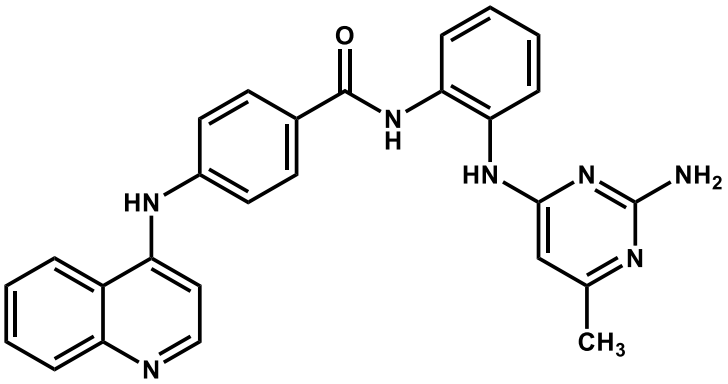

Melting point: 200-205 °C

Appearance: pale yellow solid

Yield: 72%

Recrystallization solvent: acetonitrile/methanol

^{1}H RMN (DMSO-d_6, 400 MHz) δ 2.09 (s, 3H, -CH_3), 5.88 (s, 1H, pyrimidine proton), 6.31 (bs, 2H, -NH_2-pyrimidine), 7.18-7.22 (m, 2H, benzene and quinoline protons), 7.37-7.50 (m, 4H, 7.58-7.65 (m, 2H benzene and quinoline protons), 7.72-7.77 (m, 2H, benzene protons), 7.94-7.96 (m, 2H, quinoline protons), 8.37 (d, 1H, *J* = 7.6 Hz, quinoline proton), 8.55 (bs, 1H, -N*H*-pyrimidine), 8.58 (d, 1H, *J* = 4.8 Hz, quinoline proton), 9.25 (bs, 1H, -N*H*-quinoline), 10.15 (bs, 1H, -CON*H*-) ppm

^{13}C NMR (DMSO-d6, 100 MHz) δ 23.9, 93.8, 111.4 (2C), 112.8, 118.9, 121.6, 122.8, 124.2 (2C), 125.5, 125.7, 126.1, 129.2, 129.6, 130.2 (2C), 137.9, 138.7, 147.6, 149.3, 149.7, 151.6, 163.1, 164.5, 170.2, 172.5 ppm

HRMS (ESI) $[M]^+$ $C_{27}H_{23}N_7O$ calculated: 461.1964 found: 461.1969.

Elemental analysis: calculated: C: 70.27%; H: 5.02%; N: 21.24% found: C: 70.08%; H: 4.97%; N: 21.45%

87 *N*-(4-(2-Amino-6-methylpyrimidin-4-ylamino)phenyl)-3-(quinolin-4-ylamino) benzamide

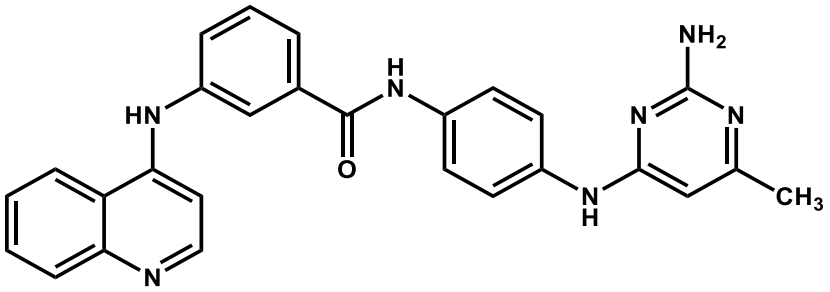

Melting point: >300 °C

Appearance: off-white solide

Yield: 83%

Recrystallization solvent: methanol

^{1}H NMR (DMSO-d_6, 400 MHz) δ 2.08 (s, 3H, -CH_3), 5.87 (s, 1H, pyrimidine proton), 6.10 (bs, 2H, -NH_2-pyrimidine), 7.06 (d, 1H, *J* = 5.6 Hz, quinoline proton), 7.54-7.74 (m, 9H, benzene and quinoline protons), 7.90 (d, 1H, *J* = 8.4 Hz quinoline proton), 8.01 (s, 1H, benzene proton), 8.46 (d, 1H, *J* = 8.4 Hz, quinoline proton), 8.51 (d, 1H, *J* = 4.0 Hz, quinoline proton), 9.01 (bs, 1H, -N*H*-pyrimidine), 9.28 (bs, 1H, -N*H*-quinoline), 10.30 (bs, 1H, -CON*H*-) ppm

^{13}C NMR (DMSO-d_6, 100 MHz) δ 23.9, 93.8, 111.8, 112.8, 117.5, 117.7 (2C), 121.2, 121.6, 122.4 (2C), 124.2, 125.7, 127.9, 129.2, 129.6, 133.9, 135.0, 136.5, 138.7, 142.5, 149.7, 151.6, 163.1, 164.5, 164.7, 170.2 ppm

HRMS (ESI) $[M]^+$ $C_{27}H_{23}N_7O$ calculated: 461.1964 found: 461.1969.

Elemental analysis: calculated: C: 70.27%; H: 5.02%; N: 21.24% found: C: 70.43%; H: 5.11%; N: 21.13%

89 ***N*-(2-(2-Amino-6-methylpyrimidin-4-ylamino)phenyl)-3-(quinolin-4-ylamino) benzamide**

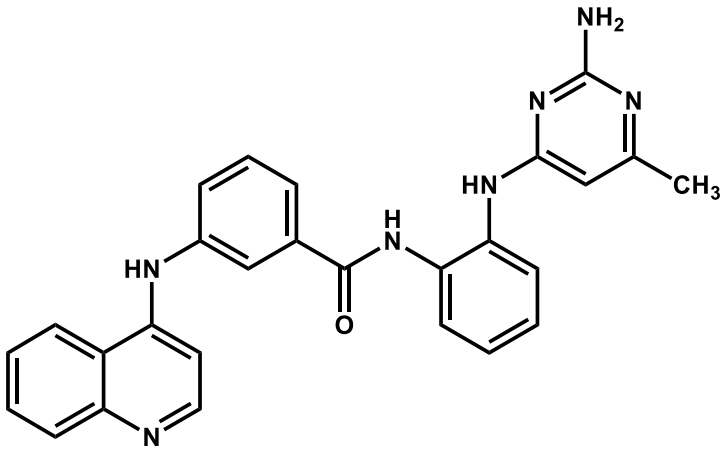

Melting point: 170-172 °C

Appearance: solide beige

Yield: 66%

Recrystallization solvent: acetonitrile

RMN ^{1}H (DMSO-d_6, 400 MHz) δ 2.05 (s, 3H, -CH_3), 5.86 (s, 1H, pyrimidine proton), 6.23 (bs, 2H, -NH_2-pyrimidine), 7.04 (d, 1H, *J* = 5.6 Hz, quinoline proton), 7.20 (m, 2H, benzene and quinoline protons), 7.51-7.74 (m, 7H, benzene and quinoline protons), 7.90-7.92 (m, 2H, benzene and quinoline protons), 8.40 (d, 1H, *J* = 8.4 Hz, quinoline proton), 8.47 (bs, 1H, -N*H*-pyrimidine), 8.51 (d, 1H, *J* = 5.4 quinoline proton), 9.11 (bs, 1H, -N*H*-quinoline), 10.19 (bs, 1H, -CON*H*-) ppm

^{13}C NMR (DMSO-d_6, 100 MHz) δ 23.9, 93.8, 111.8, 112.8, 117.5, 118.9, 121.2, 121.6, 122.8, 124.2, 125.5, 125.7, 126.1, 129.2, 129.6, 133.9, 135.0, 137.9, 138.7, 142.5, 147.6, 149.7, 151.6, 163.1, 164.5, 164.7, 170.2 ppm

HRMS (ESI) $[M]^+$ $C_{27}H_{23}N_7O$ calculated: 461.1964 found: 461.1969.

Elemental analysis: calculated: C: 70.27%; H: 5.02%; N: 21.24% found: C: 70.22%; H: 5.00%; N: 21.39%

***90N*-(4-(2-Amino-6-methylpyrimidin-4-ylamino)phenyl)-2-(quinolin-4-ylamino) benzamide**

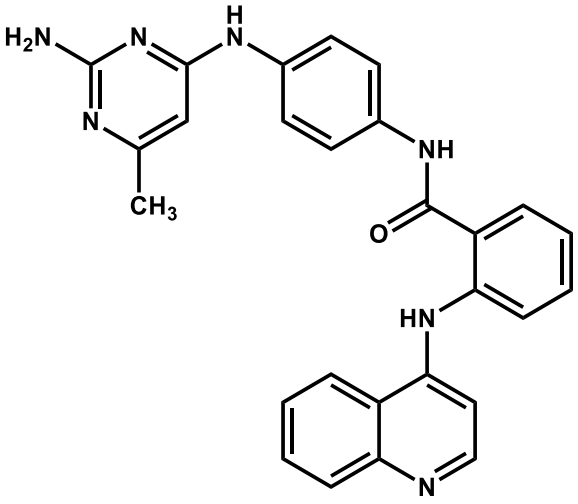

Melting point: 274-279 °C

Appearance: yellow solid

Yield: 78%

Recrystallization solvent: methanol

^{1}H NMR (DMSO-d_6, 400 MHz) δ 2.07 (s, 3H, -CH_3), 5.85 (s, 1H, pyrimidine proton), 6.08 (bs, 2H, -NH_2-pyrimidine), 7.15 (d, 1H, *J* = 5.4 Hz, quinoline proton), 7.26 (t, 1H, *J* = 6.8 Hz, quinoline proton), 7.48-7.75 (m, 9H, benzene and quinoline protons), 7.92 (m, 2H, quinoline protons), 8.16 (d, 1H, *J* = 8.0 Hz, quinoline proton), 8.55 (d, 1H, *J* = 4.0 Hz, quinoline proton), 8.95 (bs,1H, -N*H*-pyrimidine), 10.26 (bs, 1H, -N*H*-quinoline), 10.41 (bs, 1H, -CONH-) ppm

^{13}C NMR (DMSO-d_6, 100 MHz) δ 23.9, 93.8, 112.8, 116.4, 117.7 (2C), 117.9, 118.8, 121.6, 122.4 (2C), 124.2, 125.7, 127.9, 128.3, 129.2, 129.6, 132.9, 136.5, 138.7, 149.7, 151.6, 151.9, 163.1, 164.5, 167.5, 170.2 ppm

HRMS (ESI) $[M]^+$ $C_{27}H_{23}N_7O$ calculated: 461.1964 found: 461.1969.

Elemental analysis: calculated: C: 70.27%; H: 5.02%; N: 21.24% found: C: 70.37%; H: 4.95%; N: 21.12%

91 **N-(3-(2-Amino-6-methylpyrimidin-4-ylamino)phenyl)-2-(quinolin-4-ylamino) benzamide**

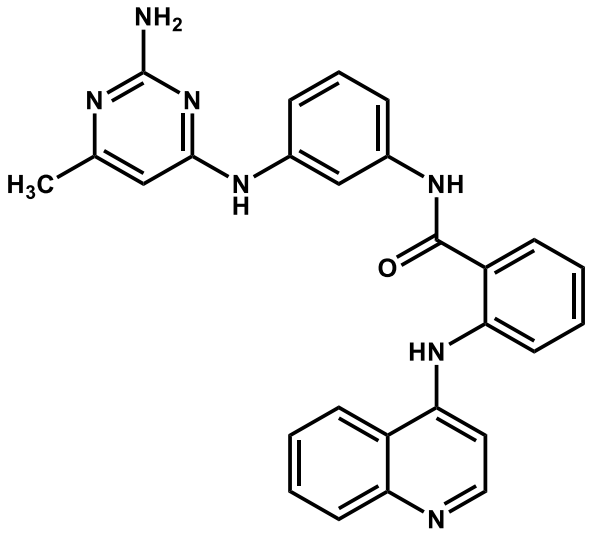

Melting point: 158-161 °C

Appearance: yellow solid

Yield: 74%

Recrystallization solvent: acetonitrile

^{1}H NMR (DMSO-d_6, 400 MHz) δ 2.08 (s, 3H, -CH_3), 5.91 (s, 1H, pyrimidine proton), 6.05 (bs, 2H, -NH_2-pyrimidine), 7.12-7.28 (m, 3H, benzene and quinoline protons), 7.61-7.73 (m, 3H, benzene and quinoline protons), 7.71-7.76 (m, 3H, benzene protons), 7.91-7.96 (m, 2H, benzene and quinoline protons), 8.16 (d, 1H, *J* = 8.0 Hz, quinoline proton), 8.55 (d, 1H, *J* = 4.8 Hz, quinoline proton), 9.02 (bs, 1H, -N*H*-pyrimidine), 10.10 (bs, 1H, -N*H*-quinoline), 10.40 (bs, 1H, -CON*H*-) ppm

^{13}C NMR (DMSO-d_6, 100 MHz, δ; ppm) δ 23.9, 93.8, 108.0, 111.6, 112.8, 113.4, 116.4, 117.9, 118.8, 121.6, 124.2, 125.7, 128.3, 129.2, 129.6, 129.7, 132.9, 136.7, 138.7, 142.6, 149.7, 151.6, 151.9, 163.1, 164.5, 167.5, 170.2 ppm

HRMS (ESI) $[M]^+$ $C_{27}H_{23}N_7O$ calculated: 461.1964 found: 461.1969.

Elemental analysis: calculated: C: 70.27%; H: 5.02%; N: 21.24% found: C: 70.12%; H: 4.90%; N: 21.54%

92 ***N*-(2-(2-Amino-6-methylpyrimidin-4-ylamino)phenyl)-2-(quinolin-4-ylamino) benzamide**

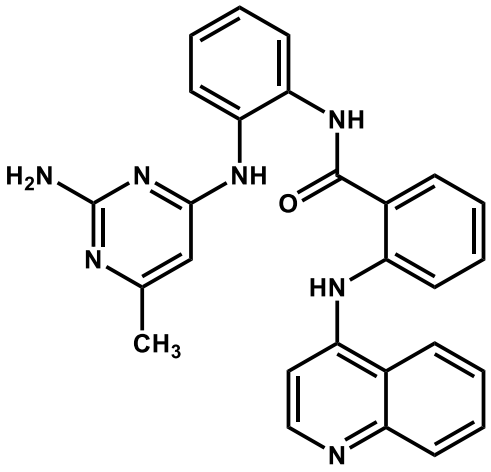

Melting point: 252-255 °C

Appearance: pale yellow solid

Yield: 68%

Recrystallization solvent: methanol

^{1}H NMR (DMSO-d_6, 400 MHz) δ 2.01 (s, 3H, -CH_3), 5.81 (s, 1H, pyrimidine proton), 6.27 (s, 2H, -NH_2-pyrimidine), 7.12-7.24 (m, 4H, benzene and quinoline protons), 7.48 (d, 1H, *J* = 7.6 Hz, benzene proton), 7.54-7.61 (m, 3H, benzene protons), 7.71-7.76 (m, 2H, benzene and quinoline protons), 7.92-7.97 (m, 2H, benzene and quinoline protons), 8.08 (d, 1H, *J* = 8.8 Hz, quinoline protons), 8.57 (m, 2H, quinoline proton and -N*H*-pyrimidine), 10.44 (bs, 1H, -N*H*-quinoline), 10.57 (bs, 1H, -CON*H*-) ppm

^{13}C NMR (DMSO-d_6, 100 MHz) δ 23.9, 93.8, 112.8, 116.4, 117.9, 118.8, 118.9, 121.6, 122.8, 124.2, 125.5, 125.7, 126.1, 128.3, 129.2, 129.6, 132.9, 137.9, 138.7, 147.6, 149.7, 151.6, 151.9, 163.1, 164.5, 167.5, 170.2 ppm

HRMS (ESI) $[M]^+$ $C_{27}H_{23}N_7O$ calculated: 461.1964 found: 461.1969.

Elemental analysis: calculated: C: 70.27%; H: 5.02%; N: 21.24% found: C: 70.32%; H: 5.07%; N: 21.12%

93 4-(Quinolin-4-ylamino)-*N*-(4-(quinolin-4-ylamino)phenyl)benzamide (10)

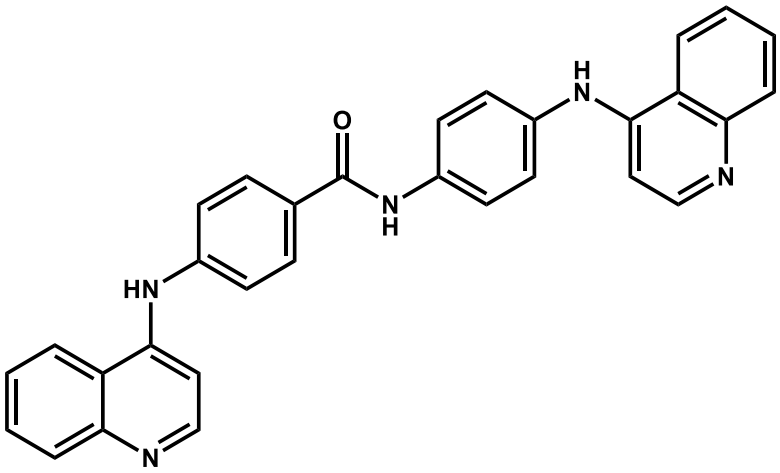

Melting point: >300 °C

Appearance: yellow solid

Yield: 77%

Recrystallization solvent: methanol

^{1}H NMR (DMSO-d_6, 400 MHz) δ 6.83 (d, 1H, *J* = 6.0 Hz, quinoline proton), 7.20 (d, 1H, *J* = 4.8 Hz, quinoline proton), 7.42 (d, 2H, *J* = 8.8 Hz, benzene protons), 7.53 (d, 2H, *J* = 8.4 Hz, benzene protons), 7.60-7.68 (m, 2H, quinoline protons), 7.79 (t, 1H, *J* = 7.2 Hz, quinoline proton), 7.83 (t, 1H, *J* = 7.2 Hz, quinoline proton), 7.94-7.97 (m, 4H, benzene and quinoline protons), 8.07 (d, 2H, *J* = 7.6 Hz, benzene protons), 8.45-8.49 (m, 2H, quinoline protons), 8.57-8.61 (m, 2H, quinoline protons), 9.49 (bs, 1H, -N*H*-quinoline), 9.82 (bs, 1H, -N*H*-quinoline), 10.35 (bs, 1H, -CON*H*-) ppm

^{13}C NMR (DMSO-d_6, 100 MHz) δ 111.4 (2C), 112.8 (2C), 117.7 (2C), 121.6 (2C), 122.4 (2C), 124.2 (3C), 125.7 (2C), 127.9, 129.2 (2C), 129.6 (2C), 130.2 (2C), 138.7 (2C), 141.5, 149.3, 149.7 (2C), 151.6 (2C), 164.7 ppm

HRMS (ESI) $[M]^+$ $C_{31}H_{23}N_5O$ calculated: 481.1903 found: 481.1908.

Elemental analysis: calculated: C: 77.32%; H: 4.81%; N: 14.54% found: C: 77.14%; H: 4.72%; N: 14.79%

94 4-(2-Amino-6-methylpyrimidin-4-ylamino)-*N*-(4-(2-amino-6-methylpyrimidin-4-ylamino) phenyl)benzamide

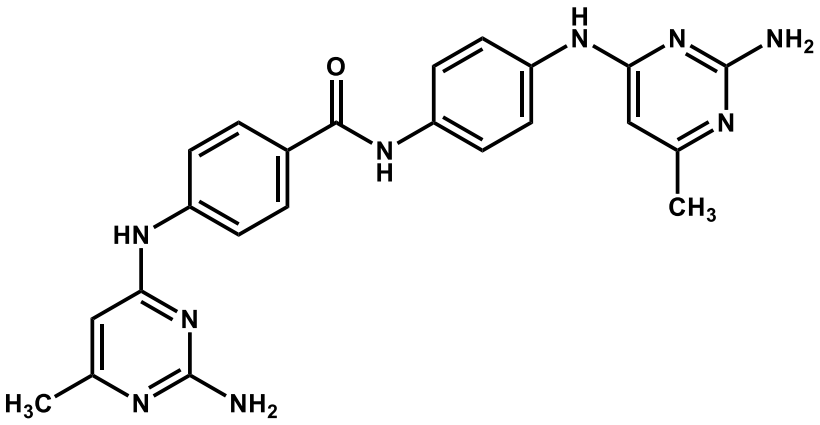

Melting point: >300 °C

Appearance: colorless solid

Yield: 73%

Recrystallization solvent: methanol

^{1}H NMR (DMSO-d_6, 400 MHz) δ 2.09 (s, 3H, -CH_3), 2.13 (s, 3H, -CH_3), 5.86 (s, 1H, pyrimidine proton), 5.95 (s, 1H, pyrimidine proton), 6.10 (bs, 2H, -NH_2-pyrimidine), 6.26 (bs, 2H, -NH_2-pyrimidine), 7.65 (m, 4H, benzene protons), 7.89 (m, 4H, benzene protons), 8.91 (bs, 1H, -N*H*-pyrimidine), 9.32 (bs, 1H, -N*H*-pyrimidine), 9.96 (bs, 1H, -CON*H*-) ppm

^{13}C NMR (DMSO-d_6, 100 MHz) δ 23.9 (2C), 93.8 (2C), 111.4 (2C), 117.7 (2C), 122.4 (2C), 124.2, 127.9, 130.2 (2C), 136.5, 144.3, 163.1 (2C), 164.5, 164.7, 167.0, 167.7, 170.2 ppm

HRMS (ESI) $[M]^+$ $C_{23}H_{23}N_9O$ calculated: 441.2026 found: 441.2023.

Elemental analysis: calculated: C: 62.57%; H: 5.25%; N: 28.55% found: C: 62.34%; H: 5.11%; N: 28.79%

***95 N*-(4-Aminophenyl)-4-(quinolin-4-ylamino)benzamide**

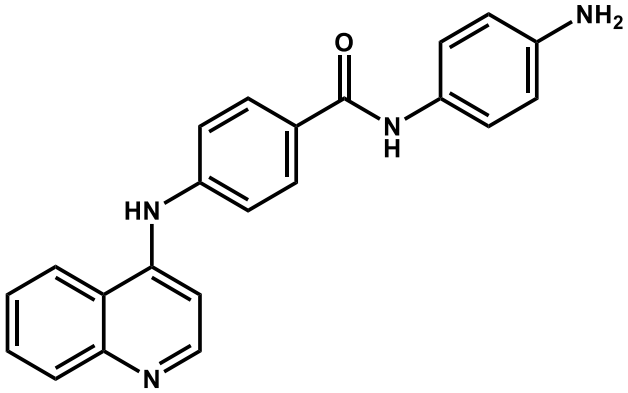

Melting point: 264-267 °C

Appearance: off-white solid

Yield: 77%

Recrystallization solvent: methanol

^{1}H NMR (DMSO-d_6, 400 MHz) δ 4.91 (bs, 2H, -NH_2-benzene), 6.56 (d, 2H, *J* = 7.6 Hz, benzene protons), 7.18 (d, 1H, *J* = 4.8 Hz, quinoline proton), 7.38 (d, 2H, *J* = 8.4 Hz, benzene protons), 7.46 (d, 2H, *J* = 8.4 Hz, benzene protons), 7.60 (t, 1H, *J* = 7.2 Hz, quinoline proton), 7.74 (t, 1H, *J* = 7.2 Hz, quinoline proton), 7.93 (d, 1H, *J* = 8.0 Hz, quinoline proton), 7.97 (d, 2H, *J* = 8.4 Hz, benzene protons), 8.38 (d, 1H, *J* = 8.4 Hz, quinoline proton), 8.57 (d, 1H, *J* = 4.4 Hz, quinoline proton), 9.20 (bs, 1H, -N*H*-quinoline), 9.79 (bs, 1H, -CON*H*-) ppm

^{13}C NMR (DMSO-d_6, 100 MHz, δ; ppm) δ 111.4 (2C), 112.8, 116.5 (2C), 121.6, 122.4 (2C), 124.2 (2C), 125.7, 127.9, 129.2, 129.6, 130.2 (2C), 138.7, 144.0, 149.3, 149.7, 151.6, 164.7 ppm

HRMS (ESI) $[M]^+$ $C_{22}H_{18}N_4O$ calculated: 354.1481 found: 354.1486.

Elemental analysis: calculated: C: 74.56%; H: 5.12%; N: 15.81% calculated: C: 74.81%; H: 5.25%; N: 15.57%

96 4-Amino-*N*-(4-(2-amino-6-methylpyrimidin-4-ylamino)phenyl)benzamide [193, 194]

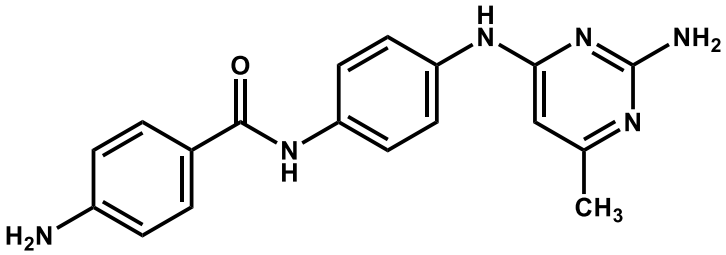

Melting point: >300 °C

Appearance: off-white solid

Yield: 75%

Recrystallization solvent: methanol

RMN ^{1}H (DMSO-d_6, 400 MHz) δ 2.06 (s, 3H, -CH_3), 5.71 (bs, 2H, -NH_2-aniline), 5.85 (s, 1H, pyrimidine proton), 6.08 (bs, 2H, -NH_2-pyrimidine), 6.60 (d, 2H, *J* = 8.4 Hz, benzene protons), 7.59-7.64 (m, 4H, benzene protons), 7.71 (d, 2H, *J* = 8.4 Hz, benzene protons), 8.88 (bs, 1H, -N*H*-pyrimidine), 9.66 (bs, 1H, -CON*H*-) ppm

RMN ^{13}C (DMSO-d_6, 100 MHz,) δ 23.9, 93.8, 114.3 (2C), 117.7 (2C), 122.4 (2C), 124.2, 127.9, 130.2 (2C), 136.5, 151.8, 163.1, 164.5, 164.7, 170.2 ppm

HRMS (ESI) $[M]^+$ $C_{18}H_{18}N_6O$ calculated: 334.1542 found: 334.1545.

Elemental analysis: calculated: C: 64.66%; H: 5.43%; N: 25.13% found: C: 64.93%; H: 5.66%; N: 24.92%

3.7.2 Biology

3.7.2.1 General introduction

The experiments described in this chapter have been conducted by the following research groups: Prof Ettore Novellino of University of Naples in Italy, Prof Xiaodong Cheng Emroy University, Atlanta, USA, Prof Marc Diederich from Laboratoire de Biologie Moléculaire et Cellulaire du Cancer, Luxembourg, Dr Paola Arimondo from USR3388 CNRS-Pierre Fabre Toulouse and Prof Elisabetta Ferretti and Prof Alberto Gulino from „La Sapienza“, University of Rome, Italy.

3.7.2.2 Nanoscale DNMT1 pre-screen. HotSpot DNMT assay

Compounds **1**-**13** were tested in 10-dose IC_{50} mode with 2-fold serial dilution at starting concentration of 500 µM against human DNMT1, using poly(dI-dC) (0.001 mg/mL) as substrate in the presence of AdoMet (1 µM) as cofactor. Control compounds, AdoHcy (S-(5'-adenosyl)-L-homocysteine) and sinefungin, were tested in 10-12 dose IC_{50} mode with 3-fold serial dilution starting at 100 µM.

3.7.2.3 DNMT1, DNMT3A2/3L, PRMT1, and GLP inhibition assays

Protein purification. Expression and purification of human DNMT1 *N*-terminal deletion of 600 residues (residues 601-1600) and human DNMT3A2/DNMT3L complex have been described [124]. Recombinant rat PRMT1[189] and human G9a-like protein (GLP) C-terminal fragment containing both the ankyrin repeats and catalytic SET domain (residues 734-1235; pXC758) [191] were purified as described.

3.7.2.4 DNMT1 inhibition assay

For DNMT1, methyl transfer activity inhibition assays were performed in 20 µL reactions containing 4.6 mM [methyl-^{3}H]-AdoMet (10.0 Ci/mmol; Perkin Elmer), 1.0 mM DNA oligonucleotides, 0.2 µM DNMT1, 1 mM EDTA and 50 mM Tris-HCl pH 7.5. The DNA substrates were 36-base pair hemi-methylated $(GAC)_{12}$. Enzymes were

pre-incubated with AdoMet and various concentrations of inhibitors for 5 min at 37 ^{O}C before the addition of substrate DNA. After 15 min incubation, the reactions were terminated by the addition of 1% sodium dodecyl sulphate and 1 mg/mL of protease K and heat at 50 ^{0}C for 15 min. The reaction mixtures were spotted on DE81 paper circles (Whatman), washed with 5 ml of cold 0.2 M NH_4HCO_3 (twice), 5 mL of deionized water (twice) and 5 mL of ethanol (once). The dried circles were subjected to liquid- scintillation counting with Cytoscint scintillant. All curves were fit individually using Origin 7.5 software (OriginLab).

3.7.2.5 DNMT3A inhibition assay

For DNMT3a2/3L complex, the inhibition assays were performed 20 µL reactions containing 4.6 mM [methyl-^{3}H]-AdoMet, 1.0 mM DNA oligonucleotides, 0.3 µM enzyme, 0.5 mM tris(2-carboxyethyl)phosphine (TCEP), 2.5% (v/v) glycerol and 50 mM Tris–HCl pH 7.5. The DNA substrates were 28-base pair containing two CpG sites: 5'-ACA GTA CGT CAA GAT CTT GAC GTA CTG T-3' and the complimentary strand.

3.7.2.6 PRMT1 and GLP inhibition assays

For histone methylation inhibitions, the assays were performed in 20 µL reactions containing 4.6 mM [methyl-^{3}H]-AdoMet, 50 µg/mL histone from calf thymus (SIGMA), 12 µg/mL (0.3 µM) PRMT1 or 10 µg/mL (0.17 µM) GLP, 100 mM KCl, 5 mM [185] dithiothreitol (DTT) and 50 mM Tris-HCl pH 8.5. Enzymes were pre-incubated with AdoMet and various concentrations of inhibitors for 5 min at 37 ^{0}C (for PRMT1) or 30 ^{0}C (for GLP) before the addition of histone substrates. After incubation (6.5 min for PRMT1 or 5 min for GLP), the reactions were terminated by the addition of 20% trichloroacetic acid (TCA, Fisher Scientific). The reaction mixtures were spotted on GF/A paper circles (Whatman), washed three times with 3 mL of 10% TCA and once with 3 ml of ethanol. The dried circles were subjected to liquid-scintillation

counting with Cytoscint scintillant. All curves were fitted individually using Origin 7.5 software (OriginLab).

3.7.2.7 Competition studies

In AdoMet-competition assays, AdoMet (0.6TBq/mmol) was varied between 0.5 µM and 15 µM with an isotopic dilution of 1*:1 at a fixed DNA duplex concentration of 1.0 µM. For each AdoMet concentration, the tested compound concentration was adjusted between its IC_{10} and its IC_{80}. In DNA-competition assays, the DNA duplex concentration was varied between 0.05 µM and 1.0 µM whereas AdoMet (0.6TBq/mmol) concentration was hold at 15 µM with an isotopic dilution of 1*:2. For each DNA duplex concentration, the tested compound concentration was adjusted between its IC_{10} and its IC_{80}. For each substrate concentration, the IC_{50} of tested compound was calculated by non-linear regression fitting with sigmoidal dose-response (variable slope). For each compound concentration, K_m^{app} and V_m^{app} of each substrate were approximated by non-linear fitting of the data with the Michaelis-Menten equation on GraphPad Prism 4.03.

3.7.2.8 Molecular modelling

Prior to docking calculations, the Epik software [195] was used to calculate the most relevant ionization and tautomeric state of compounds **1** and **5**. Then the Glide program of the Schrödinger package [196] was used to dock these compounds into the two selected DNMT1 X-ray structures (PDBs 3SWR' Hashimoto and Cheng, unpublished results, and 3PTA[192]). The receptor grid generation was performed for the box with a center in the putative binding sites of the two structures. The size of the box was determined automatically. The extra precision mode (XP) of Glide was used for docking. The ligand-scaling factor was set to 1.0. The geometry of the ligand-binding site of the complex between **1** and **5** and the DNMT1 structures was then optimized. The binding site was defined as **1** or **5** and all amino acid residues located within 8 Å from the ligands. All the receptor residues located within 2 Å

from the binding site were used as a shell. The following parameters of energy minimization were used: OPLS2005 force field was used. Water was used as an implicit solvent, and a maximum of 5000 iterations of the Polak–Ribier conjugate gradient minimization method was used with a convergence threshold of 0.01 kJ mol^{-1} $Å^{-1}$. All complex pictures were rendered employing the UCSF Chimera software [197].

3.7.2.9 U-937, RAJI, PC-3, MDA-MB-231 and PBM cellular assays

U-937 (histiocytic lymphoma), RAJI (Burkitt's lymphoma), PC-3 (prostate cancer), MDA-MB-231 (breast cancer) cell lines were purchased from Deutsche Sammlung für Mikroorganismen und Zellkulturen (DSZM). Cells were cultured in RPMI 1640 (Lonza), supplemented with 10% fetal calf serum (Lonza) and 1% antibiotic–antimycotic (Lonza). Peripheral blood mononuclear cells (PBMCs) were isolated and cultured as previously described [198]. Cells in exponential growth phase were treated with compounds at the indicated concentrations. Proliferation and viability were assessed by trypan blue exclusion analysis at the indicated time points. Morphological determination of apoptosis and necrosis was performed as described previously. [199]

3.7.2.10 Medulloblastoma cancer stem cell (MbSC) assays

Stem cell cultures and treatments

MbSCs were isolated and cultivated as already described [200]. In detail, MbSCs were isolated from fresh tumour specimens from Ptch1+/-. Cells were obtained after mechanical and enzymatic dissociation and cultured in serum-free DMEM-F12 plus glucose 0.6%, insulin 25 mg/mL, *N*-acetyl-L-cysteine 60 mg/mL, heparin 2 mg/mL, B271X, EGF 20 ng/mL and bFGF 20 ng/mL. MbSCs were also treated to differentiate in vitro after withdrawal of EGF/bFGF and addition of differentiating factors (Platelet Derived Growth Factor, PDGF) for 48 h. Compounds **2** and **5** were resuspended in DMSO at 1 mM. Cells were treated with increasing concentration of

2 or **5** (1, 10 and 50 μM) for 48 h and DMSO was used as control. Unless otherwise indicated, media and supplements were purchased from Gibco-Invitrogen (Life Science) and chemicals were from Sigma-Aldrich (St. Louis, MO).

3.7.2.11 RNA isolation and Real-Time qPCR

Total RNA was isolated with Tri-Reagent (Ambion) according to manufacturer's procedure, samples quantification was done using Nanodrop spectrophotometer (ThermoScientific). The reverse transcription was performed using High Capacity cDNA reverse transcription kit (Applied Biosystem) and quantitative RT-PCR analysis of βIII-tubulin, Pcna and DNMT1, -3a and -3b were performed using TaqMan assay from Lifetech. mRNA expression was analysed using the ABI Prism 7900HT Sequence Detection System (Applied Biosystem), using TaqMan gene expression assay according to manufacturer's protocol (Applied Biosystem). Each amplification reaction was performed in triplicate, and the average of the three threshold cycles was used to calculate the amount of transcripts in the sample (SDS 2.3 software, Applied Biosystem). mRNA quantification was expressed, in arbitrary units, as the ratio of the sample quantity to the calibrator or to the mean values of control samples. All values were normalized to three endogenous controls, β-actin, β2-microglobulin and HPRT.

3.7.2.12 Western blot assay

Cells were lysed using RIPA buffer (Tis-HCl pH7.6 50 mM, deoxycholic acid sodium salt 0.5%, NaCl 140 mM, NP40 1%, EDTA 5 mM, NaF 100 mM, sodium pyrophosphate 2 mM) and protease inhibitors. Lysate were separated on 8% acrylamide gel and immunoblotted using standard procedures. The following antibodies were used: anti-DNMT1 (sc-20701; Santa Cruz Biotechnology, CA); anti-DNMT3a (sc-365769; Santa Cruz Biotechnology, CA), anti- DNMT3b (sc-10236; Santa Cruz Biotechnology, CA).

3.7.2.13 MTT assay

MbSC were treated with 1, 10 and 50 µM of compound **2** or **5** for 48 h. Growth of drug-treated cells relative to untreated cells was measured by MTT assay. Each sample was measured in triplicates and repeated at least three times.

3.8 References

52. S.Y. Shin, M.C. Shin, J.S. Shin, K.T. Lee, and Y.S. Lee, *Synthesis of aurones and their inhibitory effects on nitric oxide and PGE(2) productions in LPS-induced RAW 264.7 cells.* Bioorganic & medicinal chemistry letters, 2011. **21**(15): p. 4520-3.
85. T. Chen, S. Hevi, F. Gay, N. Tsujimoto, T. He, B. Zhang, Y. Ueda, and E. Li, *Complete inactivation of DNMT1 leads to mitotic catastrophe in human cancer cells.* Nat Genet, 2007. **39**(3): p. 391-6.
90. C.H. Waddington, *The epigenotype. 1942.* Int J Epidemiol, 2012. **41**(1): p. 10-3.
91. A. Bird, *Perceptions of epigenetics.* Nature, 2007. **447**(7143): p. 396-8.
92. S.L. Berger, T. Kouzarides, R. Shiekhattar, and A. Shilatifard, *An operational definition of epigenetics.* Genes Dev, 2009. **23**(7): p. 781-3.
93. C.B. Yoo and P.A. Jones, *Epigenetic therapy of cancer: past, present and future.* Nat Rev Drug Discov, 2006. **5**(1): p. 37-50.
94. S.B. Baylin and P.A. Jones, *A decade of exploring the cancer epigenome - biological and translational implications.* Nat Rev Cancer, 2011. **11**(10): p. 726-34.
95. C. Florean, M. Schnekenburger, C. Grandjenette, M. Dicato, and M. Diederich, *Epigenomics of leukemia: from mechanisms to therapeutic applications.* Epigenomics, 2011. **3**(5): p. 581-609.
96. G. Egger, G. Liang, A. Aparicio, and P.A. Jones, *Epigenetics in human disease and prospects for epigenetic therapy.* Nature, 2004. **429**(6990): p. 457-63.
97. S. Takashima, M. Takehashi, J. Lee, S. Chuma, M. Okano, K. Hata, I. Suetake, N. Nakatsuji, H. Miyoshi, S. Tajima, Y. Tanaka, S. Toyokuni, H. Sasaki, M. Kanatsu-Shinohara, and T. Shinohara, *Abnormal DNA methyltransferase expression in mouse germline stem cells results in spermatogenic defects.* Biol Reprod, 2009. **81**(1): p. 155-64.
98. F. Gaudet, J.G. Hodgson, A. Eden, L. Jackson-Grusby, J. Dausman, J.W. Gray, H. Leonhardt, and R. Jaenisch, *Induction of tumors in mice by genomic hypomethylation.* Science, 2003. **300**(5618): p. 489-92.
99. A. Eden, F. Gaudet, A. Waghmare, and R. Jaenisch, *Chromosomal instability and tumors promoted by DNA hypomethylation.* Science, 2003. **300**(5618): p. 455.
100. I.A. Qureshi and M.F. Mehler, *Advances in epigenetics and epigenomics for neurodegenerative diseases.* Curr Neurol Neurosci Rep, 2011. **11**(5): p. 464-73.
101. A. Fuso, V. Nicolia, R.A. Cavallaro, and S. Scarpa, *DNA methylase and demethylase activities are modulated by one-carbon metabolism in Alzheimer's disease models.* J Nutr Biochem, 2011. **22**(3): p. 242-51.
102. F. Higuchi, S. Uchida, H. Yamagata, K. Otsuki, T. Hobara, N. Abe, T. Shibata, and Y. Watanabe, *State-dependent changes in the expression of DNA*

methyltransferases in mood disorder patients. J Psychiatr Res, 2011. **45**(10): p. 1295-300.
103. C. Lopez-Pedrera, C. Perez-Sanchez, M. Ramos-Casals, M. Santos-Gonzalez, A. Rodriguez-Ariza, and M.J. Cuadrado, *Cardiovascular risk in systemic autoimmune diseases: epigenetic mechanisms of immune regulatory functions.* Clin Dev Immunol, 2012. **2012**: p. 974648.
104. E.R. Nimmo, J.G. Prendergast, M.C. Aldhous, N.A. Kennedy, P. Henderson, H.E. Drummond, B.H. Ramsahoye, D.C. Wilson, C.A. Semple, and J. Satsangi, *Genome-wide methylation profiling in Crohn's disease identifies altered epigenetic regulation of key host defense mechanisms including the Th17 pathway.* Inflamm Bowel Dis, 2012. **18**(5): p. 889-99.
105. J. Bressler, L.C. Shimmin, E. Boerwinkle, and J.E. Hixson, *Global DNA methylation and risk of subclinical atherosclerosis in young adults: the Pathobiological Determinants of Atherosclerosis in Youth (PDAY) study.* Atherosclerosis, 2011. **219**(2): p. 958-62.
106. J.G. Herman and S.B. Baylin, *Gene silencing in cancer in association with promoter hypermethylation.* N Engl J Med, 2003. **349**(21): p. 2042-54.
107. P.A. Jones and S.B. Baylin, *The epigenomics of cancer.* Cell, 2007. **128**(4): p. 683-92.
108. L.J. Rush, Z. Dai, D.J. Smiraglia, X. Gao, F.A. Wright, M. Fruhwald, J.F. Costello, W.A. Held, L. Yu, R. Krahe, J.E. Kolitz, C.D. Bloomfield, M.A. Caligiuri, and C. Plass, *Novel methylation targets in de novo acute myeloid leukemia with prevalence of chromosome 11 loci.* Blood, 2001. **97**(10): p. 3226-33.
109. J.R. Melki, P.C. Vincent, and S.J. Clark, *Concurrent DNA hypermethylation of multiple genes in acute myeloid leukemia.* Cancer research, 1999. **59**(15): p. 3730-40.
110. A.-K. Petersen, S. Zeilinger, G. Kastenmüller, W. Römisch-Margl, M. Brugger, A. Peters, C. Meisinger, K. Strauch, C. Hengstenberg, P. Pagel, F. Huber, R.P. Mohney, H. Grallert, T. Illig, J. Adamski, M. Waldenberger, C. Gieger, and K. Suhre, *Epigenetics meets metabolomics: An epigenome-wide association study with blood serum metabolic traits.* Human Molecular Genetics, 2013.
111. T.H. Bestor, *The DNA methyltransferases of mammals.* Hum Mol Genet, 2000. **9**(16): p. 2395-402.
112. W. Reik, *Stability and flexibility of epigenetic gene regulation in mammalian development.* Nature, 2007. **447**(7143): p. 425-32.
113. J. Espada and M. Esteller, *DNA methylation and the functional organization of the nuclear compartment.* Semin Cell Dev Biol, 2010. **21**(2): p. 238-46.
114. K.D. Robertson, *DNA methylation and chromatin - unraveling the tangled web.* Oncogene, 2002. **21**(35): p. 5361-79.
115. J. Espada and M. Esteller, *Epigenetic control of nuclear architecture.* Cell Mol Life Sci, 2007. **64**(4): p. 449-57.
116. O. Bogdanovic and G.J. Veenstra, *DNA methylation and methyl-CpG binding proteins: developmental requirements and function.* Chromosoma, 2009. **118**(5): p. 549-65.

117. A.D. Riggs, Z. Xiong, L. Wang, and J.M. LeBon, *Methylation dynamics, epigenetic fidelity and X chromosome structure.* Novartis Found Symp, 1998. **214**: p. 214-25; discussion 225-32.
118. S. Sharma, T.K. Kelly, and P.A. Jones, *Epigenetics in cancer.* Carcinogenesis, 2010. **31**(1): p. 27-36.
119. A.P. Feinberg, *Epigenetics at the epicenter of modern medicine.* JAMA, 2008. **299**(11): p. 1345-50.
120. H.H. Ng and A. Bird, *DNA methylation and chromatin modification.* Curr Opin Genet Dev, 1999. **9**(2): p. 158-63.
121. T. Bestor, A. Laudano, R. Mattaliano, and V. Ingram, *Cloning and sequencing of a cDNA encoding DNA methyltransferase of mouse cells. The carboxyl-terminal domain of the mammalian enzymes is related to bacterial restriction methyltransferases.* J Mol Biol, 1988. **203**(4): p. 971-83.
122. F. Chik and M. Szyf, *Effects of specific DNMT gene depletion on cancer cell transformation and breast cancer cell invasion; toward selective DNMT inhibitors.* Carcinogenesis, 2011. **32**(2): p. 224-32.
123. F. Antequera and A. Bird, *Number of CpG islands and genes in human and mouse.* Proceedings of the National Academy of Sciences of the United States of America, 1993. **90**(24): p. 11995-9.
124. H. Hashimoto, Y. Liu, A.K. Upadhyay, Y. Chang, S.B. Howerton, P.M. Vertino, X. Zhang, and X. Cheng, *Recognition and potential mechanisms for replication and erasure of cytosine hydroxymethylation.* Nucleic Acids Res, 2012. **40**(11): p. 4841-9.
125. R.Z. Jurkowska, T.P. Jurkowski, and A. Jeltsch, *Structure and function of mammalian DNA methyltransferases.* Chembiochem, 2011. **12**(2): p. 206-22.
126. T.H. Bestor, *Activation of mammalian DNA methyltransferase by cleavage of a Zn binding regulatory domain.* EMBO J, 1992. **11**(7): p. 2611-7.
127. M. Okano, D.W. Bell, D.A. Haber, and E. Li, *DNA methyltransferases Dnmt3a and Dnmt3b are essential for de novo methylation and mammalian development.* Cell, 1999. **99**(3): p. 247-57.
128. J. Lan, S. Hua, X. He, and Y. Zhang, *DNA methyltransferases and methyl-binding proteins of mammals.* Acta Biochim Biophys Sin (Shanghai), 2010. **42**(4): p. 243-52.
129. R.S. Hansen, C. Wijmenga, P. Luo, A.M. Stanek, T.K. Canfield, C.M. Weemaes, and S.M. Gartler, *The DNMT3B DNA methyltransferase gene is mutated in the ICF immunodeficiency syndrome.* Proc Natl Acad Sci U S A, 1999. **96**(25): p. 14412-7.
130. F.I. Daniel, K. Cherubini, L.S. Yurgel, M.A. de Figueiredo, and F.G. Salum, *The role of epigenetic transcription repression and DNA methyltransferases in cancer.* Cancer, 2011. **117**(4): p. 677-87.
131. M. Esteller, *Epigenetics in cancer.* N Engl J Med, 2008. **358**(11): p. 1148-59.
132. A.P. Feinberg, R. Ohlsson, and S. Henikoff, *The epigenetic progenitor origin of human cancer.* Nat Rev Genet, 2006. **7**(1): p. 21-33.
133. E. Prokhortchouk and P.A. Defossez, *The cell biology of DNA methylation in mammals.* Biochim Biophys Acta, 2008. **1783**(11): p. 2167-73.

134. S. Ramchandani, S.K. Bhattacharya, N. Cervoni, and M. Szyf, *DNA methylation is a reversible biological signal.* Proc Natl Acad Sci U S A, 1999. **96**(11): p. 6107-12.
135. C. Gros, J. Fahy, L. Halby, I. Dufau, A. Erdmann, J.M. Gregoire, F. Ausseil, S. Vispe, and P.B. Arimondo, *DNA methylation inhibitors in cancer: Recent and future approaches.* Biochimie, 2012. **94**(11): p. 2280-96.
136. Y.G. Zheng, J. Wu, Z. Chen, and M. Goodman, *Chemical regulation of epigenetic modifications: opportunities for new cancer therapy.* Med Res Rev, 2008. **28**(5): p. 645-87.
137. T.H. Bestor and G.L. Verdine, *DNA methyltransferases.* Curr Opin Cell Biol, 1994. **6**(3): p. 380-9.
138. X. Cheng and R.M. Blumenthal, *Coordinated chromatin control: structural and functional linkage of DNA and histone methylation.* Biochemistry, 2010. **49**(14): p. 2999-3008.
139. K.D. Robertson, *DNA methylation, methyltransferases, and cancer.* Oncogene, 2001. **20**(24): p. 3139-55.
140. S. Klimasauskas, S. Kumar, R.J. Roberts, and X. Cheng, *HhaI methyltransferase flips its target base out of the DNA helix.* Cell, 1994. **76**(2): p. 357-69.
141. Z.M. Svedruzic and N.O. Reich, *Mechanism of allosteric regulation of Dnmt1's processivity.* Biochemistry, 2005. **44**(45): p. 14977-88.
142. M. Szyf, *Epigenetics, DNA methylation, and chromatin modifying drugs.* Annu Rev Pharmacol Toxicol, 2009. **49**: p. 243-63.
143. X. Yang, F. Lay, H. Han, and P.A. Jones, *Targeting DNA methylation for epigenetic therapy.* Trends in pharmacological sciences, 2010. **31**(11): p. 536-546.
144. F. Sorm and J. Vesely, *Effect of 5-aza-2'-deoxycytidine against leukemic and hemopoietic tissues in AKR mice.* Neoplasma, 1968. **15**(4): p. 339-43.
145. P.G. Constantinides, P.A. Jones, and W. Gevers, *Functional striated muscle cells from non-myoblast precursors following 5-azacytidine treatment.* Nature, 1977. **267**(5609): p. 364-6.
146. P.G. Constantinides, S.M. Taylor, and P.A. Jones, *Phenotypic conversion of cultured mouse embryo cells by aza pyrimidine nucleosides.* Dev Biol, 1978. **66**(1): p. 57-71.
147. P.A. Jones and S.M. Taylor, *Cellular differentiation, cytidine analogs and DNA methylation.* Cell, 1980. **20**(1): p. 85-93.
148. R.L. Momparler, *Pharmacology of 5-Aza-2'-deoxycytidine (decitabine).* Semin Hematol, 2005. **42**(3 Suppl 2): p. S9-16.
149. D.V. Santi, A. Norment, and C.E. Garrett, *Covalent bond formation between a DNA-cytosine methyltransferase and DNA containing 5-azacytosine.* Proc Natl Acad Sci U S A, 1984. **81**(22): p. 6993-7.
150. K. Ghoshal, J. Datta, S. Majumder, S. Bai, H. Kutay, T. Motiwala, and S.T. Jacob, *5-Aza-deoxycytidine induces selective degradation of DNA methyltransferase 1 by a proteasomal pathway that requires the KEN box, bromo-adjacent homology domain, and nuclear localization signal.* Mol Cell Biol, 2005. **25**(11): p. 4727-41.

151. C. Champion, D. Guianvarc'h, C. Senamaud-Beaufort, R.Z. Jurkowska, A. Jeltsch, L. Ponger, P.B. Arimondo, and A.L. Guieysse-Peugeot, *Mechanistic insights on the inhibition of c5 DNA methyltransferases by zebularine.* PLoS One, 2010. **5**(8): p. e12388.
152. R.L. Piekarz and S.E. Bates, *Epigenetic modifiers: basic understanding and clinical development.* Clin Cancer Res, 2009. **15**(12): p. 3918-26.
153. L.S. Kristensen, H.M. Nielsen, and L.L. Hansen, *Epigenetics and cancer treatment.* Eur J Pharmacol, 2009. **625**(1-3): p. 131-42.
154. G.L. Gravina, C. Festuccia, F. Marampon, V.M. Popov, R.G. Pestell, B.M. Zani, and V. Tombolini, *Biological rationale for the use of DNA methyltransferase inhibitors as new strategy for modulation of tumor response to chemotherapy and radiation.* Mol Cancer, 2010. **9**: p. 305.
155. J. Flynn, J.Y. Fang, J.A. Mikovits, and N.O. Reich, *A potent cell-active allosteric inhibitor of murine DNA cytosine C5 methyltransferase.* J Biol Chem, 2003. **278**(10): p. 8238-43.
156. E. Cornacchia, J. Golbus, J. Maybaum, J. Strahler, S. Hanash, and B. Richardson, *Hydralazine and procainamide inhibit T cell DNA methylation and induce autoreactivity.* J Immunol, 1988. **140**(7): p. 2197-200.
157. N. Singh, A. Duenas-Gonzalez, F. Lyko, and J.L. Medina-Franco, *Molecular modeling and molecular dynamics studies of hydralazine with human DNA methyltransferase 1.* ChemMedChem, 2009. **4**(5): p. 792-9.
158. J. Yoo and J.L. Medina-Franco, *Homology modeling, docking and structure-based pharmacophore of inhibitors of DNA methyltransferase.* J Comput Aided Mol Des, 2011. **25**(6): p. 555-67.
159. L. Halby, C. Champion, C. Senamaud-Beaufort, S. Ajjan, T. Drujon, A. Rajavelu, A. Ceccaldi, R. Jurkowska, O. Lequin, W.G. Nelson, A. Guy, A. Jeltsch, D. Guianvarc'h, C. Ferroud, and P.B. Arimondo, *Rapid synthesis of new DNMT inhibitors derivatives of procainamide.* Chembiochem, 2012. **13**(1): p. 157-65.
160. J.C. Chuang, C.B. Yoo, J.M. Kwan, T.W. Li, G. Liang, A.S. Yang, and P.A. Jones, *Comparison of biological effects of non-nucleoside DNA methylation inhibitors versus 5-aza-2'-deoxycytidine.* Mol Cancer Ther, 2005. **4**(10): p. 1515-20.
161. C. Stresemann, B. Brueckner, T. Musch, H. Stopper, and F. Lyko, *Functional diversity of DNA methyltransferase inhibitors in human cancer cell lines.* Cancer Res, 2006. **66**(5): p. 2794-800.
162. A. Villar-Garea, M.F. Fraga, J. Espada, and M. Esteller, *Procaine is a DNA-demethylating agent with growth-inhibitory effects in human cancer cells.* Cancer Res, 2003. **63**(16): p. 4984-9.
163. T.M. Attina, I.D. Drummond, L.S. Malatino, S.R. Maxwell, and D.J. Webb, *Phosphodiesterase type 5 inhibition improves arterial stiffness after exercise but not exercise capacity in hypertensive men.* Am J Hypertens, 2013. **26**(3): p. 342-50.
164. B. Brueckner, D. Kuck, and F. Lyko, *DNA methyltransferase inhibitors for cancer therapy.* Cancer J, 2007. **13**(1): p. 17-22.

165. P. Zambrano, B. Segura-Pacheco, E. Perez-Cardenas, L. Cetina, A. Revilla-Vazquez, L. Taja-Chayeb, A. Chavez-Blanco, E. Angeles, G. Cabrera, K. Sandoval, C. Trejo-Becerril, J. Chanona-Vilchis, and A. Duenas-Gonzalez, *A phase I study of hydralazine to demethylate and reactivate the expression of tumor suppressor genes.* BMC Cancer, 2005. **5**: p. 44.
166. M. Candelaria, D. Gallardo-Rincon, C. Arce, L. Cetina, J.L. Aguilar-Ponce, O. Arrieta, A. Gonzalez-Fierro, A. Chavez-Blanco, E. de la Cruz-Hernandez, M.F. Camargo, C. Trejo-Becerril, E. Perez-Cardenas, C. Perez-Plasencia, L. Taja-Chayeb, T. Wegman-Ostrosky, A. Revilla-Vazquez, and A. Duenas-Gonzalez, *A phase II study of epigenetic therapy with hydralazine and magnesium valproate to overcome chemotherapy resistance in refractory solid tumors.* Ann Oncol, 2007. **18**(9): p. 1529-38.
167. M. Candelaria, A. Herrera, J. Labardini, A. Gonzalez-Fierro, C. Trejo-Becerril, L. Taja-Chayeb, E. Perez-Cardenas, E. de la Cruz-Hernandez, D. Arias-Bofill, S. Vidal, E. Cervera, and A. Duenas-Gonzalez, *Hydralazine and magnesium valproate as epigenetic treatment for myelodysplastic syndrome. Preliminary results of a phase-II trial.* Ann Hematol, 2011. **90**(4): p. 379-87.
168. D. Kim, I.S. Lee, J.H. Jung, C.O. Lee, and S.U. Choi, *Psammaplin A, a natural phenolic compound, has inhibitory effect on human topoisomerase II and is cytotoxic to cancer cells.* Anticancer Res, 1999. **19**(5B): p. 4085-90.
169. D. Kim, I.S. Lee, J.H. Jung, and S.I. Yang, *Psammaplin A, a natural bromotyrosine derivative from a sponge, possesses the antibacterial activity against methicillin-resistant Staphylococcus aureus and the DNA gyrase-inhibitory activity.* Arch Pharm Res, 1999. **22**(1): p. 25-9.
170. I.C. Pina, J.T. Gautschi, G.Y. Wang, M.L. Sanders, F.J. Schmitz, D. France, S. Cornell-Kennon, L.C. Sambucetti, S.W. Remiszewski, L.B. Perez, K.W. Bair, and P. Crews, *Psammaplins from the sponge Pseudoceratina purpurea: inhibition of both histone deacetylase and DNA methyltransferase.* J Org Chem, 2003. **68**(10): p. 3866-73.
171. D.H. Kim, J. Shin, and H.J. Kwon, *Psammaplin A is a natural prodrug that inhibits class I histone deacetylase.* Exp Mol Med, 2007. **39**(1): p. 47-55.
172. C.S. Yang, X. Wang, G. Lu, and S.C. Picinich, *Cancer prevention by tea: animal studies, molecular mechanisms and human relevance.* Nat Rev Cancer, 2009. **9**(6): p. 429-39.
173. B.N. Singh, S. Shankar, and R.K. Srivastava, *Green tea catechin, epigallocatechin-3-gallate (EGCG): mechanisms, perspectives and clinical applications.* Biochem Pharmacol, 2011. **82**(12): p. 1807-21.
174. N. Suh and J.M. Pezzuto, *Strawberry fields forever?* Cancer Prev Res (Phila), 2012. **5**(1): p. 30-3.
175. M. Fang, D. Chen, and C.S. Yang, *Dietary polyphenols may affect DNA methylation.* J Nutr, 2007. **137**(1 Suppl): p. 223S-228S.
176. Y. Li and T.O. Tollefsbol, *Impact on DNA methylation in cancer prevention and therapy by bioactive dietary components.* Curr Med Chem, 2010. **17**(20): p. 2141-51.

177. S. Castellano, D. Kuck, M. Sala, E. Novellino, F. Lyko, and G. Sbardella, *Constrained analogues of procaine as novel small molecule inhibitors of DNA methyltransferase-1.* J Med Chem, 2008. **51**(7): p. 2321-5.
178. S. Castellano, D. Kuck, M. Viviano, J. Yoo, F. Lopez-Vallejo, P. Conti, L. Tamborini, A. Pinto, J.L. Medina-Franco, and G. Sbardella, *Synthesis and biochemical evaluation of delta(2)-isoxazoline derivatives as DNA methyltransferase 1 inhibitors.* Journal of medicinal chemistry, 2011. **54**(21): p. 7663-77.
179. Z. Liu, Z. Xie, W. Jones, R.E. Pavlovicz, S. Liu, J. Yu, P.K. Li, J. Lin, J.R. Fuchs, G. Marcucci, C. Li, and K.K. Chan, *Curcumin is a potent DNA hypomethylation agent.* Bioorg Med Chem Lett, 2009. **19**(3): p. 706-9.
180. L. Shu, T.O. Khor, J.H. Lee, S.S. Boyanapalli, Y. Huang, T.Y. Wu, C.L. Saw, K.L. Cheung, and A.N. Kong, *Epigenetic CpG demethylation of the promoter and reactivation of the expression of Neurog1 by curcumin in prostate LNCaP cells.* AAPS J, 2011. **13**(4): p. 606-14.
181. B. Brueckner, R. Garcia Boy, P. Siedlecki, T. Musch, H.C. Kliem, P. Zielenkiewicz, S. Suhai, M. Wiessler, and F. Lyko, *Epigenetic reactivation of tumor suppressor genes by a novel small-molecule inhibitor of human DNA methyltransferases.* Cancer Res, 2005. **65**(14): p. 6305-11.
182. P. Siedlecki, R. Garcia Boy, S. Comagic, R. Schirrmacher, M. Wiessler, P. Zielenkiewicz, S. Suhai, and F. Lyko, *Establishment and functional validation of a structural homology model for human DNA methyltransferase 1.* Biochem Biophys Res Commun, 2003. **306**(2): p. 558-63.
183. T. Suzuki, R. Tanaka, S. Hamada, H. Nakagawa, and N. Miyata, *Design, synthesis, inhibitory activity, and binding mode study of novel DNA methyltransferase 1 inhibitors.* Bioorg Med Chem Lett, 2010. **20**(3): p. 1124-7.
184. W.A. Denny, G.J. Atwell, B.C. Baguley, and B.F. Cain, *Potential antitumor agents. 29. Quantitative structure-activity relationships for the antileukemic bisquaternary ammonium heterocycles.* J Med Chem, 1979. **22**(2): p. 134-50.
185. J. Datta, K. Ghoshal, W.A. Denny, S.A. Gamage, D.G. Brooke, P. Phiasivongsa, S. Redkar, and S.T. Jacob, *A new class of quinoline-based DNA hypomethylating agents reactivates tumor suppressor genes by blocking DNA methyltransferase 1 activity and inducing its degradation.* Cancer Res, 2009. **69**(10): p. 4277-85.
186. Z.M. Svedruzic, *Dnmt1 structure and function.* Prog Mol Biol Transl Sci, 2011. **101**: p. 221-54.
187. M. Szyf, *Epigenetic therapeutics in autoimmune disease.* Clin Rev Allergy Immunol, 2010. **39**(1): p. 62-77.
188. J. Coste, D. Le-Nguyen, and B. Castro, *PyBOP®: A new peptide coupling reagent devoid of toxic by-product.* Tetrahedron Letters, 1990. **31**(2): p. 205-208.
189. X. Zhang and X. Cheng, *Structure of the predominant protein arginine methyltransferase PRMT1 and analysis of its binding to substrate peptides.* Structure, 2003. **11**(5): p. 509-20.

190. Y. Shinkai and M. Tachibana, *H3K9 methyltransferase G9a and the related molecule GLP.* Genes Dev, 2011. **25**(8): p. 781-8.
191. Y. Chang, X. Zhang, J.R. Horton, A.K. Upadhyay, A. Spannhoff, J. Liu, J.P. Snyder, M.T. Bedford, and X. Cheng, *Structural basis for G9a-like protein lysine methyltransferase inhibition by BIX-01294.* Nat Struct Mol Biol, 2009. **16**(3): p. 312-7.
192. J. Song, O. Rechkoblit, T.H. Bestor, and D.J. Patel, *Structure of DNMT1-DNA complex reveals a role for autoinhibition in maintenance DNA methylation.* Science, 2011. **331**(6020): p. 1036-40.
193. P. Garcia-Dominguez, C. Dell'aversana, R. Alvarez, L. Altucci, and A.R. de Lera, *Synthetic approaches to DNMT inhibitor SGI-1027 and effects on the U937 leukemia cell line.* Bioorg Med Chem Lett, 2013. **23**(6): p. 1631-5.
194. S.A. Gamage, D.G. Brooke, S. Redkar, J. Datta, S.T. Jacob, and W.A. Denny, *Structure-activity relationships for 4-anilinoquinoline derivatives as inhibitors of the DNA methyltransferase enzyme DNMT1.* Bioorg Med Chem, 2013.
195. *Epik Version 2.0*, in *Schrödinger*2009, LLC: New York: NY.
196. *Glide*, in *Schrödinger*2008, LLC New York: NY.
197. E.F. Pettersen, T.D. Goddard, C.C. Huang, G.S. Couch, D.M. Greenblatt, E.C. Meng, and T.E. Ferrin, *UCSF Chimera--a visualization system for exploratory research and analysis.* J Comput Chem, 2004. **25**(13): p. 1605-12.
198. M. Schnekenburger, C. Grandjenette, J. Ghelfi, T. Karius, B. Foliguet, M. Dicato, and M. Diederich, *Sustained exposure to the DNA demethylating agent, 2'-deoxy-5-azacytidine, leads to apoptotic cell death in chronic myeloid leukemia by promoting differentiation, senescence, and autophagy.* Biochem Pharmacol, 2011. **81**(3): p. 364-78.
199. J. Charlet, M. Schnekenburger, K.W. Brown, and M. Diederich, *DNA demethylation increases sensitivity of neuroblastoma cells to chemotherapeutic drugs.* Biochem Pharmacol, 2012. **83**(7): p. 858-65.
200. A. Po, E. Ferretti, E. Miele, E. De Smaele, A. Paganelli, G. Canettieri, S. Coni, L. Di Marcotullio, M. Biffoni, L. Massimi, C. Di Rocco, I. Screpanti, and A. Gulino, *Hedgehog controls neural stem cells through p53-independent regulation of Nanog.* EMBO J, 2010. **29**(15): p. 2646-58.

CHAPTER 4

- COUMARIN BASED CHALCONES

AS POTENTIAL NFKB INHIBITORS

4. Coumarin based chalcones as potential NF-κB inhibitors

4.1. General introduction

The transcription factor NF-κB is a dimer of proteins belonging to the Rel family. It is an ubiquitous transcription factor present in all cell types [45].To date it is one of the most complex transcription factors [201] with 5 different subunits (p50, p52, RelA, RelB, c-Rel). On one hand there is a family of inhibitors of NF-κB called IκBs and on the other activating kinase complexes (IKKα, IKKβ and IKKγ/NEMO). The sophisticated combination regulates ample physiological functions [202].

In most cells, NF-κB is found in the cytosol as inactive bound to the inhibitor of κB protein (IκB). Phosphorylation of IκB leads to its ubiquitination and subsequent proteasomal degradation. [203]The in this way activated NF-κB complex translocates to the nucleus where more than 550 target genes could be activated by binding to corresponding DNA sequences in promoter or enhancer regions [44, 203, 204]

NF-κB is generally a pro-inflammatory transcription factor expressing pro-inflammatory genes repressing other genes [205] widely involved in the initiation and progression of different cancer types. To date several factors are known to activate NF-κB pathway, including inflammatory cytokines e.g. tumour necrosis factor alpha (TNFα) and interleukin (IL)-1, carcinogens, UV radiation, hyperglycaemia and Tumor promoters [201, 204]. It plays an important role in the determination of the survival and progression or apoptosis of cancerous cells[206] [207].

It is not only an inflammation processes trigger the NF-κB activation but also the well known chemotherapeutic agents (e.g., Taxol and tamoxifen) [208] and γ-irradiation from radiotherapy [209] rendering them resistant to cancer treatments. In this regard, over the last decade the development of NF-κB inhibitors is a very promising approach towards new cancer therapies [201, 207, 210].

Chalcone-based compounds (1,3-diaryl-2-propen-1-ones), are a group of aromatic unsaturated ketones of natural or synthetic origin [210, 211]. They have been

widely reported to display a variety of biological activities, especially with regard to anti-inflammatory and anticancer activities [211]. The ease of preparation, the potential of oral administration and safety also support the feasibility of chalcone-based compounds as therapeutic agents [212-214]. Additionally, their simple and efficient synthesis makes them also attractive for cancer therapy [44, 211].

Although the modes of action of chalcones are not yet fully elucidated, enormous efforts are devoted to understand the mechanisms of their promising anti-inflammatory and anticancer activities. They have been biologically described as histone deacetylase enzymes (HDACs), anti-inflammatory compounds, cell cycle blockers, apoptosis inducers and have exert their anti-cancer properties towards several cancer cells models such as bladder, breast, colon, lung and prostate cancers. [204, 215-219]. Pharmacokinetic studies and clinical trials have shown that chalcones are well tolerated by the organism and can be detected in plasma at reasonable concentration [220-222].

Both natural and synthetic chalcones like **106** are reported in literature to inhibit the NF-κB signalling pathway, [44, 203, 210, 211]. Besides the NF-κB inhibition, interference in microtubule formation is generally thought to be responsible for the anticancer activities of chalcones [223] [224].

Another promising molecule inhibiting the NF-κB pathway is curcumin ((1E,6E)-1,7-bis(4-hydroxy-3-methoxyphenyl)hepta-1,6-diene-3,5-dione) **107**. It is a polyphenolic compound which can be found in the root of *Curcuma longa* [225]. Curcumin has been described in the literature as a multi-functional molecule that can interact with many targets, pathways and several cellular processes exhibiting interesting anti-cancer properties [226-228]. This compound is able to act as an anti-inflammatory molecule, an apoptosis inducer, a proteasome, matrix metalloproteinase and angiogenesis inhibitor [229-233].

In vitro studies have demonstrated that it has a potent cytotoxic effect towards different cancer cell lines for example leukemia cells, prostate, lung, breast, head and neck cancers [191, 234-241]. Furthermore, the influence of curcurmin on several pathways involved into cancer progression such as NF-κB, MAPK, STAT3 or Wnt pathway have been studied [227, 236, 242-244]. Whilst curcumin itself has

limited efficacy due to its low bioavailability and stability in physiological media [245], it has been the subject of many analogue studies for example the *N*-methylpiperidone analogue **108**. [246-248]

Coumarins, isolated for the first time from the plant Coumarou (*Dipteryx odorata*),are natural compounds belonging to the benzopyrone family. So far a large number of natural products bear a 2*H*-1-benzopyran-2-one (coumarin) as part of their structure [249]. 2*H*-1-benzopyran-2-ones show wide biological activity well reviewed by Riveiro et al. [250]. Experiments performed with different cancer cell line models such as leukaemia cells, colon, breast, liver, lung cancer cells but also on mice models have shown that both natural and synthetic coumarins can be classified as differentiation and apoptosis inducers, cell cycle blockers, angiogenesis and CDC25 inhibitors [67, 251-257].

Appendino et al described sesquiterpene coumarin **109** extracted from Asafetida as specific NF-κB inhibitors at a low micromolar range [258]. Therefore coumarines could be interesting as a different structural motif able to inhibit the NF-κB pathway.

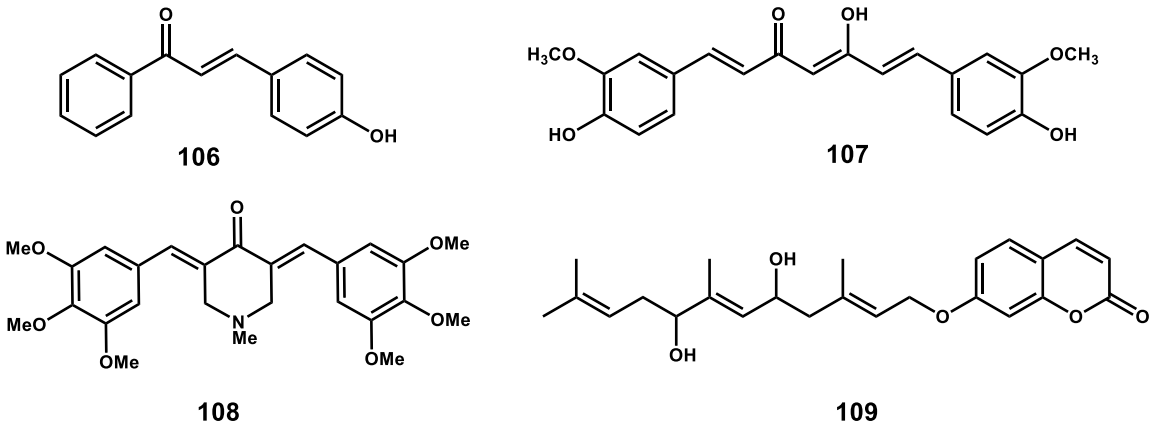

Figure 21: Known NF-*κ*B inhibitors.

Considering these structural motifs we designed new coumarin-containing curcuminoids **112a-g** and we tested all the derivatives for assessing their TNF-alpha induced NF-κB pathway inhibition activity and their effects on cell viability and apoptosis induction in K562 cell line.

4.2. Chemistry

The new series of coumarin-based curcuminoid analogues bearing an α,β-mono-unsaturated ketone at the C3 position (Scheme 18) were prepared carrying out aldolic condensation between 3-acetylcoumarin, previously synthesized by us according to the literature starting from salicylaldehyde **i** and ethylacetoacetate **ii** [259] [260], and the appropriate aldehydes following an adapted procedure of Cechinel-Filho et al. [261]. All the chemical-physical data, ^{1}H NMR and ^{13}C NMR of the compounds are described in experimental section.

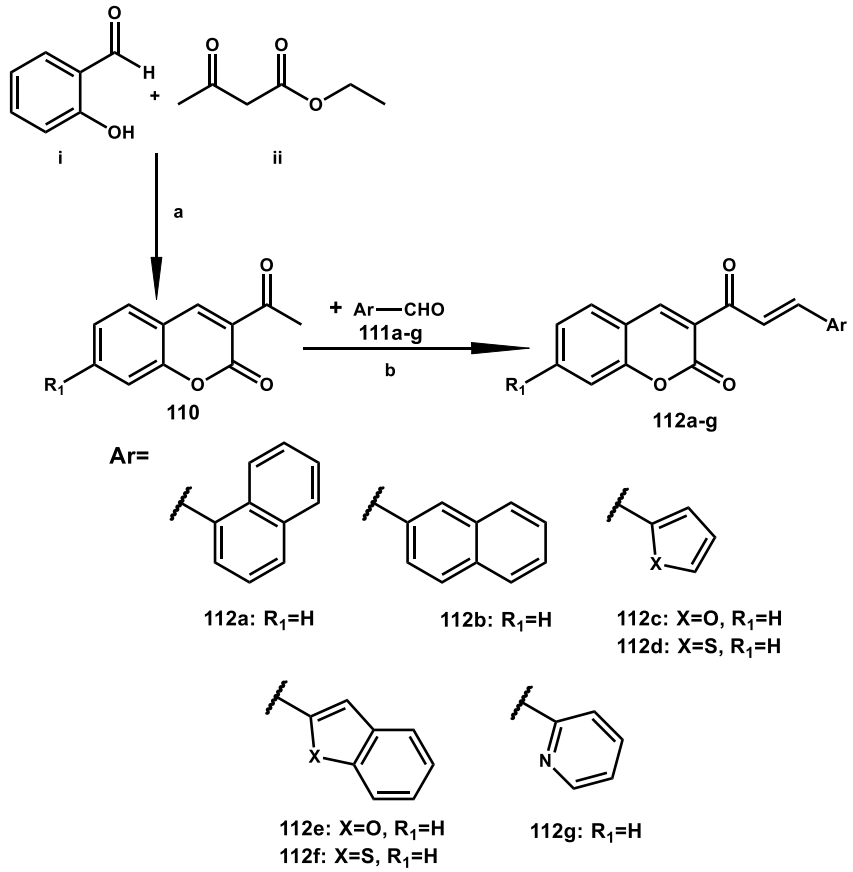

Scheme 18: Synthesis of coumarin-based compounds **112a-g: a)** cat. pyrrolidine in acetonitrile 8h at room temperature. **b)** cat. Pyrrolidine, ethanol, reflux, 1-3 h

4.3. Effect of synthetic coumarin-based molecules on the TNF-alpha induced NF-κB pathway

First, we investigated the potential ability of all new molecules to modulate the TNF-alpha induced NF-κB pathway. Transfected human chronic myelogenous leukemia K562 cells were pre-treated for 2 hours with different concentrations of coumarin derivatives and challenged for 6 hours with 20 ng/mL of TNF-alpha. However we were not able to demonstrate the involvement of the NfkB pathway so far. Therefore no biological data could be presented in here.

4.4. Conclusion and outlook

Complementary and deeper investigations need to be conducted in order to elicit deeper the biological properties of coumarin based chalcones. with the possible involvement of different pathways. In the future we should in parallel validate the biological target as well as optimize our design strategy.

4.5. Experimental part

4.5.1 Chemistry

4.5.1.1 General introduction

Please see chapter 2.10.1.1

4.5.1.2 Synthesis of potential NF-κB inhibitors

Preparation of 3-acetylcoumarin

Procedure for the synthesis of 3-acetyl coumarin or 3-acetyl-7-methoxy coumarin adapted from Hirai et al. and Starčević et al. [259] [260]. To a cold mixture of salicylaldehyde or 4-methoxy salicylaldehyde (10mM) and ethylacetoacetate (10mM) in acetonitrile, 4 drops of pyrrolidine were added under stirring. After 8 hours the reaction is diluted with water and extracted 3 times with ethylacetate. The organic layer was washed first with 2M NaOH solution and then with brine. The solvent was dried with $MgSO_4$ and then removed in vacuo. The final solid was triturated with diethyl ether and filtered.

110 3-Acetylcoumarin [259]

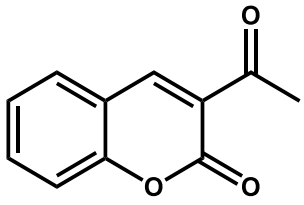

Melting point: 169-171 °C

Yield: 83%

^{1}H NMR (250 MHz, $CDCl_3$) δ 2.73 (s, 3H, -CH_3), 7.33–7.39 (m, 2H, aromatic protons), 7.64–7.69 (m, 2H, aromatic protons), 8.52 (s, 1H, coumarin proton) ppm

^{13}C NMR ($CDCl_3$, 62.5 Hz) δ 29.6, 116.1, 118.1, 125.4, 127.9, 128.3, 132.2, 137.4, 153.0, 159.4, 196.7 ppm

HRMS (ESI) [M+H]+ $C_{11}H_8O_3$ calculated: 188.0473 found: 188.0466

General procedure of preparation of (3-coumarinyl)chalcones

Following an adapted procedure from Cechinel-Filho et al. [261], a mixture of 3-acetyl coumarin **110** (5 mM) and the various heteroaromatic aldehydes **111a-g** (6mM) were refluxed in 5 ml of ethanol with 3 drops of pyrrolidine for 1 to 3 hours. The reaction was allowed to cool down to RT, kept overnight in freezer and on the next day the obtained crystals were filtered off. The precipitate was either triturated with petrol ether or recrystallized from appropriate solvent.

112a 3-(3-(Naphth-1-yl) prop-2-enoyl)-*2H*-1-benzo- pyran-2-one

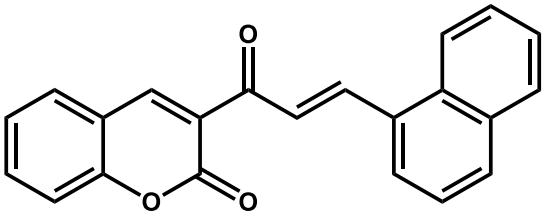

Melting point: 174-176 °C

Appearance: yellow solid

Yield: 64%

^{1}H NMR ($CDCl_3$, 250 Hz) δ 7.34–7.44 (m, 2H, aromatic protons), 7.51–7.71 (m, 5H, aromatic protons and CO-C=CH), 7.88–8.09 (m, 4H, aromatic protons), 8.32 (d, 1H, aromatic proton, J=15.3 Hz, =C*H*-Ar), 8.57 (s, 1H, coumarin proton), 8.68 (d, 1H, J=9.0 Hz aromatic proton) ppm

^{13}C NMR ($CDCl_3$, 62.5 Hz) δ 116.1, 118.1, 122.9, 124.0, 125.3, 125.4, 126.0, 126.3, 126.9, 127.9, 128.3, 128.4, 128.8, 132.0, 133.5, 133.6, 134.2, 140.2, 147.2, 153.0, 159.4, 183.7 ppm

HRMS (ESI) [M+H]+ $C_{22}H_{14}O_3$ calculated: 326.0943 found: 326.0938

112b 3-(3-(Naphth-2-yl) prop-2-enoyl)-*2H*-1-benzo- pyran-2-one

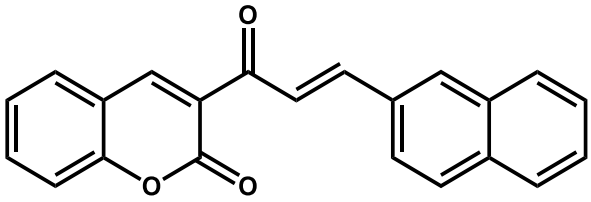

Melting point: 199-200 °C

Appearance: yellow solid

Yield: 65%

^{1}H NMR ($CDCl_3$, 250 Hz) δ 7.34–7.44 (m, 2H, aromatic protons), 7.51–7.55 (m, 2H, aromatic protons), 7.65–7.71 (m, 2H, aromatic proton et CO-C=CH), 7.83–7.90 (m, 4H, aromatic protons and =C*H*-Ar), 8.07 (s, 3H, aromatic protons), 8.63 (s, 1H, coumarin proton) ppm

^{13}C NMR ($CDCl_3$, 62.5 Hz) δ 116.1, 125.4, 125.5, 125.7, 126.0, 126.4, 127.7, 127.8, 128.1, 128.3, 128.9, 128.2, 118.1, 133.2, 133.5, 133.6, 134.2, 142.2, 147.2, 153.0, 159.4, 183.7 ppm

HRMS (ESI) [M+H]+ $C_{22}H_{14}O_3$ calculated: 326.0943 found: 326.0947

112c 3-(3-(Furan-2-yl) prop-2-enoyl)-*2H*-1-benzo- pyran-2-one [262]

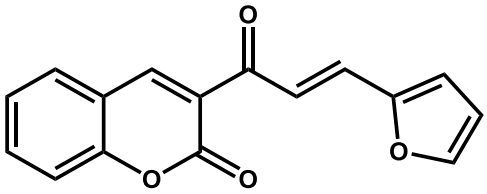

Melting point: 119-120 °C

Appearance: yellow solid

Yield: 60%

^{1}H NMR ($CDCl_3$, 250 Hz) δ 6.45 (q, 1H, aromatic proton), 6.70 (m, 1H, aromatic proton), 7.28–7.34 (m, 2H, aromatic protons), 7.48 (d, 1H, J=1,5 Hz, CO-C=CH), 7.54–7.63 (m, 3H, aromatic protons), 7.72 (d, 1H, J=15,3Hz, =C*H*-Ar), 8.49 (s, 1H, coumarin proton) ppm

^{13}C NMR ($CDCl_3$, 62.5 Hz) δ 112.7 113.8 116.1 118.1 125.4 127.9 128.3 129.3 134.2 138.9 143.7 147.2 151.5 153.0 159.4 183.7 ppm

HRMS (ESI) [M+H]+ $C_{16}H_{10}O_4$ calculated: 266.0579 found: 266.0573

112d 3-(3-(Benzofuran-2-yl)prop-2-enoyl)-*2H*-1-benzopyran-2-one [263]

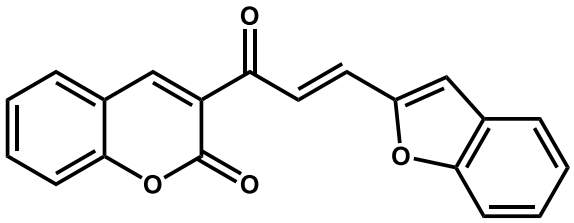

Melting point: 190-192 °C

Appearance: yellow solid

Yield: 64%

^{1}H NMR (250 Hz, CDCl3) δ 7.09 (s, 1H, aromatic proton), 7.23-7.43 (m, 4H, aromatic protons), 7.54-7.77 (m, 5H, aromatic protons and -CO-C*H*=), 8.06 (d, 1H, J=15.4 Hz, =C*H*-Ar), 8.59 (s, 1H, coumarin proton) ppm

^{13}C NMR ($CDCl_3$, 62.5 Hz) δ 106.8, 111.5, 116.1, 118.1, 120.9, 123.3, 124.7, 125.4, 127.8, 127.9, 128.3, 129.3, 134.2, 138.9, 147.2, 153.0, 157.1, 157.3, 159.4, 183.7 ppm

HRMS (ESI) [M+H]+ $C_{20}H_{12}O_4$ calculated: 316.0736 found: 316.0744

112e 3-(3-(Thiophen-2-yl) prop-2-enoyl)-*2H*-1-benzo- pyran-2-one

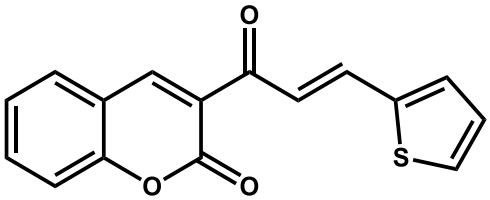

Melting point: 166-168 °C

Appearance: yellow solid

Yield: 68%

^{1}H NMR ($CDCl_3$, 250 Hz) δ 7.10 (t, 1H, aromatic proton), 7.32–7.47 (m, 4H, aromatic protons), 7.64–7.77 (m, 3H, aromatic protons and -CO-C*H*=), 8.01 (d, 1H, J=15,5 Hz, =C*H*-Ar), 8.58 (s, 1H, coumarin proton) ppm

^{13}C NMR ($CDCl_3$, 62.5 Hz) δ 116.1, 118.1, 125.4, 127.9, 128.3, 128.4, 129.1, 129.3, 130.5, 134.2, 134.7, 140.3, 147.2, 153.0, 159.4, 183.7 ppm

HRMS (ESI) [M+H]+ $C_{16}H_{10}O_3S$ calculated: 282.0351 found: 282.0348

112f 3-(3-(Benzothiophen-2-yl) prop-2-enoyl)-*2H*-1-benzopyran- 2-one

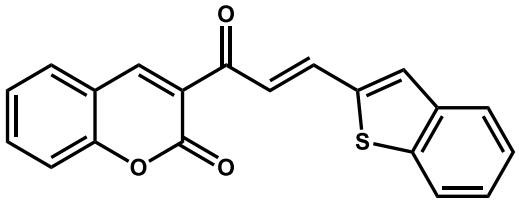

Melting point: 195-196 °C

Appearance: yellow solid

Yield: 70%

^{1}H NMR (250 Hz, $CDCl_3$) δ 7.34-7.43 (m, 4H, aromatic protons), 7.61-7.84 (m, 6H aromatic protons and -CO-C*H*=), 8.08 (d, 1H, J=15.3 Hz, =C*H*-Ar), 8.59 (s, 1H, coumarin proton) ppm

^{13}C NMR ($CDCl_3$, 62.5 Hz) δ 110.2, 116.1, 118.1, 122.8, 123.2, 124.3, 124.4, 125.4, 127.9, 128.3, 129.3, 134.2, 134.7, 138.9, 140.3, 143.3, 147.2, 153.0, 159.4, 183.7 ppm

HRMS (ESI) [M+H]+ $C_{20}H_{12}O_3S$ calculated: 332.0507 found: 332.0511

112g 3-(1-Oxo-3(2-pyridyl)-2-propenyl)-*2H*-1-benzopyran-2-one [264]

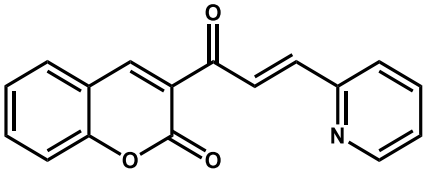

Melting point: 178-180 °C

Appearance: yellow solid

Yield: 75%

^{1}H NMR (250 MHz, $CDCl_3$) δ 7.28-7.77, (7H, m, aromatic protons), 7.84 (d, 1H, J=15,5 Hz, -CO-C*H*=), 8.26 (d, 1H, J=15,5 Hz, =C*H*- Ar), 8.56 (s, 1H, J=4,75 Hz, coumarin proton), 8.69 (d, 1H, J=4,75 Hz, pyridine proton) ppm

^{13}C NMR ($CDCl_3$, 62.5 Hz) δ 116.1, 118.1, 122.7, 124.3, 125.4, 127.9, 128.3, 129.0, 134.2, 137.0, 146.9, 147.2, 148.8, 153.0, 154.7, 159.4, 183.7 ppm

HRMS (ESI) [M+H]+ $C_{17}H_{11}NO_3$ calculated: 277.0739 found: 277.0743

4.5.2 Biology

4.5.1.3 General introduction

The experiments described in this chapter have been conducted by the following research groups: Prof Denyse Bagrel of the Université de Lorraine, Prof Marc Diederich from Laboratoire de Biologie Moléculaire et Cellulaire du Cancer, Luxembourg.

4.5.1.4 Cell culture

K562 (chronic myeloid leukaemia) cells were cultured in RPMI (Invitrogen) with 10% fetal calf serum (Hyclone), 100 U/mL penicillin

4.5.1.5 Assay to test the TNF-alpha induced NF-*κB* pathway

Transfected human chronic myelogenous leukaemia K562 cells were pre-treated for different hours with various concentrations of coumarin derivatives and challenged with 20 ng/mL of TNF-alpha. However no clear involvement of this pathway could be demonstrated so far.

4.6. References

44. B. Orlikova, D. Tasdemir, F. Golais, M. Dicato, and M. Diederich, *The aromatic ketone 4'-hydroxychalcone inhibits TNFalpha-induced NF-kappaB activation via proteasome inhibition.* Biochemical pharmacology, 2011. **82**(6): p. 620-31.
45. B. Orlikova, D. Tasdemir, F. Golais, M. Dicato, and M. Diederich, *Dietary chalcones with chemopreventive and chemotherapeutic potential.* Genes & nutrition, 2011. **6**(2): p. 125-47.
67. S. Valente, E. Bana, E. Viry, D. Bagrel, and G. Kirsch, *Synthesis and biological evaluation of novel coumarin-based inhibitors of Cdc25 phosphatases.* Bioorg Med Chem Lett, 2010. **20**(19): p. 5827-30.
191. Y. Chang, X. Zhang, J.R. Horton, A.K. Upadhyay, A. Spannhoff, J. Liu, J.P. Snyder, M.T. Bedford, and X. Cheng, *Structural basis for G9a-like protein lysine methyltransferase inhibition by BIX-01294.* Nat Struct Mol Biol, 2009. **16**(3): p. 312-7.
201. S. Vallabhapurapu and M. Karin, *Regulation and function of NF-kappaB transcription factors in the immune system.* Annu Rev Immunol, 2009. **27**: p. 693-733.
202. A. Hoffmann, G. Natoli, and G. Ghosh, *Transcriptional regulation via the NF-[kappa]B signaling module.* Oncogene, 2006. **25**(51): p. 6706-6716.
203. S.C. Gupta, C. Sundaram, S. Reuter, and B.B. Aggarwal, *Inhibiting NF-κB activation by small molecules as a therapeutic strategy.* Biochimica et Biophysica Acta (BBA) - Gene Regulatory Mechanisms, 2010. **1799**(10–12): p. 775-787.
204. B. Orlikova, M. Schnekenburger, M. Zloh, F. Golais, M. Diederich, and D. Tasdemir, *Natural chalcones as dual inhibitors of HDACs and NF-kappaB.* Oncol Rep, 2012. **28**(3): p. 797-805.
205. C.H. Lee, Y.-T. Jeon, S.-H. Kim, and Y.-S. Song, *NF-κB as a potential molecular target for cancer therapy.* BioFactors, 2007. **29**(1): p. 19-35.
206. G. Bonizzi and M. Karin, *The two NF-kappaB activation pathways and their role in innate and adaptive immunity.* Trends Immunol, 2004. **25**(6): p. 280-8.
207. J. Ling and R. Kumar, *Crosstalk between NFkB and glucocorticoid signaling: a potential target of breast cancer therapy.* Cancer Lett, 2012. **322**(2): p. 119-26.
208. Y. Zhou, C. Yau, J. Gray, K. Chew, S. Dairkee, D. Moore, U. Eppenberger, S. Eppenberger-Castori, and C. Benz, *Enhanced NFkappaB and AP-1 transcriptional activity associated with antiestrogen resistant breast cancer.* BMC Cancer, 2007. **7**(1): p. 59.
209. F. Pajonk, K. Pajonk, and W.H. McBride, *Inhibition of NF-κB, Clonogenicity, and Radiosensitivity of Human Cancer Cells.* Journal of the National Cancer Institute, 1999. **91**(22): p. 1956-1960.

210. V.R. Yadav, S. Prasad, B. Sung, and B.B. Aggarwal, *The role of chalcones in suppression of NF-κB-mediated inflammation and cancer.* International Immunopharmacology, 2011. **11**(3): p. 295-309.
211. B. Srinivasan, T.E. Johnson, R. Lad, and C. Xing, *Structure–Activity Relationship Studies of Chalcone Leading to 3-Hydroxy-4,3',4',5'-tetramethoxychalcone and Its Analogues as Potent Nuclear Factor κB Inhibitors and Their Anticancer Activities.* Journal of medicinal chemistry, 2009. **52**(22): p. 7228-7235.
212. L. Wattenberg, *Chalcones, myo-inositol and other novel inhibitors of pulmonary carcinogenesis.* J Cell Biochem Suppl, 1995. **22**: p. 162-8.
213. D.A. Israf, T.A. Khaizurin, A. Syahida, N.H. Lajis, and S. Khozirah, *Cardamonin inhibits COX and iNOS expression via inhibition of p65NF-kappaB nuclear translocation and Ikappa-B phosphorylation in RAW 264.7 macrophage cells.* Mol Immunol, 2007. **44**(5): p. 673-9.
214. M. Baba, R. Asano, I. Takigami, T. Takahashi, M. Ohmura, Y. Okada, H. Sugimoto, T. Arika, H. Nishino, and T. Okuyama, *Studies on Cancer Chemoprevention by Traditional Folk Medicines XXV.—Inhibitory Effect of Isoliquiritigenin on Azoxymethane-Induced Murine Colon Aberrant Crypt Focus Formation and Carcinogenesis.* Biological and Pharmaceutical Bulletin, 2002. **25**(2): p. 247-250.
215. A. de Vasconcelos, V.F. Campos, F. Nedel, F.K. Seixas, O.A. Dellagostin, K.R. Smith, C.M. de Pereira, F.M. Stefanello, T. Collares, and A.G. Barschak, *Cytotoxic and apoptotic effects of chalcone derivatives of 2-acetyl thiophene on human colon adenocarcinoma cells.* Cell Biochem Funct, 2013. **31**(4): p. 289-97.
216. Y.L. Hsu, P.L. Kuo, W.S. Tzeng, and C.C. Lin, *Chalcone inhibits the proliferation of human breast cancer cell by blocking cell cycle progression and inducing apoptosis.* Food Chem Toxicol, 2006. **44**(5): p. 704-13.
217. L. Pan, H. Becker, and C. Gerhauser, *Xanthohumol induces apoptosis in cultured 40-16 human colon cancer cells by activation of the death receptor- and mitochondrial pathway.* Mol Nutr Food Res, 2005. **49**(9): p. 837-43.
218. L. Yang, L. Su, C. Cao, L. Xu, D. Zhong, L. Xu, and X. Liu, *The chalcone 2'-hydroxy-4',5'-dimethoxychalcone activates death receptor 5 pathway and leads to apoptosis in human nonsmall cell lung cancer cells.* IUBMB Life, 2013.
219. J.M. Yun, M.H. Kweon, H. Kwon, J.K. Hwang, and H. Mukhtar, *Induction of apoptosis and cell cycle arrest by a chalcone panduratin A isolated from Kaempferia pandurata in androgen-independent human prostate cancer cells PC3 and DU145.* Carcinogenesis, 2006. **27**(7): p. 1454-64.
220. D.I. Batovska and I.T. Todorova, *Trends in utilization of the pharmacological potential of chalcones.* Curr Clin Pharmacol, 2010. **5**(1): p. 1-29.
221. N.K. Sahu, S.S. Balbhadra, J. Choudhary, and D.V. Kohli, *Exploring pharmacological significance of chalcone scaffold: a review.* Curr Med Chem, 2012. **19**(2): p. 209-25.
222. K.H. Shen, J.K. Chang, Y.L. Hsu, and P.L. Kuo, *Chalcone arrests cell cycle progression and induces apoptosis through induction of mitochondrial*

pathway and inhibition of nuclear factor kappa B signalling in human bladder cancer cells. Basic Clin Pharmacol Toxicol, 2007. **101**(4): p. 254-61.
223. N.J. Lawrence, A.T. McGown, S. Ducki, and J.A. Hadfield, *The interaction of chalcones with tubulin.* Anticancer Drug Des, 2000. **15**(2): p. 135-41.
224. M.L. Edwards, D.M. Stemerick, and P.S. Sunkara, *Chalcones: a new class of antimitotic agents.* Journal of medicinal chemistry, 1990. **33**(7): p. 1948-54.
225. A.M. Anderson, M.S. Mitchell, and R.S. Mohan, *Isolation of Curcumin from Turmeric.* Journal of Chemical Education, 2000. **77**(3): p. 359.
226. R.K. Maheshwari, A.K. Singh, J. Gaddipati, and R.C. Srimal, *Multiple biological activities of curcumin: a short review.* Life Sci, 2006. **78**(18): p. 2081-7.
227. J. Ravindran, S. Prasad, and B.B. Aggarwal, *Curcumin and cancer cells: how many ways can curry kill tumor cells selectively?* AAPS J, 2009. **11**(3): p. 495-510.
228. H. Zhou, C.S. Beevers, and S. Huang, *The targets of curcumin.* Curr Drug Targets, 2011. **12**(3): p. 332-47.
229. B.B. Aggarwal, *Targeting Proteasomal Pathways by Dietary Curcumin for Cancer Prevention and Treatment.* Curr Med Chem, 2013.
230. J.L. Arbiser, N. Klauber, R. Rohan, R. van Leeuwen, M.T. Huang, C. Fisher, E. Flynn, and H.R. Byers, *Curcumin is an in vivo inhibitor of angiogenesis.* Mol Med, 1998. **4**(6): p. 376-83.
231. P. Basnet and N. Skalko-Basnet, *Curcumin: an anti-inflammatory molecule from a curry spice on the path to cancer treatment.* Molecules, 2011. **16**(6): p. 4567-98.
232. D. Kumar, M. Kumar, C. Saravanan, and S.K. Singh, *Curcumin: a potential candidate for matrix metalloproteinase inhibitors.* Expert Opin Ther Targets, 2012. **16**(10): p. 959-72.
233. A. Shehzad, G. Rehman, and Y.S. Lee, *Curcumin in inflammatory diseases.* Biofactors, 2013. **39**(1): p. 69-77.
234. G.P. Nagaraju, S. Aliya, S.F. Zafar, R. Basha, R. Diaz, and B.F. El-Rayes, *The impact of curcumin on breast cancer.* Integr Biol (Camb), 2012. **4**(9): p. 996-1007.
235. G. Radhakrishna Pillai, A.S. Srivastava, T.I. Hassanein, D.P. Chauhan, and E. Carrier, *Induction of apoptosis in human lung cancer cells by curcumin.* Cancer Lett, 2004. **208**(2): p. 163-70.
236. S. Reuter, J. Charlet, T. Juncker, M.H. Teiten, M. Dicato, and M. Diederich, *Effect of curcumin on nuclear factor kappaB signaling pathways in human chronic myelogenous K562 leukemia cells.* Ann N Y Acad Sci, 2009. **1171**: p. 436-47.
237. M.H. Teiten, F. Gaascht, S. Eifes, M. Dicato, and M. Diederich, *Chemopreventive potential of curcumin in prostate cancer.* Genes Nutr, 2010. **5**(1): p. 61-74.
238. R. Wilken, M.S. Veena, M.B. Wang, and E.S. Srivatsan, *Curcumin: A review of anti-cancer properties and therapeutic activity in head and neck squamous cell carcinoma.* Mol Cancer, 2011. **10**: p. 12.

239. T.L. Chiu and C.C. Su, *Curcumin inhibits proliferation and migration by increasing the Bax to Bcl-2 ratio and decreasing NF-kappaBp65 expression in breast cancer MDA-MB-231 cells.* Int J Mol Med, 2009. **23**(4): p. 469-75.
240. H.J. Kang, S.H. Lee, J.E. Price, and L.S. Kim, *Curcumin suppresses the paclitaxel-induced nuclear factor-kappaB in breast cancer cells and potentiates the growth inhibitory effect of paclitaxel in a breast cancer nude mice model.* Breast J, 2009. **15**(3): p. 223-9.
241. C.P. Prasad, G. Rath, S. Mathur, D. Bhatnagar, and R. Ralhan, *Potent growth suppressive activity of curcumin in human breast cancer cells: Modulation of Wnt/beta-catenin signaling.* Chem Biol Interact, 2009. **181**(2): p. 263-71.
242. M.G. Alexandrow, L.J. Song, S. Altiok, J. Gray, E.B. Haura, and N.B. Kumar, *Curcumin: a novel Stat3 pathway inhibitor for chemoprevention of lung cancer.* Eur J Cancer Prev, 2012. **21**(5): p. 407-12.
243. S. Singh and B.B. Aggarwal, *Activation of transcription factor NF-kappa B is suppressed by curcumin (diferuloylmethane) [corrected].* J Biol Chem, 1995. **270**(42): p. 24995-5000.
244. M.H. Teiten, F. Gaascht, M. Cronauer, E. Henry, M. Dicato, and M. Diederich, *Anti-proliferative potential of curcumin in androgen-dependent prostate cancer cells occurs through modulation of the Wingless signaling pathway.* Int J Oncol, 2011. **38**(3): p. 603-11.
245. A.L. Cheng, C.H. Hsu, J.K. Lin, M.M. Hsu, Y.F. Ho, T.S. Shen, J.Y. Ko, J.T. Lin, B.R. Lin, W. Ming-Shiang, H.S. Yu, S.H. Jee, G.S. Chen, T.M. Chen, C.A. Chen, M.K. Lai, Y.S. Pu, M.H. Pan, Y.J. Wang, C.C. Tsai, and C.Y. Hsieh, *Phase I clinical trial of curcumin, a chemopreventive agent, in patients with high-risk or pre-malignant lesions.* Anticancer Res, 2001. **21**(4B): p. 2895-900.
246. B. Yadav, S. Taurin, R.J. Rosengren, M. Schumacher, M. Diederich, T.J. Somers-Edgar, and L. Larsen, *Synthesis and cytotoxic potential of heterocyclic cyclohexanone analogues of curcumin.* Bioorganic & medicinal chemistry, 2010. **18**(18): p. 6701-7.
247. J.R. Fuchs, B. Pandit, D. Bhasin, J.P. Etter, N. Regan, D. Abdelhamid, C. Li, J. Lin, and P.K. Li, *Structure-activity relationship studies of curcumin analogues.* Bioorganic & medicinal chemistry letters, 2009. **19**(7): p. 2065-9.
248. L. Lin, B. Hutzen, S. Ball, E. Foust, M. Sobo, S. Deangelis, B. Pandit, L. Friedman, C. Li, P.K. Li, J. Fuchs, and J. Lin, *New curcumin analogues exhibit enhanced growth-suppressive activity and inhibit AKT and signal transducer and activator of transcription 3 phosphorylation in breast and prostate cancer cells.* Cancer Sci, 2009. **100**(9): p. 1719-27.
249. I. Kostova, *Synthetic and natural coumarins as cytotoxic agents.* Curr Med Chem Anticancer Agents, 2005. **5**(1): p. 29-46.
250. M.E. Riveiro, N. De Kimpe, A. Moglioni, R. Vazquez, F. Monczor, C. Shayo, and C. Davio, *Coumarins: old compounds with novel promising therapeutic perspectives.* Current medicinal chemistry, 2010. **17**(13): p. 1325-38.
251. S.S. Bhattacharyya, S. Paul, S.K. Mandal, A. Banerjee, N. Boujedaini, and A.R. Khuda-Bukhsh, *A synthetic coumarin (4-methyl-7 hydroxy coumarin) has anti-cancer potentials against DMBA-induced skin cancer in mice.* Eur J Pharmacol, 2009. **614**(1-3): p. 128-36.

252. M.H. Jung, S.H. Lee, E.M. Ahn, and Y.M. Lee, *Decursin and decursinol angelate inhibit VEGF-induced angiogenesis via suppression of the VEGFR-2-signaling pathway.* Carcinogenesis, 2009. **30**(4): p. 655-61.
253. M.A. Musa, A. Zhou, and O.A. Sadik, *Synthesis and antiproliferative activity of new coumarin-based benzopyranone derivatives against human tumor cell lines.* Med Chem, 2011. **7**(2): p. 112-20.
254. M.A. Musa, V.L. Badisa, L.M. Latinwo, T.A. Patterson, and M.A. Owens, *Coumarin-based benzopyranone derivatives induced apoptosis in human lung (A549) cancer cells.* Anticancer Res, 2012. **32**(10): p. 4271-6.
255. R. Vazquez, M.E. Riveiro, M. Vermeulen, C. Mondillo, P.H. Coombes, N.R. Crouch, F. Ismail, D.A. Mulholland, A. Baldi, C. Shayo, and C. Davio, *Toddaculin, a natural coumarin from Toddalia asiatica, induces differentiation and apoptosis in U-937 leukemic cells.* Phytomedicine, 2012. **19**(8-9): p. 737-46.
256. C.J. Wang, Y.J. Hsieh, C.Y. Chu, Y.L. Lin, and T.H. Tseng, *Inhibition of cell cycle progression in human leukemia HL-60 cells by esculetin.* Cancer Lett, 2002. **183**(2): p. 163-8.
257. L. Zhang, G. Jiang, F. Yao, Y. He, G. Liang, Y. Zhang, B. Hu, Y. Wu, Y. Li, and H. Liu, *Growth inhibition and apoptosis induced by osthole, a natural coumarin, in hepatocellular carcinoma.* PLoS One, 2012. **7**(5): p. e37865.
258. G. Appendino, L. Maxia, M. Bascope, P.J. Houghton, G. Sanchez-Duffhues, E. Munoz, and O. Sterner, *A meroterpenoid NF-kappaB inhibitor and drimane sesquiterpenoids from Asafetida.* J Nat Prod, 2006. **69**(7): p. 1101-4.
259. T. Hirai and H. Togo, *Preparation and Synthetic Use of Polymer-Supported Acetoacetate Reagent.* Synthesis, 2005. **2005**(EFirst): p. 2664-2668.
260. S.t. Starčević, P. Brožič, S. Turk, J.k. Cesar, T. Lanišnik Rižner, and S. Gobec, *Synthesis and Biological Evaluation of (6- and 7-Phenyl) Coumarin Derivatives as Selective Nonsteroidal Inhibitors of 17β-Hydroxysteroid Dehydrogenase Type 1.* Journal of medicinal chemistry, 2010. **54**(1): p. 248-261.
261. V. Cechinel-Filho, Z.R. Vaz, L. Zunino, J.B. Calixto, and R.A. Yunes, *Synthesis of xanthoxyline derivatives with antinociceptive and antioedematogenic activities.* European journal of medicinal chemistry, 1996. **31**(10): p. 833-839.
262. O.O. Ajani and O.C. Nwinyi, *Microwave-assisted synthesis and evaluation of antimicrobial activity of 3-{3-(s-aryl and s-heteroaromatic)acryloyl}-2H-chromen-2-one derivatives.* Journal of Heterocyclic Chemistry, 2010. **47**(1): p. 179-187.
263. Y.-F. Sun and Y.-P. Cui, *The synthesis, characterization and properties of coumarin-based chromophores containing a chalcone moiety.* Dyes and Pigments, 2008. **78**(1): p. 65-76.
264. Y.R. Prasad, P.R. Kumar, C.A. Deepti, and M.V. Ramana, *Synthesis and Antimicrobial Activity of Some Novel Chalcones of 2-Hydroxy -1-Acetonapthone and 3-Acetyl Coumarin.* E-Journal of Chemistry, 2006. **3**(4): p. 236-241.

CHAPTER 5

- CONCLUSION AND PERSPECTIVES -

5. Conclusion and perspectives

During my PhD research described in this thesis we studied new potential synthetic drugs and evaluated their chemical, biochemical and biological aspects to fight cancer.

In the first part we described a series of natural compound derivatives related to aurones. We combined the benzofuranone motif of the aurone with other coumarin and chromone motifs inspired by nature. These compounds have been synthesized and evaluated against K562 human leukaemia cells. Both these chemical structures displayed anticancer activity because they are able to block the K562 cell cycle in G1 (**62b** 72%), S (**65a** 63%) or G2 (**70c** 46%) phase, and to induce high (around 24%) apoptosis (**62b**, **70b** and **70c)**. These provide a promising scaffold for medicinal chemistry bearing in mind the possibility to access heterocyclic analogues of benzofuranes. As a further step complementary investigations are planned to investigate possible other biological properties as well as the molecular mechanism of action.

We focused in the second part on oncologically relevant DNA methyltransferases as an epigenetic target. The use of specific inhibitors of DNMT (DNMTi) may reactivate tumour suppressor genes and induce the reprogramming of cancer cells, leading to their proliferation arrest and ultimately to their death. We prepared compound **88**, a novel non-nucleoside DNMTi more potent than the known molecule **SGI1027** and more selective towards other AdoMet- dependent methyltransferases (PRMT1, GLP). Differently from **SG1027**, competitive with AdoMet, **88** was found to be competitive with DNA for its DNMT1 inhibition. Tested on a panel of cancer cells (leukaemia U937, breast cancer MDA-MB-231, Burkitt's lymphoma RAJI, and prostate cancer PC- 3) as well as on PBMCs, **88** displayed comparable activity as **SGI1027** and less toxicity. In MbSCs, at 10 µM **88** significantly blocked proliferation but required higher doses (50 µM) to induce differentiation, while the related compound **85**, less potent as antiproliferative agent, showed high differentiating activity. The anticancer activity displayed by **85** and **88** in the tested cancer cells

including CSCs suggests their use as potent and selective non-nucleoside DNMTi for cancer therapy.

In a third part, coumarin-based curcuminoid analogues were projected and prepared for their potential ability to modulate the TNF-alpha induced NFkB pathway in K562 cancer cells.

However, we were not able to demonstrate the involvement of our new compounds in the NFkB pathway so far. Complementary and deeper investigations need to be conducted in order to elicit deeper biological properties of coumarin-based chalcones with the possible involvement of different pathways. In the future we should in parallel validate the biological target as well as optimize our design strategy.

In the end, the project can be seen as a successful step in developments of different classes of synthetic compounds applying different design strategies. We tried to focus on the rationale behind covalent combinations of various bioactive agents to increase their therapeutic potential. However, additional and deeper investigations should be carried out in order to elucidate the biological properties of the new molecules. All compounds described herein deserve to be further developed and explored.

CHAPTER 6

- FRENCH SUMMARY -

6. French summary

6.1. Introduction

Le cancer, connu depuis les anciens Grecs et étudié par Hippocrate qui lui a donné son nom (du mot grec *"karkinos"),* a été très longtemps une maladie incurable. "Cancer" est un terme général pour une maladie, qui peut affecter n'importe quelle partie du corps par la prolifération incontrôlée des cellules avec des conséquences pour tout l'organisme. D'autres noms sont utilisés comme néoplasme ou tumeur maligne. Même si le nombre de personnes qui guérissent augmente, les décès sont toujours importants. Les raisons, malgré un diagnostic précoce et correct, sont l'absence de traitements efficaces et l'émergence de résistances à la thérapie anticancéreuse.

C'est pourquoi les chercheurs s'intéressent aux nouvelles approches pour développer des traitements puissants et sélectifs pour vaincre le cancer.

Il est actuellement l'une des trois raisons principales de décès dans le monde, parmi les maladies cardiovasculaires et infectieuses, qui représentent environ 13% de la mortalité mondiale (7,6 millions de victimes) [1, 2] .

Les raisons outre d'un point de vue thérapeutique ainsi que le diagnostic correct sont l'absence de traitements efficaces et l'émergence de résistances aux médicaments anti-cancéreux[3-8].

Le cancer est une maladie complexe, causée par de nombreux mécanismes biologiques. Une seule cellule se transforme, évolue de forme santé à l'état tumoral via un processus en plusieurs étapes à partir d'une lésion précancéreuse. Ces changements sont le résultat de facteurs de risque génétique personnel en combinaison avec des influences externes, par exemple:

- des agents physiques tumorigènes, comme les rayonnements ultraviolets ou ionisants
- des agents chimiques tumorigènes, comme les composants de la fumée de tabac, l'aflatoxine, une contamination de la nutrition et l'arsenic en tant que contaminant de l'eau potable

- des agents biologiques tumorigènes, comme des infections causées par certains virus, bactéries ou parasites [1].

Les estimations de l'Organisation Mondiale de la Santé (OMS= WHO) montrent que le nombre de victimes du cancer va doubler jusqu'en 2030. C'est pour ces raisons, qu'il est vraiment important de développer de nouveaux traitements, plus ciblés, plus efficaces et avec moins d'effets secondaires.

Aujourd'hui, la recherche moderne essaie de synthétiser, d'isoler des molécules naturelles. En même temps, les chercheurs veulent identifier et mieux comprendre leurs mécanismes biologiques. Ils essaient d'améliorer l'efficacité des médicaments pour lutter contre différents types de cancer [9-13].

Au cours de ma thèse de doctorat j'ai voulu étudier les aspects biologiques de nouveaux composés chimiques pour vaincre le cancer.

Pendant ma thèse, l'objectif était de développer des compétences nouvelles dans la conception de médicaments. Je voulais améliorer mes compétences en chimie organique, particulièrement dans le domaine des dérivés naturels en collaboration avec des biologistes et des biochimistes pour créer de nouveaux composés bioactifs.

Dans notre première approche, nous avons développé une série de dérivés de composés naturels appelés aurones. Les aurones jouent un rôle important dans la pigmentation jaune lumineuse de certaines fleurs et certains fruits et présentent de nombreuses activités biologiques. Nous avons combiné le motif benzofuranone de l'aurone avec d'autres motifs de la coumarine et chromone. Ces nouveaux composés montrent une activité anticancéreuse prometteuse, car ils sont capables de bloquer le cycle cellulaire dans les cellules cancéreuses K562 et peuvent y induire l'apoptose.

Ensuite nous avons concentré notre attention sur un objectif épigénétique. Les méthyltransférases de l'ADN sont considérées comme une cible intéressante en oncologie. L'usage d'inhibiteurs spécifiques de la méthyltransférase de l'ADN (DNMTi) pourrait réactiver les gènes suppresseurs de tumeurs et induire la reprogrammation des cellules cancéreuses, conduisant à l'arrêt de leur prolifération

et finalement à leur mort. Nous avons amélioré le composé connu SGI1027 par modification de la structure. Nous avons obtenu de nouveaux inhibiteurs non nucléosidiques de la méthyltransférase de l'ADN, plus puissants et plus sélectifs que le composé principal.

Une troisième série d'analogues de chalcones à base de coumarine a été préparée et testée pour sa capacité potentielle à moduler la voie TNF-alpha induite par NF-kB dans les cellules cancéreuses K562. Cependant, nous n'avons pas été capable de montrer l'implication de la voie ciblée jusqu'à maintenant.

6.2. Les aurones

Les aurones jouent un rôle important dans la pigmentation de certaines fleurs et certains fruits. Elles contribuent surtout à la couleur jaune lumineuse des fleurs [15]. Elles présentent également une variété forte et large d'activités biologiques. Par exemple, elles ont été décrites comme agents antifongiques [16], en tant qu'agents insecticides [17], comme inhibiteurs de la tyrosinase [18] et comme antioxydants [19]. Rare dans la nature, les aurones sont des représentants moins fréquents et moins connus d'une sous-classe de flavonoïdes [20]. C'est probablement la raison pour laquelle elles ont reçu peu d'attention en comparaison avec les flavones et les isoflavones [21], qui sont structurellement similaires et bien étudiées.

Lawrence *et al.* [21] ont étudié les aurones isolées d'*Uvaria hamiltonii* pour la synthèse totale ainsi que pour leurs propriétés anticancéreuses dans les cellules K562 (Figure 4). Parmi elles, seulement le composé **43** a été le plus actif avec une inhibition de la croissance IC_{50} de 50 µM.

L'aurone **43** est convertie par une réaction avec du cyanure de potassium en flavone **44,** qui est un composé plus actif avec une valeur IC_{50} de 40 µm.

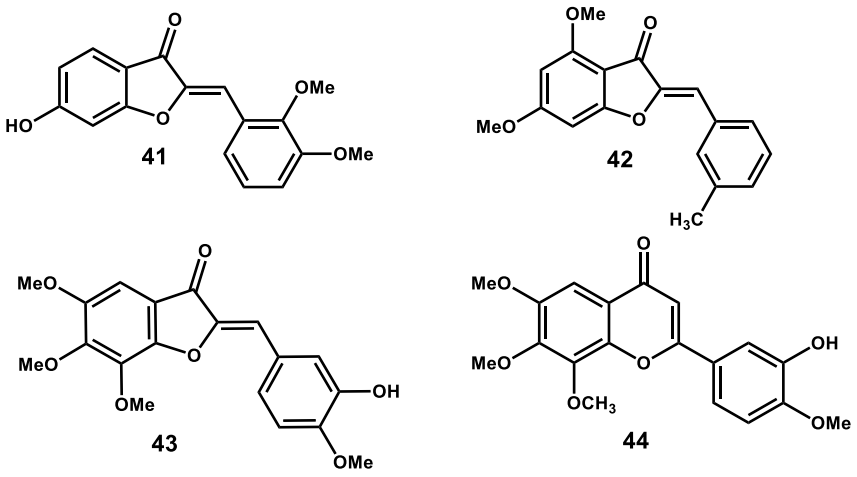

Figure 4: Les aurones **41-43** et la flavone isomérique **44,** qui possèdent des propriétés anticancéreuses postulées [21, 25, 53]

Les flavones ainsi que les aurones appartiennent à la classe des flavonoïdes et sont connues pour une activité anticancéreuse [62, 63]. Entre autres, les chromones possèdent des propriétés anticancéreuses [65]. Leurs isomères de constitution, les coumarines, présentent des activités biologiques similaires, qui ont été récemment résumées dans un article [66].

Notre idée était de créer une combinaison de la structure benzofurane ou du motif de la benzofuranone des aurones avec le motif du chromone ou le motif de la coumarine pour obtenir de nouveaux agents potentiels anticancéreux. Nous avons synthétisé et évalué nos composés dans les cellules cancéreuses K562.

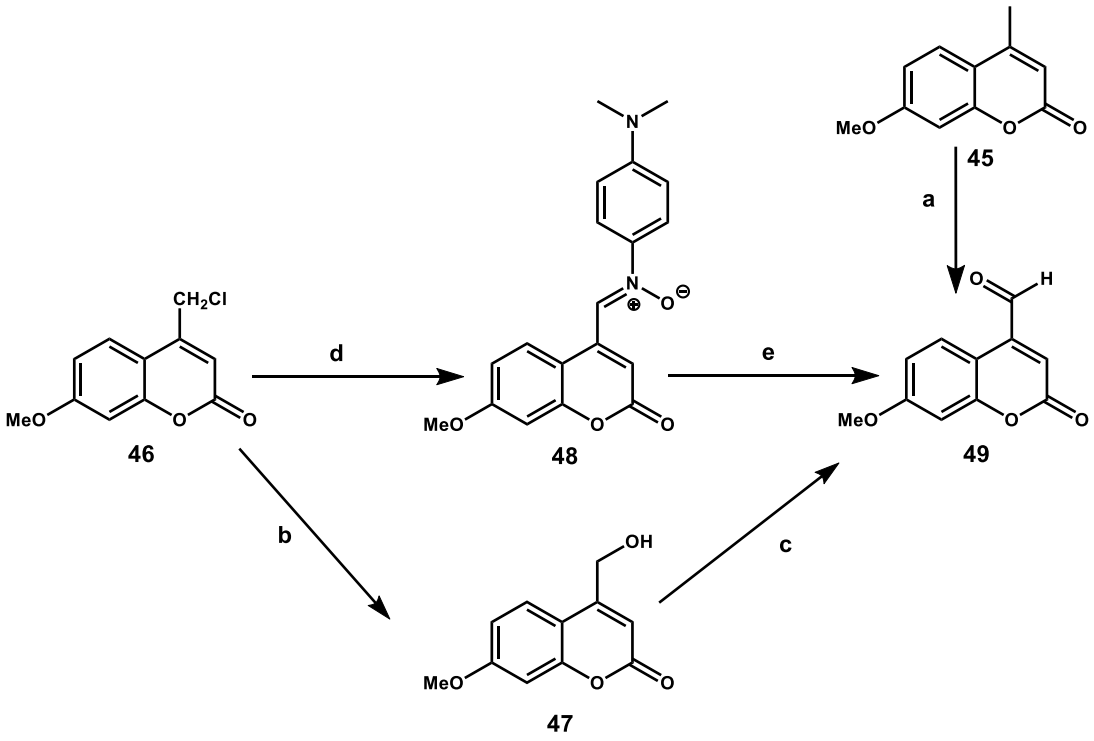

Schéma 8: Synthèse de l'aldéhyde **49** **a)** SeO_2, des solvants différents, reflux pendant 12-18 heures (voir tableau ci-dessous) **b)** de l'eau, reflux pendant 12 heures **c)** MnO_2, THF, 70 ^{0}C, 18 heures **d)** p-nitrosodiméthylaniline, éthanolate de sodium, de l'éthanol, température ambiante, 20 minutes **e)** hydrolyse 5N H_2SO_4 température ambiante, 30 minutes

Pour la préparation du coumarine-4-aldéhyde **49** comme produit de départ, nous avons d'abord utilisé l'oxydation de Riley sur la 4-methylcoumarine **45** [68]. Nous

avons également hydrolysé la 4-cloromethylcoumarine **46** en alcool **47** et puis oxydé par MnO_2. La méthode de Kröhnke avec *p-nitrosodiméthylaniline* [69] a finalement donné le meilleur résultat au départ de la 4-chloromethylcoumarine **46** (Schéma 9).

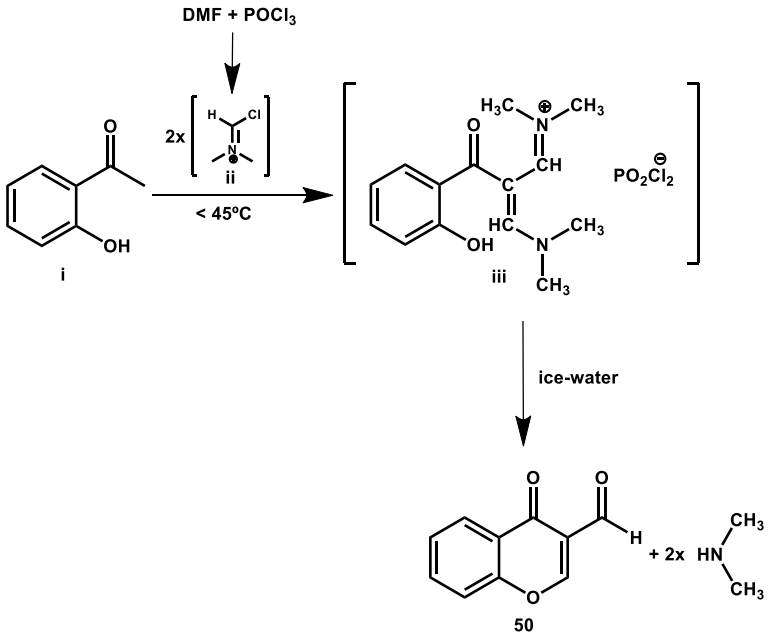

Schéma 9: Synthèse des aldéhydes de la chromone par réaction Vilsmeier-Haack: exemple **50**

Les produits de départ **50-58** ont été préparés par la réaction de Vilsmeier-Haack [21, 25, 53, 70-80]. Cette méthode peut être utilisée pour formyler des systèmes aromatiques activés dans le sens d'une acylation de Friedl-Crafts à cause de l'instabilité du dérivé chloroformylé [81]. Les benzofuranones **59a,b** et **60** ont été préparées selon une méthode développée dans notre laboratoire [61, 82].

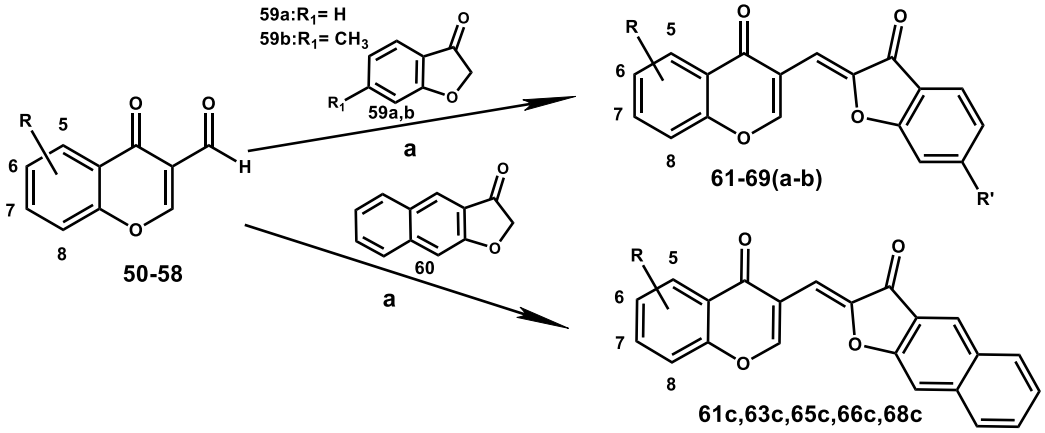

61a: R=H; R'=H
61b: R=H; R'=Me
61c: R=H
62a: R=6-Me; R'=H
62b: R=6-Me; R'=Me

63a: R=6-Me, 7-Me; R'=H
63b: R=6-Me, 7-Me; R'=Me
63c: R=6-Me, 7-Me
64a: R=7-Cl; R'=H
64b: R=7-Cl; R'=Me

65a: R=6-Cl; R'=H
65b: R=6-Cl; R'=Me
65c: R=6-Cl
66a: R=6-F; R'=H
66b: R=6-F; R'=Me

66c: R=7-F
67a: R=7-OMe; R'=H
67b: R=7-OMe; R'=Me
68a: R=5-OMe; R'=H
68b: R=5-OMe; R'=Me

68c: R=5-OMe
69a: R=7-OMe, 8-OMe; R'=H
69b: R=7-OMe, 8-OMe; R'=Me

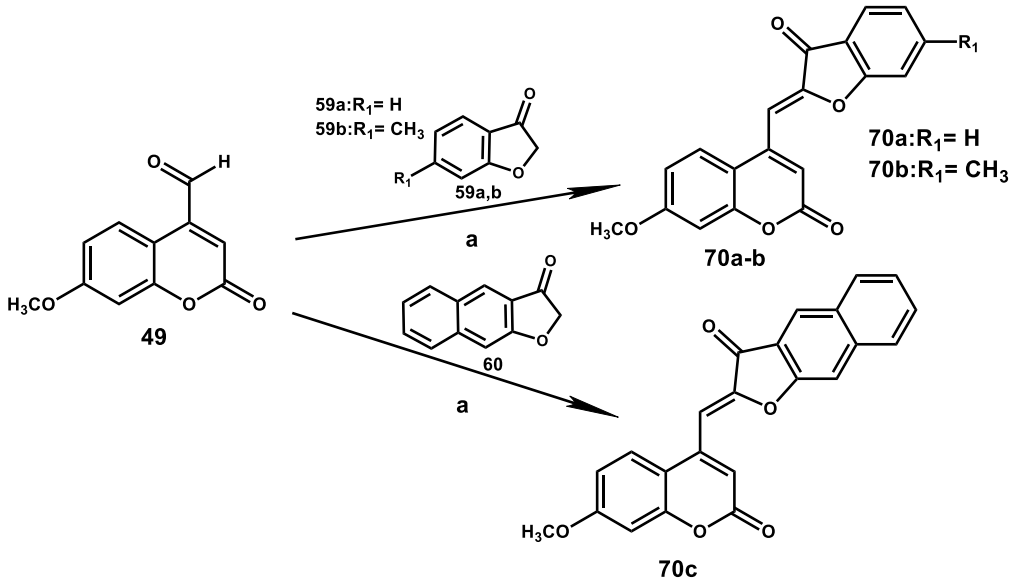

Schéma 11: Voie de synthèse a: Al_2O_3 (acide), DCM anhydre, température ambiante, 2-6 jours

Enfin, pour fournir les aurones **61-70** (Schéma 11), nous avons réalisé la condensation aldolique de l'aldéhyde avec le benzofurane par l'utilisation de l'Al_2O_3 acétique (Brockmann I) [26].

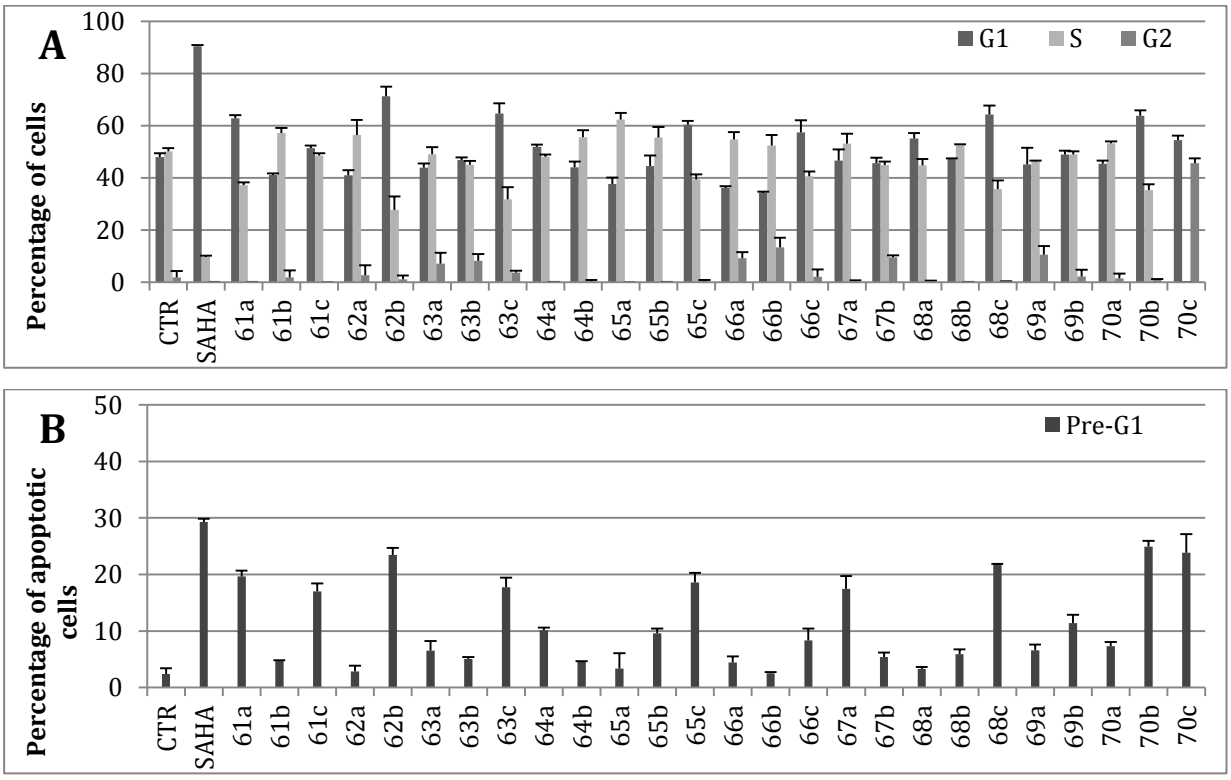

Figure 5: (A) L'analyse du cycle cellulaire et **(B)** l'induction de l'apoptose dans les cellules K562 traitées avec **61-70** à 50 pM pour 48 h.

Les dérivés coumariniques et les chromones ont des propriétés anticancéreuses, car ils sont capables de bloquer le cycle cellulaire K562 en phase G1 **(62b** 72%), S **(65a** 63%) ou phase G2 **(70c** 46%) et d'induire l'apoptose (environ 24%) **(62b, 70b** et **70c)** (Figure 5).

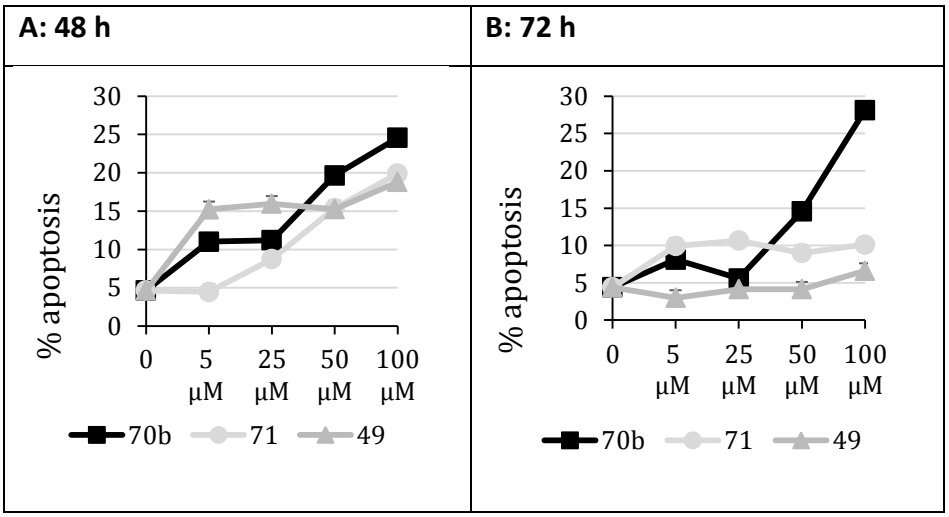

Figure 7: Dépendance de la dose d'induction de l'apoptose dans des cellules K562 traitées avec 70b, 49 et 71 pour 48 (A) et 72 (B), h. Dépendance de la dose pour l'induction de l'apoptose dans des cellules K562 traitées avec **70b, 49** et **71** pour 48 (**A**) et 72 (**B**) heures.

Nous avons choisi le produit **70b** et nous l'avons testé dans des cellules K562 aux doses de 5 à 100 µM, en comparaison avec **8,** le coumarine-4-aldehyde; un produit de départ pour la synthèse de **70b;** et avec **71,** une aurone simple et classique (Figure 6) Après 48 h et respectivement 72 h de traitement, **70b** a montré aux doses élevées (50 et 100 µM), la plus forte induction de l'apoptose. **70b** plus efficace que le composé **49** et **71** (Figure 7). Ces résultats suggèrent que la combinaison d'une structure « aurone-like » avec une chromone ou coumarine peut donner de nouveaux composés intéressants pour l'apoptose dans les cellules leucémiques K562. Ils sont prometteux pour la chimie médicinale grâce à la possibilité d'obtenir des analogues hétérocycliques du benzofurane.

6.3. Les inhibiteurs de la méthyltransférase de l'ADN

Parmi les cinq événements épigénétiques, la méthylation de l'ADN a été largement étudiée. Ces méthylations jouent un rôle important dans la modulation de l'expression des gènes [96]. Elles sont cruciales pour le développement embryonnaire ou la différentiation des cellules [85, 97-99]. Les méthylations de l'ADN aberrantes sont associées à la sous- ou sur-expression de certaines protéines, qui conduisent aux pathologies diverses comme la maladie d'Alzheimer [100, 101], la dépression, le trouble bipolaire, la schizophrénie [101, 102], des maladies auto-immunes [103] et même certains troubles génétiques [104, 105]. Par ailleurs les profils de la méthylation aberrante de l'ADN ont été abondamment décrits dans la bibliographie dans de nombreux syndromes myélodysplasiques et la leucémie myéloïde aiguë (AML), la leucémie myélomonocytaire chronique (LMMC) [106-109]. Peterson *et al.* ont montré très récemment que la méthylation de l'ADN est dépendante du style de vie individuelle comme par exemple la nutrition ou le tabagisme. Ces changements dans l'épigénome peuvent conduire aux pathologies différentes [110] .

Même si les origines génétiques du cancer sont bien acceptées aujourd'hui, il est évident que des modifications épigénétiques sont des événements précoces de la tumorigenèse [118, 132, 133]. Les modifications épigénétiques sont réversibles, contrairement aux mutations génétiques [134].

Les inhibiteurs de la méthyltransférase de l'ADN (DNMTi) sont utiles pour la réactivation des gènes suppresseurs de tumeur et pour la reprogrammation des cellules cancéreuses vers l'arrêt de croissance et la mort [135, 136].

Pourquoi est-ce que la conception de nouveaux inhibiteurs de la DNMT est intéressante? D'une part, ils peuvent être utilisés afin d'élucider le rôle de la méthylation de l'ADN dans les conditions normales de même que cancéreuses [186] et d'autre part, la méthylation de l'ADN est une cible thérapeutique prometteuse dans les différents types de cancer, mais aussi dans d'autres maladies comme les maladies neurologiques [187]. Bien que les premiers inhibiteurs non-sélectifs aient été découverts dans les années 1960, il y a encore beaucoup à découvrir sur la

route des futures thérapies efficaces et sélectives. À ce jour, aucun des inhibiteurs non- nucléosidiques décrits dans la bibliographie n'est pour le moment au stade du développement clinique. Il y a donc une longue route à parcourir avant que ces composés puissent atteindre le chevet du patient. Aujourd'hui, un effet directement cytotoxique n'est plus voulu par contre dans la thérapie épigénétique, on veut que le cancer est traité par une reprogrammation des cellules qui elles-mêmes décident de leur propre sort [135].

Nous rapportons ici les résultats d'une étude d'optimisation du composé non-nucléosidique SGI-1027 **(84)** [135]. La conception rationnelle, les routes de la synthèse et l'évaluation biologique seront présentées.

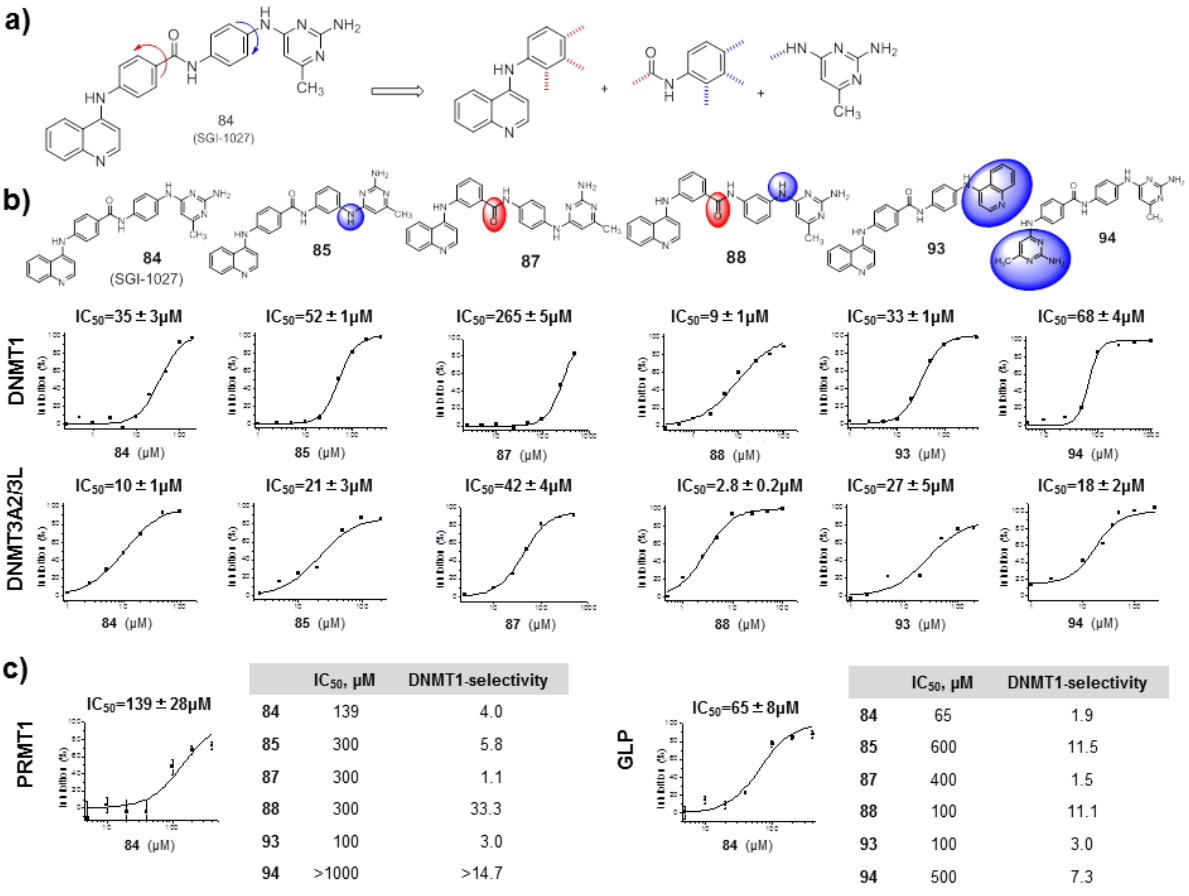

	IC_{50}, μM	DNMT1-selectivity
84	139	4.0
85	300	5.8
87	300	1.1
88	300	33.3
93	100	3.0
94	>1000	>14.7

	IC_{50}, μM	DNMT1-selectivity
84	65	1.9
85	600	11.5
87	400	1.5
88	100	11.1
93	100	3.0
94	500	7.3

Figure 15: Nouveaux inhibiteurs non-nucléosidiques à base de quinoléine de la méthyltransférase de l'ADN. (a) La conception des régioisomères de **84**, (b) les activités inhibitrices de **84, 85, 87, 88, 93** et **94** contre DNMT1 humaine (substrat

hémiméthylé) et le complex d8 DNMT3A2/DNMT3L (substrat non méthylé). (c) Selectivité **de 84, 85, 87, 88, 93** et **94** contre PRMT1 et GPL.

Le composé **84** identifié parmi une série de composés quinoléiniques et développé comme un médicament anticancéreux, a attiré notre attention en raison de sa forte activité dans les tests enzymatiques et cellulaires [185]. Puisque la structure de **84** a quatre fragments (4-quinoléine + 4-acide-3-aminobenzoique + 1,4-phénylènediamine + 2,4-diamino-6-methylpyrimidine) liés en séquence avec *para* / *para* orientation, nous avons préparé une série des régioisomères **84.** Nous avons déplacé la liaison de chaque fragment de position *para* en *méta* ou *ortho*, et donc obtenu les composés **85 à 92** (Figure 15) en utilisant l'amidation avec du PyBOP (Schéma 15).

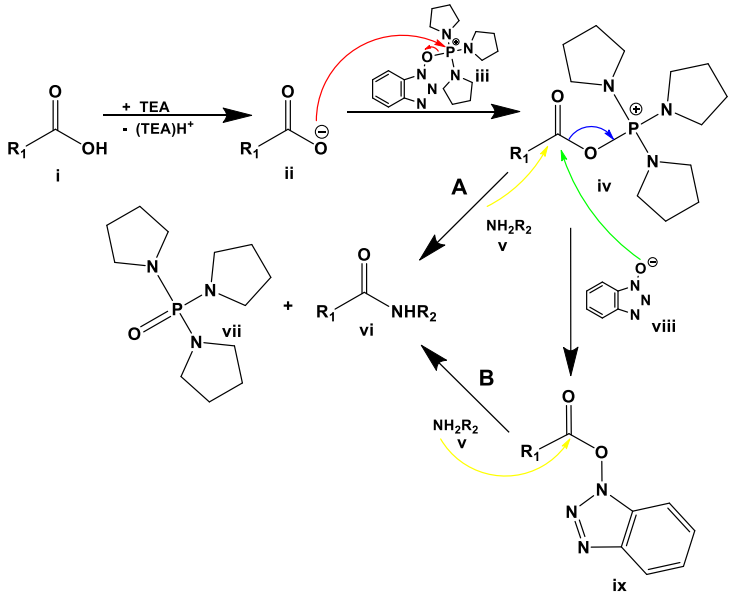

Schéma 15: Le mécanisme général de l'amidation avec du PyBOP, la flèche rouge représente une attaque nucléophile du PyBOP pour activer l'acide, la verte représente la transestérification et les jaunes l'attaque nucléophile pour former finalement l'amide désiré

De plus, nous avons préparé quelques composés similaires, qui montrent soit une structure bis-quinoléine soit une structure bis-pyrimidine **(93, 94)** et deux composés

tronqués **(95, 96)** qui n'ont pas la pyrimidine dans la partie «droite» ou la partie du quinolone à «gauche».

Nous avons identifié par la modulation appliquée à la structure **84** le composé **88,** un dérivé non-nucléosidique plus puissant et plus sélectif envers les autres methyltransférases AdoMet-dépendantes (PRMT1, BPL) que le composé **84**. Le composé **88** a été trouvé compétitif avec l'ADN, alors que le composé initial **84** était compétitif avec AdoMet. Le composé **88** affiche une activité comparable à **84** et une toxicité moindre pendant les tests sur un panneau de cellules cancéreuses (leucémie U937, cancer du sein MDA-MB-231, lymphome de Burkitt et cancer de la prostate PC-3) ainsi que sur les PBMCs (cellules sanguines périphériques mononucléaires).

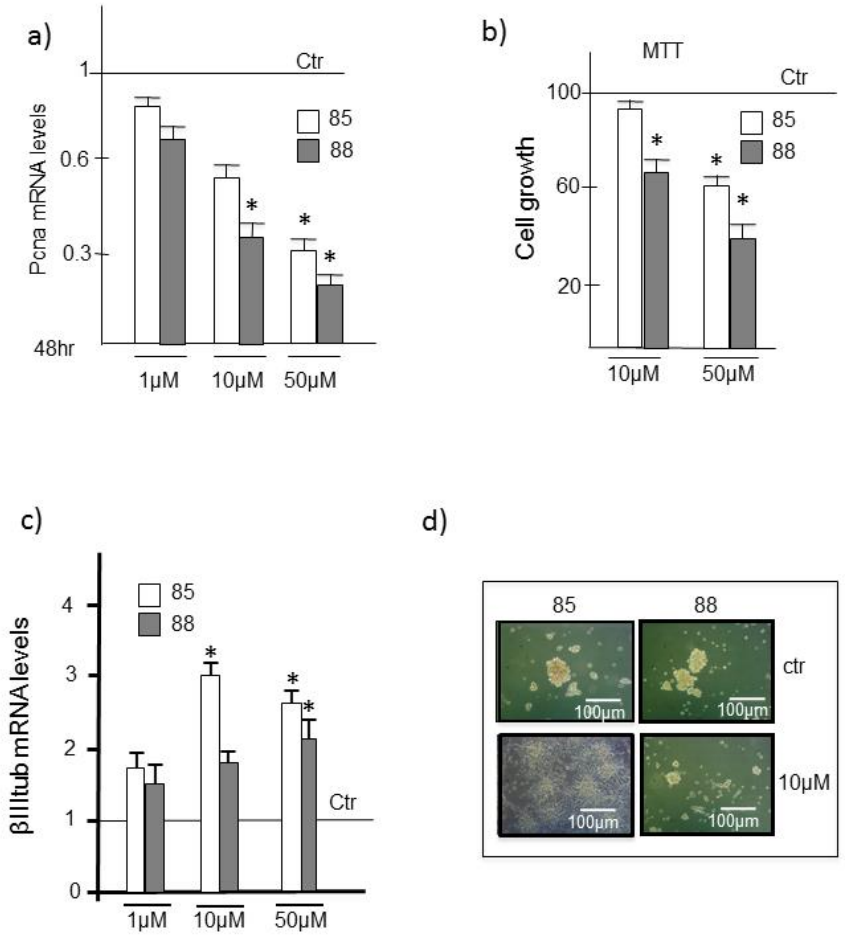

Figure 20: Effets de 85 et 88 dans les cellules souches du médulloblastome : (**a**) les niveaux de l'ARNm, (**b**) le test MTT après 48 h de traitement du compose **85**

respectivement **88**, ou le DMSO comme contrôle (CTR). * P <0,05 par rapport aux cellules non traitées (CTR), (**c**) les niveaux de ARNm dans les cellules traitées avec 85 ou 88 pour 48 h (DMSO utilisé comme contrôle, (**d**) des images de champ lumineux des cellules souches du médulloblastome après le traitement du compose **85** respectivement **88** (48 h, 10 UM) ou du DMSO comme contrôle.

Sur les cellules souches du médulloblastome, le composé **88** (à 10 µM) a bloqué significativement la prolifération, mais des doses plus élevées sont requises (50 µM) pour induire la différentiation. Par contre le composé **85** était moins puissant en tant qu'agent anti-prolifératif, mais a montré une activité élevée dans la différentiation (Figure 20). L'activité anticancéreuse des composés **85** et **88** sur des cellules cancéreuses testées, y compris des cellules souches du cancer, suggère leur utilisation comme inhibiteurs non- nucléosidiques de la méthyltransférase de l'ADN puissants et sélectifs pour la thérapie du cancer.

6.4. Chalcones à base de coumarine comme des inhibiteurs potentiels de NF-κB

Le facteur de transcription NF-κB est un dimère de protéines, qui appartient à la famille Rel. C'est un facteur de transcription ubiquitaire présent dans tous les types cellulaires [45]. Jusqu'à présent, il est l'un des facteurs de transcription le plus complexe [201] avec 5 sous-unités différentes (p50, p52, RelA, RelB, c-Rel).

NF-κB est généralement un facteur de transcription pro-inflammatoire, qui exprime des gènes pro-inflammatoires et en même temps réprime d'autres gènes [205]. Il est impliqué dans l'initiation et la progression des différents types de cancer. À ce jour plusieurs facteurs sont connus pour activer la voie de NF-κB, y compris les cytokines inflammatoires, par exemple le facteur de nécrose tumorale alpha (TNFα) et l'interleukine (IL) -1, les rayons UV, l'hyperglycémie et des promoteurs de tumeurs [45, 201]. NF-κB joue un rôle important dans la détermination de la survie et de la progression ou de l'apoptose des cellules cancéreuses [206, 207].

Au cours de la dernière décennie, le développement d'inhibiteurs de NF-kB est une approche très prometteuse vers de nouvelles thérapies contre le cancer [201, 207, 210].

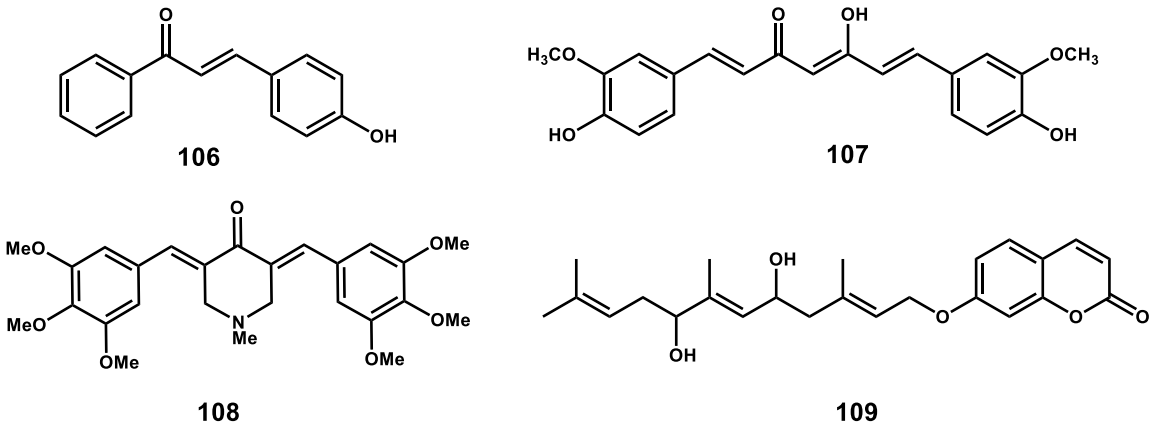

Figure 21: Inhibiteurs connus de NF-κB.

Les composés à base des chalcones (1,3-diaryl-2-propène-1-ones) sont un groupe de cétones insaturées aromatiques d'origine naturelle ou synthétique [210, 211]. Ils ont été largement rapportés de posséder une variété d'activités biologiques,

particulièrement celles, qui concernent les activités anti-inflammatoires et anticancéreuses [211].

Les chalcones, naturelles et synthétiques, comme **106,** sont rapportées dans la bibliographie comme inhibiteurs de la voie de signalisation NF-kB, [44, 203, 210, 211].

Une autre molécule prometteuse est la curcumine **107.** Des études in vitro ont montré qu'il y a un effet cytotoxique par plusieurs voies, comme NF-kB, MAPK, STAT3 ou voie Wnt [227, 236, 242-244], concernant des cellules différentes cancéreuses comme par exemple des cellules de leucémie, du cancer de la prostate, du cancer du poumon, du cancer du sein, du cancer du cerveau [191, 234-241].

Appendino *et al.* ont extrait un sesquiterpene coumarinique **109** d'Asafetida comme un fort inhibiteur spécifique de NF-kB [258]. Par conséquence, les coumarines pourraient être intéressantes comme un motif structural différent, capable d'inhiber la voie de signalisation de NF-kB.

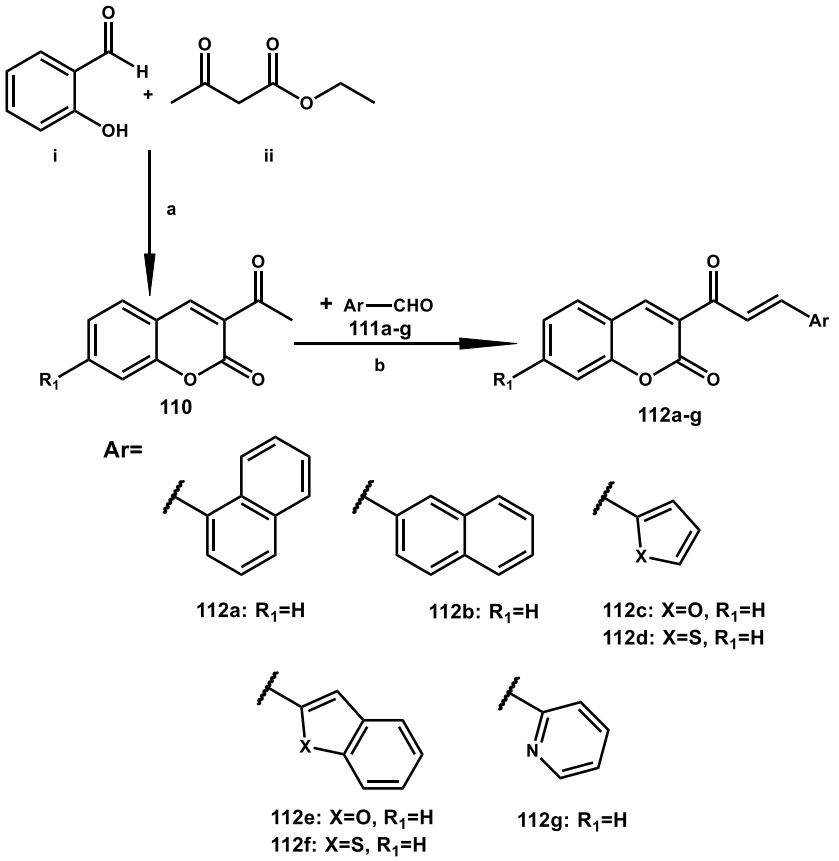

Schéma 18: Synthèse des dérivés coumariniques **112a-g**

Nous avons combiné ces motifs structuraux pour créer une nouvelle série de chalcones avec une base coumarinique. Les composés **112a-g**, portant un cétone α, β-mono-insaturé à la position C3, sont préparés par une condensation aldolique entre la 3-acétylcoumarine, précédemment synthétisée par notre laboratoire selon la bibliographie [259, 260], et les aldéhydes appropriés suivant une procédure de à Cechinel-Filho *et al.* adaptée [261] (Schéma 18).

Tout d'abord, nous avons étudié l'aptitude potentielle de toutes nouvelles molécules pour moduler la voie NF-κB, induite par le TNFα. Jusqu'à présent nous nous n'avons pas réussi à montrer l'implication de nos composés à la voie NF-κB. Par conséquence, aucun résultat biologique ne peut être présenté jusqu'à présent.
Des études complémentaires et plus approfondies doivent être menées afin d'estimer les propriétés biologiques de ces composés dans la participation éventuelle aux voies différentes. Dans l'avenir, nous devrons valider la cible biologique parallèlement à l'optimisation de notre stratégie de conception et de synthèse.

6.5. Conclusion et perspectives

Pendant ma thèse, nous avons étudié la synthèse de nouvelles molécules et nous avons évalué leur activité biologique potentielle pour vaincre le cancer.

Dans la première partie, nous avons décrit une série de dérivés de composés naturels, notamment des aurones. Nous avons combiné le motif de la benzofuranone des aurones avec le motif coumarinique ou chromonique. Ces composés ont été synthétisés et évalués dans des cellules leucémiques K562. Ils ont montré des activités anticancéreuses, car ils sont capables de bloquer le cycle cellulaire en phase G1 **(62b** 72%), en phase S **(65a** 63%) ou en phase G2 **(70c** 46%) et d'induire l'apoptose (environ 24%) **(62b, 70b** et **70c).** Des études complémentaires et plus approfondies doivent être menées afin d'estimer les propriétés biologiques de ces composés dans la participation éventuelle aux voies différentes ainsi que le mécanisme d'action moléculaire.

Dans la deuxième partie, nous avons travaillé sur une cible épigénétique notamment les méthyltransférases de l'ADN. L'utilisation d'inhibiteurs spécifiques des méthyltransférases de l'ADN peut réactiver les gènes suppresseurs des tumeurs et induire la reprogrammation des cellules cancéreuses, qui conduit à l'arrêt de la prolifération et finalement à leur mort contrôlée. Nous avons préparé le composé non-nucléosidique **88,** plus puissant que la molécule connue SGI1027 **(84)** et plus sélectif envers les autres methyltransférases AdoMet-dépendantes (PRMT1, BPL).

Le composé **88** a été trouvé compétitif avec l'ADN, par contre le composé initial **84** était compétitif avec AdoMet. Le composé **88** affiche une activité comparable à **84,** mais moins toxique pendant les tests sur un panneau de cellules de cancer (leucémie U937, cancer du sein MDA-MB-231, lymphome de Burkitt et cancer de la prostate PC-3) ainsi que sur les PBMCs. Sur les cellules souches du médulloblastome, le composé **88** (à 10 µM) a bloqué la prolifération significativement, mais des doses plus élevées sont requises (50 µM) pour induire la différentiation. Par contre le composé **85** était moins puissant comme agent anti-prolifératif, mais a montré une activité élevée dans la différentiation. L'activité anticancéreuse des composés **85** et **88** dans des cellules cancéreuses testées, y

compris des cellules souches du cancer, suggère leur utilisation comme des inhibiteurs de la méthyltransférase de l'ADN non-nucléosidique puissants et sélectifs pour la thérapie du cancer.

Dans une troisième partie, des chalcones avec une base coumarinique ont été projetées et préparées pour leur aptitude potentielle à moduler la voie NF-kB, induite par le TNFα dans les cellules cancéreuses K562.

Jusqu'à présent nous n'avons pas réussi à montrer l'implication de nos composés dans la voie NF-κB.

Par conséquence, des études complémentaires et plus approfondies doivent être menées afin d'estimer les propriétés biologiques de ces composés dans la participation éventuelle aux voies différentes. Dans l'avenir, nous devrions en parallèle valider la cible biologique ainsi qu'optimiser notre stratégie dans la conception et la synthèse.

À la fin du projet, on peut considérer notre travail comme une première étape réussie dans le développement de différentes classes de composés synthétiques en appliquant différentes stratégies de conception. Nous avons essayé de nous concentrer sur la combinaison de divers agents bioactifs pour améliorer leur potentiel thérapeutique. Dans l'avenir, il serait intéressant de mener des investigations supplémentaires et plus profondes pour élucider plus les propriétés biologiques de nos nouvelles molécules.

Tous les composés décrits ici méritent d'être développés et davantage étudiés dans l'avenir.

6.6. References

1. WHO. *Cancer Fact Sheet*. 2013 [cited 2013 16. September]; Available from: http://www.who.int/medicantre/factsheets/fs297.
2. J. Ferlay, D.M. Parkin, and E. Steliarova-Foucher, *Estimates of cancer incidence and mortality in Europe in 2008.* Eur J Cancer, 2010. **46**(4): p. 765-81.
3. M. Dean, *ABC transporters, drug resistance, and cancer stem cells.* J Mammary Gland Biol Neoplasia, 2009. **14**(1): p. 3-9.
4. S. Dermime, *Cancer Diagnosis, Treatment and Therapy.* J Carcinogene Mutagene S, 2013. **14**.
5. J. Ferlay, H.R. Shin, F. Bray, D. Forman, C. Mathers, and D.M. Parkin, *Estimates of worldwide burden of cancer in 2008: GLOBOCAN 2008.* Int J Cancer, 2010. **127**(12): p. 2893-917.
6. F.S. Liu, *Mechanisms of chemotherapeutic drug resistance in cancer therapy--a quick review.* Taiwan J Obstet Gynecol, 2009. **48**(3): p. 239-44.
7. R. Siegel, C. DeSantis, K. Virgo, K. Stein, A. Mariotto, T. Smith, D. Cooper, T. Gansler, C. Lerro, S. Fedewa, C. Lin, C. Leach, R.S. Cannady, H. Cho, S. Scoppa, M. Hachey, R. Kirch, A. Jemal, and E. Ward, *Cancer treatment and survivorship statistics, 2012.* CA Cancer J Clin, 2012. **62**(4): p. 220-41.
8. R. Siegel, D. Naishadham, and A. Jemal, *Cancer statistics, 2012.* CA Cancer J Clin, 2012. **62**(1): p. 10-29.
9. G.M. Cragg and D.J. Newman, *Natural products: A continuing source of novel drug leads.* Biochim Biophys Acta, 2013.
10. T. Efferth, P.C. Li, V.S. Konkimalla, and B. Kaina, *From traditional Chinese medicine to rational cancer therapy.* Trends Mol Med, 2007. **13**(8): p. 353-61.
11. D.J. Newman and G.M. Cragg, *Natural products as sources of new drugs over the 30 years from 1981 to 2010.* J Nat Prod, 2012. **75**(3): p. 311-35.
12. S. Nobili, D. Lippi, E. Witort, M. Donnini, L. Bausi, E. Mini, and S. Capaccioli, *Natural compounds for cancer treatment and prevention.* Pharmacol Res, 2009. **59**(6): p. 365-78.
13. M. Schumacher, M. Kelkel, M. Dicato, and M. Diederich, *Gold from the sea: marine compounds as inhibitors of the hallmarks of cancer.* Biotechnol Adv, 2011. **29**(5): p. 531-47.
15. E. Ono, M. Fukuchi-Mizutani, N. Nakamura, Y. Fukui, K. Yonekura-Sakakibara, M. Yamaguchi, T. Nakayama, T. Tanaka, T. Kusumi, and Y. Tanaka, *Yellow flowers generated by expression of the aurone biosynthetic pathway.* Proceedings of the National Academy of Sciences of the United States of America, 2006. **103**(29): p. 11075-80.
16. C.J.W. Brooks and D.G. Watson, *Phytoalexins.* Natural Product Reports, 1985. **2**(5): p. 427-459.

17. M. Morimoto, H. Fukumoto, T. Nozoe, A. Hagiwara, and K. Komai, *Synthesis and insect antifeedant activity of aurones against Spodoptera litura larvae.* Journal of agricultural and food chemistry, 2007. **55**(3): p. 700-5.
18. S. Okombi, D. Rival, S. Bonnet, A.M. Mariotte, E. Perrier, and A. Boumendjel, *Discovery of benzylidenebenzofuran-3(2H)-one (aurones) as inhibitors of tyrosinase derived from human melanocytes.* Journal of medicinal chemistry, 2006. **49**(1): p. 329-33.
19. S. Venkateswarlu, G.K. Panchagnula, and G.V. Subbaraju, *Synthesis and antioxidative activity of 3',4',6,7-tetrahydroxyaurone, a metabolite of Bidens frondosa.* Bioscience, biotechnology, and biochemistry, 2004. **68**(10): p. 2183-5.
20. A. Boumendjel, *Aurones: a subclass of flavones with promising biological potential.* Current medicinal chemistry, 2003. **10**(23): p. 2621-30.
21. N.J. Lawrence, D. Rennison, A.T. McGown, and J.A. Hadfield, *The total synthesis of an aurone isolated from Uvaria hamiltonii: aurones and flavones as anticancer agents.* Bioorganic & medicinal chemistry letters, 2003. **13**(21): p. 3759-63.
25. H. Cheng, L. Zhang, Y. Liu, S. Chen, H. Cheng, X. Lu, Z. Zheng, and G.-C. Zhou, *Design, synthesis and discovery of 5-hydroxyaurone derivatives as growth inhibitors against HUVEC and some cancer cell lines.* European journal of medicinal chemistry, 2010. **45**(12): p. 5950-5957.
26. R.S. Varma and M. Varma, *Alluminia-mediated condensation. A simple synthesis of Aurones.* Tetrahedron Letters, 1992. **33**(40): p. 5937-5940.
44. B. Orlikova, D. Tasdemir, F. Golais, M. Dicato, and M. Diederich, *The aromatic ketone 4'-hydroxychalcone inhibits TNFalpha-induced NF-kappaB activation via proteasome inhibition.* Biochemical pharmacology, 2011. **82**(6): p. 620-31.
45. B. Orlikova, D. Tasdemir, F. Golais, M. Dicato, and M. Diederich, *Dietary chalcones with chemopreventive and chemotherapeutic potential.* Genes & nutrition, 2011. **6**(2): p. 125-47.
53. H.M. Sim, C.Y. Lee, P.L. Ee, and M.L. Go, *Dimethoxyaurones: Potent inhibitors of ABCG2 (breast cancer resistance protein).* European journal of pharmaceutical sciences : official journal of the European Federation for Pharmaceutical Sciences, 2008. **35**(4): p. 293-306.
61. P. Cagniant, G. Kirsch, and P. Legendre, *Contribution à l'étude du naphto-[2.3-b]furanne et de son analogue sélénié le naphto-[2.3-b] sélénophène.* C. R. Acad. Sci., Ser. C, 1973. **276**(Copyright (C) 2013 American Chemical Society (ACS). All Rights Reserved.): p. 1629-31.
62. J.A. Beutler, E. Hamel, A.J. Vlietinck, A. Haemers, P. Rajan, J.N. Roitman, J.H. Cardellina, and M.R. Boyd, *Structure–Activity Requirements for Flavone Cytotoxicity and Binding to Tubulin.* Journal of medicinal chemistry, 1998. **41**(13): p. 2333-2338.
63. M. Lopez-Lazaro, *Distribution and biological activities of the flavonoid luteolin.* Mini Rev Med Chem, 2009. **9**(1): p. 31-59.
65. R. Ali, Z. Mirza, G.M.D. Ashraf, M.A. Kamal, S.A. Ansari, G.A. Damanhouri, A.M. Abuzenadah, A.G. Chaudhary, and I.A. Sheikh, *New Anticancer Agents:*

Recent Developments in Tumor Therapy. Anticancer Res, 2012. **32**(7): p. 2999-3005.
66. C. Kontogiorgis, A. Detsi, and D. Hadjipavlou-Litina, *Coumarin-based drugs: a patent review (2008 – present).* Expert Opin Ther Pat, 2012. **22**(4): p. 437-454.
68. K. Ito and J. Sawanobori, *4-Diazomethyl-7-Methoxycoumarin as a New Type of Stable Aryldiazomethane Reagent.* Synthetic Communications, 1982. **12**(9): p. 665-671.
69. F. Kröhnke and E. Börner, *Über α-Keto-aldonitrone und eine neue Darstellungsweise von α-Keto-aldehyden.* Berichte der deutschen chemischen Gesellschaft (A and B Series), 1936. **69**(8): p. 2006-2016.
70. H. Harnisch, *Chromon-3-carbaldehyde.* Justus Liebigs Annalen der Chemie, 1973. **765**(1): p. 8-14.
71. R. Araya-Maturana, J. Heredia-Moya, H. Pessoa-Mahana, and B. Weiss-López, *Improved Selective Reduction of 3-Formylchromones Using Basic Alumina and 2-Propanol.* Synthetic Communications, 2003. **33**(18): p. 3225-3231.
72. T. Shankar, R. Gandhidasan, and S. Venkataraman, *Synthesis and characterization and anti-inflammatory and antibacterial evaluation of 3-arylidene-7-methoxychroman-4-ones.* Indian J. Chem., Sect. B: Org. Chem. Incl. Med. Chem., 2011. **50B**(Copyright (C) 2012 American Chemical Society (ACS). All Rights Reserved.): p. 1202-1207.
73. A. Caşcaval, *2-Hydroxyketone, V. Darstellung substituierter Chromone.* Liebigs Annalen der Chemie, 1980. **1980**(5): p. 669-672.
74. T. Patonay, A. Kiss-Szikszai, V.M.L. Silva, A.M.S. Silva, D.C.G.A. Pinto, J.A.S. Cavaleiro, and J. Jekő, *Microwave-Induced Synthesis and Regio- and Stereoselective Epoxidation of 3-Styrylchromones.* European Journal of Organic Chemistry, 2008. **2008**(11): p. 1937-1946.
75. P.-L. Zhao, J. Li, and G.-F. Yang, *Synthesis and insecticidal activity of chromanone and chromone analogues of diacylhydrazines.* Bioorganic & Medicinal Chemistry, 2007. **15**(5): p. 1888-1895.
76. K.F. Shelke, B.R. Madje, S.B. Sapkal, B.B. Shingate, and M.S. Shingare, *An efficient ionic liquid promoted Knoevenagel condensation of 4-oxo-4H-benzopyran-3-carbaldehyde with Meldrum's acid.* Green Chemistry Letters and Reviews, 2009. **2**(1): p. 3-7.
77. J. Alderete, J. Belmar, M. Parra, C. Zúñiga, and V. Jimenez, *Esters derived from 7-decanoyloxychromone-3-carboxylic acid: synthesis and mesomorphic properties.* Liquid Crystals, 2003. **30**(11): p. 1319-1325.
78. H. Dueckert, V. Khedkar, H. Waldmann, and K. Kumar, *Lewis Base Catalyzed [4+2] Annulation of Electron-Deficient Chromone-Derived Heterodienes and Acetylenes.* Chem.--Eur. J., 2011. **17**(Copyright (C) 2012 American Chemical Society (ACS). All Rights Reserved.): p. 5130-5137, S5130/1-S5130/20.
79. A.M. Piloto, A.S.C. Fonseca, S.P.G. Costa, and M.S.T. Gonçalves, *Carboxylic fused furans for amino acid fluorescent labelling.* Tetrahedron, 2006. **62**(39): p. 9258-9267.

80. N. Hadj-Esfandiari, L. Navidpour, H. Shadnia, M. Amini, N. Samadi, M.A. Faramarzi, and A. Shafiee, *Synthesis, antibacterial activity, and quantitative structure-activity relationships of new (Z)-2-(nitroimidazolylmethylene)-3(2H)-benzofuranone derivatives.* Bioorg. Med. Chem. Lett., 2007. **17**(Copyright (C) 2013 American Chemical Society (ACS). All Rights Reserved.): p. 6354-6363.
81. G. Jones and S.P. Stanforth, *The Vilsmeier Reaction of Non-Aromatic Compounds*, in *Organic Reactions*. 2004, John Wiley & Sons, Inc.
82. P. Cagniant and G. Kirsch, *Méthode de synthése des [2H] benzofurannones-3 mono et polysubstituées et des benzo [b] furannes correspondants.* C. R. Acad. Sci., Ser. C, 1976. **282**(Copyright (C) 2013 American Chemical Society (ACS). All Rights Reserved.
): p. 993-96.
85. T. Chen, S. Hevi, F. Gay, N. Tsujimoto, T. He, B. Zhang, Y. Ueda, and E. Li, *Complete inactivation of DNMT1 leads to mitotic catastrophe in human cancer cells.* Nat Genet, 2007. **39**(3): p. 391-6.
96. G. Egger, G. Liang, A. Aparicio, and P.A. Jones, *Epigenetics in human disease and prospects for epigenetic therapy.* Nature, 2004. **429**(6990): p. 457-63.
97. S. Takashima, M. Takehashi, J. Lee, S. Chuma, M. Okano, K. Hata, I. Suetake, N. Nakatsuji, H. Miyoshi, S. Tajima, Y. Tanaka, S. Toyokuni, H. Sasaki, M. Kanatsu-Shinohara, and T. Shinohara, *Abnormal DNA methyltransferase expression in mouse germline stem cells results in spermatogenic defects.* Biol Reprod, 2009. **81**(1): p. 155-64.
98. F. Gaudet, J.G. Hodgson, A. Eden, L. Jackson-Grusby, J. Dausman, J.W. Gray, H. Leonhardt, and R. Jaenisch, *Induction of tumors in mice by genomic hypomethylation.* Science, 2003. **300**(5618): p. 489-92.
99. A. Eden, F. Gaudet, A. Waghmare, and R. Jaenisch, *Chromosomal instability and tumors promoted by DNA hypomethylation.* Science, 2003. **300**(5618): p. 455.
100. I.A. Qureshi and M.F. Mehler, *Advances in epigenetics and epigenomics for neurodegenerative diseases.* Curr Neurol Neurosci Rep, 2011. **11**(5): p. 464-73.
101. A. Fuso, V. Nicolia, R.A. Cavallaro, and S. Scarpa, *DNA methylase and demethylase activities are modulated by one-carbon metabolism in Alzheimer's disease models.* J Nutr Biochem, 2011. **22**(3): p. 242-51.
102. F. Higuchi, S. Uchida, H. Yamagata, K. Otsuki, T. Hobara, N. Abe, T. Shibata, and Y. Watanabe, *State-dependent changes in the expression of DNA methyltransferases in mood disorder patients.* J Psychiatr Res, 2011. **45**(10): p. 1295-300.
103. C. Lopez-Pedrera, C. Perez-Sanchez, M. Ramos-Casals, M. Santos-Gonzalez, A. Rodriguez-Ariza, and M.J. Cuadrado, *Cardiovascular risk in systemic autoimmune diseases: epigenetic mechanisms of immune regulatory functions.* Clin Dev Immunol, 2012. **2012**: p. 974648.
104. E.R. Nimmo, J.G. Prendergast, M.C. Aldhous, N.A. Kennedy, P. Henderson, H.E. Drummond, B.H. Ramsahoye, D.C. Wilson, C.A. Semple, and J. Satsangi, *Genome-wide methylation profiling in Crohn's disease identifies altered*

epigenetic regulation of key host defense mechanisms including the Th17 pathway. Inflamm Bowel Dis, 2012. **18**(5): p. 889-99.

105. J. Bressler, L.C. Shimmin, E. Boerwinkle, and J.E. Hixson, *Global DNA methylation and risk of subclinical atherosclerosis in young adults: the Pathobiological Determinants of Atherosclerosis in Youth (PDAY) study.* Atherosclerosis, 2011. **219**(2): p. 958-62.
106. J.G. Herman and S.B. Baylin, *Gene silencing in cancer in association with promoter hypermethylation.* N Engl J Med, 2003. **349**(21): p. 2042-54.
107. P.A. Jones and S.B. Baylin, *The epigenomics of cancer.* Cell, 2007. **128**(4): p. 683-92.
108. L.J. Rush, Z. Dai, D.J. Smiraglia, X. Gao, F.A. Wright, M. Fruhwald, J.F. Costello, W.A. Held, L. Yu, R. Krahe, J.E. Kolitz, C.D. Bloomfield, M.A. Caligiuri, and C. Plass, *Novel methylation targets in de novo acute myeloid leukemia with prevalence of chromosome 11 loci.* Blood, 2001. **97**(10): p. 3226-33.
109. J.R. Melki, P.C. Vincent, and S.J. Clark, *Concurrent DNA hypermethylation of multiple genes in acute myeloid leukemia.* Cancer research, 1999. **59**(15): p. 3730-40.
110. A.-K. Petersen, S. Zeilinger, G. Kastenmüller, W. Römisch-Margl, M. Brugger, A. Peters, C. Meisinger, K. Strauch, C. Hengstenberg, P. Pagel, F. Huber, R.P. Mohney, H. Grallert, T. Illig, J. Adamski, M. Waldenberger, C. Gieger, and K. Suhre, *Epigenetics meets metabolomics: An epigenome-wide association study with blood serum metabolic traits.* Human Molecular Genetics, 2013.
118. S. Sharma, T.K. Kelly, and P.A. Jones, *Epigenetics in cancer.* Carcinogenesis, 2010. **31**(1): p. 27-36.
132. A.P. Feinberg, R. Ohlsson, and S. Henikoff, *The epigenetic progenitor origin of human cancer.* Nat Rev Genet, 2006. **7**(1): p. 21-33.
133. E. Prokhortchouk and P.A. Defossez, *The cell biology of DNA methylation in mammals.* Biochim Biophys Acta, 2008. **1783**(11): p. 2167-73.
134. S. Ramchandani, S.K. Bhattacharya, N. Cervoni, and M. Szyf, *DNA methylation is a reversible biological signal.* Proc Natl Acad Sci U S A, 1999. **96**(11): p. 6107-12.
135. C. Gros, J. Fahy, L. Halby, I. Dufau, A. Erdmann, J.M. Gregoire, F. Ausseil, S. Vispe, and P.B. Arimondo, *DNA methylation inhibitors in cancer: Recent and future approaches.* Biochimie, 2012. **94**(11): p. 2280-96.
136. Y.G. Zheng, J. Wu, Z. Chen, and M. Goodman, *Chemical regulation of epigenetic modifications: opportunities for new cancer therapy.* Med Res Rev, 2008. **28**(5): p. 645-87.
185. J. Datta, K. Ghoshal, W.A. Denny, S.A. Gamage, D.G. Brooke, P. Phiasivongsa, S. Redkar, and S.T. Jacob, *A new class of quinoline-based DNA hypomethylating agents reactivates tumor suppressor genes by blocking DNA methyltransferase 1 activity and inducing its degradation.* Cancer Res, 2009. **69**(10): p. 4277-85.
186. Z.M. Svedruzic, *Dnmt1 structure and function.* Prog Mol Biol Transl Sci, 2011. **101**: p. 221-54.

187. M. Szyf, *Epigenetic therapeutics in autoimmune disease.* Clin Rev Allergy Immunol, 2010. **39**(1): p. 62-77.
191. Y. Chang, X. Zhang, J.R. Horton, A.K. Upadhyay, A. Spannhoff, J. Liu, J.P. Snyder, M.T. Bedford, and X. Cheng, *Structural basis for G9a-like protein lysine methyltransferase inhibition by BIX-01294.* Nat Struct Mol Biol, 2009. **16**(3): p. 312-7.
201. S. Vallabhapurapu and M. Karin, *Regulation and function of NF-kappaB transcription factors in the immune system.* Annu Rev Immunol, 2009. **27**: p. 693-733.
203. S.C. Gupta, C. Sundaram, S. Reuter, and B.B. Aggarwal, *Inhibiting NF-κB activation by small molecules as a therapeutic strategy.* Biochimica et Biophysica Acta (BBA) - Gene Regulatory Mechanisms, 2010. **1799**(10–12): p. 775-787.
205. C.H. Lee, Y.-T. Jeon, S.-H. Kim, and Y.-S. Song, *NF-κB as a potential molecular target for cancer therapy.* BioFactors, 2007. **29**(1): p. 19-35.
206. G. Bonizzi and M. Karin, *The two NF-kappaB activation pathways and their role in innate and adaptive immunity.* Trends Immunol, 2004. **25**(6): p. 280-8.
207. J. Ling and R. Kumar, *Crosstalk between NFkB and glucocorticoid signaling: a potential target of breast cancer therapy.* Cancer Lett, 2012. **322**(2): p. 119-26.
210. V.R. Yadav, S. Prasad, B. Sung, and B.B. Aggarwal, *The role of chalcones in suppression of NF-κB-mediated inflammation and cancer.* International Immunopharmacology, 2011. **11**(3): p. 295-309.
211. B. Srinivasan, T.E. Johnson, R. Lad, and C. Xing, *Structure–Activity Relationship Studies of Chalcone Leading to 3-Hydroxy-4,3',4',5'-tetramethoxychalcone and Its Analogues as Potent Nuclear Factor κB Inhibitors and Their Anticancer Activities.* Journal of medicinal chemistry, 2009. **52**(22): p. 7228-7235.
227. J. Ravindran, S. Prasad, and B.B. Aggarwal, *Curcumin and cancer cells: how many ways can curry kill tumor cells selectively?* AAPS J, 2009. **11**(3): p. 495-510.
234. G.P. Nagaraju, S. Aliya, S.F. Zafar, R. Basha, R. Diaz, and B.F. El-Rayes, *The impact of curcumin on breast cancer.* Integr Biol (Camb), 2012. **4**(9): p. 996-1007.
235. G. Radhakrishna Pillai, A.S. Srivastava, T.I. Hassanein, D.P. Chauhan, and E. Carrier, *Induction of apoptosis in human lung cancer cells by curcumin.* Cancer Lett, 2004. **208**(2): p. 163-70.
236. S. Reuter, J. Charlet, T. Juncker, M.H. Teiten, M. Dicato, and M. Diederich, *Effect of curcumin on nuclear factor kappaB signaling pathways in human chronic myelogenous K562 leukemia cells.* Ann N Y Acad Sci, 2009. **1171**: p. 436-47.
237. M.H. Teiten, F. Gaascht, S. Eifes, M. Dicato, and M. Diederich, *Chemopreventive potential of curcumin in prostate cancer.* Genes Nutr, 2010. **5**(1): p. 61-74.

238. R. Wilken, M.S. Veena, M.B. Wang, and E.S. Srivatsan, *Curcumin: A review of anti-cancer properties and therapeutic activity in head and neck squamous cell carcinoma.* Mol Cancer, 2011. **10**: p. 12.
239. T.L. Chiu and C.C. Su, *Curcumin inhibits proliferation and migration by increasing the Bax to Bcl-2 ratio and decreasing NF-kappaBp65 expression in breast cancer MDA-MB-231 cells.* Int J Mol Med, 2009. **23**(4): p. 469-75.
240. H.J. Kang, S.H. Lee, J.E. Price, and L.S. Kim, *Curcumin suppresses the paclitaxel-induced nuclear factor-kappaB in breast cancer cells and potentiates the growth inhibitory effect of paclitaxel in a breast cancer nude mice model.* Breast J, 2009. **15**(3): p. 223-9.
241. C.P. Prasad, G. Rath, S. Mathur, D. Bhatnagar, and R. Ralhan, *Potent growth suppressive activity of curcumin in human breast cancer cells: Modulation of Wnt/beta-catenin signaling.* Chem Biol Interact, 2009. **181**(2): p. 263-71.
242. M.G. Alexandrow, L.J. Song, S. Altiok, J. Gray, E.B. Haura, and N.B. Kumar, *Curcumin: a novel Stat3 pathway inhibitor for chemoprevention of lung cancer.* Eur J Cancer Prev, 2012. **21**(5): p. 407-12.
243. S. Singh and B.B. Aggarwal, *Activation of transcription factor NF-kappa B is suppressed by curcumin (diferuloylmethane) [corrected].* J Biol Chem, 1995. **270**(42): p. 24995-5000.
244. M.H. Teiten, F. Gaascht, M. Cronauer, E. Henry, M. Dicato, and M. Diederich, *Anti-proliferative potential of curcumin in androgen-dependent prostate cancer cells occurs through modulation of the Wingless signaling pathway.* Int J Oncol, 2011. **38**(3): p. 603-11.
258. G. Appendino, L. Maxia, M. Bascope, P.J. Houghton, G. Sanchez-Duffhues, E. Munoz, and O. Sterner, *A meroterpenoid NF-kappaB inhibitor and drimane sesquiterpenoids from Asafetida.* J Nat Prod, 2006. **69**(7): p. 1101-4.
259. T. Hirai and H. Togo, *Preparation and Synthetic Use of Polymer-Supported Acetoacetate Reagent.* Synthesis, 2005. **2005**(EFirst): p. 2664-2668.
260. S.t. Starčević, P. Brožič, S. Turk, J.k. Cesar, T. Lanišnik Rižner, and S. Gobec, *Synthesis and Biological Evaluation of (6- and 7-Phenyl) Coumarin Derivatives as Selective Nonsteroidal Inhibitors of 17β-Hydroxysteroid Dehydrogenase Type 1.* Journal of medicinal chemistry, 2010. **54**(1): p. 248-261.
261. V. Cechinel-Filho, Z.R. Vaz, L. Zunino, J.B. Calixto, and R.A. Yunes, *Synthesis of xanthoxyline derivatives with antinociceptive and antioedematogenic activities.* European journal of medicinal chemistry, 1996. **31**(10): p. 833-839.

Summary of the scientific titles (participation in scientific programs, publications, oral communications, poster communications) and complementary modules

(1) Scientific programs/ poster communications / oral contributions:

07/2013	ESMEC Urbino, Italy; Poster Presentation, PhD project: Structure-Based Lead-Optimization of Quinoline-Based DNA Hypomethylating Agents as DNMT1 Inhibitors C. Zwergel S. Valente, Y. Liu, M. Schnekenburger, S. Cosconati, C. Gros, M. Tardugno, D. Labella, C. Florean, S. Minden, H. Hashimoto, Y. Chang, X. Zhang, G. Kirsch, E. Novellino, P. B. Arimondo, E. Miele, E. Ferretti, A. Gulino, M. Diederich, X. Cheng and A. Mai
05/2013	COST Epigenetic Rome Training School: Active participation in the organization of the PhD-school as well as attendance in the plenary lectures, lab courses and journal clubs.
11/2012:	3rd meeting on medicinal chemistry, 3enqt, Aveiro, Portugal; Poster Presentation: Structure-Based Lead-Optimization of Quinoline-Based DNA Hypomethylating Agents as DNMT1 Inhibitors S. Valente, M. Schnekenburger, C. Zwergel, C. Florean, M. Diederich, G. Kirsch and A. Mai
11/2012:	Final RedCat Meeting, Aveiro, Portugal; Poster and oral presentation: Coumarine and Chromone based derivatives and study of their biological activities C. Zwergel, S. Valente, F. Gaascht, L. Altucci, M. Diederich and G. Kirsch
11/2012:	Ecole Doctorale de Chimie et Physique Moléculaires SESAMES Journée de rentrée, Metz, France; Oral Presentation: Overview over the PhD project C. Zwergel, G. Kirsch
07/2012:	ESMEC Urbino, Italy; Poster and Oral Presentation: PhD project: Coumarine and Chromone based derivatives and study of their biological activities C. Zwergel, S. Valente, G. Kirsch
03/2012:	SCF Grand Est 7 Reims, France; Poster Presentation: Preparation of novel aurones from coumarin-4-aldehyde and 3-formylchromone C. Zwergel, Z. Xu, S. Valente, G. Kirsch
02/2012:	SCT Journées Jeunes Chercheurs 2012 Paris, France; Poster Presentation: Preparation of novel aurones from coumarin-4-aldehyde and 3-formylchromone C. Zwergel, Z. Xu, S. Valente, G. Kirsch

01/2012: Meeting on Redox regulation - Natural compounds as regulators of inflammation signalling, Luxemburg; Poster Presentation: Preparation of novel aurones from coumarin-4-aldehyde and 3-formylchromone
C. Zwergel, Z. Xu, S. Valente, G. Kirsch

11/2011: Ecole Doctorale de Chimie et Physique Moléculaires SESAMES Journée Scientifique de rentrée, Metz, France; Poster Presentation: 4-Vinyl-2*H*-1-benzopyran-2-one reactivity for [4+2] thermal cycloaddition: access to novel steroid-like coumarin-based heterocycles
C. Zwergel, Z. Xu, S. Valente, A. M. S. Silva, G. Kirsch

08/2011: ASMC St. Petersburg, Russia; Poster Presentation: 4-Vinyl-2*H*-1-benzopyran-2-one reactivity for [4+2] thermal cycloaddition: access to novel steroid-like coumarin-based heterocycles
Z. Xu, C. Zwergel, S. Valente, A. M. S. Silva, G. Kirsch

05/2011: Ecole Doctorale de Chimie et Physique Moléculaires SESAMES Journé Scientifique de rentrée, Nancy, France; oral communication: 4-Butoxyvinyl coumarins and 4-Acetyl coumarins as starting material fc polycyclic systems
C. Zwergel, S. Valente, Z. Xu, G. Kirsch

04/2011: Annual Gathering 2011 of the RedCat project, Metz, France; oral communication: 2*H*-chromen-2-one (Coumarin) as scaffold for new anticancer agents
C. Zwergel, S. Valente, Z. Xu, G. Kirsch

(2) Publications

A) Medicinal Chemistry Communications, 2011, 2, 196-200
Interactions of polysulfanes with components of red blood cells
Thomas Schneider, Lalla Aicha Ba, Khairan Khairan, Clemens Zwergel, Nguyen Duc Bach, Ingolf Bernhardt, Wolfgang Brandt, Ludger Wessjohann, Marc Diederich and Claus Jacob

B) Natural Products Communications, 2012; 7,3 389-394
Aurones: Interesting Natural and Synthetic Compounds with Emerging Biological Potential
Clemens Zwergel, François Gaascht, Sergio Valente, Marc Diederich, Denyse Bagrel and Gilbert Kirsch

C) European Journal of Organic Chemistry 2013; 2869-2877
Reactivity of 4-Vinyl-2H-1-benzopyran-2-ones in Diels–Alder Cycloaddition Reactions: Access to Coumarin-Based Polycycles with Cdc25 Phosphatase-Inhibiting Activity
Sergio Valente, Zhanjie Xu, Emilie Bana, Clemens Zwergel, Antonello Mai, Claus Jacob, Peter Meiser, Denyse Bagrel, Artur M. S. Silva and Gilbert Kirsch

D) Medicinal Chemistry Communications 2013, **4**, 1571-1579
Novel benzofuran-chromone and –coumarine derivatives: Synthesis and biological activity in K562 human leukemia cells
Clemens Zwergel, Sergio Valente, Angela Salvato, Zhanjie Xu, Oualid Talhi, Antonello Mai, Artur Silva, Lucia Altucci and Gilbert Kirsch

Accepted
E) Journal of Medicinal Chemistry 2013
Selective Non-Nucleoside Inhibitors of Human DNA Methyltransferases Active in Cancer Including Cancer Stem Cells
Sergio Valente, Liu Yiwei, Michael Schnekenburger, Clemens Zwergel, Sandro Cosconati, Christina Gros, Maria Tardugno, Donatella Labella, Cristina Florean, Steve Minden, Hideharu Hashimoto, Yanqi Chang, Xing Zhang, Gilbert Kirsch, Ettore Novellino, Paola Arimondo, Evelina Miele, Elisabetta Ferretti, Alberto Gulino, Marc Diederich, Xiaodong Cheng and Antonello Mai

3) Complementary Modules

A) Within the RedCat training network
1) Project Management and Communication
2) Science and Society
3) Science and Industry
4) Fit to Europe
Each Module was granted 5 ECTS credits.

B) Université de Lorraine
1) Scientifc writing combined with English Course
2) French language course for foreign students

C) Universita degli Studi di Roma "Sapienza"
1) NMR-Training
2) External Italian course for foreign students